LITHUANIAN UNIVERSITY OF HEALTH SCIENCES

Ali Aldujeli

CORONARY MICROVASCULAR DYSFUNCTION IN PATIENTS WITH ST-ELEVATION MYOCARDIAL INFARCTION: DIAGNOSTICS, AND OUTCOMES

Doctoral Dissertation
Medical and Health Sciences,
Medicine (M 001)

Kaunas, 2024

Dissertation has been prepared at the Laboratory of Molecular Cardiology of the Institute of Cardiology of the Lithuanian University of Health Sciences during the period of 2020–2024.

Scientific Supervisor

Prof. Dr. Ramūnas Unikas (Lithuanian University of Health Sciences, Medical and Health Sciences, Medicine – M 001).

Consultant

Assoc. Prof. Dr. Vacis Tatarūnas (Lithuanian University of Health Sciences, Natural Sciences, Biology – N 010).

Dissertation is defended at the Medical Research Council of the Lithuanian University of Health Sciences:

Chairperson

Prof. Dr. Andrius Macas (Lithuanian University of Health Sciences, Medical and Health Sciences, Medicine – M 001).

Members:

Prof. Dr. Raimondas Kubilius (Lithuanian University of Health Sciences, Medical and Health Sciences, Medicine – M 001);
Prof. Dr. Dainius Haroldas Pauža (Lithuanian University of Health Sciences, Natural Sciences, Biology – N 010);
Prof. Dr. Pranas Šerpytis (Vilnius University, Medical and Health Sciences, Medicine – M 001);
Prof. Dr. Mohaned Egred (University of Sunderland, Medical and Health Sciences, Medicine – M 001).

Dissertation will be defended at the open session of the Medical Research Council of the Lithuanian University of Health Sciences on the 5th of July 2024, at 12 p.m. in the Conference Hall of the Institute of Cardiology of the Lithuanian University of Health Sciences.
Address: Sukilėlių 15, LT-50162 Kaunas, Lithuania.

LIETUVOS SVEIKATOS MOKSLŲ UNIVERSITETAS

Ali Aldujeli

PACIENTŲ, SERGANČIŲ MIOKARDO INFARKTU, KAI S–T SEGMENTAS PAKILĘS, VAINIKINIŲ MIKROKRAUJAGYSLIŲ DISFUNKCIJA: DIAGNOSTIKA IR BAIGTYS

Daktaro disertacija
Medicinos ir sveikatos mokslai,
medicina (M 001)

Kaunas, 2024

Disertacija rengta 2020–2024 metais Lietuvos sveikatos mokslų universiteto Kardiologijos instituto Molekulinės kardiologijos laboratorijoje.

Mokslinis vadovas

prof. dr. Ramūnas Unikas (Lietuvos sveikatos mokslų universitetas, medicinos ir sveikatos mokslai, medicina – M 001).

Konsultantas

doc. dr. Vacis Tatarūnas (Lietuvos sveikatos mokslų universitetas, gamtos mokslai, biologija – N 010).

Disertacija ginama Lietuvos sveikatos mokslų universiteto Medicinos mokslo krypties taryboje:

Pirmininkas

prof. dr. Andrius Macas (Lietuvos sveikatos mokslų universitetas, medicinos ir sveikatos mokslai, medicina – M 001).

Nariai:

prof. dr. Raimondas Kubilius (Lietuvos sveikatos mokslų universitetas, medicinos ir sveikatos mokslai, medicina – M 001);
prof. dr. Dainius Haroldas Pauža (Lietuvos sveikatos mokslų universitetas, gamtos mokslai, biologija – N 010);
prof. dr. Pranas Šerpytis (Vilniaus universitetas, medicinos ir sveikatos mokslai, medicina – M 001);
prof. dr. Mohaned Egred (Sanderlando universitetas, medicinos ir sveikatos mokslai, medicina – M 001).

Disertacija bus ginama viešame Medicinos mokslo krypties tarybos posėdyje 2024 m. liepos 5 d. 12 val. Lietuvos sveikatos mokslų universiteto Kardiologijos instituto Posėdžių salėje.
Adresas: Sukilėlių pr. 15, LT-50162 Kaunas, Lietuva.

CONTENTS

ABBREVIATIONS

ACS	–	acute coronary syndrome
ADA	–	American diabetes association
ADR	–	epinephrine (adrenaline)
ADP	–	adenosine diphosphate
AMI	–	acute myocardial infarction
ANP	–	atrial natriuretic peptide
APV	–	average peak velocity
ASE	–	American society of echocardiography
AUC	–	area under the curve
BMI	–	body mass index
BNP	–	B-type natriuretic peptide
CABG	–	coronary artery bypass graft
CAD	–	coronary artery disease
CCS	–	chronic coronary syndrome
CFR	–	coronary flow reserve
CFVR	–	coronary flow velocity reserve
CI	–	confidence interval
CICU	–	cardiology intensive care unit
CMR	–	cardiovascular magnetic resonance
CMD	–	coronary microvascular dysfunction
CRP	–	C-reactive protein
CT	–	computed tomography
cTFC	–	corrected thrombolysis in myocardial infarction frame count
CV	–	cross-validation
CVD	–	cardiovascular disease
Discrete SL	–	discrete super learner
EAS	–	European atherosclerosis society
ECG	–	electrocardiogram
ELISA	–	enzyme-linked immunosorbent assay
ESC	–	European society of cardiology
ESH	–	European society of hypertension
ESR	–	erythrocyte sedimentation rate
FFR	–	fractional flow reserve
FLVR	–	functional left ventricular remodelling
FMO	–	flavin-containing monooxygenase
FXR	–	farnesoid X receptor
GBB	–	γ-Butyrobetaine
GBM	–	gradient boosting machine
HDL	–	high-density lipoprotein
HMR	–	hyperemic microvascular resistance
Hs-CRP	–	high sensitivity C-reactive protein
HSPs	–	heat shock proteins
IQR	–	interquartile range
IMR	–	index of microcirculatory resistance
IMR_{angio}	–	index of microcirculatory resistance by angiography
LA	–	left atrial/left atrium

LBBB	–	left bundle branch block
LDL	–	low-density lipoprotein
LV	–	left ventricular
LVEF	–	left ventricular ejection fraction
LVEDP	–	left ventricular end-diastolic pressure
LVEDV	–	left ventricular end diastolic volume
MACE	–	major adverse cardiovascular events
MBG	–	myocardial blush grade
MI	–	myocardial infarction
MRR	–	microvascular resistance reserve
NLR	–	neutrophil-to-lymphocyte ratio
NLRP	–	nucleotide-binding oligomerization domain, leucine rich repeat and pyrin domain containing
NH-IMR_{angio}	–	non-hyperemic IMR_{angio}
NPV	–	negative predictive value
OOB	–	out-of-bag
ox-LDL	–	oxidized low-density lipoprotein
P_a	–	aortic pressure
PCI	–	percutaneous coronary intervention
PET	–	positron emission tomography
P_d	–	distal coronary pressure
PLT	–	platelets
PPV	–	positive predictive value
PRRs	–	pattern recognition receptors
POCE	–	patient-oriented composite endpoint
Pzf	–	zero-flow pressure
QFR	–	quantitative flow ratio
QuBE	–	quantitative blush evaluator
RDW	–	red cell distribution width
RCT	–	reverse cholesterol transport
relVIM	–	relative variable importance measures
RF	–	random forest
ROC	–	receiver operating characteristic
SD	–	standard deviations
SL	–	super learner
SMOTE	–	synthetic minority over-sampling technique
SRs	–	scavenger receptors
STEMI	–	ST-elevation myocardial infarction
SVM	–	support vector machine
suPAR	–	soluble urokinase plasminogen activator receptor
TAMIR	–	impact of trimethylamine-N-oxide on index of microcirculatory resistance
TC	–	total cholesterol
TFG	–	thrombolysis in myocardial infarction flow grade
TG	–	triglycerides
TIMI	–	thrombolysis in myocardial infarction
TMA	–	trimethylamine
TMAO	–	trimethylamine N-oxide
TMPG	–	thrombolysis in myocardial infarction myocardial perfusion grade

T_{mn}	–	mean transit time
TnI	–	troponin I
TRpV	–	tricuspid regurgitation peak velocity
WBC	–	white blood cells
WIA	–	wave intensity analysis
XGBoost	–	eXtreme Gradient Boosting
3D-PDP	–	3-dimensional partial dependence plots

INTRODUCTION

Cardiovascular diseases (CVD) are the leading cause of mortality globally, responsible for a significant number of deaths and disabilities [1]. In 2021 alone, CVDs accounted for 20.5 million deaths, comprising approximately one-third of all global deaths. Over the European continent, CVD accounts for half of all deaths [2]. Despite improvements in the management of ischemic heart diseases, ST-Elevation Myocardial Infarction (STEMI) remains the cornerstone of these deaths [3]. In the vast and ever-evolving landscape of

Early reperfusion with primary percutaneous coronary intervention (PCI) is the standard of care for the contemporary management of STEMI [4]. Despite the established efficacy of PCI in reestablishing 95% of epicardial vessel patency, the restoration of coronary microcirculation and complete myocardial perfusion may not be achieved in up to 50% of patients [5]. Inadequate myocardial perfusion may lead to the cascade of ischemic heart disease: diastolic dysfunction, systolic dysfunction, and adverse left ventricular remodelling. Further investigations have revealed that up to 15.5% of STEMI patients continue to experience anginal symptoms even after successful reperfusion of epicardial arteries, which can be attributed to disruption of coronary microvasculature, independently associated with ongoing anginal symptoms, poor recovery of left ventricular function, and adverse clinical outcomes [6].

CMD involve a spectrum of anatomical and functional aberrations of the cardiac microcirculation that curtail the necessary coronary blood supply to the myocardium, culminating in myocardial ischemia [7]. In STEMI patients, CMD may be caused by several pathophysiologic pathways, including microvascular occlusion, intramyocardial hemorrhage, and inflammation [8].

Coronary microvasculature is not visible on conventional angiography. Thus, the diagnosis of CMD requires invasive physiology tests or advanced imaging techniques, all of which can be costly, time-consuming, and carry a risk of complication, contributing to its underdiagnosis [9, 10]. Among these, the thermodilution-derived evaluation of Coronary Flow Reserve (CFR) and the Index of Microcirculatory Resistance (IMR) using a pressure-temperature sensor coronary guidewire are the most widely adopted, reproducible, and streamlined diagnostic strategies, with CFR representing the functional vasodilatory capacity and IMR representing the microvascular resistance [11]. The link between abnormal CFR, IMR, and unfavorable clinical outcomes in STEMI patients has been repeatedly demonstrated [12].

In this thesis, the investigation focuses on a thorough exploration of CMD within the context of STEMI. The work is structured, comprising a series of in-

depth studies that systematically address various dimensions of CMD. These investigations range from evaluating interventional strategies in STEMI management to the enhancement of CMD diagnostics through the utilization of machine learning algorithms. Additionally, the identification and validation of novel biomarkers form a crucial part of this work, culminating in an extensive examination of their implications on patient outcomes.

The initial segment of the research offers a critical comparison of various interventional approaches in STEMI, such as direct stenting, aspiration thrombectomy, and the administration of intracoronary glycoprotein IIb/IIIa inhibitors. Emphasis is placed on assessing the impact of these strategies on the prevalence of CMD and the incidence of Major Adverse Cardiac Events (MACE), providing insights crucial for optimizing treatment protocols.

Subsequently, the thesis then delves into the development of a novel machine learning algorithm, a significant innovation in the diagnosis of CMD. This algorithm is grounded in data-driven analytics and is designed to assess the probability of CMD by analyzing a suite of biomarkers, which have been identified in previous literature as being associated with CMD. The research progresses towards a critical phase that includes both internal and external validations of this algorithm. These steps are instrumental in marking a substantial advancement in CMD diagnostics. The ultimate aim is to establish this algorithm as a reliable, blood test-based tool for the identification of CMD in patients with STEMI.

Following the implementation of the machine learning algorithm, the thesis progresses by selecting the most relevant biomarker identified through this analysis for further exploration. This subsequent phase delves into examining the chosen biomarker's role in diagnosing CMD in STEMI patients. It highlights the biomarker's correlation with crucial clinical outcomes, including Left Ventricular (LV) recovery post-STEMI.

Additionally, the thesis investigates the prognostic value of Microvascular Resistance Reserve (MRR) in STEMI patients. While MRR has been validated in Chronic Coronary Syndrome (CCS), its utility in STEMI was hitherto unexplored. This study fills this gap, validating MRR as a robust prognostic indicator and comparing it with other coronary physiological parameters.

One of the first comprehensive efforts to categorize CMD endotypes in STEMI patients is also presented. This research delves into the prevalence and clinical implications of various CMD endotypes, paving the way for more targeted therapeutic interventions based on distinct CMD profiles.

The final part of the thesis examines the long-term implications of CMD on cardiac remodelling, particularly focusing on Functional LV Remodelling (FLVR) and diastolic dysfunction post-STEMI. This research establishes

CMD as an early marker for predicting future LV remodelling and increased MACE risk, underscoring the importance of early CMD diagnosis for improving patient monitoring and long-term outcomes.

This thesis stands as a significant milestone in our understanding of CMD within the STEMI framework. Each chapter meticulously unravels different facets of CMD, blending innovative methodologies, critical analyses, and pioneering discoveries to enhance diagnostic accuracy, therapeutic efficacy, and patient outcomes in cardiovascular care. This introduction sets the stage for a journey through groundbreaking research, with each subsequent part building upon the last to present a comprehensive view of CMD in the STEMI landscape.

1. THE AIM AND OBJECTIVES OF THE STUDY

1.1. The aim of the study

The primary aim of the PhD thesis is to enhance the understanding and management of CMD in patients suffering from STEMI, ultimately contributing to improved patient outcomes and the advancement of cardiovascular medicine.

1.2. The objectives of the PhD thesis

1. To evaluate the efficacy of various interventional strategies in STEMI management, focusing on their impact on the prevalence of CMD and incidence of MACE.
2. To introduce and validate a machine learning algorithm for CMD diagnosis in patients who suffered from STEMI, emphasizing its utility in diverse patient populations.
3. To investigate the biomarker deemed most relevant by the machine learning algorithm for CMD in STEMI patients, aiming to determine its cut-off value, compare it with other presumed biomarkers, and analyze its correlation with clinical outcomes and LV recovery post-STEMI.
4. To assess and validate the prognostic value of the novel coronary physiology parameter, MRR, in STEMI patients, and to conduct comparative analyses with other established coronary physiological parameters.
5. To explore the prevalence of different CMD endotypes in STEMI patients and their respective clinical implications, paving the way for personalized treatment approaches.
6. To study the long-term effects of CMD on LV function post-STEMI, focusing on functional remodelling and diastolic dysfunction.

1.3. Scientific novelty of the PhD thesis

This thesis introduces groundbreaking elements to cardiovascular research, particularly in the realm of CMD and STEMI:

1. Pioneering Percutaneous Coronary Intervention (PCI) Technique Evaluation in STEMI: This research breaks new ground by systematically identifying the most effective PCI technique for STEMI patients [13]. It introduces a novel analytical approach, setting a precedent in comparative interventional research and potentially influencing future studies in cardiac care.
2. Breakthrough in Artificial Intelligence-Driven CMD Diagnosis: The integration of a machine learning algorithm in CMD diagnosis repre-

sents a groundbreaking development in cardiovascular diagnostics. This research marks a novel application of artificial intelligence, utilizing advanced data analytics to interpret complex biomarker information for CMD detection. This approach is pioneering in its combination of machine learning with cardiovascular diagnostic processes.

3. Groundbreaking Biomarker Research: This thesis delves into an in-depth investigation of the biomarker identified as most relevant through the previously mentioned machine learning algorithm for CMD in STEMI patients, heralding a new era in cardiac research. By focusing on the metabolic indicators and their link to CMD, this research holds the potential to revolutionize our understanding of CMD mechanism and diagnostics. It lays a foundation for innovative diagnostic approaches, thereby significantly contributing to the advancement of cardiac health knowledge and practice.
4. Pioneering MRR Prognostic Evaluation in STEMI: This research represents a novel foray into validating MRR as a prognostic marker specifically in STEMI patients. This investigation is groundbreaking, as it extends the application of MRR from CCS to STEMI, a relatively uncharted territory in microvascular health research. It establishes a new precedent in understanding the long-term implications of microvascular health in heart disease.
5. Charting Unexplored Terrain in CMD Endotypes: This segment of the study breaks new ground by comprehensively exploring CMD endotypes in STEMI patients. It marks one of the first extensive efforts to classify and understand the diversity of CMD presentations within this patient group. This exploration adds a novel perspective to the field of precision cardiovascular care, potentially revolutionizing the approach to treatment by tailoring it to specific CMD endotypes.
6. Unraveling CMD's Impact on LV Recovery Post-STEMI: This part of the study pioneers in unraveling the complex relationship between CMD and diverse patterns of LV recovery following STEMI. It offers a novel perspective by identifying CMD as a critical factor influencing the varied trajectories of cardiac recovery or decline. This groundbreaking approach provides a deeper understanding of the mechanisms behind different recovery patterns in both systolic and diastolic heart function post-STEMI. The study's advanced methods in assessing functional LV remodelling and diastolic dysfunction represent a significant advancement in cardiac prognosis research.

1.4. The practical value of the PhD thesis

This PhD thesis offers significant practical contributions to the field of cardiovascular medicine, particularly in the management and understanding of CMD in STEMI patients:

1. Enhanced STEMI Management Strategies: The practical implications of this study are profound for clinical practice. By offering a detailed assessment of various PCI strategies, the research equips clinicians with evidence-based insights to refine STEMI treatment protocols. This directly contributes to improved patient management, potentially reducing the incidence of CMD and MACE, and enhancing overall patient outcomes in STEMI care.
2. Enhancing Diagnostic Precision in CMD: The practical application of this machine learning algorithm for CMD diagnosis in STEMI patients is transformative. By offering a validated, data-driven method, this tool enhances diagnostic accuracy, facilitating early detection and more precise management of CMD. Its effectiveness across diverse patient demographics marks a significant step forward in improving patient care and outcomes in cardiovascular health.
3. Biomarker-Based Personalized Care in CMD: The in-depth exploration of the biomarker identified by the machine learning algorithm as being most relevant in diagnosing CMD marks a significant leap in diagnostic and therapeutic realms. This research goes beyond enhancing diagnostic capabilities; it profoundly impacts patient care. By elucidating the intricate relationship between this blood biomarker, CMD diagnosis, clinical outcomes, and LV recovery post-STEMI, the study paves the way for tailored and effective treatment strategies. It underscores the transformative potential of biomarker-based approaches in refining the precision and efficacy of patient management following STEMI, thereby charting a course towards personalized cardiac healthcare.
4. Enhancing STEMI Patient Risk Stratification with MRR: The successful validation of MRR as a prognostic tool for MACE in STEMI patients adds a significant layer to cardiac risk assessment. By enabling clinicians to identify high-risk individuals accurately, this research fosters a targeted and efficient approach to patient care. It empowers healthcare providers with a powerful tool to prioritize and intensify treatment for those most in need, potentially improving patient outcomes and management strategies.
5. Tailoring Treatment with CMD Endotype Insights: The investigation into the various CMD endotypes and their clinical significance

in STEMI patients paves the way for a more nuanced and personalized approach to patient care. By identifying specific endotypes and understanding their unique clinical implications, this research empowers clinicians to develop more targeted and effective treatment strategies. It signifies a substantial step towards enhancing the quality and specificity of care for STEMI patients, moving closer to a personalized medicine model in cardiology.

6. Enhancing Post-STEMI Cardiac Care through CMD Insights: The insights gained from this study about the long-term effects of CMD on LV remodelling and diastolic dysfunction are invaluable for patient care following STEMI. By establishing CMD as a marker for future cardiac function, the research equips clinicians with critical information for proactive and personalized patient management. This understanding is vital for the ongoing monitoring and intervention, aiming to mitigate further deterioration and optimize recovery, ultimately enhancing the quality of life and long-term outcomes for STEMI patients.

2. LITERATURE REVIEW

2.1. Chapter overview

The prevailing paradigm in the management of STEMI predominantly relies upon the expeditious mechanical reperfusion of the occluded epicardial coronary artery, primarily executed via PCI. This interventionist approach has demonstrated considerable efficacy, with a success rate exceeding 95% in re-establishing patency within the epicardial coronary artery, thereby substantially diminishing mortality rates in STEMI cohorts [14]. Nonetheless, despite the angiographically ascertained restoration of unimpeded flow in the epicardial coronary artery, a significant proportion – approximately 50% – of patients continue to exhibit a phenomenon of incomplete microvascular perfusion in the distal segments of the coronary microvasculature. This phenomenon of suboptimal reperfusion is inextricably linked with escalated risks of morbidity and mortality [15].

Intriguingly, experimental investigations employing animal models have elucidated that the genesis of regions within the coronary microvasculature, characterized by diminished or absent perfusion, predominantly manifests during the reperfusion phase [16, 17]. This observation accentuates the paradoxical propensity of reperfusion to amplify myocardial damage. The initial correlation between structural manifestations of microvascular injury and corresponding regions within the intramural myocardium, exhibiting poor or null perfusion, was reported in the seminal year of 1974 [18]. The intervening years have witnessed a proliferation of documentation on the nuances of reperfusion injury. More contemporaneously, the discourse regarding the coronary microcirculation has evolved from a passive bystander to an active therapeutic target in the quest to ameliorate reperfusion injury.

The intricate pathophysiological mechanisms underpinning this process, however, remain a subject mired in scholarly debate [19]. Within the ambit of this comprehensive review, we endeavor to dissect and elucidate the prevailing understanding of CMD within the STEMI context. Primarily, our discourse will offer an integrative analysis of the pathophysiological mechanisms predisposing to coronary microvascular injury concomitant with the STEMI event. Furthermore, we will discuss the modalities used for diagnosis and quantification of CMD. Additionally, this review will delve into the critical biomarkers (including Trimethylamine N-oxide (TMAO)) associated with microvascular injury, examining their role and significance in CMD. Alongside this, we will review key clinical trials related to CMD, focusing on their findings and implications for clinical outcomes in STEMI.

2.2. Definitions

Within the scope of scholarly literature, a variety of terminologies have been employed to characterize the occurrence of reduced myocardial perfusion subsequent to reperfused STEMI. To facilitate clarity and understanding for the reader, we commence by presenting a concise exposition, replete with the relevant nomenclature and definitions, thereby elucidating this complex phenomenon.

2.2.1. No-reflow

As early as 1966, Krug and his colleagues identified perturbations in blood flow following the alleviation of coronary artery blockage in feline models [20]. However, this early finding did not specifically link these alterations to microvascular compromise. The concept of "no-reflow" was initially introduced in a rabbit model investigating cerebral ischemia [21]. Later, Kloner et al. explored the no-reflow phenomenon in a canine model of ACS, observing continuous inadequate or absent myocardial blood supply in vast areas of the reperfused cardiac muscle, despite clear epicardial coronary arteries, correlating this state with microvascular damage [18].

In the subsequent years, the term no-reflow continued to be prevalent, mainly stemming from animal experiments utilizing flow indicators like carbon black or microspheres, or vascular cell dyes such as Thioflavin S. The lack of these markers in certain areas of the heart muscle was interpreted as evidence of no-reflow zones following ischemia [22]. In human studies, the recognition of coronary no-reflow trailed its experimental discovery. Schofer and his team delivered scintigraphic evidence of no-reflow in a STEMI patient undergoing thrombolysis [23]. This observation was soon augmented by Bates et al., who presented angiographic proof of no-reflow, measuring coronary circulation using the opacity of angiographic contrast [24]. The key concepts of the no-reflow phenomenon are presented in Fig. 2.2.1.1.

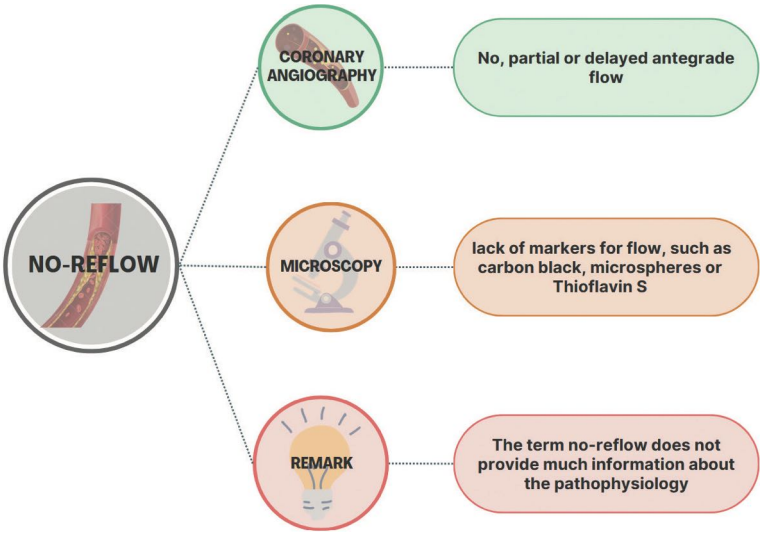

Fig. 2.2.1.1. *Key concepts in no-reflow phenomenon: diagnostic techniques and pathophysiological considerations*

With the introduction of primary PCI, the detection of no-reflow became more common via immediate angiographic analysis [25]. The absence of angiographic no-reflow was considered a benchmark for procedural success, reflecting its link with negative patient outcomes. However, the term no-reflow, although descriptive, provides limited understanding of its pathophysiological basis. It covers a range of clinical features, with microvascular obstruction, microvascular damage, intramyocardial hemorrhage, and CMD being the key elements. In modern clinical practice, angiographic no-reflow is noted in fewer than 5% of patients, a statistic that considerably underrepresents the true frequency, especially when compared with the incidence of myocardial perfusion impairments detected through Cardiovascular Magnetic Resonance (CMR) following STEMI [26].

2.2.2. Microvascular obstruction

The realization that angiographic no-reflow lacked the sensitivity to adequately detect microvascular perfusion deficits led to the incorporation of CMR for this evaluative purpose. Utilizing CMR, a distinct pattern emerged, characterized by a contrast-enhanced infarct region surrounding a core devoid of contrast uptake, a phenomenon subsequently termed microvascular obstruction (Fig. 2.2.2.1). This term was predicated on the assumption that microvascular obstruction was the principal mechanism inhibiting the penetration of contrast into the infarct core. The genesis of microvascular obstruction was hypothesized to involve a confluence of factors: distal embo-

lization, intraluminal obstruction from circulating blood cells, in situ formation of microvascular thrombi, and extravascular compression. However, clinical trials aimed at addressing these factors have not yielded positive outcomes, suggesting that the role of microvascular obstruction in the context of reperfusion injury might be more circumscribed than initially perceived [27, 28]. Additionally, CMR-defined microvascular obstruction has been observed to be reversible in some cases [29]. It has also become evident that CMR-defined microvascular obstruction frequently encapsulates a broader spectrum of microvascular injury, including complete microvascular destruction and intramyocardial hemorrhage [30, 31]. Consequently, the usage of the term microvascular obstruction should be confined to the histological verification of microvessel obstruction, rather than encompassing the entire clinical spectrum of failed primary reperfusion. The key concepts of microvascular obstruction are presented in Fig. 2.2.2.2.

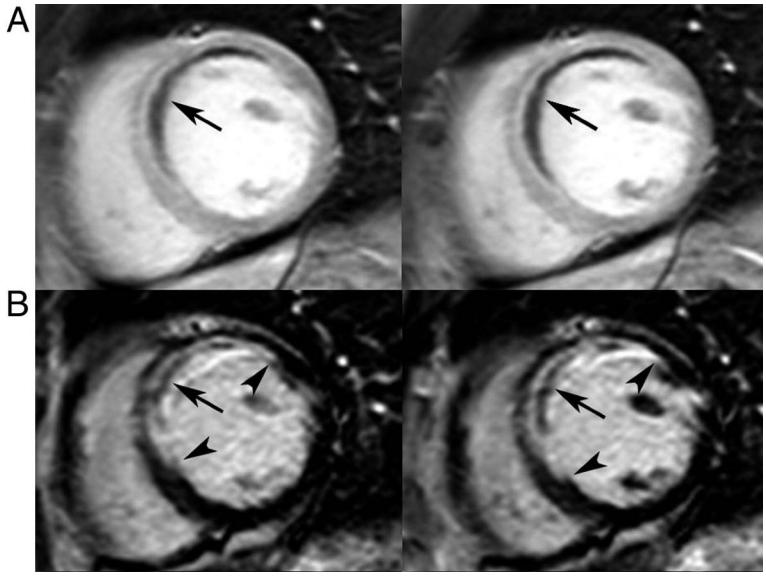

Fig. 2.2.2.1. *Identifying microvascular obstruction through cardiovascular magnetic resonance*

This figure describes two sets of short-axis images taken from cardiovascular magnetic resonance imaging using a 3-dimensional inversion recovery gradient-echo pulse sequence. The first image **(A)** is captured early (2 minutes after contrast injection) and shows a central area of reduced enhancement in the anteroseptal region, indicative of early microvascular obstruction (highlighted by arrows). The second image **(B)** is taken later (10 minutes after contrast injection) and displays hyperenhancement in the anteroseptal region, consistent with myocardial infarction (marked by arrowheads), along with a central zone of microvascular obstruction (shown by arrows). Notably, the area of late microvascular obstruction is smaller than that of the early obstruction, suggesting gradual penetration of the contrast agent over time.

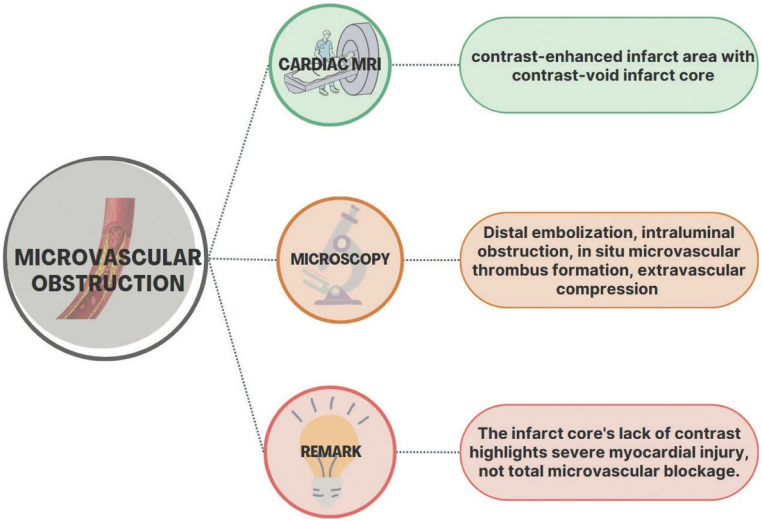

Fig. 2.2.2.2. *Key concepts in microvascular obstruction phenomenon: diagnostic techniques and pathophysiological considerations*

2.2.3. Intramyocardial hemorrhage

Intramyocardial hemorrhage manifests as an irrevocable pathological outcome of severe microvascular injury [32]. While certain instances of microvascular obstruction may exhibit resolution, such as the restoration of perfusion following the dissipation of edema, intramyocardial hemorrhage signifies a level of capillary destruction that is irremediable [29]. Experimental evidence indicates that reperfusion is a critical factor in the genesis of Intramyocardial hemorrhage, characterized by the disintegration of interendothelial cell connections and the subsequent perivascular seepage of red blood cells [33]. Additionally, a significant congruence has been observed between the dimensions and locations of CMR-defined microvascular obstruction and histologically confirmed Intramyocardial hemorrhage, further emphasizing the severity and irreversible nature of the damage wrought by intramyocardial hemorrhage in the myocardial tissue [31, 33]. The key concepts of the intramyocardial hemorrhage phenomenon are presented in Fig. 2.2.3.1.

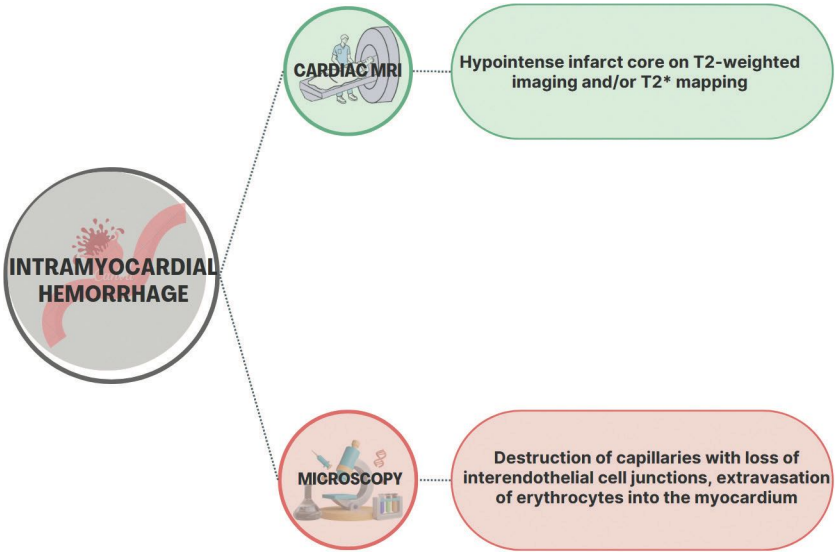

Fig. 2.2.3.1. *Key concepts in intramyocardial hemorrhage phenomenon: diagnostic techniques*

2.3. Coronary microvascular dysfunction in the context of ST-elevation myocardial infarction

The etiology of reperfusion injury is complex and multifaceted, encompassing a spectrum of factors such as compromised vasomotor functionality, microvascular obstruction, microvascular injury, intramyocardial hemorrhage, and inflammatory processes [27]. Consequently, the term CMD in the context of STEMI more aptly encapsulates the diverse pathophysiological facets contributing to myocardial reperfusion deficits, which arise from an amalgam of pathological mechanisms. It is noteworthy that the terminology of CMD is contemporarily employed in scenarios involving ischemia in the absence of obstructive Coronary Artery Disease (CAD).

2.3.1. Physiology and anatomy of coronary microcirculation

The coronary arterial network is intricately structured into three primary segments: expansive conductive arteries (with diameters exceeding 500 μm), intermediary prearterioles (ranging from 100 to 500 μm in diameter), and the finer arterioles (diameters less than 100 μm). The latter two categories collectively form the coronary microcirculation [34–40].

Coronary blood flow is propelled by the differential pressure existing between the aortic root and the capillary beds. Each segment within this tripartite system exerts distinct regulatory control over vascular tone, ultimately governed by the metabolic demands of the cardiac muscle.

The larger epicardial arteries and the proximal segments of prearterioles, accounting for a mere 10% of the total resistance in coronary vasculature, primarily function as conduits for blood delivery. Their vasomotor activity is largely dictated by flow-mediated dilation, a process dependent on the endothelial response.

In contrast, the distal prearterioles and arterioles, which are pivotal in the coronary microcirculation, play a significant role in regulating the total resting vascular resistance. The distal prearterioles are particularly sensitive to alterations in intravascular pressure, playing a central role in the autoregulation of coronary blood flow. This myogenic control mechanism involves the vascular smooth muscle cells' reaction to intraluminal pressure shifts, resulting in constriction or dilation as the pressure fluctuates.

Arterioles, meanwhile, are acutely attuned to variations in intramyocardial metabolite levels, primarily steering the metabolic regulation of coronary blood flow. Elevated metabolic activity induces vasodilation in these smaller arterioles, reducing pressure in the distal prearterioles, which in turn triggers myogenic dilation. This cascade effect enhances upstream flow, culminating in endothelium-dependent vasodilation.

At the terminal end of the coronary circulation lie the capillaries and venules. Though they contribute only about 10% to the overall coronary blood flow resistance, they function predominantly as capacitance vessels, harboring 90% of the myocardial blood volume. This zone is pivotal for the effective exchange between myocardial tissues and the blood within the capillaries, often described as the critical 'business end' of circulation, crucial for the delivery of oxygen and nutrients and the removal of metabolic by-products.

Dysfunctions or structural anomalies within the coronary microcirculation can disrupt the regulation of myocardial blood flow, thereby playing a contributory role in the development of myocardial ischemia.

2.3.2. Pathophysiological mechanisms of microvascular injury in ST-elevation myocardial infarction

The rapid restoration of full and lasting blood flow in the epicardial arteries is essential to save the ischemic myocardium from becoming infarcted. Nonetheless, the prompt reconstitution of coronary flow via the revascularization of the occluded infarct-related artery may paradoxically precipitate injury within the coronary microvascular network, and this intervention does not instantaneously halt the progression of cardiomyocyte demise within the myocardial region at risk. Amidst the phases of coronary occlusion and subsequent reperfusion, a spectrum of dynamic pathological transformations within both the microvascular and interstitial realms significantly exacerbates

the ongoing deterioration of cardiomyocytes in the subtended myocardial zone [41]. The functional and structural ramifications emanating from this procession of pathological alterations, which unfold both temporally and spatially across the successive segments of myocardial circulation, appear to critically influence the ultimate destiny of the affected myocardial territory (Table 2.3.2.1).

Table 2.3.2.1. *Myocardial circulation changes during occlusion and post-reperfusion*

Phase	Site				Total Coronary Resistance	Coronary Flow
	Epicardial Coronaries	**Arterioles**	**Capillaries**	**Cardiomyocytes and Interstitium**		
Early ischemia	Complete Occlusion	Adaptive Dilation Response		Cellular Dysfunction and Edematous State	Elevated (due to Macrocirculation)	No-flow
Prolonged ischemia	Persistent Occlusion	Paralysis (both ischemic insult and adaptive response)	Permeability Augmentation, Structural Disruption	Necrotic Transformation	Elevated (due to Macrocirculation)	No-flow
Initial phase of reper-fusion	Luminal Reopening	Paralysis	Occlusion from Intraluminal Plugs	Interstitial Fluid Accumulation	Low (due to microcirculation)	Overflow
Late phase of reper-fusion	Maintained Vascular Patency	Partial Restoration of Constrictor Tone	More plugged, leakier	Aggravated Edema, Intramyocardial Hemorrhage	High (due to microcirculation)	Normal, slow or “no-reflow”

The protracted duration of ischemia is acknowledged as the paramount determinant in dictating the severity of microvascular injury and its subsequent recuperation post-STEMI [42]. However, recent empirical evidence derived from rodent models of Acute Myocardial Infarction (AMI) suggests that ischemia, in isolation, precipitates only nominal morphological alterations within the coronary microcirculatory system, albeit with a concomitant augmentation in vascular permeability. Contrastingly, ischemia succeeded by reperfusion is implicated in the genesis of substantial microvascular trauma [33]. In this context, on a chronological spectrum commencing from the preocclusion phase, the intricate interplay among the dynamic processes unfolding during both coronary occlusion and subsequent reperfusion appears to be pivotal in determining the ultimate extent of microvascular

impairment and cardiomyocyte attrition within the microcirculatory domain subjugated by the occlusion over time (Table 2.3.2.1).

In this context, the adoption of the classification paradigm (Fig. 2.3.2.1) that was adopted by Sezer et al. to facilitate a deeper understanding of the discrete contributions of various elements to the pathology of CMD post-primary PCI, as well as foster a reevaluation of their potential interactions [27]. Post-reperfusion, the factors leading to microvascular damage within the myocardium supplied by the culprit artery are broadly classified into two main categories: intraluminal microvascular obstruction and extravascular compression of the microcirculation.

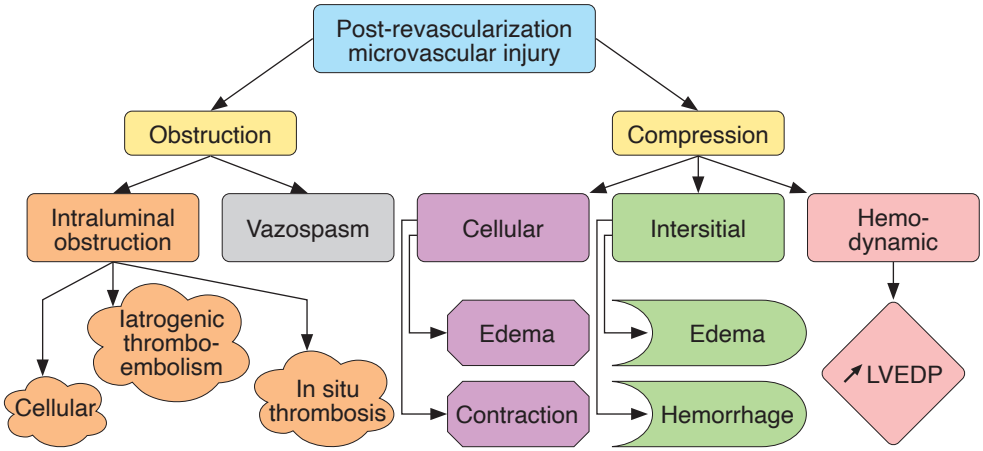

Fig. 2.3.2.1. *Pathophysiological mechanism of microvascular injury post revascularization LVEDP*

LVEDP – Left ventricular end-diastolic pressure.

Intraluminal obstruction primarily results from a series of pathologies including distal thromboembolization, the formation of thrombosis in situ, cellular obstruction within the vessels, and vasospasm. These conditions collectively contribute to blocking the blood flow within the microvascular lumen, impeding proper circulation.

On the other hand, the microcirculation can also be externally compressed, which is attributed to different pathological processes. Cellular edema, interstitial fluid accumulation, and intramyocardial hemorrhage can exert an outward pressure on the microvessels. Additionally, elevated LV end-diastolic pressure (LVEDP) can further exacerbate this external compression, leading to a significant impairment of the coronary microcirculation. This composite of internal obstruction and external pressure on the microvessels effectively

summarizes the intricate interplay of factors that contribute to microvascular injury after the reperfusion of blood flow to the myocardium.

2.3.3. Coronary microvascular obstruction

2.3.3.1. Coronary intraluminal obstruction

Within the context of reperfusion during STEMI, the etiology of coronary microvascular intraluminal obstruction predominantly arises from phenomena such as iatrogenic thromboembolism, occlusion by circulating cells, and in situ thrombosis. Intraluminal microvascular obstruction is identified as the primary pathological mechanism underpinning myocardial malperfusion after primary PCI. Pathologically, microvascular obstruction initially manifests in the infarct core and subsequently undergoes spatial and temporal expansion, correlating with the progressive myocardial deterioration following the revascularization of the culprit coronary artery. Notably, the obstruction zone expands for a duration of up to two days after restoration of epicardial coronary flow [43]. In the aftermath of an ischemic episode, it has been documented that the majority of the capillaries within the myocardial area at risk remain devoid of restored blood flow even after the reestablishment of epicardial patency [44]. In myocardium subjected to ischemic reperfusion, there is an initial hyperemic response in certain microvascular territories during the inaugural minutes of reperfusion [45]. This is followed by a rapid and progressive diminution in regional blood flow within the myocardium, culminating in a constant stable phase within the subsequent few hours after revascularization, which consequently results in an approximate tripling of the anatomical microvascular obstruction zone [16, 45]. This delayed, progressive decline in blood flow in initially adequately perfused myocardial areas is believed to result from the simultaneous activation of intraluminal obstructive and extravascular compressive pathologies, both of which are incited by the reperfusion process itself. Experimental and clinical investigations have consistently underscored a robust correlation between zones of microvascular obstruction and myocardial necrosis [42, 46]. Additionally, an experimental study involving female Fisher rats, designed to investigate the dynamics of coronary occlusion and reperfusion, has revealed that the phenomenon of microvascular obstruction can resolve itself approximately one month following the revascularization procedure [47].

2.3.3.1.1. Iatrogenic thromboembolization

Within the procedural milieu of interventional revascularization, it is postulated that atherothrombotic embolization, emanating from the culprit lesion and reported in approximately 13.4% of cases, stands as a predominant factor contributing to microvascular obstruction during the reperfusion of STEMI [48]. The mechanism underlying this phenomenon involves the distal dissemination of the thrombus, which not only exerts a physical blockage but also incites the activation of coagulative and inflammatory cascades within the distal microcirculatory network.

In previous literature, it has been observed that subjects exhibiting distal embolization shortly following reperfusion are predisposed to larger Myocardial Infarction (MI) sizes and more pronounced microvascular damage [49]. Conversely, a study employing advanced modalities to quantify embolized particles during the reperfusion of STEMI patients through interventional means, indicated that while distal embolization might transiently impede coronary flow, its impact on MI size and cardiac function may not be significantly pronounced [50]. In contrary, angiographic evidence of distal embolization during reperfusion of STEMI patients through interventional means, has been reported to contribute to myocardial injury and rates of heart failure hospitalizations; however, its impact on major cardiovascular outcomes appears to not be avoidable even when distal embolization protection devices are being utilized [51].

In the STEMI therapeutic landscape, utilizing aspiration catheter devices in the culprit arteries is postulated to substantially mitigate the risk of distal embolization, ostensibly leading to a marked decrement in the extent of microvascular obstruction and myocardial necrosis. Paradoxically, despite the achievement of comparatively lower rates of distal embolization with aspiration catheters versus balloon pre-dilatation followed by stenting, aspiration of thrombus mass does not appear to correspond with an enhancement in myocardial perfusion, a finding at odds with earlier meta-analytic observations [52, 53].

More critically, a preponderance of trials investigating the advantages of the utilization of aspiration catheters during primary PCI has not substantiated any diminution in MI size [54]. Similarly, thrombus removal, whether applied as a regular or selective intervention, has not demonstrated benefits in outcomes [55–57].

The medical community continues to debate the effectiveness of thrombus aspiration in treating epicardial thrombus during the initiation of reperfusion. Clinical trials and meta-analyses have produced conflicting results, highlighting the complexity of this issue. There are various approaches

to managing this condition, including standard primary PCI and adjunctive thrombectomy before stenting. However, there is still rigorous debate over these methods due to the different outcomes and experiences reported in clinical practice. A key point of contention is the role of iatrogenic embolization, originating from the culprit lesion, in worsening microvascular and myocardial damage during primary PCI. This topic remains highly debated due to its complexity and the varied perspectives within the field.

2.3.3.1.2. Cellular intraluminal obstruction

In the context of STEMI, after revascularization by interventional means, such as primary PCI, microvascular obstruction is exacerbated by phenomena such as white blood cell and thrombocyte adhesion and erythrocyte clustering [58, 59]. Following the re-establishment of flow in the culprit coronary artery, neutrophils contribute to the impairment of microvascular flow by adhering to the endothelium alongside thrombocytes and releasing inflammatory cytokines [60, 61]. In non-perfused zones, capillary segments are often blocked due to extensive white blood cell entrapment, leading to upstream congestion of red cells and rouleaux formation, which can potentially cause mechanical obstruction [44].

The deformability of circulating cells and the smoothness of the endothelial surface layer are crucial for maintaining blood flow through coronary microvascular segments, particularly when capillary diameters are smaller than the diameters of red blood cells. However, microvascular resistance increases due to the effects of ischemia-reperfusion, which damages the endothelial glycocalyx layer. This damage leads to reduced endothelial permeability and alters the properties of the vascular surface, increasing the likelihood of capillary blockage by cellular plugging [62].

Despite these potential ways that circulatory cells obstruct microvascular flow, clinical trials in patients with acute coronary syndrome have not demonstrated beneficial results from treatments like complement inhibition, antagonism of white blood cell integrin receptors, or enhanced local thrombocyte inhibition [63–65]. This suggests that circulating cells have a limited impact on acute CMD following primary PCI, although they may contribute to intraluminal obstruction after reperfusion. White blood cell invasion into the microvasculature, on the other hand, seems to play a more significant role in myocardial remodelling and infarct healing, rather than in defining CMD zone or size of the culprit vessel. Therefore, the clinical efficacy of targeting cellular interactions and endothelial changes that contribute to microvascular obstruction in STEMI patients after primary PCI continues to be debated within the medical community. This is due to the complex interplay of white

blood cells, thrombocytes, and endothelial factors in coronary microvascular dysfunction. Understanding these dynamics is crucial to unraveling the intricacies of CMD and its contributing factors.

2.3.3.1.3. In situ thrombosis

In STEMI, particularly within the culprit coronary artery, the microcirculation distal to the occlusion site becomes highly procoagulant, favoring the development of in situ microvascular thrombosis. This environment leads to hypoxia, which in turn triggers coagulative processes. These processes activate hemostatic responses in the compromised endothelium, potentially resulting in microvascular thrombosis and in situ fibrin formation at sites of endothelial injury [66]. The expression of tissue factor by predominantly hypoxic and damaged endothelial cells, in conjunction with vascular stasis, serves as a potent catalyst for the activation of the coagulation cascade and subsequent de novo fibrin generation at the microvascular echelon (Fig. 2.3.3.1.3.1).

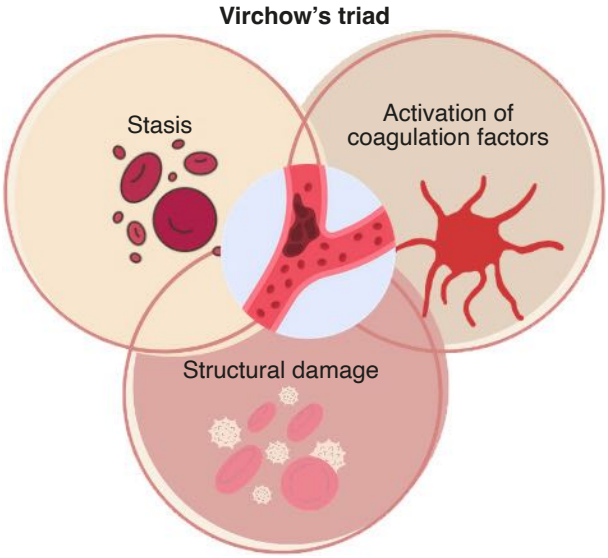

Fig. 2.3.3.1.3.1. *Pathogenesis of microvascular thrombosis in ST-elevation myocardial infarction – the role of virchow's triad*

This illustration depicts the intricate and multifaceted pathophysiological process initiated by epicardial occlusion in ST-elevation Myocardial Infarction. It intricately outlines the sequence of events starting with hypoxic injury to the endothelium, leading to stasis and activation of coagulation and tissue factors. This sequence potently triggers the components of Virchow's Triad, setting the stage for the progression to in situ microvascular fibrin formation, thereby illustrating the intricate dynamics of a self-perpetuating thrombotic cycle.

Moreover, the reperfusion phase subsequent to ischemic insult is characterized by a marked dysfunction in endogenous fibrinolysis, as delineated by the significantly diminished release of tissue plasminogen activator from the endothelium, which could contribute to the persistence of fibrin deposits within the coronary microvasculature [67]. The entrenched fibrin, which tenaciously adheres to the vascular wall through interactions with intercellular cadherin receptors, poses a formidable challenge to elimination by the mere reestablishment of blood flow to the infarcted zone [68].

Exacerbating this condition, all mobile hematologic constituents intrinsically exhibit a propensity for adherence to the fibrin matrix that augments within the microcirculatory channels, a process that occurs passively and is further facilitated by direct interaction with distinct fibrin receptors located on their cellular membranes [69]. Consequently, even minimal intraluminal fibrin presence can act as a viscous snare for formed blood elements introduced during reperfusion, thereby potentially impeding the restorative process once the obstructed epicardial artery is recanalized. Despite the paucity of focus on in situ fibrin deposition within the cardiac microvasculature following ischemia-reperfusion events, the existence of in situ fibrin depositions in the microcirculation has been unequivocally evidenced in ischemia-reperfusion models pertaining to cerebral, intestinal, and renal domains [70–73].

Under circumstances characterized by reduced circulatory dynamics, which give rise to diminished shear stress, fibrinogen significantly augments resistance within the microvascular flow. It accomplishes this through its role in promoting aggregation of erythrocytes, fostering adherence between leukocytes and the endothelial lining, and enhancing post-ischemic leukocyte-thrombocyte conjugation [74–76].

From a therapeutic standpoint, the successful removal of fibrin deposits from the microvascular network may serve to significantly enhance perfusion at this critical juncture. Evidence supporting this therapeutic strategy is found in the administration of adjunctive, low-dose intracoronary fibrinolytic medications like streptokinase and urokinase during primary PCI in STEMI patients, which has been associated with a notable improvement in microvascular perfusion, a reduction in the size of myocardial infarctions, the preservation of LV function, and overall enhancement of patient outcomes [77–79]. The auspicious results gleaned from these interventions have provided impetus for further investigation into the effects of fibrin clearance from the microvasculature using diverse fibrinolytic agents, as evidenced by large-scale clinical trials such as the Trial of Low-Dose Adjunctive Alteplase During Primary PCI (T-TIME) [80, 81].

Within this context, the in situ generation of fibrin in the distal coronary microcirculation, leading to thrombotic microvascular obstruction at the local

level, may be pivotal in the etiology of microvascular dysfunction precipitated by ischemia-reperfusion events. It is clear, however, that extensive clinical trials, exemplified by the T-TIME trial, are crucial to obtaining conclusive evidence regarding the phenomenon of in situ microvascular thrombosis.

2.3.3.2. Vasospasm

In instances of STEMI and presence of a complete occlusion in the culprit coronary artery, the microcirculatory system distal of the blockage is typically found in a state of pronounced vasodilation, this being a result of the overwhelmed autoregulatory capabilities of the arteriolar sphincters. Intriguingly, even in the face of severe myocardial ischemia, which is acknowledged as the most intense vasodilatory stimulus known, there often remains a pharmacologically accessible reserve for vasodilation [82]. Additionally, during STEMI the microvascular structures exhibit an increased responsiveness to α-adrenergic stimuli known to induce coronary constriction. This phenomenon, combined with the release of soluble vasoconstrictors like serotonin and thromboxane A2 from fragmented plaques and platelet clusters into the microcirculation, contributes to the development of a vasospastic state during STEMI [83].

Predicated on such premises, the administration of vasodilators into the culprit artery, particularly adenosine (A2 receptor activator leading to vasodilation of microvasculature) have been rigorously evaluated in numerous clinical trials focusing on the reduction of CMD during STEMI [84]. While initial studies yielded promising results, more recent clinical research has revealed that the targeted use of adenosine and sodium nitroprusside for microvascular bed dilation was ineffective in reducing CMD in STEMI patients [85]. Significantly, high doses of adenosine were linked with an increase in necrotic zone and a decrease in LV ejection fraction (LVEF) compared to the control group.

Crucially, the control of vasomotor function in regulating pressure in the microvasculature is vital to prevent an uncontrolled and rapid increase in capillary pressure during recanalization of STEMI patients. This serves as a protective mechanism against myocardial edema and intramyocardial hemorrhage. Thus, in light of adverse outcomes from recent studies that employ potent vasodilators along with STEMI, it is apparent that preserving vasomotor function at the arteriolar level is essential.

2.3.4. External compression

The process of extravascular compression within the microcirculation involves an external narrowing of capillary pathways, primarily instigated by both interstitial and cellular forms of myocardial edema, in conjunction with intramyocardial hemorrhage, which materialize in the heart muscle as a result of primary PCI of the culprit vessel. This external pressure plays a significant part in aggravating myocardial malperfusion after primary PCI, chiefly by intensifying the overall resistance in the microvascular framework.

Under normal cardiac conditions, the capillaries in the coronary system typically do not impede myocardial blood circulation significantly. Nonetheless, this vascular network is acutely susceptible to external constriction caused by adjacent edema and intramyocardial hemorrhage, due to its inherently limited capacity to withstand radial pressure. Such constriction results in a narrowing of the capillary diameter, with each incremental reduction leading to a disproportionately large increase in resistance, which could significantly reduce myocardial blood flow in the microvasculature. Theoretically, the calculation of extravascular pressure involves assessing the additional volume introduced into the cardiac tissue relative to the tissue's ability to accommodate this volume, known as myocardial compliance. Situations involving intramyocardial hemorrhage and edema lead to an expansion in the volume of the interstitial space and concurrently reduce myocardial compliance, thereby resulting in a significant rise in extravascular pressure, which in turn leads to pronounced external compression of the microvasculature [86].

During instances of STEMI, the extended time of ischemia trigger a hypoxia-induced disruption in endothelial integrity, leading to impaired functionality of the microvascular barrier and subsequent microvascular leakage [87]. This leakage serves as the fundamental anatomical basis for the development of myocardial edema and hemorrhage following primary PCI. CMR imaging in clinical settings has linked the deterioration of microvascular barrier integrity in cases of STEMI with the emergence of edema and intramyocardial hemorrhage [88]. Therefore, both edema and intramyocardial hemorrhage, as the primary factors driving extravascular compression, are regarded as consequences of microvascular leakage.

In advanced studies utilizing murine models of ischemia/reperfusion, the application of late gadolinium enhancement in CMR imaging, acknowledged as a marker for extravascular volume, alongside detailed histological examinations of microvascular leakage, both demonstrated a robust correlation [89]. This observation underscores a compromise in the microvascular barrier integrity reperfusion, culminating in microvascular leakage, during STEMI

acute stage. Importantly, within the ischemic zone, the region impacted by microvascular leakage exceeded both the infarct size and the microvascular obstruction zone in the initial phase of STEMI. During the protracted phase, a discernible link was noted between the extent of microvascular leakage and a reduction in the LVEF. Collectively, these insights portray MVL as a primary pathological manifestation of recanalized culprit vessel in STEMI patients.

2.3.4.1. Edema

In the early phases of STEMI, there is a disruption in the energy-dependent sodium-potassium pump, leading to the onset of myocardial edema. As the ischemia becomes more severe, there is accompanying harm to endothelial cells, including their protective glycocalyx layer and the walls of the capillaries, resulting in increased microvascular permeability and capillary leakage. Simultaneously, during occurrences of coronary occlusion, a significant rise in myocardial demand (an adaptive widening of blood vessels) combined with the impact of ischemic harm (reduced muscle contraction ability) is believed to impair the arteriolar sphincters ability to constrict vessels. This leaves the microvascular segments downstream vulnerable, without the protection of the arterioles that usually regulate pressure, especially during sudden reperfusion. Upon reperfusion during primary PCI, before the restoration of coronary self-regulation, this exposed and defenseless microcirculation faces a surge in pressure due to a rapid increase in capillary hydrostatic pressure, causing interstitial myocardial edema in the early reperfusion hyperemia phase [90].

Remarkably, myocardial edema worsens when blood flow is restored to the ischemic microvascular region. Interestingly, without reperfusion, the initial wave of edema is almost completely prevented, highlighting a direct link between revascularization via primary PCI and the development of myocardial edema. Challenging conventional views, recent studies suggest that myocardial edema is not a stationary event but follows a two-phase pattern [91]. The first spike in edema related to recanalization is seen quickly at two hours after reperfusion, while a later edema is thought to stem from the healing process in the following week after reperfusion [91]. However, a study conducted in the United Kingdom found that the severity of edema follows this two-phase timeline only in patients who also suffer from intramyocardial hemorrhage. In the study, patients without intramyocardial hemorrhage exhibited a steady, singular progression of myocardial edema [29]. Another study, which was a retrospective synthesis of data from three separate studies, refuted the hypothesis of a two-phase pattern of edema

following the revascularization of STEMI patients. However, the validity of this conclusion is limited by the fact that most subjects in these studies underwent only a single CMR scan at varying times, lacking consistent, sequential evaluations [92]. The most recent clinical and experimental research, specifically designed to investigate the edematous response of the heart muscle to ACS, has confirmed that the post-heart attack edema reaction is indeed dynamic and follows the two-phase pattern previously described, regardless of the presence or severity of intramyocardial hemorrhage [93].

Initially, myocardial edema exerts an external compressive force on the capillary bed, thereby increasing the hydrostatic pressure in the surrounding tissue space. Subsequently, the heightened stiffness and diminished elasticity of the edematous cardiac muscle tissue lead to increased LVEDP, which further imposes external pressure on the microcirculation. These processes collectively elevate the resistance to blood flow in the myocardium, potentially exacerbating the severity of muscle death within the infarct zone [86].

2.3.4.2. Intramyocardial hemorrhage

Intramyocardial hemorrhage is recognized as a critical marker of severe microvascular damage, occurring in about half of patients following primary PCI for STEMI [29]. CMR imaging has demonstrated that intramyocardial hemorrhage generally worsens, reaching its peak approximately two days after primary PCI in patients with STEMI [94]. There is a notable association between myocardial hemorrhage and larger necrotic zone, detrimental changes in heart structure, reduction in LVEF, arrhythmias, and generally poorer clinical outcomes [29, 31, 94–96]. A multi-institutional observational study identified that infarcts occurring in the anterior region and the use of periprocedural glycoprotein IIb/IIIa inhibitors are key indicators of myocardial hemorrhage following primary PCI [97].

The loss of endothelial integrity caused by low oxygen levels during extended culprit artery occlusion results in fragile capillary walls [66]. Prior to reperfusion, both the adaptive response to widen blood vessels and the ischemic effects on arteriolar sphincters leave the distal microcirculation exposed to the sudden spike in hydrostatic pressure that comes with recanalization of culprit vessel. In such cases, rapid blood flow, as achieved through effective primary PCI, can lead to a trauma-like impact on the already compromised, permeable capillaries, causing red blood cells to leak from the microvascular network into the surrounding tissue, thus resulting in myocardial hemorrhage. Conversely, blockages that do not undergo primary PCI lead to cell edema but not hemorrhage [98]. Intramyocardial hemorrhage was significantly less common in patients where primary PCI was not accomplished

and was rare in patients with untreated ACS [99, 100]. In the initial phase, the aggregation of red blood cells in the interstitial space creates an external compressive mass on the capillaries, while in the later stages, it triggers macrophage infiltration, production of reactive oxygen species, inflammation, and fibrosis [101]. Therefore, intramyocardial hemorrhage is seen as a more severe form of myocardial edema and represents the most extreme case of microvascular dysfunction.

Imaging studies have consistently found that nearly all patients with intramyocardial hemorrhage show signs of microvascular obstruction on CMR [31]. Additionally, recent animal studies have shown that the areas affected by intramyocardial hemorrhage and microvascular obstruction during STEMI as identified in CMR closely correspond to areas of intramyocardial hemorrhage confirmed through histopathology [31]. This connection between intramyocardial hemorrhage and severe microvascular obstruction suggests that hemorrhage primarily occurs in areas with substantial microvascular obstruction. Moreover, the IMR measured right after primary PCI was notably higher in STEMI patients with intramyocardial hemorrhage compared to those without [102]. A high microvascular resistance was recently identified as an independent factor predicting intramyocardial hemorrhage in patients undergoing primary PCI [103]. Once established, intramyocardial hemorrhage severely worsens microvascular damage in the infarct area by creating an external compressive force on the microvascular bed.

2.3.4.3. Increased left ventricular end diastolic pressure

The complex interaction between vascular and heart muscle compartments makes the vessels within the myocardium highly responsive to hemodynamic changes in the surrounding cardiac tissue and the LV chamber. In cases of STEMI, an increase in LVEDP arises due to a sudden decrease in cardiac output, coupled with increased stiffness and reduced flexibility of the cardiac muscle, a result of edema and intramyocardial hemorrhage. This leads to a diminished capacity of the intramyocardial vessels, negatively affecting blood flow during the later part of the diastole. The heightened pressures within the heart chamber, which are partially transmitted, play a role in externally compressing the coronary microvasculature, particularly in the subendocardial areas, which are more susceptible to increases in LV filling pressure. Consistent with this, studies in patients with STEMI have shown a relationship between LVEDP and zero flow pressure, a measure largely indicative of the external force applied to the coronary microvasculature [104].

Thus, in STEMI scenarios, diastolic LV dysfunction, leading to increased LV filling pressure, may further restrict the microvascular space.

However, LV filling pressure isn't the only factor influencing myocardial interstitial pressure. In the case of post-primary PCI STEMI patients, the formation of intramyocardial edema and hemorrhage, resulting from significant microvascular damage in the affected cardiac muscle, can notably raise interstitial pressure, especially in a cardiac muscle with limited elasticity. Additionally, this extra volume added to an already rigid cardiac chamber may cause interstitial pressure to exceed diastolic intraventricular pressure levels.

2.3.5. Post-reperfusion microvascular injury in acute myocardial infarction

While the advent of successful primary PCI has markedly altered the trajectory of STEMI management, it remains insufficient in halting the progression of cardiomyocyte loss, particularly in the presence of severe microvascular damage. This review examined the pathophysiological mechanisms of CMD during STEMI, focusing on the potential impact of both intra- and extravascular elements on microvascular integrity and, consequently, the survival of cardiomyocytes in ischemic regions post-epicardial reperfusion, through an integrated and comprehensive analysis. The complex interplay of intravascular obstructions and extravascular compressive forces is fundamental to the development of microvascular injury post-primary PCI. Following the blockage of an epicardial artery and subsequent reperfusion, a complex, multifactorial cascade of interrelated pathologies leads to the progressive deterioration of the microvasculature and subsequent cardiomyocyte attrition in the affected zone (Fig. 2.3.5.1). Consequently, this progressive damage to the microvascular structure and myocardial tissue following reperfusion might be mitigated through innovative therapeutic approaches that address mechanisms linked to both intraluminal obstruction (such as localized pharmacological interventions for microvascular thrombolysis) and extravascular compression of the microcirculation (such as controlled-pressure, gradual reperfusion techniques).

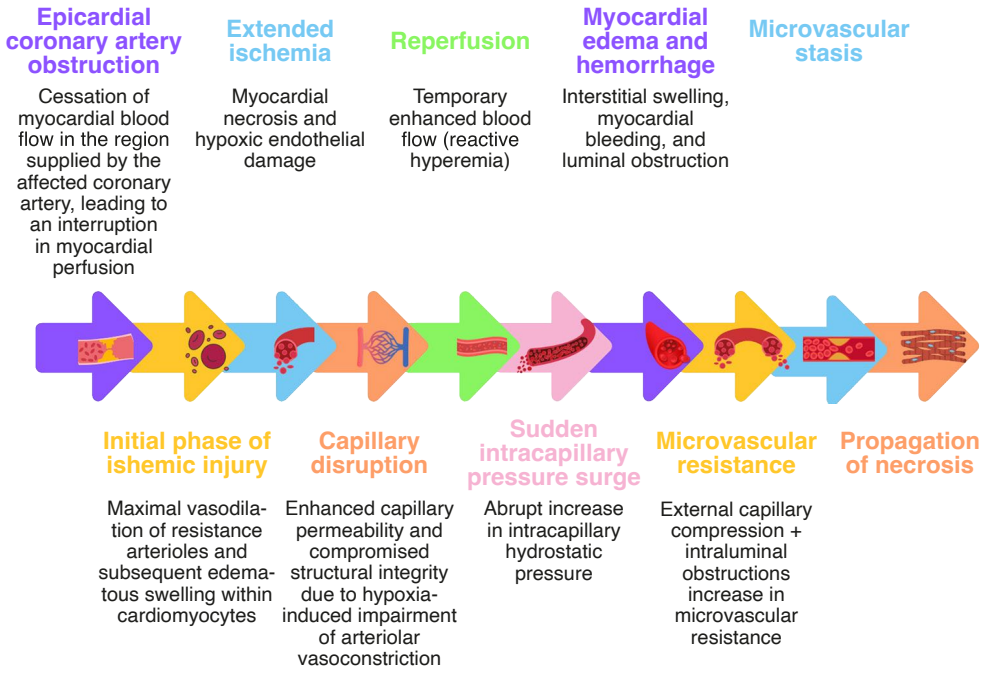

Fig. 2.3.5.1. *Key phases of ischemic and reperfusion-induced myocardial damage from a hemodynamic perspective*

2.4. Assessment of CMD

2.4.1. Assessing coronary microvascular dysfunction noninvasively

The noninvasive assessment of CMD focuses on examining coronary vasomotor function, which includes evaluating both regional and overall myocardial blood circulation at rest and during stress, assessing microvascular resistance, and measuring CFR. CFR, defined as the ratio of myocardial blood flow during hyperemia to its flow at rest, acts as a comprehensive indicator of coronary vasomotor impairment. It encompasses the combined hemodynamic effects of localized, widespread, and small-vessel disorders on the blood supply to myocardial tissue. In clinical practice, CMD is recognized by a reduction in CFR, particularly in the absence of significant epicardial CAD, suggesting impaired downstream vasomotor control.

Delving deeper into this field, it becomes apparent that some patients may have both localized obstructive CAD and CMD simultaneously, while others may show signs of CMD without any noticeable atherosclerosis. Importantly, a considerable number of individuals are found to have CMD along with widespread, but not obstructive, CAD. Although measuring localized myocardial ischemia and regional CFR is crucial in assessing focally

obstructive CAD, this part of the review mainly focuses on the use of overall measurements of myocardial blood flow and CFR. These comprehensive evaluations are essential for both diagnosis and prognosis of CMD, especially in assessing the overall condition of the LV system.

2.4.1.1. Positron emission tomography

Positron Emission Tomography (PET) is recognized as the most thoroughly validated and accurate noninvasive technique for quantitatively evaluating coronary vasomotor function. Recent technological advancements have allowed for the incorporation of these assessments into routine PET myocardial perfusion stress testing procedures [105]. This imaging method employs a two-phase protocol, consisting of a resting phase and a stress test for myocardial perfusion, each following the injection of a specific blood flow tracer [82]. Rubidium and 13N-ammonia, both approved by the U.S. Food and Drug Administration for this purpose). The subsequent analysis of the gathered rest and stress images enables the precise measurement of both localized and total myocardial blood flow (measured in ml/min/g of heart muscle tissue) and facilitates the calculation of CFR, which is determined as the ratio of myocardial blood flow during stress compared to the resting state.

Recent studies confirm that a significant number of individuals with confirmed or suspected CAD exhibit coronary vascular dysfunction, as indicated by reduced CFR [106]. This impairment aggravates the severity of potential myocardial ischemia (beyond the effects of blockages in the epicardial coronary arteries) and plays a role in asymptomatic heart muscle damage [107]. Additionally, a decreased CFR as detected by PET is a strong indicator of MACE, including death due to heart-related causes [108–110]. The precision of PET in noninvasively measuring myocardial blood flow and CFR has been extensively validated through both animal experiments and human clinical studies, and the consistency of this method has been well-established [105].

2.4.1.2. Cardiovascular magnetic resonance

CMR presents an alternative technique for measuring myocardial perfusion, using methods similar to those in PET [105]. Nonetheless, CMR's post-processing is considerably complex and time-consuming. Like PET, CMR adopts a two-phase imaging strategy that includes a resting phase and a vasodilator-stress first-pass myocardial perfusion scan, each following the injection of a gadolinium-based contrast medium [105]. Analyzing these resting and stress images allows for the assessment of both localized and overall myocardial perfusion, using either semi-quantitative methods (like the

myocardial perfusion reserve index) or fully quantitative models (such as CFR) (Fig. 2.2.2.1). Recently, a new T1 mapping-based, gadolinium-free stress CMR approach has been introduced, providing diagnostic capabilities for myocardial ischemia, regardless of the presence of obstructive CAD [111].

CMR has multiple benefits, including its superior spatial resolution that facilitates detailed assessment of myocardial blood flow across heart muscle layers, and its lack of ionizing radiation exposure. It also enables a thorough analysis of cardiovascular anatomy and function. The significance of a diminished myocardial perfusion reserve index in evaluating CMD has been shown, with potential prognostic value, although research in this field is still in development and relatively limited [112].

2.4.1.3. Doppler echocardiography

Doppler echocardiography, especially when applied to the left anterior descending coronary artery, serves as another method for assessing coronary blood flow velocity, both under normal conditions and during vasodilator stress induced pharmacologically (Fig. 2.4.1.3.1). Utilizing pulsed-wave Doppler techniques, precise measurements of coronary flow velocities are obtained, focusing on the diastolic peak velocities in both resting and peak hyperemic conditions. The coronary flow velocity reserve is computed as the ratio of hyperemic to resting coronary flow velocity. This technique is recognized for its cost-efficiency, the lack of ionizing radiation, and its potential for broad application. However, it's crucial to acknowledge that this method heavily relies on the expertise and proficiency of the practitioner. Furthermore, it requires effective echocardiographic imaging of the proximal coronary arteries, which can be challenging, particularly in individuals with obesity. A growing body of research indicates that a reduced coronary flow velocity reserve index plays a critical role in detecting CMD and provides important prognostic information [113–115].

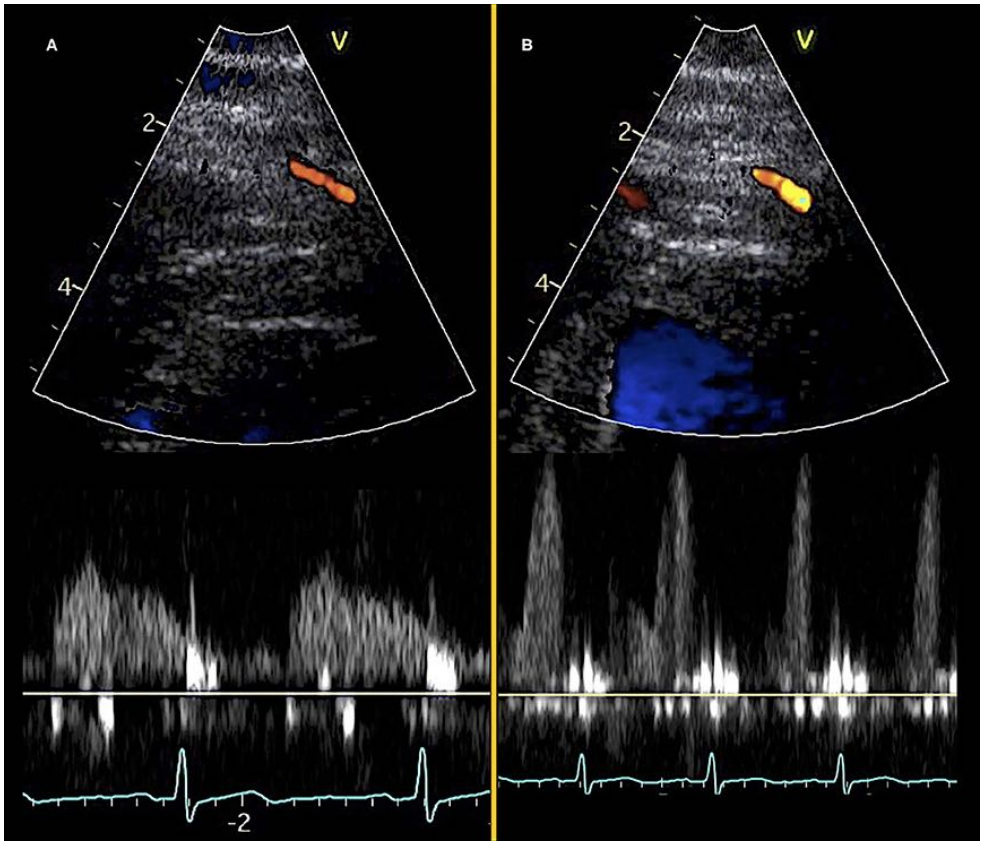

Fig. 2.4.1.3.1. *Identifying coronary microvascular dysfunction via doppler echocardiography shows transthoracic doppler echocardiography of the mid-distal left anterior descending artery*

Top: color doppler images. Bottom: diastolic flow velocity curves. **(A)** Resting state, **(B)** Adenosine stress.

2.4.1.4. Dynamic myocardial perfusion computed tomography

Dynamic myocardial perfusion Computed Tomography (CT) offers an alternative method for estimating myocardial blood flow, using techniques similar to those in CMR perfusion imaging. This method involves conducting dynamic CT scans after administering an iodinated contrast medium, using prospective electrocardiographic synchronization to capture the initial passage of the contrast through the heart [105]. The acquired dynamic imaging data are then used to calculate myocardial blood flow estimates, utilizing methods originally developed for CMR. Key advantages of this approach include CT's exceptional spatial resolution, along with the ability to perform detailed anatomical and functional assessments of both the myocardial tissue and

coronary arteries in a single examination. However, it's important to consider the trade-off of increased radiation exposure for the patient with this method.

2.4.2. Assessing CMD invasively

2.4.2.1. Angiography

Coronary angiography serves as a foundational technique for appraising the state of coronary microcirculation, primarily through the direct observation of contrast dye dynamics within the infarct-related artery. The flow velocity of this contrast medium offers a readily accessible and semi-quantitative approximation of CMD, which generally shows a congruent relationship with the presence and severity of CMD as determined by CMR, as well as with prognostic outcomes. However, it is widely acknowledged that such anatomical evaluations do not fully encapsulate the complexities of the coronary microvascular bed under the domain of the culprit artery. Thus, alternative methodologies that more accurately gauge coronary physiology are often preferred. Despite this, angiographic techniques for CMD detection retain clinical utility as expedient estimations during interventional procedures and have laid the groundwork for the evolution of more sophisticated diagnostic tools.

2.4.2.2. TIMI flow grade

The Thrombolysis In Myocardial Infarction (TIMI) Flow Grade (TFG) constitutes a visual assessment scale used in angiography to evaluate anterograde flow through an epicardial vessel, assigning a score from 0 (denoting no antegrade flow past the lesion, indicative of an occluded vessel) to 3 (representing normal anterograde flow) (Table 2.4.2.2.1, Fig. 2.4.2.2.1) [116]. In the Primary Angioplasty in Myocardial Infarction (PAMI) trial, TFG 3 was redefined to encompass complete opacification of the epicardial vessel within three cardiac cycles [117]. While microvascular obstruction, an acute form of CMD, may be inferred in cases of a TFG less than 3 with no significant epicardial stenosis after undergoing PCI, this assessment remains a semi-quantitative measure and is subject to considerable interobserver variability. Notably, even reperfused culprit arteries with TFG 3 have been shown to exhibit CMD in a substantial percentage of cases as identified by CMR [118, 119]. Nonetheless, TFG remains an effective tool for prognosticating MACE in STEMI patients with reperfused culprit arteries [120].

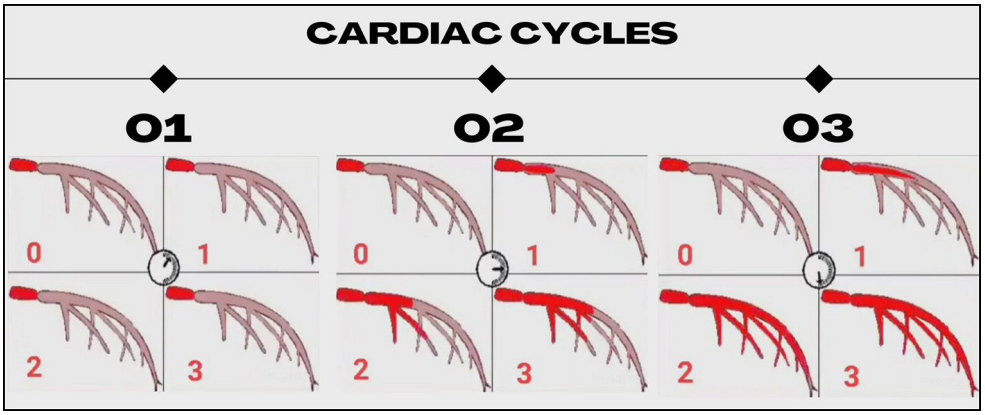

Fig. 2.4.2.2.1. *Visualization of TIMI flow grades across three consecutive cardiac cycles*

Each panel shows the progression of blood flow through a coronary artery, graded from 0 (no perfusion) to 3 (full perfusion), demonstrating the TIMI flow grades during different phases of the cardiac cycle.

Table 2.4.2.2.1. *Evaluation criteria for thrombolysis in myocardial infarction grade flow: acquisition process and grading scale*

	Acquisition	Scale
TIMI Grade Flow	Begin at the frame when contrast touches both side of the ostium and travels distally with > 70% vessel opacification	0: No anterograde flow
		1: Anterograde flow with no opacification of capillary bed
	Visual assessment of anterograde flow and opacification of capillary bed	2: Anterograde flow with partial opacification of capillary bed
		3: Anterograde flow with complete opacification of capillary bed

TIMI – Thrombolysis In Myocardial Infarction.

2.4.2.3. Corrected TIMI frame count

The corrected TIMI frame count (cTFC) was developed to enhance objectivity and reduce variability in quantifying myocardial perfusion (Table 2.4.2.3.1). It involves counting the number of cine frames required for contrast to traverse from a coronary ostium to a predetermined distal landmark [121]. The application of cTFC has been instrumental in diminishing both inter- and intraobserver variability, with sources of variance being restricted to factors such as nitroglycerin usage, patient-specific attributes (gender, weight, blood pressure), and the rate of contrast injection [122]. Critically, cTFC shows correlation with, and can facilitate the calculation of CFR and average peak velocity, both serving as proxies for microvascular resistance [122, 123]. While direct comparative studies between cTFC and

CMD as determined by CMR in STEMI patients are yet to be conducted, a higher cTFC has been correlated with increased mortality, even in cases exhibiting TFG 3 [124]. For a detailed overview of the evaluation criteria for TIMI grade flow and acquisition Process refer to Table 2.4.2.3.1.

Table 2.4.2.3.1. *Evaluation criteria for corrected thrombolysis in myocardial infarction grade flow: acquisition process and grading scale*

	Acquisition	Scale
Corrected TIMI Frame Count	Begin at the frame when contrast touch both side of the ostium and travels distally with > 70% vessel opacification	Frame counts above a range of 21 +/–3 indicate hypoperfusion. *Note: the frame counts for the LAD must be divided by 1.7 to correct for its longer course
	Count the number of frames until each standard landmark is reach below: – LAD: opacification of distal bifurcation of the apical segment (Whale tail branch) – LCX: opacification of most distal branch of the obtuse marginal artery – RCA: opacification of the first branchof the postero-lateral artery	
	The standard frame acquisition rate is 30 fps. If a lower rate is used (ie. 15 fps), the multiple to equal 30 (ie. 2) must be multiplied by the cTFC for the artery	

TIMI – thrombolysis in myocardial infarction; LAD – left anterior descending artery; LCX – left circumflex artery; RCA – right coronary artery.

2.4.2.4. Myocardial blush grade and TIMI myocardial perfusion grade

While TFG and cTFC primarily assess epicardial patency and flow, there is a recognized need for metrics that directly evaluate microcirculation and myocardial perfusion. This necessity led to the development of additional semi-quantitative measures, such as the Myocardial Blush Grade (MBG) and the TIMI Myocardial Perfusion Grade (TMPG).

MBG is a scoring system designed to quantify the extent of contrast density within the myocardium, colloquially referred to as ‘blush’. It ranges from 0, indicating no ‘blush’ of the culprit coronary artery microcirculation, to 3, denoting normal density, similar to that observed in non-culprit territories [125].

On the other hand, the TMPG is a mechanism to evaluate the clearance of the contrast medium from the microcirculation. It is graded on a scale from 0 to 3, where 0 signifies an absence of ‘blush’ and 3 indicates a sustained, mild to moderate ‘blush’ across three cardiac cycles, akin to that observed in non-culprit coronary arteries [126].

For accurate assessment, it is imperative to utilize specific imaging angles tailored to the involved coronary artery. This approach minimizes the impact of overlapping capillary beds on the perceived density and clearance duration of the contrast agent (Table 2.4.2.4.1).

Table 2.4.2.4.1. *Evaluation criteria for myocardial blush grade and thrombolysis in myocardial infarction myocardial perfusion grade: acquisition process and grading scale*

<table>
<tr><th></th><th>Acquisition</th><th colspan="2">Scale</th></tr>
<tr><td rowspan="4">Myocardial Blush Grade
TIMI Myocardial Perfusion Grade</td><td rowspan="2">Acquisition rate set to 30 fps</td><td colspan="2">Graded by comparing to a non- culprit coronary artery</td></tr>
<tr><td>MBG</td><td>TMPG</td></tr>
<tr><td>Prolonged cine-acquisition to ensure contrast is visualized entering and leaving the microcirculation</td><td rowspan="2">0: No myocardial contrast density or blush
1: Minimal blush
2: Moderate blush
3: Normal blush</td><td rowspan="2">0: No or minimal blush
1: Blush persists for –30 seconds
2: Blush strongly persists for over 3 cardiac cycles
3: Blush mildly/moderately persists for over 3 cardiac cycles</td></tr>
<tr><td>Specific angiographic views for the culprit artery to minimize superimposition with non-culprit capillary bed.
– LAD: RAO 40°, CRA 40°
– LCx: RAO 0°, CAU 20°
– RCA: RAO 30°, CRA 0°</td></tr>
</table>

MBG – myocardial blush grade; TMPG – TIMI myocardial perfusion grade; LAD – left anterior descending artery; LCX – left circumflex artery; RCA – right coronary artery; RAO – right anterior oblique; CRA – cranial; CAU – caudal.

Despite TMPG demonstrating a higher correlation with infarct size and reductions in LVEF than MBG, the latter is often preferred in clinical settings. This preference is due to MBG's clearly delineated grading system compared to TMPG [127, 128]. In a study involving STEMI patients undergoing primary PCI, an MBG score of 0 or 1 was associated with CMD as determined by CMR. Subsequently, an MBG score of less than 2 exhibited a sensitivity of 53.8% and a specificity of 74% for CMD [129, 130]. In a smaller cohort study of 21 patients, TMPG scores of less than 3 were aligned with the presence of microvascular obstruction on CMR. This finding demonstrated a sensitivity of 90% and was associated with larger infarct sizes and lower LVEF compared to TMPG 3 [131].

2.4.2.5. Quantitative blush evaluator

In an endeavor to refine the objectivity of MBG and TMPG assessments, the Quantitative Blush Evaluator (QuBE) was introduced. This technique employs computerized analysis to quantify variations in myocardial 'blush' over time, thereby standardizing measurements (Table 2.4.2.5.1). QuBE synthesizes the advantages of both contrast density changes and wash-out durations by automatically generating a "perfusion curve" specific to the culprit coronary artery [132]. In a study encompassing 52 STEMI patients who underwent reperfusion via primary PCI, QuBE demonstrated a sensitivity of 81% and a specificity of 80% in detecting CMD, in comparison to CMR, yielding an area under the receiver operating curve (AUC) of 0.88. A QuBE score below 3 was indicative of an 80% positive-predictive value for CMD [133]. The acquisition technique for QuBE is analogous to that of MBG and TMPG, albeit with a frame rate adjustment to 12.5 frames per second, diverging from the standard 30.

Table 2.4.2.5.1. *Evaluation criteria for quantitative blush evaluator: acquisition process and grading scale*

	Acquisition	Scale
Quantitative blush evaluator	Acquisition rate set to 12.5 fps	Range of value from 1 to 40 with higher values representing less coronary microvascular disease.
	Minimize panning	
	Similar angiographic views to MBG and TMPG	

MBG – myocardial blush grade; TMPG – TIMI myocardial perfusion grade.

2.4.2.6. Intracoronary doppler assessment

The advent of guidewires equipped with Doppler-flow and pressure-sensing capabilities has revolutionized the measurement of coronary flow velocity and pressure within the continuity of the coronary artery. Moreover, coronary velocity can be used as a surrogate for coronary flow as demonstrated in the continuity equation [134]:

$$\text{Flow} = \text{Velocity} \times \text{Cross sectional area}$$

These measurements are obtained using a 0.014" Doppler wire (FlowWire, Volcano Therapeutics), featuring a mounted transducer at its apex (Fig. 2.4.2.6.1). The incorporation of a 12-megahertz ultrasound transducer modality on the Doppler flow wire enhances both accuracy and reproducibility compared to indirect measurement techniques. However, these direct measures necessitate the induction of hyperemia and the instrumentation of the culprit coronary artery, which are associated with specific procedural risks.

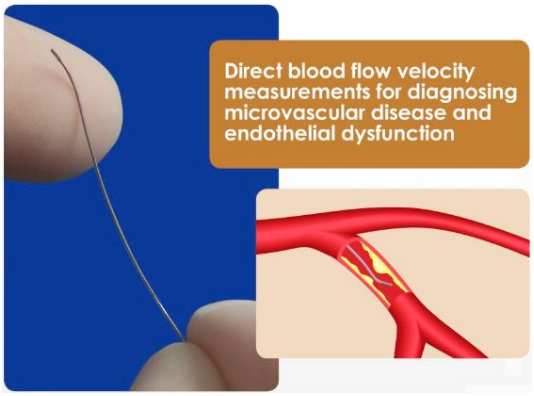

Fig. 2.4.2.6.1. *Flow-wire doppler wire for coronary velocity and pressure measurement*

2.4.2.6.1. Diastolic flow deceleration and systolic flow reversal

Patterns of coronary flow velocity, such as diastolic flow deceleration and systolic flow reversal, can be directly quantified using Doppler guidewires. In the context of STEMI after primary PCI, the manifestation of these flow patterns has been linked with suboptimal myocardial reperfusion [124]. In scenarios of severe CMD after primary PCI, alterations in coronary flow are predominantly dictated by increased microvascular resistance. This results in a characteristic pattern involving shortened diastolic flow deceleration time, systolic flow reversal, and ultimately the cessation of anterograde flow, which can be depicted schematically (Fig. 2.4.2.6.1.1).

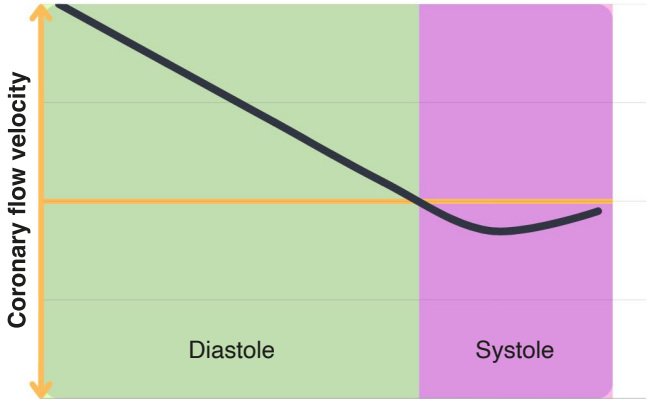

Fig. 2.4.2.6.1.1. *Diastolic deceleration and systolic reversal in microvascular disease*

This figure depicts the rapid diastolic flow deceleration (green) and reversal of systolic flow (violet) in severe coronary microvascular disease, driven by myocardial contraction.

In an investigative study encompassing 23 STEMI patients after primary PCI, a diastolic flow deceleration time of 600 milliseconds was associated with a sensitivity of 86% and a specificity of 89% for CMD, in comparison to Coronary Flow Velocity Reserve (CFVR) [135]. Other research has demonstrated that, following STEMI and PCI, progressively shorter deceleration times were correlated with decreased LVEF and severe CMD as determined by CMR, particularly when myocardial involvement exceeded 16% of wall segments with a threshold of less than 382 milliseconds [136]. Moreover, a diastolic deceleration time of less than 600 milliseconds emerged as an independent prognostic indicator for mortality, recurrent myocardial infarction, and heart failure over an average follow-up period of 4 years [137].

2.4.2.6.2. Coronary flow velocity reserve

The notion of CFVR was originally delineated by Gould et al. in 1974, conceptualizing it as the proportion of coronary flow during hyperemic states to that in resting conditions. This reserve metric is instrumental in ascertaining the physiological impact of an epicardial stenosis, with a CFR value of 2.0 or higher typically regarded as normal for epicardial vessels [138]. Conversely, in scenarios devoid of epicardial disease, CFR emerges as a diagnostic indicator for CMD [139]. This inference is rooted in the principles of Ohm's law, expressed as:

$$\text{Pressure} = \text{Flow} \times \text{Resistance}$$

In conditions where resistance is minimized, such as during hyperemic states, pressure becomes directly proportional to flow. Furthermore, since flow is inherently related to velocity, assessments of velocity under both hyperemic and resting states serve as effective surrogate markers for CFR evaluation. Consequently, the calculation of CFVR is derived as follows:

$$\text{CFVR} = \frac{\text{APV}_{\text{hyperemia}}}{\text{APV}_{\text{baseline}}}$$

In this formula, the Average Peak Velocity (APV) of blood flow is directly ascertained using a Doppler wire positioned in the distal third of the culprit coronary artery. CFVR's efficacy and reliability have been corroborated through numerous research studies focusing on STEMI patients after undergoing primary PCI (Table 2.4.2.6.2.1) [140–144]. It is crucial to distinguish between CFVR and CFR in scientific literature, as they are occasionally used interchangeably; however, CFVR specifically refers to velocity measurements as opposed to direct flow assessments. In STEMI presentations, comparative analyses of various prognostic markers, including TFG, cTFC,

MBG, coronary Doppler flow velocity, ST-segment resolution on ECG, and CFVR, revealed that CFVR uniquely predicted both global and regional recovery at a 6-month follow-up interval [140]. In terms of long-term outcomes within a similar patient cohort, those exhibiting a CFVR ≤ 2.1 had a significantly higher likelihood of cardiac mortality [141]. Furthermore, CFVR mirrors the extent and severity of CMD as depicted on CMR, although precise sensitivity and specificity metrics remain unspecified [142].

Table 2.4.2.6.2.1. *Coronary flow velocity reserve prognostic impact in ST-elevation myocardial infarction patients*

PMID	Sample	CFVR cut-off	Time Frame	Conclusion
17719324 [144]	118	1.3	CFVR immediately after PCI for STEMI	CFVR < 1.3: larger infarct size by CK, lower LVEF, and larger LVEDV; worse long-term outcomes (mean follow-up of 62 months) including HF, cardiac death, and total cardiac events
14975460 [140]	73	2.0	CFVR immediately after PCI for STEMI	CFVR ≥ 2.0: no LVEF recovery at 6-month; CFVR was superior and only predictor for LVEF compared to TFG, cTFC, MBG, and Doppler flow velocity indices
23735476 [141]	100	2.1	CFVR immediately and 6 months after primary PCI	CFVR ≥ 2.1: after PCI, had larger infarct size by CK, greater NT-proBNP; at 6-months, had greater WMSI and lower CFVR; at 10-years were 4.09 times more likely to have cardiac mortality
18534269 [136]	27	2.0	CFVR immediately after PCI for STEMI and CFVR with CMR within 8 days	CFVR < 2.0: lower CFVR was associated with increased severity of microvascular obstruction as determined by CMR
24135835 [142]	44	2.0	CFVR immediately after PCI for STEMI and at day 1. CMR at day 1 and at 6-month follow-up	Higher CFVR post-PCI and increase in CFVR from PCI to day 1 were associated with higher salvage index. Persistently low CFVR is associated with microvascular obstruction by CMR

CFVR – coronary flow velocity reserve; PCI – percutaneous coronary intervention, STEMI – ST-elevated myocardial infarction; CMR – cardiac magnetic resonance; CK – creatine kinase; LVEF – left ventricular ejection fraction; LVEDV – left ventricular end-diastolic volume; HF – heart failure; PMID – PubMed Index.

Despite its diagnostic value, the integration of CFVR into routine clinical practice is limited due to several factors, including the influence of patient hemodynamics on APV measurements and the methods lack of specificity for microvascular disease [143]. Efforts to address these challenges have included the utilization of pressure-derived flow ratios and the computation of a relative CFVR by comparing CFVR values in non-culprit and culprit

territories, under the assumption of CMD absence in non-culprit territories [145, 146]. Nevertheless, the significance of CFVR in evaluating CMD remains paramount. The innovative linkage of CFVR with APV, as measured by Doppler-wire technology, paves the way for the utilization of alternate velocity surrogates and fosters the development of new indices for diagnosing and understanding CMD, such as those based on thermodilution-derived CFR.

2.4.2.6.3. Hyperemic Microvascular Resistance

Hyperemic Microvascular Resistance (HMR) is an index conceptualized during hyperemic conditions, as proposed by Kitabata et al. The index is calculated using the formula [147]:

$$\mathrm{HMR} = \frac{\mathrm{P_d}}{\mathrm{APV_{hyperemia}}}$$

In this equation, P_d denotes the distal coronary pressure ascertained via a pressure-flow wire. Measurements are conducted during hyperemia employing a dual-function pressure and Doppler-flow guidewire (Combo-wire, Volcano Therapeutics), enabling the acquisition of simultaneous measurements over three successive cardiac cycles to determine average values.

The exploration of HMR in the context of STEMI has been relatively limited. In a cohort of 27 patients undergoing primary PCI for STEMI, heightened HMR values recorded immediately post-revascularization exhibited a significant correlation with infarct size, as indicated by peak creatinine-kinase levels and CMR, as well as with the transmural extent of the infarction. HMR demonstrated enhanced sensitivity, specificity, and diagnostic accuracy (75%, 89%, and 85%, respectively) using a threshold of 3.25 mmHg/cm/s, in comparison to CFVR and diastolic deceleration time [147]. In a subsequent study involving 24 of these patients, an HMR value exceeding 2.96 mmHg/cm/s was predictive of LV remodelling within 1 year [148].

In a research study involving 60 patients, of which 48 had complete data sets, HMR was found to correlate with CMD and reduced myocardial blood flow, as verified by CMR and PET, respectively. An optimal threshold of 2.5 mmHg/cm/s was established, yielding a sensitivity and specificity of 71% and 63%, respectively, for the prediction of any CMD, and 93% and 65%, respectively, for extensive CMD [149]. However, considering these variations, a universally accepted cut-off for HMR is yet to be established, with larger trials suggesting a higher threshold for predicting long-term clinical outcomes. In two separate studies encompassing 176 patients (130 with STEMI and 46 with non-STEMI) and 145 STEMI patients, HMR values exceeding 3.0 and

2.82 were associated with hospital admissions for heart failure and mortality, respectively, over median and average follow-up periods of 3.2 years and 85 months [150, 151].

It is important to note that HMR measurements may be inflated in cases of severe epicardial disease, as is the case with thermodilution-derived IMR. In instances of pronounced stenoses, where fractional flow reserve is below 0.6, HMR needs to be adjusted for coronary wedge pressure, similar to the adjustments made for IMR, according to the following formula:

$$\mathrm{HMR} = (\mathrm{P_d}/\mathrm{V}) \times (\mathrm{P_d} - \mathrm{P_w})/(\mathrm{P_a} - \mathrm{P_w})$$

In this equation, P_a represents aortic pressure, P_d symbolizes distal coronary pressure, and P_w denotes coronary wedge pressure.

2.4.2.6.4. Zero-flow pressure

Zero-flow pressure (Pzf) is conceptualized as the distal coronary pressure (P_d) in the culprit coronary artery at which the blood flow velocity ceases entirely [152]. Utilizing a Doppler-pressure wire, both P_d and velocity are meticulously measured across multiple cardiac cycles, with dedicated software automatically generating an average pressure-velocity loop. A regression line is then constructed from data points along the diastolic phase of this loop, extrapolating to the point on the x-axis where velocity equals zero, thereby denoting the zero-flow pressure (Fig. 2.4.2.6.4.1). Notably, during diastole, the pressure derived from Pzf is not influenced by myocardial contraction occurring in systole. Consequently, Pzf primarily reflects the pressure impacting the microcirculation due to impaired myocardial relaxation or augmented myocardial stiffness, conditions that are exacerbated in the presence of CMD and microvascular obstruction as a consequence of edema or intramyocardial hemorrhage, subsequently hindering perfusion within the coronary microvasculature [104, 152, 153].

In the inaugural study employing Pzf, 27 STEMI patients after primary PCI underwent Pzf and CFR measurements, which were then juxtaposed with myocardial viability assessments via PET [154]. Pzf demonstrated a correlation with myocardial viability, unlike CFR, thereby asserting its superior prognostic utility. A subsequent investigation involving 34 STEMI patients after PCI revealed that Pzf, as measured at the time of PCI, surpassed HMR and IMR in predicting the extent of infarct transmurality, size, salvage index, and the reduction in LVEF over a 6-month follow-up period [152]. While a Pzf threshold of 42 mmHg is recognized as the optimal benchmark for predicting a ≥ 24% LV infarction and ≥ 50% transmurality at six months, as well as ≥ 70% ST-segment resolution (with 49 mmHg as the cutoff for

predicting an LVEF ≥ 50%), this criterion does not distinctly differentiate between patients with CMD and those without. However, it does discern between individuals with more pronounced myocardial edema and those with less, likely indicative of the severity of ischemia-reperfusion injury.

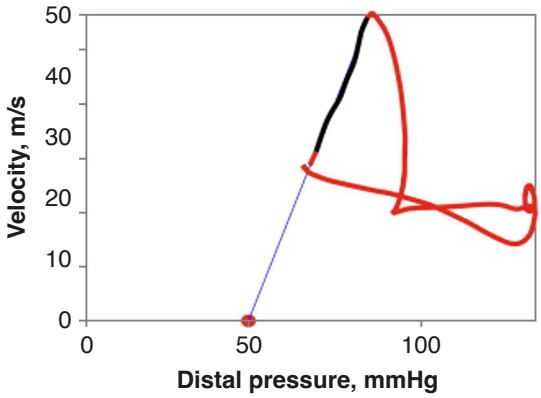

Fig. 2.4.2.6.4.1. *Pressure-velocity curve used to calculate zero-flow pressure*

2.4.2.6.5. Advanced wave intensity analysis

Wave Intensity Analysis (WIA) is predicated on the concept that the dynamics of blood flow in the coronary circulation are more intricate than the straightforward pressure gradient observed in other organ systems. In the coronary arteries, the interplay between constant aortic pressure and fluctuating resistance within the microvasculature due to myocardial contractions culminates in distinct periods within the cardiac cycle that facilitate optimal antegrade blood flow. This understanding posits that these evolving pressure differentials are critical in driving myocardial perfusion. These dynamics can be categorized into six distinct "waves" during the cardiac cycle, each providing intricate insights into the pressure, timing, and location of flow [155, 156].

While the application of WIA in the context of CMD in STEMI is still emerging, preliminary studies show promise. In one particular investigation, the backward-traveling expansion wave, which originates in the microvasculature as a response to the relaxation of the myocardium, exhibited an inverse relationship with infarct size as depicted on CMR. Additionally, it showed a positive correlation with LV recovery at a 3-month follow-up, demonstrating high sensitivity and specificity [157]. These findings suggest that WIA could be a valuable tool in the future for the assessment of CMD during the acute phase of STEMI.

2.4.2.7. Intracoronary thermodilution assessment

2.4.2.7.1. Thermodilution-derived coronary flow reserve

Thermodilution-derived CFR represents a nuanced technique diverging from traditional CFVR, which relies on blood flow velocity ratios. CFR instead employs the proportionality of transit times for assessment. This method involves utilizing a pressure guidewire equipped with dual temperature sensors, advanced towards the distal third of the desired coronary artery. Sequential injections of room temperature saline (3 mL each) into the artery facilitate the measurement of time from the nadir of temperature change back to baseline, averaged over three trials to determine the mean baseline transit time ($T_{mn\ (rest)}$) (Fig. 2.4.2.7.1) [147]. This procedure is replicated under hyperemic conditions to ascertain the mean hyperemic transit time ($T_{mn\ (hyperemia)}$).

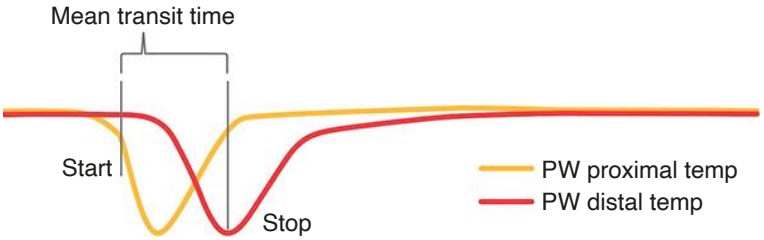

Fig. 2.4.2.7.1. *Measurement of transit time by thermodilution*

The estimate of coronary flow is made by measuring the time it takes for saline to travel from the proximal to the distal sensors. The acronym Tmn stands for "mean transit time", and it is measured in seconds. PW – Pressure wire.

Given that the spatial separation between the two temperature sensors remains constant, the distance elements within the velocity ratios of CFVR effectively negate each other, thereby simplifying CFR into a ratio of transit times. These transit times at rest and during hyperemia serve as proxies for velocity, which in turn, is a surrogate for blood flow. For optimal reproducibility, the temperature sensor should be positioned a minimum of 50 mm from the tip of the guiding catheter. The catheter tip should remain immobile, with precautions taken to avoid displacement following the initial saline injection. The use of side-hole guiding catheters or 5 Fr catheters is generally discouraged. Importantly, the units for mean transit times are in inverse seconds, thus allowing for the calculation of CFR as:

$$CFR = (1/T_{mn\ (hyperemia)})/(1/T_{mn\ (rest)}) = T_{mn\ (rest)}/T_{mn\ (hyperemia)}$$

CFR has undergone similar validation and is applicable in much the same way as CFVR. In a cohort study involving 82 STEMI patients post-primary

PCI, invasive CMD assessment was conducted concurrently with the intervention and subsequently reassessed, along with CMR, at one day and six months post-procedure. Initial low CFR readings at the time of PCI and at one day were indicative of CMD, as evidenced by CMR on day one, though this association did not persist at the six-month mark [158]. This suggests a progressive improvement in CFR over this period, indicative of microcirculatory recovery. Conversely, in a reevaluation of 44 patients from this group, those exhibiting persistently reduced LVEF at six months, compared to those with preserved LVEF, showed an association between low CFR at one day and higher troponin-I AUC as well as more severe CMD on CMR. At six months, these patients displayed reduced myocardial salvage and more pronounced CMD on CMR [159]. In a separate study of 288 STEMI patients where both CFR and IMR were measured, a CFR value below 2.0 mirrored the extent and severity of CMD on CMR, with a sensitivity of 79% and specificity of 34%, and an AUC of 0.57. However, there was no correlation with changes in LV end-diastolic volume at follow-up, nor with all-cause mortality or heart failure hospitalizations, whereas IMR showed high accuracy and correlations with these outcomes [142]. Typically, CFR values > 2.0 units are considered normal, with lower values indicative of more pronounced epicardial stenosis or CMD [160]. Despite similarities to CFVR, CFR is not specific to microvasculature and may be influenced by hemodynamic variations.

2.4.2.7.2. Thermodilution-derived index of microcirculatory resistance

The IMR via Thermodilution was pioneered by Fearon et al. as a specialized method to evaluate the microcirculatory system. This technique involves advancing a pressure guidewire, equipped with a distal temperature sensor, into the distal third of the culprit coronary artery) [161]. Upon induction of hyperemia, the distal coronary pressure (P_d) is recorded, and the mean hyperemic transit time ($T_{mn\,(hyperemia)}$) is ascertained, akin to the methodology used in CFR calculations. IMR is derived using the following equation:

$$IMR = P_d/(1/T_{mean\,(hyperemia)}) = P_d \times T_{mean\,(hyperemia)}$$

A distinctive feature of IMR is its independence from patient-specific hemodynamic variables, as both parameters in the IMR equation are gauged during hyperemia. While generally unaffected by the presence of epicardial stenosis, IMR values could be inflated in cases of severe epicardial disease. This inflation stems from a lesion-induced elevation in $T_{mn\,(hyperemia)}$ and an augmented P_d, consequent to collateral flow impacts on the microcirculation

of the culprit territory. In such scenarios, correctional formulas incorporating coronary wedge pressure (P_w) may be utilized to adjust for collateral effects [162,163]:

$$IMR = P_a \times T_{mn\,(hyperemia)} \times [(P_d - P_w)/(P_a - P_w)]$$

Typically, IMR values ≤ 25 units are considered normal, with higher values indicative of more pronounced CMD (Fig. 2.4.2.7.2.1) [160].

Fig. 2.4.2.7.2.1. *Index of microcirculatory resistance established cut-off value*

IMR has been the subject of extensive research in post-PCI STEMI patient populations (Table 2.4.2.7.2.1) [102, 103, 164–169]. Among various CMD markers, including TBG, TFC, CFR, ST-segment elevation resolution, and IMR, in STEMI presentations, IMR emerged as the most robust predictor of peak creatine kinase levels, wall motion score at 3 months, and LVEF recovery [164]. Additionally, IMR has consistently shown correlation with infarct size and CMD as determined by CMR, exhibiting a sensitivity of 58% and specificity of 72%, with an AUC of 0.65 when an IMR threshold > 27 is applied [142, 165, 169]. In STEMI patients undergoing primary PCI, an IMR > 40 has been identified as a predictor for acute cardiac complications within 30 days after primary PCI, including cardiac death, cardiogenic shock, arrhythmias, and wall rupture, as well as long-term outcomes like heart failure hospitalization and mortality over an average follow-up of 2.8 years [166, 167]. This underscores the utility of an IMR threshold of 40 for risk stratification and prognostication in STEMI contexts.

It is noteworthy, however, that discordance between IMR and CMR can occur in up to 36.4% of cases, particularly concerning the detection of microvascular obstruction and infarct size at six months follow-up [170]. While CMR offers direct insights into structural damage within the coronary microvasculature, IMR provides an assessment of the anatomical extent of injury, microvascular functionality, and potential reversibility. An IMR value < 40 units may suggest a potential for CMD resolution, even in the presence of microvascular obstruction as evidenced by CMR.

Table 2.4.2.7.2.1. *Index of microcirculatory resistance prognostic impact in ST-elevation myocardial infarction patients*

PMID	Sample	IMR cut-off	Time Frame	Conclusion
18237685 [165]	29	32	IMR immediately after primary PCI. Echocardiography within 1 day and at 3-month follow-up	IMR >32: larger infarct size by CK, less wall motion recovery at 3 months
20650433 [169]	57	35	IMR immediately after PCI for STEMI. CMR within 2 days and at 3-month follow-up	IMR >35: larger troponin-I peak, lower LVEF and greater infarct volume at 2 days and 3 months, presence of microvascular obstruction on CMR
27017370 [166]	40	36	IMR immediately after PCI for STEMI. CMR within 7 days and at 3-month follow-up	IMR >36: presence of microvascular obstruction on CMR
27699259 [171]	288	25	IMR immediately after PCI for STEMI. CMR within 2 days and at 6-month follow-up	IMR >25: lower LV ejection fraction at 2 days and at 6 months, greater infarct size and myocardial edema, and microvascular obstruction all as determined by CMR
23681066 [167]	253	40	IMR immediately after PCI for STEMI. Follow-up at mean 2.8 years	IMR >40: increased risk of death or rehospitalization from heart failure
29113999 [168]	261	40	IMR immediately after PCI for STEMI. Follow-up at 1-month	IMR >40: predicts cardiac death, cardiogenic shock, arrhythmia, and wall rupture; predictive power superior to CFR, PAMI-II, and Zwolle score
27803036 [103]	288	40	IMR immediately after PCI for STEMI. CMR within 2 days and 6 months. Follow-up at mean 845 days	IMR >40: lower LV ejection fraction, greater infarct size and myocardial edema, lower myocardial salvage index, microvascular obstruction all as determined by CMR, and all-cause death or first hospitalization for heart failure
23130166 [102]	108	28	IMR immediately after PCI for STEMI. CMR within 2 days and at 3-month follow-up	IMR >28: lower LV ejection fraction and greater infarct size, and lower myocardial salvage index

IMR – Index of Microcirculatory resistance by thermodilution; PCI – percutaneous coronary intervention; STEMI – ST-elevated myocardial infarction; CMR – cardiac magnetic resonance; CK – creatine kinase; LV– left ventricular; CFR – coronary flow reserve.

2.4.2.7.3. Absolute coronary blood flow

The methodologies previously delineated predominantly employ proxy indicators such as flow velocity and mean transit time to gauge coronary flow. A novel approach for calculating absolute coronary blood flow has been developed, utilizing a continuous infusion of room temperature saline, as delineated by the following formula [172]:

$$Q_b = 1.08 \times Q_i \times [(T_b - T_i)/(T_i - T)]$$

In this equation, Q_b signifies the absolute flow, Q_i denotes the rate of continuous saline infusion, T_b represents the temperature of the blood post-infusion, T_i is the pre-infusion blood temperature, and T corresponds to the temperature of the saline-blood mixture. If T_b is normalized to 0, and both T_i and T are measured relative to T_b, the equation simplifies to:

$$Q_b = 1.08 \times Q_i \times (T_i/T)$$

The infusion rate Q_i is operator-defined, typically ranging from 8 mm/min to 25 mm/min. This infusion is administered via a specialized microcatheter (RayFlow, Hexacath), while temperatures (T_i and T) are measured using a conventional pressure wire equipped with a distal temperature sensor. The factor 1.08 serves as a corrective coefficient to account for the disparity in specific heat capacities between normal saline and blood. Intriguingly, the infusion of room temperature saline can elicit hyperemia akin to that induced by continuous adenosine infusion, albeit devoid of its associated adverse effects [173]. With Q_b thus determined, distal pressure (P_d) can be directly measured using a pressure wire, enabling the calculation of absolute resistance (AR) as:

$$AR = P_d/Q_b$$

In an exploratory study involving 20 STEMI patients, AR was quantified immediately post-primary PCI and then again between three to five days afterward, CMR was additionally performed in 15 of these patients. The study observed an increase in flow and a concomitant decrease in resistance post-PCI, although these findings did not reach statistical significance. Furthermore, no correlation was established between AR and the detection of CMD via CMR. However, AR measurements were feasibly conducted within twenty minutes in the catheterization suite, signifying a safe and rapid procedure [174]. While the utility of AR in clinical settings remains a subject of ongoing research, the continuous monitoring of coronary blood flow represents a significant leap forward in the assessment of coronary microvascular dysfunction.

2.4.2.7.4. Microvascular resistance reserve

The concept of MRR was innovatively introduced and substantiated by De Bruyne et al. in 2021, within a study encompassing 37 patients, as a methodology to intricately assess the vasodilatory reserve capacity of the coronary microvasculature [175]. This assessment notably factors in the concurrent presence of epicardial disease and the hemodynamic alterations induced by potent vasodilators on aortic pressure. Initially conceptualized from absolute coronary flow metrics obtained via continuous thermodilution techniques, MRR's theoretical foundation allows for its application across various modalities, contingent upon the precise acquisition of coronary flow and pressure data.

The derivation of MRR, as proposed by De Bruyne et al., integrates the dynamic interplay of CFR and Fractional Flow Reserve (FFR), further adjusted for the hemodynamic shifts transitioning from non-hyperemic to hyperemic states. The refined formula employed in their analysis is articulated as:

$$\mathrm{MRR} = (\mathrm{CFR}/\mathrm{FFR}) \times (\mathrm{P_{a\ (rest)}}/\mathrm{P_{a\ (hyperemia)}})$$

Here, CFR represents the quotient of coronary flow (or velocity) under maximal hyperemia relative to its non-hyperemic baseline, and FFR denotes the ratio of distal coronary pressure to aortic pressure at peak hyperemia. $P_{a\ (rest)}$ and $P_{a\ (hyperemia)}$ correspond to aortic pressures during non-hyperemic conditions and maximal hyperemia, respectively. Thus, MRR adjusts the coronary circulation's vasodilatory reserve capacity, as expressed by CFR, to account for the severity of epicardial CAD, as indicated by FFR, and the influence of pharmacological vasodilation on perfusion pressure, as denoted by the ratio of resting to hyperemic aortic pressure.

The diagnostic and prognostic efficacy of MRR was further explored by De Bruyne et al. within the ILIAS registry, where they successfully established an MRR value of < 3 as the optimal threshold for CMD diagnosis. MRR demonstrated an independent association with MACE over a 5-year follow-up period, exhibiting a hazard ratio of 0.78, thereby underscoring its long-term prognostic significance in cardiac outcomes [176].

It is imperative to note, in a distinct consideration, that while the MRR has undergone rigorous validation and testing within populations diagnosed with CCS, its efficacy and applicability in patients experiencing STEMI remain yet unexplored and undetermined.

2.4.2.8. Index of microcirculatory resistance by angiography

The evolution of pressure-wire independent analogues of fractional flow reserve has marked a pivotal shift in the analysis of the physiological impact of epicardial stenoses [177]. In this vein, De Maria et al. have innovated an angiography-based, pressure-wire free Index of Microcirculatory Resistance (IMR_{angio}) [168]. Utilizing the foundational principles of the original IMR, an equation for IMR_{angio} was formulated. This integrates an angiography-derived fractional flow reserve surrogate, such as the Quantitative Flow Ratio (QFR; Medis Medical Imaging Systems B.V., The Netherlands), with frame count rate and aortic pressure data (Fig. 2.4.2.8.1).

$$IMR_{Thermo} = P_{distal} \times Time_{Transit}$$

$$\text{Given } P_{distal} = P_{aortic} \times (P_{distal}/P_{aortic}) = P_{aortic} \times (P_{distal}/P_{aortic}) \times Time_{Transit}$$

$$\text{Given } QFR = (P_{distal}/P_{aortic}) = P_{aortic} \times QFR \times Time_{Transit}$$

$$\text{Given } Time_{Transit} = (N_{frames(hyperemia)}/FPS)$$

$$IMR_{angio} = P_{aortic} \times QFR \times (N_{frames(hyperemia)}/FPS)$$

Fig. 2.4.2.8.1. *Derivation of index of microcirculatory resistance (IMR)*

The novel IMR angio measures distal pressure and transit time similar to IMR thermo, however, uses the unique relationship of QFR to aortic pressure along with the frame count on angiography as surrogate markers for these values.QFR: quantitative flow ratio; fps: frames per second.

In an initial study comprising 45 STEMI patients who underwent primary PCI, both thermodilution-derived IMR and IMR_{angio} were measured post-restoration of blood flow in the culprit territories. Subsequent to stenting, these measurements were repeated, and CMR was conducted 48 hours later. It was observed that IMR derived from thermodilution and IMR_{angio} demonstrated correlation in infarct related arteries both pre- and post-stenting, as well as in non-infarct related arteries, exhibiting an area under the curve (AUC) of 0.96. The sensitivity and specificity for predicting an $IMR_{angio} \geq 40$ U were 83.0% and 100.0%, respectively, when employing a thermodilution-derived IMR cutoff of > 40 U. Moreover, IMR_{angio} > 40 U exhibited a diagnostic accuracy of 76.5% in predicting CMD post-PCI, as verified by CMR [168]. These findings received further validation in subsequent research involving patients with STEMI, NSTEMI, and stable angina [178]. However, an IMR_angio cutoff of > 25 U was utilized for NSTEMI and stable angina, yielding diagnostic accuracies of 73.3% and 78.4%, respectively.

A non-hyperemic variant of IMR_{angio} (NH-IMR_{angio}) was also examined and revealed commendable diagnostic accuracy for an IMR > 40 in STEMI, with an AUC of 0.82, albeit less precise than its hyperemic counterpart. NH-

IMR_{angio} demonstrated moderate diagnostic accuracy for NSTEMI and stable angina. In detecting CMD as identified on CMR, NH-IMR_{angio} achieved an AUC of 0.71, comparable to the IMR_angio AUC of 0.76. Consequently, a hybrid IMR_{angio} methodology could be proposed for STEMI patients, employing NH-IMR_{angio} < 30 U to exclude CMD and NH-IMR_{angio} > 90 U to confirm CMD, with cases falling within this range undergoing further assessment via hyperemic IMR_{angio}. Finally, in a retrospective analysis of 262 STEMI patients post-PCI, an NH-IMR_{angio} value > 43 U was identified as an independent predictor of all-cause mortality, resuscitated cardiac arrest, and heart failure, paralleling the prognostic value of hyperemic IMR_{angio} [179].

In summary, the field of CMD evaluation features a broad spectrum of both noninvasive and invasive methods, each with its distinct advantages and limitations, as delineated in Fig. 2.4.2.8.2. In the sphere of invasive diagnostics, while basic angiographic techniques offer the benefit of rapid assessment, they are limited by their accuracy and the dependency on the observer's interpretation. The introduction of CFRV as an invasive diagnostic innovation represents a significant advancement in CMD assessment, leading to the development of more sophisticated techniques, as outlined in Table 2.4.2.8.1. Most of these methodologies are characterized by high accuracy and reproducibility, and have been extensively validated in STEMI scenarios, except for MRR, which has yet to be validated in the STEMI context.

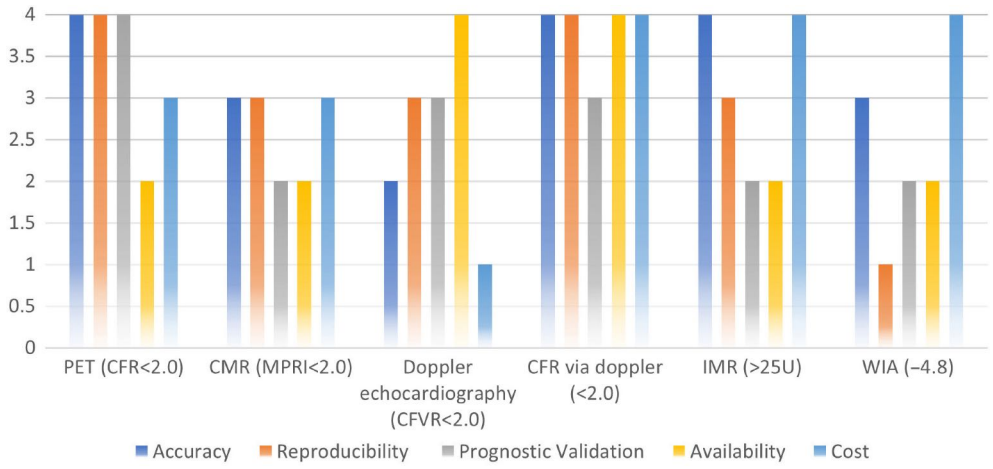

Fig. 2.4.2.8.2. *Strengths and limitations of selected diagnostic techniques with their cut-off values for the evaluation of CMD*

CFR – coronary flow reserve; CFVR – coronary flow velocity reserve; CMD – coronary microvascular disease; CMR – cardiac magnetic resonance; CT – computed tomography; IMR – Index of Microcirculatory resistance; MPRI – myocardial perfusion reserve index; PET – positron emission tomography; WIA – wave intensity analysis.

Table 2.4.2.8.1. *Comparative analysis of coronary microvascular assessment through invasive techniques*

	CFR_{thermo}	**Diastolic flow deceleration**	**IMR_{thermo}**	**HMR**	**Pzf**	**WIA**
Strengths	Well-validated	Specific to microvascular disease. Well-validated. Automated, simple measurement	Specific to microvascular disease. Highly reproducible. Well-validated. Not affectted by hemodynamic variations	Specific to microvascular disease. Highly reproducible. Well-validated	Specific to microvascular disease	Specific to microvascular disease. Not affected by epicardial stenosis
Weaknesses	Affected by epicardial stenosis. Affected by hemodynamic variations. Unspecific to microvascular disease	Affected by hemodynamic variations.	May be affected by epicardial stenosis	May be affected by epicardial stenosis	Lack of clinical validation in STEMI. Affected by hemodynamic variations. Lack of real-time analysis	Lack of clinical validation in STEMI. Time-consuming. Complex methodology. Lack of real-time analysis
Instrumentation of culprit artery	Yes	Yes	Yes	Yes	Yes	Yes
Hyperemia needed	Yes	Yes	Yes	Yes	Yes	Yes
Cut-off	Velocity at hyperemia to baseline ratio ≥ 2.0 is normal	Deceleration time > 600 milliseconds is normal	IMR ≤ 40 (in STEMI) and < 25 (in stable CAD)	HMR < 2.5 mmHg/cm/s is normal*	Pzf < 42 mmHg is normal	Unknown

$CFR_{thermos}$ – thermodilution-derived coronary flow reserve; CFVR – coronary flow velocity reserve; IMR – Index of Microcirculatory resistance by thermodilution; HMR – hyperemic microvascular resistance; MVO – microvascular obstruction; Pzf – zero-flow pressure; WIA – wave intensity analysis; STEMI – ST-elevated myocardial infarction; IRA– infarct related artery.

2.5. Novel biomarkers of coronary microvascular disease

2.5.1. Overview

The endothelial cells lining the coronary arteries execute numerous critical roles, including the generation of vasodilatory agents such as prostacyclin and nitric oxide. They respond to various stimuli, like inflammation or oxidative stress, and take part in hemostasis processes. When subjected to stress, compromised endothelium and minor arterioles may fail to dilate adequately or may even undergo paradoxical constriction. This leads to reduced perfusion of the myocardial tissue, manifesting as ischemic symptoms and anginal pain. The fundamental driver behind endothelial dysfunction is the skewed balance between the production and degradation of nitric oxide, with a propensity towards increased consumption and diminished synthesis. Furthermore, endothelial impairment fosters an environment conducive to the aggregation of platelets and the adhesion of leukocytes [180–182]. Hence, biomarkers related to inflammatory processes, oxidative stress, and coagulation pathways could be pivotal in conducting research on CMD.

2.5.2. Biomarkers of inflammation

Inflammation and immune dysregulation are crucial factors in the onset of endothelial dysfunction and the development of CAD. In line with these findings, CMD has been linked to various inflammatory biomarkers.

2.5.2.1. High sensitivity C-reactive protein

High sensitivity C-Reactive Protein (Hs-CRP), a generalized marker of systemic inflammation, has been extensively recognized for its role in predicting cardiovascular risk, particularly in females [183–185]. The Reynolds Risk Score, derived from the Women's Health Study which monitored 24,558 healthy females over an average of 10.2 years, includes Hs-CRP along with classic risk factors like age, smoking habits, familial history, and cholesterol levels to forecast the 10-year likelihood of MACE [184]. Given the historical perception of CMD as predominantly affecting females, these epidemiological studies suggest that hs-CRP could be a relevant biomarker for CMD. Patients with CMD typically exhibit elevated hs-CRP levels, often mirroring those seen in individuals with chronic CAD [186–190]. Nevertheless, hs-CRP levels can vary throughout the day due to its association with various metabolic processes affecting endothelial cell function, thereby complicating its interpretation over extended durations [191, 192].

2.5.2.2. Erythrocyte sedimentation rate

An elevated Erythrocyte Sedimentation Rate (ESR) is indicative of systemic inflammation, yet a reduced ESR may occur in conditions like polycythemia vera. Despite cytokines playing a central role in inflammatory states, ESR remains a crucial diagnostic and monitoring tool for various conditions including rheumatoid arthritis, temporal arteritis, sickle cell disease, and osteomyelitis, as well as in non-inflammatory states like stroke, CAD, and prostate cancer [193].

Andresdottir et al. explored the link between ESR and CAD risk in a cohort study, concluding that ESR can function as an independent prognostic factor for CAD in both genders, rooted in the inflammatory nature of atherosclerosis [194]. However, ESR is not recommended for screening or routine evaluations in asymptomatic individuals. Gillum et al. also noted an increased ESR as a risk factor for CAD, a finding corroborated by their study which also observed elevated other inflammatory markers, thus reinforcing the hypothesis of inflammation as a foundational element in atherosclerosis development [195].

In a clinical observational study by Natali et al., a connection between coronary atherosclerosis and ESR was identified, with seven patients diagnosed with coronary atherosclerosis *via* cardiac catheterization showing prolonged ESR in three arteriosclerosis cases [196].

Josef Yayan, in his retrospective study, discovered that ESR was extended in patients with CAD and CMD, with an ESR specificity for CAD of 70.59% and a sensitivity of 67.65% [197].

2.5.2.3. Soluble urokinase plasminogen activator receptor

The Soluble Urokinase-type Plasminogen Activator Receptor (suPAR) serves as a key proinflammatory biomarker and chemotactic substance, originating from the cleavage of Urokinase-type Plasminogen Activator Receptor (uPAR), a protein ubiquitously present on various cell types, including hematopoietic, endothelial, and smooth muscle cells [198, 199]. Distinct from hs-CRP, suPAR demonstrates remarkable stability and lacks susceptibility to diurnal fluctuations [199]. Despite a moderate correlation with hs-CRP, extensive longitudinal studies within diverse population cohorts have consistently associated elevated suPAR levels with an augmented risk of cardiovascular diseases and mortality, independent of conventional risk factors and hs-CRP levels [200–204]. In a focused investigation involving 47 individuals, heightened plasma suPAR concentrations were observed to negatively correlate with CFR in patients presenting with nonobstructive CAD [205].

2.5.2.4. Leukocytes and their distinct subtypes

Leukocytes and their distinct subtypes are recognized as robust markers of inflammation and have been implicated in the development of CMD in STEMI patients [206]. Emerging research has proposed several mechanisms to explain this association, including leukocyte-induced hypercoagulability and systemic inflammatory cytokine-induced cardiotoxic effects [207, 208]. Elevated leukocyte counts have been associated with increased thrombus formation in the infarct-related artery and a heightened resistance to thrombolysis [209]. Neutrophils, specifically, play a critical role in synthesizing and regulating a range of inflammatory mediators, such as myeloperoxidase, reactive oxygen species, elastase, and others, which can induce endothelial dysfunction and contribute to the development of CMD in later stages [210, 211].

Conversely, lymphocytes serve pivotal functions in the regulation of immune responses. An inverse relationship has been noted between lymphocyte levels and inflammatory cytokines, which are linked to endothelial dysfunction [212]. This inverse correlation may present a potential risk factor for CMD. The Neutrophil-to-Lymphocyte Ratio (NLR), which derives its value from the juxtaposition of these two leukocytes subtypes, becomes significantly elevated in the context of increased neutrophil counts coupled with decreased lymphocyte levels. Such elevated NLR values are indicative of heightened inflammatory states and damage to the endothelial microvasculature, particularly in patients with acute coronary syndrome.

Moreover, collaborative interactions between thrombocytes and monocytes have been implicated in the exacerbation of microvascular obstruction following primary PCI [58]. Correlations of clinical significance have been observed between microvascular obstruction presence, neutrophil concentrations, and thrombocyte activity [213, 214]. Elevated neutrophil counts, increased thrombocyte volumes, and a heightened neutrophil-to-lymphocyte ratio have been associated with CMD in STEMI patients, underscoring the obstructive potential of the previously mentioned markers [206, 215].

Impaired microcirculation are identified as critical prognostic factors following reperfusion therapy in STEMI cases [216]. Prior studies have established a link between elevated WBC counts and increased NLR with diminished myocardial perfusion [217]. Consequently, it is plausible to consider that a heightened NLR might signal compromised coronary microcirculation post-effective reperfusion in patients with STEMI.

2.5.3. Biomarkers of oxidation

The pivotal role of oxidative stress in disrupting endothelium-dependent vasodilation, contributing to the complexity of CMD and atherosclerotic pathogenesis, is increasingly recognized. This phenomenon manifests at the cellular level through an imbalance in redox signaling and regulation, where pro-oxidant elements overpower the cell's antioxidant defenses [218]. The reduced synthesis and augmented consumption of nitric oxide, a primary endogenous vasodilator, precipitate endothelial dysfunction and angina-like symptoms, observable even in individuals devoid of angiographic evidence of atherosclerosis.

Endothelial nitric oxide synthase is instrumental in the endothelium for the biosynthesis of nitric oxide from l-arginine and tetrahydrobiopterin [219–221]. Endothelial nitric oxide synthase function is critical in preserving endothelial health, influencing vasodilation, modulating local cellular proliferation, and safeguarding vascular integrity [222]. An upsurge in reactive oxygen species disrupts this nitric oxide synthesis pathway by depleting endothelial nitric oxide synthase cofactors, leading to a shift in endothelial nitric oxide synthase activity towards the production of superoxide and hydrogen peroxide instead of nitric oxide. This 'uncoupling' of endothelial nitric oxide synthase not only diminishes the bioavailability of nitric oxide but exacerbates oxidative stress, thereby amplifying endothelial dysfunction [223–225]. A variety of circulating biomarkers linked to this disruption in nitric oxide homeostasis have been identified, suggesting their potential as indicators of CMD.

2.5.3.1. Erythrocyte morphological characteristics

Within the microvascular network, blood flow dynamics are intricately linked to the deformability of red blood cells, a property closely associated with nitric oxide release. RBC morphology can be quantitatively assessed through parameters such as erythrocyte count, average RBC size, and Red Blood Cell Distribution Width (RDW). Initial studies, albeit small in scale, have indicated that patients with CMD tend to exhibit elevated Red Blood Cell Distribution values when compared to healthy individuals [226, 227].

2.5.3.2. Aminothiol biomarkers

Glutathione, a critical aminothiol, plays a vital role in maintaining the reduced states of thiol groups in enzymes and other biomolecules, as well as in preventing the peroxidation of membrane lipids [228]. It is also posited to facilitate the transport of nitric oxide from larger epicardial vessels to the distal microvasculature [229]. Observations have highlighted a positive

correlation between glutathione concentrations and CFR, implying that heightened levels of glutathione may signify a more robust microvascular health, whereas lower levels could reflect increased oxidative stress, potentially correlating with CMD [226, 228].

2.5.3.3. Low-density lipoprotein

Low-Density Lipoprotein (LDL) cholesterol levels have long been the archetypal biomarker for CAD [191]. Elevated LDL cholesterol levels have been directly linked to coronary microvascular function, as measured by the IMR, irrespective of the presence of coronary atherosclerosis [230]. Reactive oxygen species interact with methylene carbons in polyunsaturated fatty acids within vascular walls, leading to the formation of oxidized LDL [191]. This process triggers chronic inflammation and atherosclerotic plaque development. The presence of oxidized LDL in arterial walls stimulates the upregulation of adhesion molecules and the secretion of chemokines that attract leukocytes, further accelerating atherosclerosis [231]. The unique role of oxidized LDL in bridging lipoprotein disorders with the inflammation driving atherosclerosis is well recognized, positioning it as a potential biomarker for CMD.

The incursion of oxidized LDL into endothelial cells escalates gene expression and post-transcriptional activities of key oxidative enzymes like NADPH oxidase and xanthine oxidase, located on endothelial cell membranes [232]. This results in an amplified production of ROS. Additionally, oxidized LDL has been shown to augment the release of Von Willebrand factor and exert direct cytotoxic effects on endothelial cells [233]. The integrity of endothelial cell membranes is compromised by the self-sustaining reactions of lipid peroxides, leading to heightened membrane permeability and irreversible cellular damage [228]. However, the in vivo assessment of oxidized LDL levels presents significant challenges due to its minimal presence in plasma and the difficulty of accurate measurement, limiting its practicality as a biomarker [233].

2.5.4. Biomarkers of platelet function

Platelet activation and aggregation processes involve critical inducers such as adenosine diphosphate (ADP), thromboxane A2 (TxA2), and epinephrine, which contribute to the development of cardiovascular disease [234, 235]. ADP is the main substance that triggers platelet aggregation. The effect of other platelet aggregation inducers depends on the release of ADP. ADP attaches itself to two different types of platelet surface membrane receptors, namely P2Y1 (linked to Gq) and P2Y12 (linked to Gi). When ADP activates

the P2Y12 receptor, platelets undergo shape change and aggregation [236]. ADP is stored in the dense granules of platelets and gets released when the platelets are activated [237]. In combination with ADP, vasopressor epinephrine induces platelet aggregation. Although epinephrine is not a true platelet aggregation inducer, it plays a substantial role in determining platelets' aggregatory function. A study by Martin and colleagues showed that epinephrine may restore the effect of ADP on ADP-sensitive receptors blocked by ticagrelor [235]. TxA2 is synthesized from arachidonic acid by the action of cyclooxygenase (COX) and thromboxane synthase. The resulting TxA2 binds to its receptor, thromboxane/prostaglandin H2 (PGH2) receptor, and triggers platelet activation by increasing intracellular calcium levels [238, 239].

2.5.5. Cardiac biomarkers

2.5.5.1. Natriuretic peptide dynamics

Among the well-recognized natriuretic peptides, Atrial Natriuretic Peptide (ANP) is released in response to atrial wall distension, while BNP is secreted due to ventricular wall stretching.

The microvascular impact of ANP infusion is observed to be contingent on dosage. Studies involving individuals on a high-sodium diet revealed that low-dose ANP infusion led to constriction within the skin's microvascular network, a functional diminution in conjunctival capillary density, and an elevation in renal vascular resistance [240]. The researchers posited that ANP exerted a direct influence on microvascular structures, as the microvascular alterations were not aligned with potential confounding variables such as blood pressure, heart rate, or the renin–angiotensin–aldosterone system's activity. Conversely, higher doses of ANP were found to induce skin vasodilation, accompanied by a decrease in blood pressure and an elevation in heart rate.

While the prognostic significance of elevated BNP levels in systolic heart failure is well documented, there is a paucity of research linking BNP levels with CMD. Elevated resting NT-proBNP levels were noted in CMD patients experiencing complications such as left bundle branch block and LV diastolic dysfunction, in contrast to normal subjects; however, NT-proBNP levels in CMD patients without left bundle branch block were more akin to those of control groups [241]. A detailed imaging study involving ten controls and 18 patients with symptomatic hypertrophic cardiomyopathy and unobstructed coronary arteries utilized PET-derived hyperemic myocardial blood flow as a CMD indicator. In this research, while hyperemic myocardial blood flow was attenuated in hypertrophic cardiomyopathy patients compared to controls, NT-proBNP exhibited an inverse and independent correlation with

hyperemic myocardial blood flow [242]. Additionally, myocardial perfusion reserve during hyperemia, as assessed via MRI in 184 asymptomatic adults devoid of overt CAD from the multi-ethnic study of atherosclerosis, demonstrated a correlation between elevated NT-proBNP levels and reduced myocardial perfusion reserve [243].

2.5.5.2. Troponin dynamics

Troponin, an exquisitely sensitive biomarker for myocardial injury, has been extensively investigated in patients with CMD, particularly following PCI. Among individuals with stable angina, post-PCI IMR readings, indicative of microvascular impairment, were significantly elevated in patients exhibiting abnormal troponin I spikes compared to those without [244]. Furthermore, an inquiry involving 55 patients undergoing PCI demonstrated a direct correlation between post-PCI CFR and cardiac enzyme levels [245].

While cardiac enzymes are firmly established as markers for acute myocardial damage, their utility in managing stable CMD remains less clear. A study examining 58 heart failure patients for CMD (characterized by CFR < 2.0) noted that troponin levels were markedly higher in CMD-afflicted patients than in those without CMD [246]. Another analysis involving 19 stable patients, who underwent simultaneous troponin assessments and coronary physiological evaluations, reported a weak correlation between troponin values and CFR and a somewhat stronger correlation with IMR [247]. In a more extensive study, 761 patients suspected of CAD but without explicit manifestations were monitored over a median duration of 2.8 years. This study revealed that individuals with any positive troponin readings exhibited lower CFR than those with negative troponin tests. Moreover, those with both diminished CFR and positive troponin readings faced an elevated risk of major adverse cardiovascular events [107].

2.6. Trimethylamine N-oxide and cardiovascular diseases

2.6.1. Trimethylamine N-oxide metabolism

Nutrients like choline, L-carnitine, betaine, and similar compounds rich in choline serve as primary building blocks for TMAO, a metabolite linked to heart-related diseases, through a process reliant on gut bacteria [248]. These elements, common in diets, are converted to Trimethylamine (TMA) by intestinal flora and a variety of enzymes [249]. Once formed, TMA is taken up by the intestines and transported to the liver via the bloodstream, where it transforms into TMAO under the action of liver-specific enzymes, Flavin-Containing Monooxygenase (FMO), fish have high pre-existing

TMAO levels, which are readily absorbed upon ingestion and later eliminated through urine [250, 251].

Dietary patterns play a pivotal role in TMAO synthesis. Foods of animal origin, like red meats, poultry products, eggs, and certain seafood, are the main sources of L-carnitine and choline. In contrast, plants predominantly contain betaine [252]. Excessive red meat consumption, rich in L-carnitine, has been associated with heightened atherosclerosis risk due to microbial composition shifts in the gut and increased TMA and TMAO production [253]. A comprehensive study highlighted a significant correlation between high red meat intake and increased CAD incidents [254]. Continual red meat consumption leads to higher TMAO levels from carnitine, impacts TMAO excretion through kidneys, and TMAO levels are observed to decrease following the cessation of red meat intake [248]. γ-Butyrobetaine (GBB), a derivative of dietary L-carnitine, plays a role in converting L-carnitine into TMAO [255]. Studies revealed that omnivores tend to have elevated TMAO levels compared to vegans or vegetarians after L-carnitine supplementation. Further research indicates the gut microbiota's conversion of GBB to TMA is influenced by dietary habits, particularly omnivorous diets and prolonged L-carnitine consumption [256]. However, the relationship between dietary intake of choline/betaine and cardiovascular health risks is not definitively established. Elevated plasma levels of these nutrients are primarily concerning when accompanied by high TMAO levels [257]. Diets high in fats or typical Western dietary habits have been linked to increased plasma TMAO, whereas Mediterranean diets have been shown to have advantageous impacts [258].

The intestinal microbiome is also a critical component in TMAO creation, proving essential in the conversion of diet-derived compounds into TMA in both controlled mouse environments and human studies [248, 259–261]. Alterations in the gut microbiome significantly influence TMAO levels. Stroke patients, for instance, exhibited significant changes in their gut bacteria and lower TMAO levels [262]. Mice studies showed that exposure to certain environmental chemicals can result in substantial shifts in gut microbial populations, leading to an increase in fecal TMA [263]. Nine gut bacteria strains known for TMA production from choline have been identified. Mice with minimal colonization by these bacteria experienced a notable rise in plasma TMAO [264]. Mice with diets rich in choline and implanted with gut bacteria from high TMAO-producing strains exhibited more arterial lesions than those with bacteria from low TMAO-producing strains [265].

The conversion of TMA to TMAO involves the FMO enzyme group, especially FMO1 and FMO3. FMO3 demonstrates a higher activity level than FMO1, making it a key player in TMAO synthesis [266]. FMO3 was significantly down-regulated by testosterone in mice, suggesting the mecha-

nism why in both humans and mice, the expression of hepatic FMO3 was lower in males than in females [266].

Female mice with gut bacteria that produce TMA showed increased TMAO levels and higher liver FMO3 activity compared to males [264]. Additionally, FMO3 regulation is subject to control by the bile acid-activated Farnesoid X Receptor (FXR), with FXR activators promoting FMO3 expression and TMAO production in mice [266].

A significant relationship exists between TMAO levels and body mass index (BMI) in adults, with TMAO concentrations rising with age in both humans and mice [267, 268].

2.6.2. Immune mechanism of Trimethylamine N-oxide

Atherosclerosis, a chronic condition characterized by inflammation, involves responses from both the innate and adaptive immune systems to a range of internal and external factors, highlighting its complex nature [269]. Studies have shown that immune responses generally aggravate atherosclerosis, leading to its potential classification as an autoimmune disease to some extent [270].

As atherosclerosis progresses, the modification of autoantigens activates both innate and adaptive immune responses. Heat shock proteins (HSPs), which are found in atherosclerotic plaques and the bloodstream, are a primary type of autoantigen in this context [271]. Georg Wick and colleagues identified the autoimmune response to HSP60 as an initiating factor in atherosclerosis development [272]. Established risk factors for atherosclerosis prompt a cellular immune response in macrophages, characterized by increased expression of stress-induced HSPs [273]. These proteins are highly similar across various species, from microbes to humans [274]. Both microbial and human HSP60 can bind to endothelial cells via Toll-like receptors, sparking autoimmune responses [272]. Recent findings indicate that TMAO, a compound derived from gut microbes, can modify the expression or structure of HSPs. In murine J774A.1 macrophages, for instance, TMAO induced stress leading to an upregulation of Glucose-Regulated Protein (GRP) 94 and HSP70 proteins, potentially linked to abnormal macrophage activation and subsequent foam cell formation, a key aspect of atherosclerosis [275]. Additionally, TMAO increases the mRNA expression of stress-induced heat shock proteins such as HSP60 and GRP78, markers of endoplasmic reticulum stress, which is associated with an increased risk of atherosclerosis [276].

The innate immune system identifies pathogens through various Pattern Recognition Receptors (PRRs), leading to an immune response that includes the release of inflammatory cytokines [277]. Among these PRRs are scaven-

ger receptors (SRs) like SR-A and Cluster of Differentiation (CD)36, located on macrophages. These receptors play a crucial role in recognizing and internalizing oxidized low-density lipoprotein (ox-LDL), an important autoantigen in the development of atherosclerosis [278]. This uptake process, which doesn't have a negative feedback mechanism from intracellular cholesterol, leads to the transformation of macrophages into foam cells, a key early sign of atherosclerosis [279]. TMAO has been shown to increase the expression of SR-A1 and CD36 in macrophages, thus enhancing ox-LDL uptake and foam cell formation [248]. Interestingly, reducing TMAO production through antibiotics lessened macrophage presence and foam cell formation in aortic lesions in ApoE−/− mice [248]. Further studies indicated that TMAO amplifies CD36 expression and ox-LDL-induced foam cell formation, which can be mitigated by CD36 Small interfering RNA (siRNA) knockdown and inhibition of the Mitogen-activated protein kinases (MAPK) (SB230580) and c-Jun N-terminal Kinase (JNK) (SP600125) pathways, suggesting a critical role for the CD36/MAPK/JNK pathway in TMAO-induced foam cell formation [280]. Destruction of CD36 also hindered atherosclerotic lesion development in mice [281]. However, contrasting findings showed that different TMAO concentrations did not impact foam cell formation in mouse macrophages in vitro [282].

The Nucleotide-binding oligomerization domain, Leucine rich Repeat and Pyrin domain containing (NLRP)3 inflammasome, a complex formed by PRR activation, has been recently recognized as vital in atherosclerosis progression [283]. Activation of the NLRP3 inflammasome leads to the conversion of pro-caspase-1 into active caspase-1, facilitating the maturation and release of Interleukin (IL)-18 and IL-1β, and triggering inflammatory and immune responses [284]. Elevated TMAO levels have been shown to activate the NLRP3 inflammasome. For instance, studies with carotid artery endothelial cells and wild-type mice demonstrated that TMAO significantly activates the NLRP3 inflammasome, increasing caspase-1 activity, IL-1β production, and cell permeability, thus contributing to endothelial damage, a key initiator of atherosclerosis [285]. This activation is thought to be linked to lysosomal dysfunction and redox regulation. Additionally, the essential role of intracellular Reactive Oxygen Species (ROS) in NLRP3 activation was confirmed in hyperhomocysteinemia (HHcy) mouse models [286]. TMAO-induced endothelial NLRP3 inflammasome activation was diminished by mitochondrial ROS scavengers or Sirtuin (SIRT)3 overexpression in human umbilical vein endothelial cells, implicating the SIRT3- Superoxide Dismutase (SOD)2-Mitochondrial ROS (mtROS) signaling pathway in the activation process [287]. Other research proposed the ROS- Thioredoxin Interacting Protein (TXNIP) pathway as a mediator [288]. TXNIP is a well-studied protein

connecting ROS with NLRP3 inflammasome activation. TMAO triggers oxidative stress and TXNIP-NLRP3 inflammasome activation, leading to the dose- and time-dependent release of inflammatory cytokines IL-18 and IL-1β [289]. Furthermore, experiments in fetal human colon cells revealed that TMAO causes increases in NLRP3 inflammasome activation and ROS production in a dose- and time-dependent manner [290].

2.6.3. Inflammatory mechanism of Trimethylamine N-oxide

Atherosclerosis, a disease marked by chronic inflammation, experiences continuous inflammatory activation [291]. Research has linked higher plasma levels of TMAO with increased pro-inflammatory cytokines. For instance, obesity in mice, induced by a western diet, a known risk factor for atherosclerosis, resulted in elevated TMAO and pro-inflammatory cytokines like Tumour Necrosis Factor alpha (TNF-α) and IL-1β, while anti-inflammatory IL-10 decreased [292]. A study involving 271 German adults found a positive correlation between TMAO plasma levels and low-grade inflammation, with elevated levels of TNF-α and its receptors, though IL-6 and CRP levels showed no significant difference [293]. Further, TMAO levels were positively associated with IL-1β and high-sensitivity CRP (hsCRP) in patients with stable angina, emphasizing the need to explore TMAO-CRP relationships further, given CRP's established role in assessing atherosclerosis risk. In vitro studies indicated that TMAO promoted inflammation and oxidative stress in endothelial progenitor cells [294].

The NF-κB pathway, known to regulate several atherosclerosis-related pro-inflammatory genes, was found to be upregulated by TMAO [295]. Seldin et al. showed that TMAO increased inflammatory gene expression in aortic endothelial and smooth muscle cells, enhancing leukocyte adhesion, a process dependent on MAPK and NF-κB signaling [296]. TMAO also upregulated pro-atherogenic inflammatory proteins such as cyclooxygenase 2 and E-selectin by activating NF-κB. This pathway is also crucial in atherosclerotic thrombosis, with studies showing TMAO-induced upregulation of Vascular Cell Adhesion Molecule (VCAM)-1 and tissue factor via NF-κB signaling in human endothelial cells, promoting atherothrombosis [297, 298].

Lastly, the IL-23–IL-22 axis appears to play a role in TMAO regulation. Fatkhullina et al. proposed that this pathway, through inhibiting pro-atherogenic microbiota and metabolites like TMAO, could suppress atherosclerosis [299]. IL-22, primarily produced by Th17 cells and regulated by IL-23, has been implicated in metabolic disorders in diabetes, but its specific role in atherosclerosis warrants further investigation [300].

2.6.4. Trimethylamine N-oxide and lipid metabolism

TMAO significantly influences lipid metabolism, as evidenced in various studies. Research in mice indicates that TMAO, along with choline and carnitine, can impair Reverse Cholesterol Transport (RCT), a process that removes excess cholesterol from tissues to the liver and intestines [252]. Ross and Glomset initially suggested that atherosclerosis could result from an imbalance in arterial cholesterol deposition and removal [301]. The primary pathway for cholesterol elimination involves converting it into bile acids in the liver [302]. Studies have shown that TMAO reduces the total bile acid pool in mice, and in ApoE−/− mice, TMAO was found to suppress bile acid synthesis in the liver by inhibiting CYP7a1, potentially through FXR and Small Heterodimer Partner (SHP) activation, thereby exacerbating atherosclerosis [249, 303].

In experiments with peritoneal macrophages from C57BL/6J mice, TMAO exposure modestly increased ABCG1 and ABCA1 expression, enhancing cholesterol efflux. Dietary TMAO also reduced the expression of cholesterol transporters Npc1L1 and ABCG5/8 in the gut [249, 304]. However, the specific role of these transporter changes in TMAO-induced RCT reduction remains unclear.

Furthermore, the gut microbiota-driven TMA/FMO3/TMAO pathway is a key regulator of lipid metabolism [305]. The enzyme FMO3, involved in TMAO production, has been shown to decrease RCT and alter the bile acid pool's composition and size [306]. Liver X receptor's (LXR) critical role in cholesterol metabolism is highlighted by studies showing that mice lacking LXR couldn't induce CYP7a transcription [307]. In cholesterol-fed mice, FMO3 knockdown, stimulated by LXR, enhanced macrophage RCT, improving cholesterol balance and protecting against atherosclerosis [305].

2.6.5. Trimethylamine N-oxide and thrombosis

TMAO has been implicated in directly causing atherosclerosis and thrombosis in animal studies [308]. Atherosclerotic Cardiovascular Disease (ASCVD) like oxidative stress and hyperlipidemia often see heightened risks of platelet hyperreactivity and thrombosis [309]. Research in both humans and animals indicates that TMAO may enhance platelet hyperreactivity, thereby increasing thrombosis risk [310, 311]. This increase is associated with higher risks of coronary events, myocardial injury, and death [312]. Platelets exposed directly to TMAO showed heightened activation in response to various agonists, primarily through increased intracellular Ca2+ release [310]. In atherosclerosis and hyperlipidemia, oxLDL has been known to activate platelets via a CD36-dependent pathway, with the activation of

MAPK JNK2 and Extracellular signal-Regulated Kinases (ERK)5 playing a key role [313]. TMAO also contributes to foam cell formation and vascular inflammation by upregulating MAPK/JNK and MAPK/ERK pathways [280]. TMAO also promotes atherothrombosis through increased Tissue factor (TF) expression, monocyte adhesion, and leukocyte adhesion to endothelial cells, all mediated by the NF-κB pathway [296–298].

Further studies in germ-free mice highlighted that microbial TMA/TMAO production, dependent on Copper Homeostasis Protein (CutC), is sufficient to increase platelet reactivity and thrombosis risk [314]. The administration of CutC/D inhibitors significantly lowered plasma TMAO levels and reduced diet-induced platelet hyperreactivity and thrombosis, without notable toxicity or increased bleeding risk [315]. Additionally, FMO3-knockout mice exhibitted markedly reduced TMAO levels and thrombosis potential [316]. Recent research suggests that targeting gut microbial proteins related to TMAO production could be a promising approach to reduce platelet aggregation and arterial thrombosis [317].

2.6.6. Trimethylamine N-oxide and clinical outcomes

TMAO is gaining recognition as a potential biomarker for atherosclerosis. A significant link between TMAO and CVD was established in a large study involving 1,876 participants [248]. Elevated TMAO levels were found in CAD patients compared to those with healthy arteries and were identified as an independent predictor in CAD patients with or without type 2 diabetes mellitus [318, 319]. Urinary TMAO was correlated with an increased risk and progression of CAD [320]. High TMAO levels in STEMI patients indicated severe coronary atherosclerosis [321]. While TMAO showed a positive correlation with carotid intima-media thickness, no significant changes were observed in TMAO levels concerning carotid plaque presence over a decade, suggesting its limited role in early atherosclerotic disease in healthy adults [262, 322, 323].

Prospective studies indicate that higher plasma levels of TMAO are linked to an increased risk of MACE in individuals with existing atherosclerosis. A study involving 4,007 patients undergoing coronary angiography over three years showed a strong correlation between high TMAO levels and a greater risk of MACE (stroke, myocardial infarction, or death) [324]. In cases of chest pain and acute coronary syndromes, TMAO and its precursor TML were effective in predicting both short-term and long-term cardiovascular event risks [325]. Elevated TMAO levels were also predictive of 5-year mortality in patients with stable CAD, heart failure, and peripheral

artery disease, with respective increases in mortality risk by factors of 4, 3.4, and 2.7 [259, 326].

Additionally, TMAO was a predictor of all-cause mortality or reinfarction two years post-hospitalization for acute myocardial infarction, although it did not predict these outcomes at 6 months. However, it did aid in reclassifying the risk of death/MI at 6 months [327]. A similar graded relationship was observed between TMAO levels and subsequent cardiovascular events in patients with a recent ischemic stroke [328]. Elevated levels of L-carnitine, choline, and betaine also indicated higher CVD and MACE risks, but this was significant only in those with high TMAO levels [329]. However, a meta-analysis did not support this association [257]. Moreover, several studies found no significant link between TMAO levels and CAD history, incident cardiovascular events, or cardiovascular mortality [330–332].

2.6.7. Trimethylamine N-oxide therapeutic regulation

The potential of targeting TMAO as a therapeutic approach in atherosclerosis is gaining interest. Key dietary precursors of TMAO include choline, L-carnitine, betaine, and other choline-rich foods. These are initially metabolized to TMA by gut bacteria and various enzymes. TMA is then absorbed by the intestines, transported to the liver via the portal vein, and transformed into TMAO by the enzyme FMO3. There are several strategies to target TMAO:

1. Dietary Changes: Adjustments in diet, supplements, and lifestyle can significantly alter TMAO levels. The Mediterranean diet is one example of a dietary approach that might influence TMAO levels.
2. Gut Microbiota Modulation: Using antibiotics, probiotics, functional probiotic products, and specific natural compounds can effectively reduce TMA and TMAO levels by altering gut microbiota composition.
3. TMA Generation Inhibition: Compounds like plant sterol esters, meldonium, 3,3-dimethyl-1-butanol, and CutC/D inhibitors can suppress TMA production.
4. Inhibiting TMA to TMAO Conversion: Substances like trigonelline and guggulsterone can potentially block the conversion of TMA into TMAO by inhibiting the FMO3 enzyme.

In conclusion, this comprehensive review outlined the multifaceted approach to understanding, diagnosing, and managing coronary CMD and its broader implications on cardiovascular health. It delved into the crucial roles played by endothelial function, novel biomarkers of inflammation, oxidative stress, and platelet function in the pathophysiology of CMD, providing a

detailed account of how factors like hs-CRP, ESR, suPAR, and others served as indicators of disease presence and severity. Furthermore, it extended into the metabolic contributions to CMD, particularly emphasizing the role of TMAO, a gut microbiota-derived metabolite. TMAO's association with diet and its impact on atherosclerosis, lipid metabolism, endothelial dysfunction and thrombosis was highlighted, revealing its potential as a biomarker for CMD. The review collectively underscored the complexity of CMD, emphasizing the need for a holistic understanding that spans biological markers, metabolic processes, and the gut microbiome, to better predict, prevent, and treat CMD and its associated cardiovascular complications.

3. METHODS

3.1. Study design

3.1.1. Overview of the research

This research is based on a comprehensive, prospective, observational, and validation-focused cohort study conducted at the Hospital of the Lithuanian University of Health Sciences Kauno klinikos. The overarching goal of the study is to explore the multifaceted aspects of CMD within the context of STEMI and its associated prognostic implications. This research approach includes several critical dimensions:

1. Impact of PCI strategies during STEMI on the prevalence of CMD.
2. Prediction of CMD in STEMI patients via a machine learning approach.
3. Investigation of the biomarker identified as most relevant by the machine learning prediction algorithm for CMD in STEMI patients. This includes determining its cut-off value for predicting CMD, assessing its sole ability in predicting CMD, and evaluating its impact on patient outcomes.
4. Validation of the prognostic performance of the novel parameter MRR in STEMI Patients.
5. Prevalence and prognostic impact of CMD endotypes on clinical outcomes in STEMI patients
6. Impact of CMD on FLVR, diastolic dysfunction, and clinical outcomes.

3.1.2. Study setting

3.1.2.1. Location of the study

The research was conducted at the Hospital of the Lithuanian University of Health Sciences Kauno klinikos, a prominent medical facility located in Kaunas, Republic of Lithuania. This hospital is a major healthcare hub, boasting 2,249 hospital beds and accommodating over 1.3 million patient visits and 91,000 hospital admissions annually. Its substantial capacity and high patient turnover make it an ideal setting for conducting extensive medical research, particularly in the field of cardiology.

3.1.2.2. Cardiology intensive care unit

The Cardiology Intensive Care Unit (CICU) at the Hospital of the Lithuanian University of Health Sciences Kauno klinikos, equipped with 18

advanced beds, is central to this study. Each bed features sophisticated monitoring and interventional tools, ensuring superior care for patients. Serving as the first response unit and initial admission point for all STEMI patients in our study. Post-urgent primary PCI, these patients were brought back to the CICU for at least 24 hours of detailed monitoring, highlighting the CICU's integral role as a connector between the out-of-hospital settings and the catheterization laboratory.

3.1.2.3. Catheterization laboratory

Central to this study are the hospital's advanced catheterization lab facilities. There are three fully equipped catheterization labs, operational 24 hours a day, providing round-the-clock service for emergency and scheduled cardiac procedures. These labs are equipped with cutting-edge technologies for coronary physiology assessment and imaging, making them perfectly suited for the intricate procedures and evaluations involved in this study. Additionally, the facility maintains a ready cardiac surgery backup, ensuring comprehensive care for all patients undergoing cardiac interventions.

3.2. Inclusion, exclusion and withdrawal criteria

3.2.1. Demographics of the study population

The study's goal was to capture a wide and representative sample of the adult population, mirroring real-world clinical scenarios. It included a diverse group of individuals from different demographic backgrounds, without limitations based on gender, education, or residency. The inclusion of patients from both urban and rural areas provided a holistic view of the STEMI patient demographic, ensuring diversity in experiences and health outcomes. Such inclusivity in age and gender was crucial for understanding the varied manifestations of STEMI and CMD, thereby enhancing the relevance and applicability of the findings to the general adult population in clinical settings.

3.2.2. Inclusion criteria

The study established precise inclusion criteria to accurately identify the target patient population for this research. Eligibility was confined to adults aged 40 and above with STEMI diagnoses. A crucial criterion was the receipt of dual antiplatelet therapy before successful primary PCI on the culprit vessel, typically combining acetylsalicylic acid (300 mg) with either ticagrelor (180 mg) or clopidogrel (600 mg), following clinical guidelines. Moreover, candidates were those scheduled for a subsequent PCI on the non-culprit vessel three months after the initial procedure. This approach was vital for

the study's longitudinal nature, as it enabled a thorough evaluation of coronary microvascular function over time.

3.2.3. Exclusion criteria

A detailed set of exclusion criteria was carefully established to ensure the specificity and validity of the study's findings:

1. **History of ACS:** Patients were excluded to mitigate the impact of pre-existing microvascular obstruction, which could confound the assessment of newly developed CMD post-STEMI.
2. **Fibrinolysis:** Patients who underwent fibrinolysis were excluded because those patients had altered clinical outcomes and prognosis.
3. **Absence of requirement for staged PCI:** Exclusion of patients who did not require staged PCI was crucial, as coronary physiology assessment was planned during this procedure, scheduled 3 months post-index PCI.
4. **Atrial fibrillation:** Excluded due to the potential confounding effects on coronary physiology assessment, and the inability to evaluate diastolic function accurately, which is one of the outcomes monitored in the study.
5. **Sever comorbid conditions:** Patients with these conditions such as septicemia, autoimmune disorders, terminal hepatic disease, advanced kidney dysfunction, or malignant solid tumors were excluded due to their known effects in causing severe systemic inflammation, altering clinical outcomes and worsening prognosis.
6. **Severe valvular heart disease:** Patients with severe valvular heart diseases were excluded to avoid complications related to altered coronary physiology and the risk of degenerative arrhythmias during hyperemia.
7. **Coronary artery bypass grafts (CABG):** Patients with a history of CABG were excluded due to the potential alteration in coronary circulation, impacting the accurate assessment of CMD.
8. **Allergy to contrast media and adenosine intolerance:** These conditions were critical exclusion criteria, as they are vital components of the diagnostic procedures and coronary physiology assessments used in the study.
9. **Informed consent refusal:** Participation was contingent upon voluntary informed consent, ensuring ethical compliance and patient autonomy.
10. **Dementia:** Excluded due to potential challenges in obtaining informed consent and ensuring adherence to the study protocol.

11. **Pregnancy:** Excluded due to ethical considerations and the potential impact of physiological changes during pregnancy.

3.2.4. Withdrawal criteria

To ensure the integrity and validity of the longitudinal data, specific criteria were established for participant withdrawal from the study. These criteria were applied to manage instances where participants, initially included in the study, could no longer contribute to the meaningful progression of the research. The withdrawal criteria included:

1. **Withdrawal of consent:** Participants who chose to withdraw their consent at any point during the study were respectfully removed from the cohort. Their right to discontinue participation without any repercussions was upheld in accordance with ethical research practices.
2. **Inability to complete follow-up assessments:** Participants who, for any reason, were unable to attend or complete the scheduled three-month coronary physiology assessment or the 12-month follow-up were excluded from the final analysis. This ensured that the data remained consistent and robust, representing those who completed the entire study protocol.
3. **Development of exclusion criteria post-enrollment:** In cases where participants developed conditions post-enrollment that would have initially qualified them for exclusion (e.g., pregnancy, severe comorbidity), they were withdrawn from the study. This was crucial to maintain the scientific rigor, ethics and homogeneity of the study population.
4. **Data integrity and continuity concerns:** any situation that compromised the integrity or continuity of the data collected (e.g., incomeplete data collection, significant protocol deviations) resulted in participant withdrawal. This criterion was vital for ensuring the reliability and validity of the study findings.

3.3. Participant recruitment and enrollment

3.3.1. Patient recruitment and enrolment flow chart

The study commenced with a cohort of 624 STEMI patients who underwent primary PCI, from which 400 were identified with non-culprit lesions suitable for staged PCI. During the selection process, 172 patients were excluded for meeting exclusion criteria. This left 228 patients in the primary analysis group. However, 18 additional patients withdrew due to the development of new exclusion criteria, inability to complete follow-up, or voluntary

withdrawal, resulting in a final cohort of 210 patients for the study's analysis (Fig. 3.3.1.1).

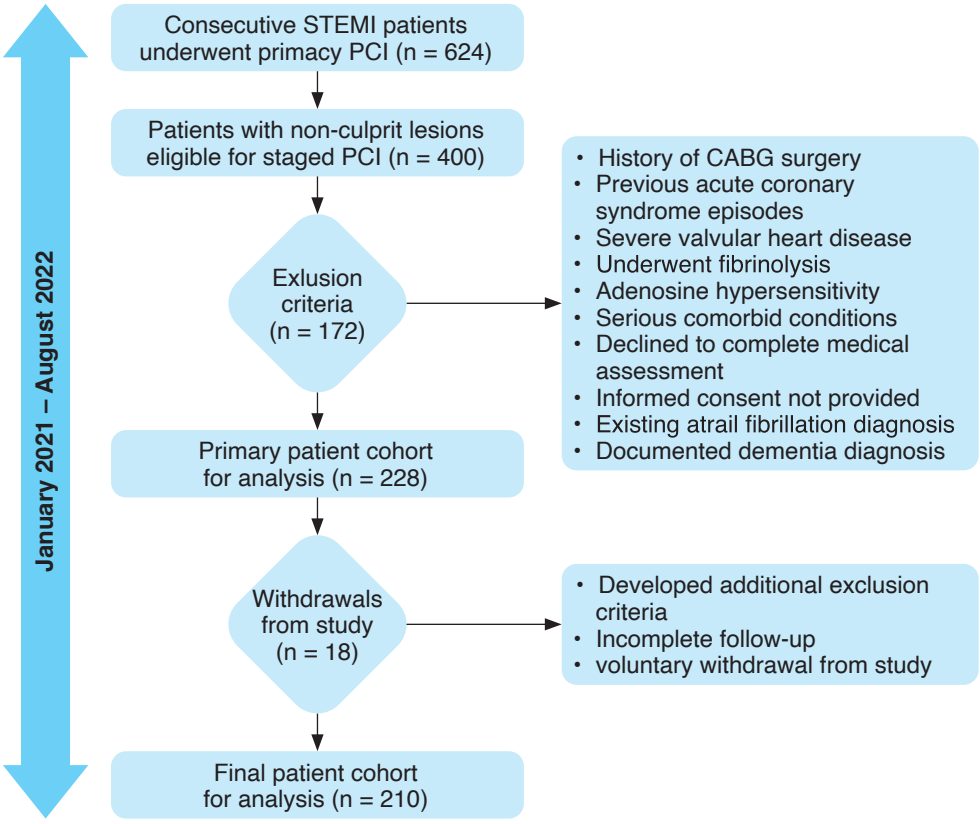

Fig. 3.3.1.1. *Patient recruitment and enrolment flow chart*

PCI – Percutaneous Coronary Intervention; CABG – coronary artery bypass graft.

3.3.2. Recruitment strategy

The recruitment strategy for this study was designed to capture a comprehensive and representative sample of the STEMI patient population. We focused on enrolling all consecutive patients who were admitted to the cardiology intensive care unit for urgent primary PCI. This approach was intended to minimize selection bias and ensure that the study population accurately reflected the diverse range of individuals typically treated for STEMI.

3.3.3. Process of identifying eligible participants

Upon admission to the cardiology intensive care unit, patients were initially assessed to determine their eligibility for the study. This assessment involved a review of their medical history and current clinical presentation to confirm the diagnosis of STEMI. The study team worked collaboratively to identify potential participants, ensuring that each patient who met the study criteria was considered for inclusion.

3.3.4. Engagement and informed consent

Once a patient was identified as a potential participant, a member of the research team approached them for enrollment. The engagement process involved providing detailed information about the study's purpose, procedures, potential risks and benefits, and the rights of the participants, including their right to withdraw from the study at any point. If the patient expressed interest and agreed to participate, written informed consent was obtained. This process was conducted with utmost respect for patient autonomy and in strict adherence to ethical guidelines.

3.3.5. Continuous enrolment and monitoring

Enrollment of participants was a continuous process, maintained throughout the study period from January 2021 to August 2022. The research team closely monitored admissions to ensure that every eligible STEMI patient was considered for inclusion. Regular meetings were held to discuss enrollment progress and address any challenges encountered, ensuring that the recruitment process remained efficient and effective.

3.4. Sequential protocol for study participants follow-up

The study's patient enrollment period was from January 2021 to August 2022. The chosen PCI strategy, either direct stenting or balloon pre-dilation followed by stenting, was determined by physicians based on each patient's unique clinical condition. Initial assessments, including echocardiography and blood sample collection, were carried out within the first 24 hours after the procedure. At the three-month follow-up, additional blood tests and coronary physiology evaluations were conducted to identify microvascular dysfunction. Though enrollment ended in August 2022, the follow-up continued until August 2023. The critical twelve-month follow-up involved another echocardiography to assess cardiac structure and function one-year post-STEMI. Along with patient-oriented composite endpoints, major adverse

cardiovascular events, and other significant health events within the first year following the STEMI incident, were also monitored (Fig. 3.4.1).

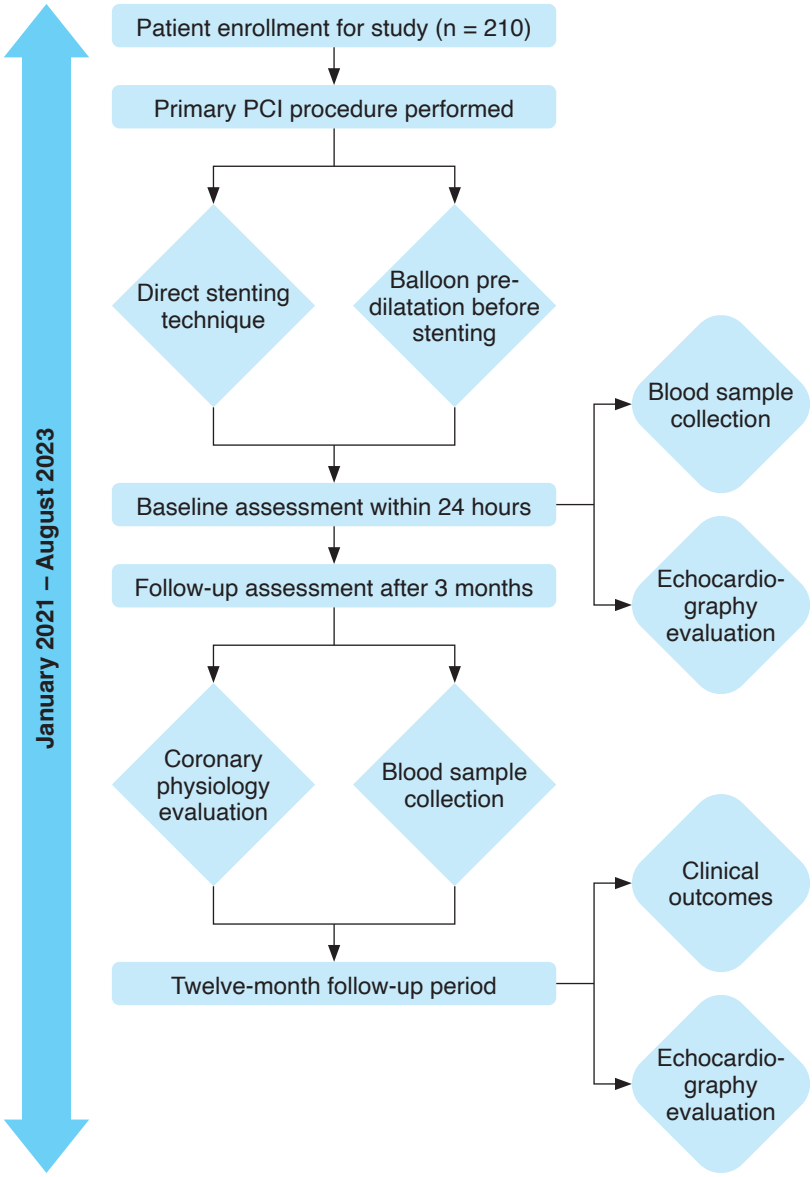

Fig. 3.4.1. *Sequential protocol for study participants follow-up*

PCI – Percutaneous Coronary Intervention.

3.5. On-admission study procedures

3.5.1. Coronary angiography and primary percutaneous coronary intervention procedures

3.5.1.1. Procedure overview

Coronary angiography and primary PCI were conducted using 6-French guiding catheters via radial or femoral arterial approaches (Fig. 3.5.1.1.1). This approach selection provided flexibility, accommodating patient-specific factors and operator preferences. Such adaptability demonstrates the procedure's versatility across different clinical scenarios.

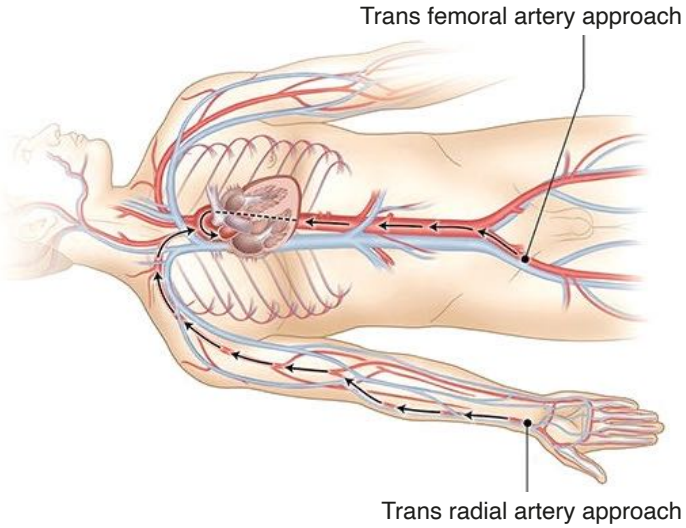

Fig. 3.5.1.1.1. *Comparative illustration of trans femoral and trans radial artery approaches for coronary angiography*

3.5.1.2. Anticoagulation protocol

Since all patients included in the study underwent primary PCI, they were anticoagulated using a heparin bolus ranging from 70 to 100 U/kg. The administration of heparin was versatile, being injected either peripherally through the arterial sheath, intravenously through a venous catheter, or directly into the coronary artery via the guiding catheter. This crucial step in the procedure was tailored to individual patient needs, with the route of heparin administration left to the discretion of the operator. The decision-making process and specifics of the heparin administration were prospectively recorded, ensuring detailed documentation of this aspect of the intervention.

3.5.1.3. Angiographic assessment

Angiographic assessments were critically conducted by two interventional cardiologists, both blinded to treatment allocation and study data, to ensure objectivity and minimize bias in evaluating angiographic outcomes. Their primary task included the identification of the culprit artery responsible for STEMI, achieved through careful examination of coronary angiograms to determine the location and severity of the blockage. This step was pivotal for guiding the PCI procedure and understanding individual coronary pathologies. A key focus of the assessment was the TIMI flow score, evaluated both at baseline and immediately after the primary PCI procedure (Fig. 2.4.2.2.1, Table 2.4.2.2.1). The baseline TIMI flow score offered insights into the initial severity of coronary occlusion, while the post-PCI TIMI score was instrumental in determining the intervention's effectiveness in restoring blood flow. Beyond the TIMI score, additional angiographic parameters, such as the degree of coronary stenosis, collateral circulation, and arterial blockage characteristics, were also scrutinized. These comprehensive evaluations provided a deeper understanding of coronary anatomy and pathology in each patient. Throughout the process, all findings were documented, and any discrepancies between the cardiologists' interpretations were resolved through a consensus approach, ensuring accuracy and consistency in the angiographic data.

3.5.1.4. Contrast agent

Iopromide (Ultravist, Bayer HealthCare Pharmaceuticals, Leverkusen, Germany), a well-established contrast agent, was utilized during the procedure. It is non-ionic, low-osmolality contrast agent known for its effectiveness and safety in coronary angiography. The choice of Iopromide was based on its excellent track record in providing clear coronary angiographic images, essential for accurate diagnosis and intervention. The total volume used, concentration, and administration rate were documented to analyze the potential impact on patient outcomes, especially in the context of renal function and the risk of contrast-induced nephropathy.

3.5.1.5. Stenting techniques and post-dilation practices

Operators were given the choice between balloon pre-dilatation followed by stenting and direct stenting, based on their clinical assessment and the individual case characteristics. Regardless of the selected method, post-dilation with non-compliant balloons was consistently applied after stent implantation for all patients. This step was vital to ensure optimal stent placement and expansion, reducing the risks of stent under-expansion or

malapposition. Comprehensive documentation of procedural details, such as stent diameter and length, along with maximum inflation pressure, was maintained. This level of detailed recording was crucial for the study, allowing for an in-depth analysis of procedural variables and their potential impacts.

3.5.1.6. Use of aspiration catheter and intracoronary glycoprotein IIb/IIIa inhibitors

The choice to use an aspiration catheter (Thrombuster II manual thrombus aspiration catheter, Kaneka Inc., Osaka, Japan) was left to the discretion of the treating physician and was prospectively documented. The use of the intracoronary glycoprotein IIb/IIIa inhibitor, specifically Eptifibatide (Integrilin, Millennium Pharmaceuticals), followed institutional protocols. It was primarily administered when a TIMI flow score of 3 was not achieved after revascularization. However, in cases with relative contraindications, such as advanced age, low hemoglobin levels, or a history of hemorrhagic complications, the decision to administer Eptifibatide was made with caution by the treating physician and duly recorded.

3.5.1.7. Procedural decision-making and documentation

Every step of the PCI procedure, from anticoagulation to stent deployment and post-procedural care, was guided by a combination of clinical guidelines, physician expertise, and patient-specific factors. The accurate documentation of each decision and procedural detail was integral to the study, providing a comprehensive dataset for subsequent analysis and interpretation.

3.5.2. Baseline assessment procedures

3.5.2.1. Blood sampling

The blood sampling procedure for this study was conducted with stringent adherence to protocol to ensure the accuracy and reliability of results. Performed by skilled nurses at the Lithuanian University of Health Sciences Kauno klinikos Cardiology Intensive Care Unit, the process commenced with patient preparation, including a brief medical history to identify any conditions that might complicate venipuncture. Utilizing aseptic techniques, the nurse selected an appropriate puncture site, typically the median cubital vein located in the antecubital fossa of the arm, which is favored for its accessibility and reduced likelihood of complications. In some cases, alternative sites like the dorsal hand veins were used, depending on the

patient's vascular anatomy and condition. The area around the selected venipuncture site was cleansed with an alcohol swab in a circular motion, moving outward, and allowed to air dry to minimize contamination risk. The patient's arm was then positioned to ensure venous distension, aided by a tourniquet applied 3–4 inches above the puncture site to engorge the veins, though care was taken to release the tourniquet as soon as blood flow was established to prevent hemoconcentration. The nurse then inserted a sterile, single-use needle swiftly and smoothly into the vein at an angle of 15 to 30 degrees with the bevel up, minimizing discomfort for the patient. Once the needle was in place and blood flow was confirmed, the nurse collected the required volume of blood into vacutainer tubes. The needle was withdrawn, pressure was applied to the puncture site with a clean gauze pad to prevent bruising, and a bandage was placed once bleeding had ceased. In alignment with data privacy regulations, each sample was coded, ensuring no direct patient identifiers were present on the labels. The coding system maintained patient anonymity while allowing for accurate sample identification and traceability. After labeling, the samples were promptly placed on ice or in a cool transport container when necessary and were swiftly conveyed to the laboratory for processing.

3.5.2.2. Echocardiographic evaluation

3.5.2.2.1. Execution and timing of echocardiography

The echocardiographic evaluations, integral to the study, were performed by experienced cardiologist who was deliberately kept unaware of the specific study data. This measure was taken to ensure objectivity and impartiality in the evaluations. The first echocardiographic assessment was conducted within 24 hours following the STEMI occurrence, a critical timeframe for capturing acute cardiac responses post-event. The second assessment took place at the 1-year mark, offering insights into the longer-term cardiac repercussions of CMD on STEMI patients.

3.5.2.2.2. Echocardiography equipment and settings

All echocardiographic assessments were performed with the EPIQ 7 ultrasound system provided by Phillips Ultrasound, Inc., headquartered in Washington, USA. All echocardiographic assessments were synchronized with ECG gating to correlate the imagery with specific phases of the cardiac cycle, ensuring highly accurate temporal resolution and cardiac event timing. To optimize image quality and ensure the most accurate readings, echocardiograms were conducted in a specialized darkened room. This controlled lighting environment minimized glare and reflections on the monitor, thereby

enhancing the cardiologist's ability to discern fine details in the ultrasound images. During each session, patient comfort and privacy were of utmost importance. The room was arranged to afford a private and secure space, shielding the patient from outside observation during the procedure. Patients were draped appropriately, with only the necessary area of the chest exposed for the ultrasound transducer. The echocardiography machine settings were calibrated before each examination to ensure consistency across all measurements. Standardized protocols for transducer placement and image acquisition were strictly followed. Each patient's study was saved under a unique identifier code, corresponding to the anonymized patient data, to ensure confidentiality.

3.5.2.2.3. Detailed measurement techniques

1. **LVEF assessment:** LVEF was precisely measured using Simpson's biplane method, conforming to the standards set by the European Association of Cardiovascular Imaging (EACVI) and the American Society of Echocardiography (Fig. 3.5.2.2.3.1) [333]. This method calculates LVEF with the formula:

$$\text{LVEF} = [(\text{EDV} - \text{ESV})) \ / \ \text{EDV}] \times 100\%$$

where EDV represents End-Diastolic Volume and ESV is End-Systolic Volume.

These volumes are derived using the equation:

$$\text{Volume} = 8 \times (\text{Area1} \times \text{Area2})/(3\pi \times \text{Length})$$

Here, Area1 and Area2 denote the cross-sectional areas of the left ventricle in the apical four-chamber and two-chamber views, respectively, while Length is the longest dimension of the left ventricle measured in these views.

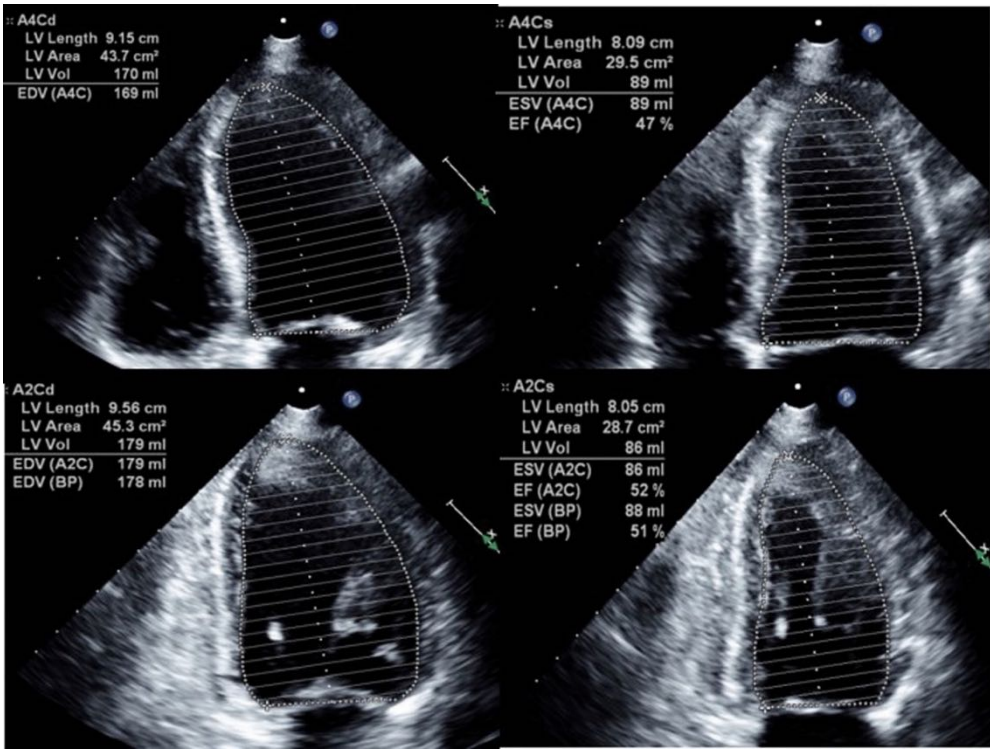

Fig. 3.5.2.2.3.1. *Visualization of left ventricular ejection fraction estimation via the Simpson's biplane technique*

Assessment of left ventricular ejection fraction via the application of Simpson's biplane method. the top panels depict the 4-chamber view, while the bottom panels display the 2-chamber view, with diastole shown on the left and systole on the right.

2. **Left Atrial (LA) volume estimation:** The LA volume was quantified using the modified Simpson method, leveraging apical 4-chamber and apical 2-chamber views at the point of ventricular end-systole (representing the maximum LA size) (Fig. 3.5.2.2.3.2) [334]. The formula for this method is:

$$\pi/4 \sum_{i=1}^{20} a_i \times b_i \times L/20$$

where a_i and b_i represent the 20 disks obtained from orthogonal views, and L represent the length measured from the mitral annular plane to the back wall. The precision of this method, particularly in calculating dimensions from multiple disk-shaped sections obtained from orthogonal views, provided a nuanced understanding of LA size and volume.

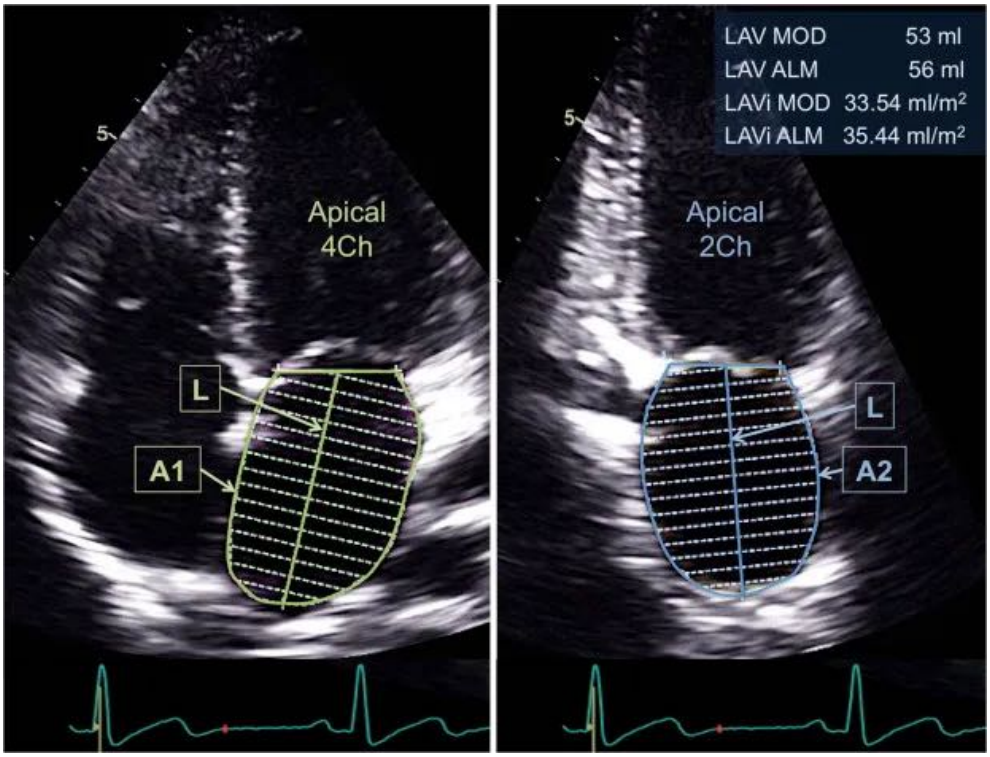

Fig. 3.5.2.2.3.2. *Methodology of assessing of left atrium volume via the modified Simpson's biplane technique*

Assessment of left atrial volume via the application of modified Simpson's biplane method. the left panel depict the 4-chamber view, while the right panel display the 2-chamber view

3. **Diastolic function analysis:** Following the American Society of Echocardiography 2016 guidelines, various diastolic parameters were analyzed [335]. This included pulsed doppler imaging to measure the mitral peak early (E) and late (A) diastolic inflow velocities, and pulsed tissue doppler for assessing the average peak early diastolic velocity (e') of the annulus (Fig. 3.5.2.2.3.3, 3.5.2.2.3.4). Continuous wave Doppler was used to measure the tricuspid regurgitation peak velocity (TRpV) (Fig. 3.5.2.2.3.5).

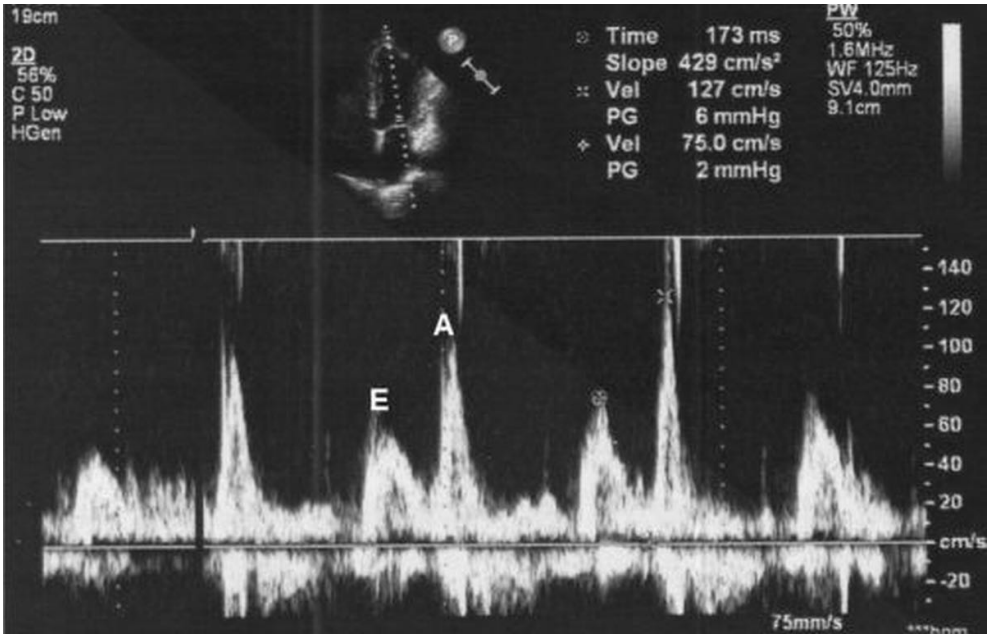

Fig. 3.5.2.2.3.3. *Demonstration of the methodology of acquiring the mitral peak early* ***(E)*** *and late* ***(A)*** *diastolic inflow velocities via pulsed doppler technique*

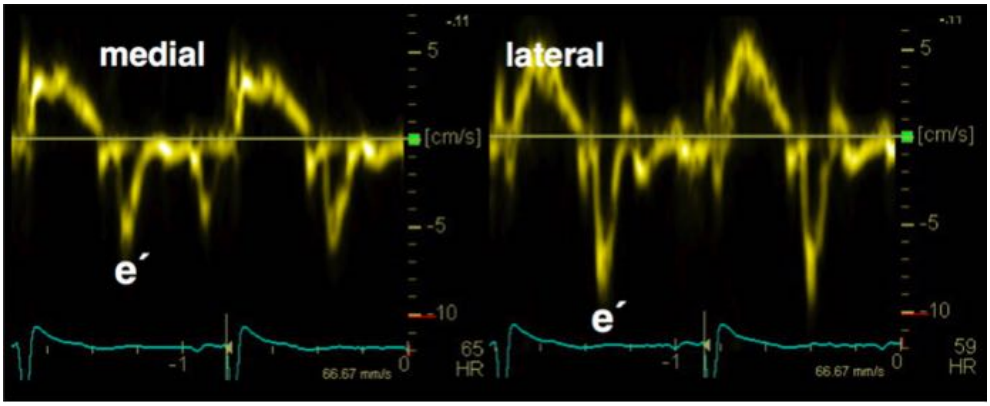

Fig. 3.5.2.2.3.4. *Demonstration of the methodology of acquiring the average peak early diastolic velocity (e') of the mitral annulus via pulsed tissue doppler technique*

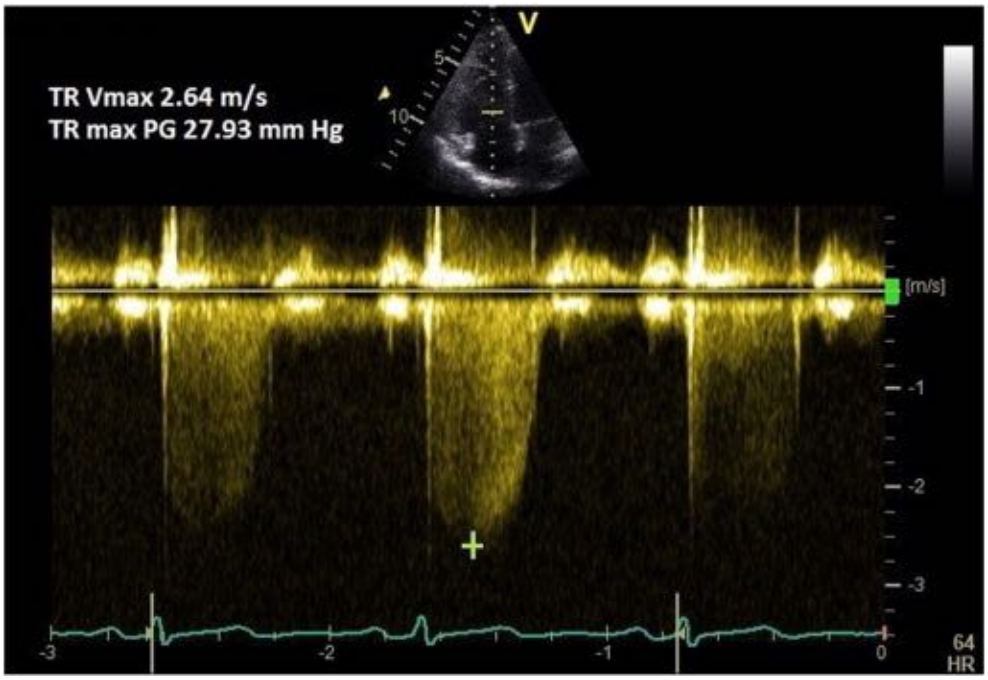

Fig. 3.5.2.2.3.5. *Demonstration of the methodology of acquiring the tricuspid regurgitation peak velocity via continuous wave doppler technique*

3.6. Follow-up study procedures

3.6.1. Coronary physiology assessment

3.6.1.1. Procedure overview and timing

The coronary physiology assessments, a pivotal element of this study, were conducted with precision 3 months after the occurrence of STEMI. This specific timing was deliberately selected based on previous literature, which suggests that microvascular obstruction post-STEMI typically resolves within a month. Assessing at 3 months provided a window for evaluating coronary physiology and microcirculation once these acute obstructions had subsided, thereby ensuring more accurate and meaningful measurements. To preserve the integrity and unbiased nature of the assessment, an experienced interventionalist, purposefully blinded to each patient's data, as well as the revascularization techniques implemented during primary PCI, performed the measurements. This strategic approach to blinding was critical to eliminate any potential bias, thereby upholding the objectivity and reliability of the physiological assessments.

3.6.1.2. Equipment and techniques used

For the assessment of coronary physiology in this study, the CoroFlow system (Coroventis Research AB, Uppsala, Sweden) was chosen for its precision and reliability, particularly in measuring critical parameters such as CFR, FFR, and IMR (Fig. 3.6.1.2.1). Recognized for its advanced technological capabilities, the CoroFlow system is essential in the diagnostics of microcirculation and microcirculation, adeptly assessing both the flow capacity and hemodynamic impact of coronary artery stenosis, as well as the nuances of coronary microvascular dysfunction. Enhanced by the integration with a pressure/temperature sensor-tipped guidewire, notably the Pressure Wire X (Abbott Vascular, Santa Clara, CA, United States), the system provides simultaneous and accurate measurements of pressure gradients and temperature fluctuations (Fig. 3.6.1.2.1). This harmonious integration is pivotal for an all-encompassing evaluation of coronary hemodynamics, with a particular focus on calculating IMR, a key indicator of microvascular health. Additionally, the adenosine served as the hyperemic agent due to its potent vasodilatory effects on microvascular systems. It primarily interacts with A_2-receptors on vascular smooth muscle, an action largely independent of endothelial function, yet it also prompts NO release from endothelial cells. For maximal hyperemia, adenosine should be administered in 100 µg and 200 µg for right and left coronary arteries, respectively.

Fig. 3.6.1.2.1. *CoroFlow coroventis system featuring the pressure wire X: a pressure/temperature sensor-tipped guidewire*

3.6.1.3. Procedure for coronary physiology measurement

The procedure for measuring coronary physiology in this study was conducted following standard validated protocols with meticulous care to ensure the accuracy of data (Fig. 3.6.1.3.1) [336]. The procedure began with the aortic pressure transducer being zeroed to air, following which routine preparation, including the administration of nitroglycerin (100 to 200 μg) via the guiding catheter. This administration was crucial for dilating the coronary arteries, thereby preventing coronary spasm and avoiding false assessments. Following this, the coronary pressure/temperature sensor-tipped guidewire, specifically the Pressure Wire X (Abbott Vascular, Santa Clara, CA, United States), was employed. The wire was carefully equalized to match the aortic pressure, ensuring that the readings taken were reflective of the true coronary pressure. This equalization was conducted at the tip of the guiding catheter positioned at the aortic sinus, a strategic point for obtaining accurate pressure readings. Once the pressure wire was appropriately calibrated, it was advanced into the coronary artery, specifically targeting the distal two-thirds of the infarct-related artery. Positioning the sensor in this location was critical for obtaining readings that accurately reflect the conditions in the area most affected by the STEMI event. Once the pressure wire was suitably positioned in the distal two-thirds of the infarct-related artery, thermodilution curves were obtained by briskly injecting 3 mL of saline at room temperature through the guiding catheter and this was repeated 3 times, allowing for calculation of the non-hyperemic mean transit time (T_{mn}). Then, the process of inducing maximal hyperemia began. To achieve this state, repeated boluses of intracoronary adenosine were administered, with at least three boluses given for acquiring the three desired $T_{mn\ (hyperemia)}$ measurements. Once stable hyperemia was verified, thermodilution curves under hyperemic conditions were recorded, adhering to the same method used for establishing baseline conditions. To expedite the process of administering the three saline bolus injections during intracoronary adenosine-induced hyperemia, a tripartite stopcock system was employed. This setup connected the manifold to a reservoir containing heparinized saline and a 3 mL syringe, while reserving the third outlet for adenosine administration. After performing these procedures Corflow system provide various coronary physiology parameters as shown in Fig. 3.6.1.3.2.

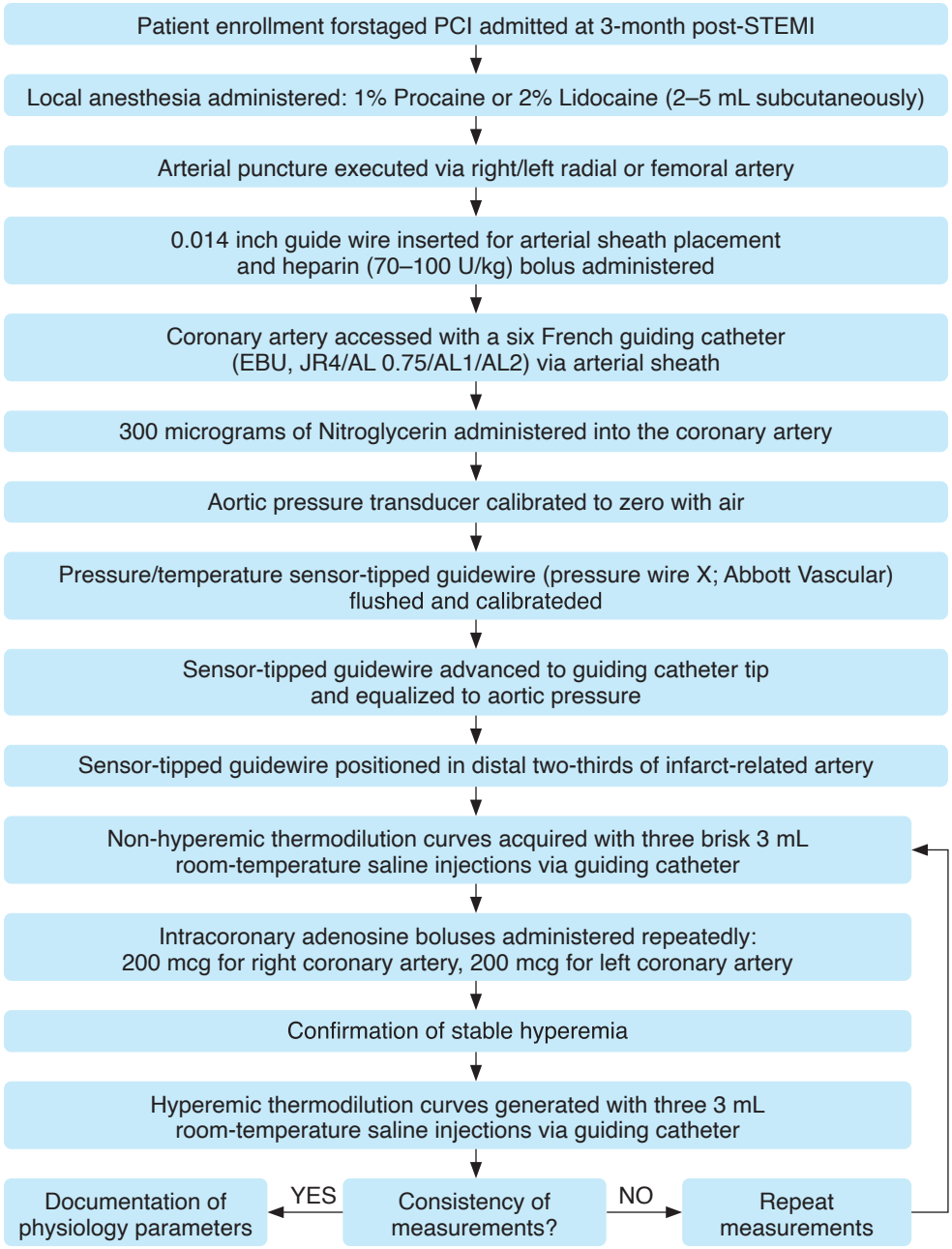

Fig. 3.6.1.3.1. *Detailed step-by-step protocol for coronary physiology assessments*

PCI – Percutaneous Coronary Intervention; STEMI – ST-Elevation Myocardial Infarction; EBU – Extra-Backup; JR – Judkins Right; AL – Amplatz left.

Fig. 3.6.1.3.2. *Invasive physiological traces of pressure and temperature curves during bolus thermodilution displayed on a Coroflow console (Coroventis; Abbott)*

CFR – coronary flow reserve; CFR_{norm} – normalised coronary flow reserve; FFR – fractional flow reserve; Hyp – hyperaemic; IMR – index of microcirculatory resistance; IMR_{cor} – corrected index of microcirculatory resistance; LAD Prox – proximal left anterior descending artery; P_a – aortic pressure; PB-CFR – pressure-bounded coronary flow reserve; PCI – percutaneous coronary intervention; P_d = distal coronary pressure; RRR = resistive reserve ratio.

3.6.1.4. Calculation of fractional flow reserve, coronary flow reserve, index of microcirculatory resistance and microvascular resistance reserve.

1. **CFR:** This physiological index evaluates the entire coronary bed's capability, from the epicardial vessels to the microvasculature, to dynamically adjust in response to the myocardium's heightened oxygen needs. To determine this adaptability, the CFR is calculated using the following formula:

$$CFR = (1/T_{mn\ (hyperemia)})/(1/T_{mn\ (rest)}) = T_{mn\ (rest)}/T_{mn\ (hyperemia)}$$

which compares the mean transit time (T_{mn}) of blood during rest to that during hyperemia [147].

2. **IMR:** This is a physiological index that measures the resistance within the microvascular network of the coronary bed. It reflects the microvasculature's capacity to permit blood flow under conditions of increased demand, as observed during maximal hyperemia. To calculate the IMR, the formula:

$$\mathrm{IMR} = \mathrm{P_d}/(1/\mathrm{T_{mean\ (hyperemia)}}) \ = \ \mathrm{P_d} \times \mathrm{T_{mean\ (hyperemia)}}$$

where P_d represents the distal coronary pressure and T_{mn} signifies the mean transit time, both measured during the hyperemic state [161].

3. **FFR:** This is a physiological index used to assess the physiological impact of coronary artery stenosis. It provides an index of the potential for any given coronary stenosis to cause myocardial ischemia. The FFR is calculated during maximal hyperemia using the formula:

$$\mathrm{FFR} = \ \mathrm{P_d}/\mathrm{P_a}$$

where 'P_d' denotes the mean distal coronary pressure, and 'P_a' stands for the mean aortic pressure. This ratio offers a valuable assessment of the hemodynamic severity of coronary artery narrowing [337].

4. **MRR:** is a calculated index that evaluates the microvascular resistance independently of any epicardial resistance to flow, offering a specific view of the microvascular function [175]. The MRR is derived using the formula:

$$\mathrm{MRR} = (\mathrm{CFR}/\mathrm{FFR}) \times (\mathrm{P_{a\ (rest)}}/\mathrm{P_{a\ (hyperemia)}})$$

where CFR represents the coronary flow reserve, FFR the fractional flow reserve, $P_{a\ (rest)}$ the aortic pressure at rest, and $P_{a\ (hyper)}$ the aortic pressure during maximal hyperemia. This calculation allows for the isolation of microvascular resistance, and when epicardial resistance is negligible, the MRR is equivalent to CFR. This distinction is particularly relevant in patients where the condition of the epicardial arteries may influence the assessment of microvascular function.

3.6.2. 12-month echocardiographic evaluation

During the follow-up phase of the study, participants underwent echocardiographic evaluations at 12-month to monitor changes in cardiac function and structure. These assessments were performed in accordance with the protocols outlined previously.

3.7. Blood and biomarkers analysis

All blood tests in this study were meticulously analyzed at the Lithuanian University of Health Sciences Kauno klinikos Laboratories and the Institute of Cardiology Molecular Laboratory, both renowned for their state-of-the-art technology and experienced staff. These facilities uphold rigorous quality control standards, ensuring unparalleled accuracy and reliability in our analyses. Every procedure, from sample preparation to final analysis, was executed with precision, leveraging advanced automated systems alongside detailed manual techniques.

3.7.1. Complete blood count

The complete blood count was conducted using an advanced hematological analyzer. This device drew a small volume of blood into a mixing chamber, where it was diluted with a reagent to separate the cells. Using electrical impedance for cell counting and sizing, and photometric analysis for hemoglobin concentration, the machine provided a detailed count of red and white blood cells, platelets, hemoglobin levels, and hematocrit values.

3.7.2. Troponin I levels

Troponin I levels were analyzed at two critical points: admission and peak concentration. A high-sensitivity assay was employed, which involved adding the blood sample to a solution containing specific antibodies. These antibodies, tagged with a color-changing enzyme, bound to troponin I molecules, leading to a color change proportional to the troponin concentration, which was then measured photometrically.

3.7.3. Erythrocyte sedimentation rate

The ESR test began by mixing the blood with an anticoagulant to prevent clotting. The sample was then placed in a vertical Westergren tube and left undisturbed for one hour. The distance the red blood cells fell in this time, due to gravity, was measured.

3.7.4. Creatinine levels

Creatinine levels were measured using the Jaffe method, a well-established colorimetric assay. Initially, blood samples were collected and centrifuged to obtain serum, the preferred sample type for this assay. The key reagent, an alkaline picric acid solution, was prepared to react with creatinine in the serum. Upon mixing the serum with this solution, creatinine reacted with picric acid to form a red-colored complex, creatinine-picrate. This reaction

mixture was then incubated for a specific duration to allow the reaction to complete fully. The intensity of the resulting color change, which is directly proportional to the creatinine concentration in the sample, was measured using a spectrophotometer at a specific wavelength (around 490 nm). For accurate quantification of creatinine levels, the absorbance values obtained from the spectrophotometer were compared against a pre-established calibretion curve, created using standards with known creatinine concentrations. Additionally, control samples with defined creatinine levels were included in each batch of tests to ensure the assay's accuracy and reliability.

3.7.5. High sensitivity C-reactive protein

The hs-CRP levels were precisely determined using an advanced immunoturbidimetric assay, a method renowned for its sensitivity and accuracy in detecting low concentrations of hs-CRP. This process began with the careful collection and preparation of blood serum from the participants. The serum was then introduced into a prepared reagent containing anti-CRP antibodies. These antibodies were conjugated to latex particles, a crucial component that enhanced the assay's sensitivity and specificity. Upon mixing the serum with this reagent, the anti-CRP antibodies bound to any CRP molecules present, forming antibody-CRP complexes. These complexes caused an increase in the turbidity of the solution due to the light-scattering properties of the latex particles. The next step involved incubating the mixture for a specific period under controlled conditions to ensure optimal binding and reaction. Following incubation, the turbidity of the mixture was assessed using a sophisticated photometric device. This device measured the amount of light scattered by the latex-enhanced complexes, with the degree of light scattering being directly proportional to the concentration of CRP in the serum. To accurately quantify the CRP levels, a calibration curve was employed. This curve was generated using standard solutions with known CRP concentrations, providing a reference for interpreting the test results. By comparing the photometric readings of the participant samples against this calibration curve, the precise concentration of hs-CRP in each sample was determined. This method's high sensitivity allowed for the detection of even very low levels of CRP, which is critical in assessing subtle inflammatory changes and cardiovascular risk in patients.

3.7.6. Lipid levels

For the majority of the lipid parameters, enzymatic hydrolysis was the cornerstone of our methodology. Blood serum samples were treated with specific enzymes that targeted each type of lipid. These enzymes catalyzed

reactions that broke down the lipids into smaller components, leading to the production of colorimetrically measurable end products. The intensity of the color change in these reactions was directly proportional to the concentration of each lipid type, allowing us to quantify levels of total cholesterol (TC), triglycerides, and High-Density Lipoprotein (HDL) cholesterol. For LDL cholesterol, however, a different approach was taken. Given that direct measurement of LDL cholesterol can be challenging and resource-intensive, we employed the Friedewald formula, a widely accepted calculation method in lipidology [338]. This formula calculates LDL cholesterol as follows LDL Cholesterol (mmol/L) = Total Cholesterol (mmol/L) – HDL Cholesterol (mmol/L) – (Triglycerides (mmol/L) / 2.2). This calculation is based on the principle that the TC in the serum is the sum of LDL cholesterol, HDL cholesterol, and VLDL cholesterol. Since VLDL cholesterol is roughly one-fifth the triglyceride value in most individuals with normal lipid metabolism, this ratio is used in the formula. The accuracy of the Friedewald formula relies on precise measurements of TC, HDL cholesterol, and triglycerides. It's important to note that this formula is most reliable when triglyceride levels are below 4.5 mmol/L. In cases where triglyceride levels are significantly higher, direct LDL measurement was done.

3.7.7. B-type natriuretic peptide

The BNP levels were measured using a highly accurate sandwich immunoassay technique. This process was carried out both during patient admission and at the 3-month follow-up to monitor changes over time. Initially, patient blood samples were collected and prepared to isolate the serum. The assay involved introducing the serum into a solution containing two types of highly specific antibodies against BNP. One antibody was immobilized on a solid phase, typically a microplate, and the other was in a fluid phase, labeled with an enzyme that could trigger a color change upon binding. As BNP molecules from the serum bound to these antibodies, they formed a 'sandwich' complex. The enzyme attached to the fluid-phase antibody catalyzed a reaction in the presence of a substrate, leading to a measurable color change. The intensity of this color change was directly proportional to the BNP concentration in the sample. A spectrophotometer was then used to quantify this color intensity, translating it into BNP concentration values.

3.7.8. Plasma TMAO levels

Plasma TMAO levels were quantified using an Enzyme-linked Immunosorbent Assay (ELISA) kit provided by Bioassay Technology Laboratory, Shanghai, China. Initially, blood samples were collected and centrifuged to

separate the plasma, which was then stored at −80 °C to preserve sample integrity. For the assay, the plasma was thawed and added to wells in an ELISA plate pre-coated with TMAO-specific antibodies. A labeled TMAO analog was also added, competing with plasma TMAO for antibody binding. The plate underwent incubation, allowing binding between the antibodies and either the plasma TMAO or the analog. The color change intensity in each well, measured by an ELISA reader, was inversely proportional to the plasma TMAO concentration; more plasma TMAO resulted in less analog binding and a weaker color change. These readings were compared against a standard curve of known TMAO concentrations, enabling accurate quantification of TMAO levels in the plasma samples.

3.7.9. Platelet aggregation

The assessment of platelet aggregation was carried out using a state-of-the-art STAGO TA-8V platelet aggregometer (STAGO, Frouard, France), employing the classical Born method to provide detailed insights into blood clotting dynamics. Blood samples were drawn into specialized vacutainer tubes (Greiner Bio-One Vacuette North America, Inc, Monroe, NC), which contained a 3.2% sodium citrate solution.

The blood samples were then treated with adenosine diphosphate (ADP) and epinephrine (ADR), which served as induction agents for platelet aggregation.

These agents play a pivotal role in stimulating the platelets to aggregate, mimicking the physiological process of clot formation. Once treated, the samples were placed in the aggregometer, which monitored changes in light transmission through the blood. As the platelets aggregated in response to the induction agents, they formed aggregates, leading to a decrease in light transmission through the sample. This change in light transmission was precisely measured by the aggregometer, providing quantitative data on the extent of platelet aggregation.

3.8. Study endpoints

The overarching objectives of this PhD thesis were to investigate the clinical and physiological outcomes in post- STEMI patients, with a particular focus on CMD and its prognostic implications. Several endpoints were defined to explore the multifaceted nature of CMD post-STEMI.

A. 3-month follow-up endpoints
    1. Prevalence of CMD.
    2. Prevalence of CMD endotypes.

B. 12-month follow-up endpoints
1. Functional left ventricular remodelling grade
2. Diastolic dysfunction grade.
3. The occurrence of the patient-oriented composite endpoint (POCE) and MACE with its individual components.

3.9. Data collection

Data collection for this observational study was orchestrated and adhered to standardized protocols, ensuring robust and reliable data across all phases of the patient journey. From initial enrollment through the twelve-month follow-up, each data point was systematically captured. Following the primary PCI procedure, real-time data entry methods were employed to document the specifics of the intervention, such as direct stenting, balloon pre-dilatation, aspiration thrombectomy, and intracoronary glycoprotein IIb/IIIa inhibitor infusion. Within the first 24 hours post-procedure, a comprehensive baseline was established through echocardiographic evaluations and blood sample collections, with all samples immediately coded for anonymity and processed using validated instruments. By the three-month mark, a structured follow-up assessment ensured continuity in tracking coronary physiology and biomarker trajectories, with stringent quality checks in place to validate data accuracy. The culmination of data collection at twelve months involved repeat echocardiography and careful monitoring of clinical outcomes, including POCE and MACE, to ascertain the full spectrum of patient health outcomes. Robust training and detailed audit trails for all personnel involved in data handling reinforced the integrity of the process. Additionally, adverse events were diligently recorded, providing a comprehensive dataset for analyzing the interplay between coronary microvascular dysfunction and patient outcomes. Each stage of data collection was precisely aligned with the study's timeline, and redundant systems were in place to protect data integrity, ensuring the final dataset's strength for significant clinical insights.

3.10. Definitions

3.10.1. Alcohol abuse

Alcohol Abuse was defined by regularly consuming alcohol in amounts greater than the equivalent of 14 standard drinks per week for men and 7 standard drinks per week for women, with one standard drink defined as approximately 0.6 ounces (17.7 milliliters) of pure alcohol. This typically translates to 12 ounces (355 milliliters) of beer, 5 ounces (148 milliliters) of wine, or 1.5 ounces (44 milliliters) of distilled spirits per drink [339].

3.10.2. STEMI

STEMI, delineated in accordance with the 2023 European Society of Cardiology (ESC) Guidelines for the management of acute coronary syndromes, manifests as an ST-segment elevation at the J-point observed in two contiguous ECG leads, with an elevation threshold of ≥ 2 mm in chest leads or ≥ 1 mm in limb leads, adhering to specified gender and age-based criteria. Additionally, a new onset or presumed new left bundle branch block (LBBB) augments the clinical suspicion of STEMI [4]. A definitive diagnosis is contingent upon the clinical presentation of ischemic symptoms and is substantiated by the evidentiary confirmation of obstructive CAD via coronary angiography. In instances where coronary angiography does not reveal obstructive CAD, the patient would not be classified as having experienced a STEMI, regardless of the fulfilment of the aforementioned electrocardiographic and clinical criteria.

3.10.3. Dyslipidemia

In alignment with the 2019 ESC/ European Atherosclerosis Society Guidelines for the management of dyslipidemias, it was defined by having a fasting LDL cholesterol level exceeding 1.4 mmol/L or the ongoing use of lipid-lowering medications [340].

3.10.4. Hypertension

In accordance with the 2018 ESC/European society of hypertension clinical practice guidelines for the management of arterial hypertension, hypertension is diagnosed by a systolic blood pressure at or above 140 millimeters of mercury (mmHg) and/or diastolic blood pressure at or above 90 mmHg [341]. This diagnosis must be based on blood pressure measurements that are confirmed on at least two separate occasions, ensuring consistency in the elevated readings. The measurements should be taken using validated and calibrated techniques to guarantee accuracy. Furthermore, the definition of hypertension also includes individuals who are actively taking medication to lower their blood pressure, regardless of their current measured values. This encompasses those who have been prescribed antihypertensive therapy as part of their treatment plan to manage high blood pressure.

3.10.5. Diabetes mellitus

Drawing on the standards set forth by the 2019 American Diabetes Association (ADA) Standards of Medical Care in Diabetes, diabetes mellitus was defined through multiple criteria [342]. One criterion is a fasting plasma

glucose level of 7.0 mmol/L (126 mg/dL) or greater. Fasting is defined as no caloric intake for at least 8 hours. Alternatively, diabetes was also defined by an HbA1c level of 6.5% or higher, which reflects the average plasma glucose over the previous 2 to 3 months. Additionally, patients who are actively using blood glucose-lowering medications were also considered as diabetics.

3.10.6. KILLIP classification

Killip classification was defined based on the following criteria [343]:

1. **Killip Class I:** Denotes patients who show no clinical signs of heart failure. This includes the absence of rales, a third heart sound (S3), and normal findings on chest radiography.
2. **Killip Class II:** Represents patients with mild to moderate heart failure. Indicators include the presence of rales in the lower half of the lung fields, a potential S3, and elevated jugular venous pressure.
3. **Killip Class III:** Identifies patients with severe heart failure, characterized by extensive rales across lung fields, marked hypoxemia, and frequently, an audible S3. This class is commonly associated with acute pulmonary edema.
4. **Killip Class IV:** Corresponds to patients in cardiogenic shock or experiencing hypotension (systolic blood pressure < 90 mmHg), alongside signs of peripheral vasoconstriction like oliguria, cyanosis, or diaphoresis.

3.10.7. Creatinine clearance

In this study, the evaluation of renal function was primarily conducted through the assessment of creatinine clearance, utilizing the Cockcroft-Gault equation [344]. This established formula calculates creatinine clearance by considering the patient's serum creatinine level, age, body weight, and gender. The resulting value provides an estimate of the kidneys' glomerular filtration rate, reflecting the body's ability to clear creatinine from the blood.

3.10.8. Successful PCI

Successful PCI was defined by the implantation of a second-generation drug-eluting stent into the targeted lesions. The measure of success was twofold: visually, there needed to be a reduction of the lesion's stenosis to less than 20%, and functionally, there had to be a restoration of coronary blood flow. This restoration was quantified as achieving TIMI flow grades of either 2 or 3, indicating substantial blood flow restoration through the treated coronary artery. These criteria collectively constitute the benchmark for a

successful PCI, encapsulating both mechanical success in stent placement and the effective restoration of coronary blood flow [345].

3.10.9. Pain-to-door time

Defined by the 2023 ESC guidelines for the management of acute coronary syndromes, pain-to-door time denotes the elapsed duration, measured in minutes, from the initial manifestation of symptoms indicative of an acute coronary syndrome – typically chest pain – to the moment the patient presents at a medical facility, such as the emergency department of a hospital [4]. This critical temporal metric is utilized in evaluating the responsiveness and efficacy of emergency medical services and the healthcare delivery system in acute cardiac care. Additionally, it depends on patient awareness in recognizing and acting upon critical cardiac symptoms.

3.10.10. Door-to-balloon time

Defined as the measured time interval, expressed in minutes, from the patient's initial arrival at a medical facility, typically the emergency department, to the precise moment of balloon inflation during PCI in the culprit artery. This time frame is pivotal in the context of STEMI management, as it encapsulates the entire process of patient evaluation, diagnosis, preparation for catheterization, and the actual interventional procedure. This metric serves as a benchmark for evaluating the quality of care and is a key factor in determining the prognosis of patients undergoing treatment for STEMI [346].

3.10.11. TIMI flow

In the study, TIMI flow grades is defined as follows [116]:

1. **TIMI Grade 0 (No Perfusion):** Characterized by the complete absence of antegrade flow through the coronary artery beyond the point of occlusion.
2. **TIMI Grade 1 (Penetration Without Perfusion):** This grade indicates the presence of contrast material penetration beyond the occlusion site but without successful perfusion of the distal coronary bed.
3. **TIMI Grade 2 (Partial Perfusion):** Denotes a scenario where contrast material passes the site of occlusion, but the flow is reduced and delayed, leading to incomplete or late filling of the distal coronary bed.
4. **TIMI Grade 3 (Complete Perfusion):** Represents normal flow, characterized by prompt and complete perfusion of the distal coronary territory, indicative of successful revascularization.

These TIMI flow grades, as defined in the study, are utilized to evaluate the extent of coronary artery perfusion, particularly in the context of ACS and post-interventional assessment in PCI. The optimal clinical outcome is reflected by achieving a TIMI Grade 3 flow, whereas TIMI Grades 0 to 2 are indicative of reduced or absent perfusion, often requiring additional clinical interventions for optimal patient care.

3.10.12. Coronary physiology indices

The assessment of coronary physiology was anchored by established cut-off values for FFR, CFR, IMR and MMR.

1. **Normal FFR** was defined as a value greater than 0.80, indicating adequate coronary blood flow [337].
2. **Normal CFR** was defined as a value of 2.0 or higher, reflecting sufficient blood flow increase in response to stress [160].
3. **Normal IMR** was defined as a value of less than 25 units, signifying unimpeded microvascular flow [160].
4. **Normal MRR** was defined as a value of 3 or higher, derived from non-invasive stress test data and clinical outcomes from prior studies [176].

3.10.13. CMD

Microcirculatory dysfunction was defined by either an IMR value of 25 or higher or a CFR value below 2.0, indicating impaired microvascular function [160]. Additionally, our study utilized a subset analysis where microcirculatory dysfunction was further classified based on the novel parameter MRR. Also an MRR value below 3 indicated the presence of CMD, which was then sub-divided into functional-CMD for IMR values below 25, and structural-CMD for IMR values of 25 or higher [160].

3.10.14. Functional Left Ventricular Remodelling

FLVR in this study was categorized based on a classification system outlined by Surenjav Chimed et al. This system stratifies patients into four distinct groups based on changes in LV dimensions and ejection fraction [347]:

1. **Group 1:** Encompasses patients who exhibit no significant dynamic changes in both LV diameter and LVEF, indicating stable cardiac dimensions and function.

2. **Group 2:** Included in this category are patients who do not show LV dilatation; however, they experience a notable decrease in LVEF, defined as an absolute reduction of more than 5%. This suggests a decline in cardiac contractility without dimensional changes.
3. **Group 3:** Patients classified in this group exhibit an increase in Left Ventricular End-Diastolic Volume (LVEDV) of 20% or more, but without impairment in LVEF. This indicates an enlargement of the ventricular chamber while maintaining functional pumping efficiency.
4. **Group 4:** This final group consists of patients who show both an increase in LVEDV by 20% or more and a significant reduction in LVEF (an absolute decrease of more than 5%). This group represents the most pronounced form of LV remodelling, involving both dimensional and functional cardiac alteration**s.**

3.10.15. Diastolic dysfunction

Diastolic dysfunction was defined and categorized according to the ASE 2016 algorithm and definitions [335]. The grading system is as follows:

1. **Grade I dysfunction or normal LV filling pressure:** This is identified by an E/A ratio of 0.8 or lower, coupled with a peak E velocity not exceeding 50 cm/s, indicating normal diastolic function or mild diastolic dysfunction.
2. **Intermediate diastolic dysfunction (Grade II):** For E/A ratios between 0.8 and 2, the assessment requires additional parameters: average E/e', tricuspid regurgitant peak velocity (TRpV), and left atrial volume index (LAVI). A diagnosis of grade II dysfunction, suggestive of elevated LV filling pressures, is made if two or three of these parameters are positive. Conversely, if two or three parameters are negative, grade I dysfunction with normal filling pressures is indicated.
3. **Mixed diastolic dysfunction:** In cases where the readings of the supplementary parameters are mixed, the pulmonary vein S/D ratio is considered. A ratio less than 1 indicates grade II diastolic dysfunction, implying increased LV filling pressures.
4. **Advanced diastolic dysfunction (Grade III):** An E/A ratio exceeding 2 is indicative of grade III diastolic dysfunction, representing significantly elevated LV filling pressures.

3.10.16. Major adverse cardiac events and patient-oriented composite endpoint

MACE was defined comprehensively to include both POCE and hospitalization due to heart failure. This definition aligns with the aim to capture a wide spectrum of significant adverse cardiac outcomes post-intervention. The POCE itself was defined in accordance with the Academic Research Consortium (ARC) II consensus, which encompasses a collective of critical events: all-cause mortality, any instance of myocardial infarction, any revascularization procedures undertaken (including target vessel revascularization), and strokes [348].

3.11. Ethics

3.11.1. Ethical compliance and approval

This research was meticulously designed and executed in full compliance with the ethical standards outlined in the Declaration of Helsinki. The study received ethical approval from the Kaunas Regional Biomedical Research Ethics Committee, in the Republic of Lithuania. The committee recognized and sanctioned the study's methodologies, objectives, and implications, granting approval under reference number BE-2-5. This endorsement, received in January 2021, underscored the study's adherence to the highest ethical standards in biomedical research.

3.11.2. Informed consent process

A cornerstone of our ethical conduct was the informed consent process. Every participant, or their legal representatives where applicable, was provided with comprehensive information about the study. This included a detailed explanation of the study's purpose, the procedures involved, potential risks and benefits, and the confidentiality measures in place to protect their privacy. After ensuring understanding and addressing any queries, written informed consent was obtained from each participant or their legal representative. This process not only adhered to ethical guidelines but also fostered trust and transparency between the researchers and the participants.

3.11.3. Data privacy and confidentiality measures

We took stringent measures to uphold the privacy and confidentiality of all participants. From the outset, data anonymization protocols were rigorously applied. All identifying information was detached from the datasets to ensure that individual participants could not be identified in any published

material. Data storage and handling were conducted under strict security protocols to prevent unauthorized access and ensure data integrity. These measures reflect our unwavering commitment to protecting participant confidentiality and upholding ethical research practices.

3.11.4. Registration and compliance with regulations

In an effort to maintain transparency and public trust, our study was registered in the clinical trials registry, bearing the identifier NCT05406297. This registration provided a public record of our study, facilitating its accessibility and scrutiny by the broader scientific community and the public. It also served as a testament to our commitment to ethical standards and regulatory compliance in clinical research.

3.12. Data analysis: statistical analysis and software

3.12.1. Overview

In this doctoral research, various statistical methods were employed to analyze data across different studies. The methods chosen were contingent on the nature of the data, which included continuous and categorical variables, and the specific requirements of each analysis. The overarching goal was to provide a rigorous and detailed statistical examination of the findings, ensuring the reliability and validity of the results.

3.12.2. Data presentation and comparison

Continuous variables, depending on their distribution, were presented either as means with standard deviations (SD) or medians with interquartile ranges (IQR). Categorical variables were consistently represented as frequencies and percentages. To compare these variables between different study groups, a suite of tests was utilized. The choice of test – Student's t-test, Mann–Whitney U test, Wilcoxon Rank sum test, Chi-square test, or Fisher's exact test – was based on the type of data (continuous or categorical) and its distribution.

3.12.3. Multivariable analysis

A key aspect of the analysis involved the creation of multivariable logistic regression models. These models were instrumental in identifying procedural factors associated with CMD, LV diastolic dysfunction, and functional LV remodelling. For this, stepwise selection was employed. Similarly, multivariable Cox regression models were utilized to calculate hazard ratios for MACE per unit increase of specific indicators like TMAO, FFR,

and MRR. All models were adjusted for pertinent patient demographics, medical history, clinical course, laboratory values, and angiographic characteristics, with a significance level of $p < 0.05$ for inclusion.

3.12.4. Survival analysis

Kaplan-Meier analysis was a pivotal tool in assessing MACE-free survival rates across the studies. Differences in survival rates were evaluated using the log-rank test. This method provided a non-parametric estimation of survival probabilities, allowing for a clear visual representation of survival data over time.

3.12.5. Dose-response relationships and receiver operating characteristic curve analysis

To explore the dose-response relationships between variables like TMAO, CMD, and MACE, restricted cubic spline curves were created. Additionally, Receiver Operating Characteristic (ROC) curve analysis, supplemented with the Delong test and Youden index, was employed. This was particularly useful in identifying optimal cutoffs for indicators like TMAO, FFR, IMR, CFR, and MRR. This analysis provided a robust method for assessing the diagnostic performance of these indicators.

3.12.6. Data collection and descriptive statistics for the machine learning approach

The study involved data collection from patients over two distinct time periods: from January 12, 2021, to July 31, 2022, and from August 1, 2022, to January 31, 2023. In these cohorts, descriptive statistics were computed to provide an initial overview of the data. For quantitative variables, this included calculating the mean, SD, median, first and third quartiles (Q1, Q3), and range (minimum to maximum). Categorical variables were presented in terms of frequencies and percentages. To discern any significant differences (p-value < 0.05) between subpopulations, data were stratified based on qualitative variables and analyzed using the Wilcoxon Rank Sum test for quantitative variables, the Ordered test for ordinal variables, and the Fisher exact test for qualitative variables.

3.12.7. Objective and model selection for the machine learning approach

The primary objective was to predict the presence or absence of CMD in STEMI patients using selected biomarkers (covariates collected at baseline). Various models were estimated and compared on the first sample (the training set) which comprised 149 patients (74.5% of the entire sample), to identify the most accurate one.

3.12.8. Multicollinearity check and data balancing for the machine learning approach

A crucial step involved checking for multicollinearity in the data using Spearman correlations (ρ_s) between pairs of quantitative variables, visualized through a correlation plot. The plot used a color-coded system to indicate the nature and intensity of correlations. To address the moderate prevalence of CMD in the training set, which could lead to biased predictions, a sophisticated oversampling method called SMOTE (Synthetic Minority Over-sampling Technique) was used to balance the dataset.

3.12.9. Machine learning algorithms and model comparison

The focus was on Machine Learning algorithms due to their suitability in handling classification problems with correlated covariates and outliers. Ensemble methods like Random Forest (RF), Gradient Boosting Machine (GBM), Support Vector Machines (SVM), XGBoost algorithm, Super Learner, and Discrete Super Learner (Discrete SL) were applied to the balanced dataset. Their performance was evaluated using 10-fold Cross-Validation (CV) risk estimates, and comparisons were made against classical Logistic regression and a meta-learner (SL.mean) to identify the best performing model.

3.12.10. Model validation and tools for interpretation for the machine learning approach

RF emerged as the best predictor, and its AUC was compared with competing models using the DeLong test. To further understand the relationship between covariates and the outcome, the RF model provided two tools: the relative Variable Importance Measure (relVIM) and the 3D Partial Dependence Plot (3D-PDP). The relVIM was represented using a lollipop plot, and the 3D-PDP visualized the joint variation of the three most important covariates in predicting CMD risk.

3.12.11. Model testing and performance metrics for the machine learning approach

The RF model, trained on SMOTE data, was then tested on the second sample to evaluate its performance on new data and to check for overfitting. This was complemented by comparing its accuracy to an RF model estimated on the original data using the DeLong test and analyzing Out-Of-Bag (OOB) errors. Performance metrics such as Accuracy (95% CI), Sensitivity, Specificity, Positive Predicted Value, Negative Predictive Value, and Precision were reported for the RF models on both the balanced training set and the test set.

3.12.12. Significance level and software

Throughout the analysis, a probability level of $p < \alpha$, with α set at 0.05, was used to determine statistical significance. This standard threshold ensured a balance between sensitivity and the risk of type I error. Data processing and analysis were performed using IBM SPSS Statistics 27, and for specific tasks, R (version 4.1.3) on R Studio (Build 576) software was utilized. These tools provided a comprehensive platform for statistical analysis, ensuring accuracy and efficiency in handling large datasets.

4. RESULTS

4.1. The impact of percutaneous coronary intervention strategies during ST-elevation myocardial infarction on the prevalence of coronary microvascular dysfunction

4.1.1. Study population characteristics

This cohort was stratified based on stenting strategy (direct stenting *vs.* balloon pre-dilatation followed by stenting). Two hundred and ten patients were included in the study, of which 98 patients (46.66%) underwent direct stenting and 112 patients (53.33%) did undergo balloon pre-dilatation followed by stenting. In total 125 males took part in the study, which accounts for 59.52% of the total population of the study; however, there were no differences in gender between the two groups of participants in the study. The study population's median age was 65 years, with an interquartile range of 58 to 76 years. While patients undergoing direct stenting tended to be older, with a median age of 67 years, the age difference between the two groups participating in the study was not statistically significant. Between these two groups, there was no discernible difference in terms of body mass index, body surface area, or the location of STEMI events. It is essential to take note of the fact that 51 participants, or 24.29% of the total population of the study, were diagnosed with diabetes; despite this, diabetics were almost equally distributed between the two groups. A total of 109 patients, representing 51.90% of the study's STEMI population, were identified as current or former smokers. Despite this, smokers were almost evenly distributed across study groups. The baseline CHADS2-VASc score was relatively comparable across study groups. The two groups did not differ from one another in any of the risk factors, such as arterial hypertension, dyslipidemia, Killip classification, or a history of alcohol abuse, stroke and CAD. In conclusion, patients within the study groups were fairly similar, with no statistically significant differences in terms of general characteristics (Table 4.1.1.1).

Table 4.1.1.1. *Characteristics of ST-elevation myocardial infarction patients classified by percutaneous coronary intervention technique*

Characteristic	Overall (n =210)	Direct stenting (n = 98)	Balloon pre-dilatation stenting (n = 112)	*p*-value
Sex (Female)	85 (40.48%)	35 (35.71%)	50 (44.64%)	0.240
Age (years)	65.0 [58, 76]	67.0 [58.25, 76.0]	63.50 [56.0, 75.0]	0.477
Body mass index (kg/m^2)	27.39 [24.56, 30.69]	27.71 [25.32, 30.60]	26.38 [24.29, 31.10]	0.443
Body surface area (m^2)	1.93 [1.81, 2.10]	1.94 [1.81, 2.10]	1.92 [1.83, 2.12]	0.768
Primary diagnosis				
Anterior STEMI	116 (55.24%)	53 (54.08%)	63 (56.25%)	0.860
Inferior STEMI	94 (44.76%)	45 (45.92%)	49 (43.75%)	
Arterial hypertension	123 (58.57%)	58 (59.18%)	65 (58.04%)	0.978
History of coronary artery disease	59 (28.10%)	27 (27.55%)	32 (28.57%)	0.992
History of PCI	26 (12.38%)	11 (11.22%)	15 (13.39%)	0.790
History of stroke	27 (12.86%)	11 (11.22%)	15 (13.39%)	0.649
History of diabetes mellitus	51 (24.29%)	21 (21.43%)	30 (26.79%)	0.458
History of dyslipidemia	119 (56.67%)	60 (61.22%)	59 (52.68%)	0.268
Smoker (former/current)	109 (51.90%)	51 (52.04%)	58 (51.79%)	1
History of alcohol abuse	20 (9.52%)	8 (8.16%)	12 (10.71%)	0.695
Baseline CHADS2-VASc score	3 [2, 4]	3 [2, 4]	3 [2, 4]	0.851
KILLIP class				
I	62 (29.52%)	27 (27.55%)	35 (31.25%)	0.519
II	111 (52.86%)	53 (54.08%)	58 (51.79%)	
III	27 (12.86%)	15 (15.31%)	12 (10.71%)	
IV	10 (4.76%)	3 (3.06%)	7 (6.25%)	

STEMI – ST elevation myocardial infarction; PCI – Percutaneous Coronary Intervention. Values are n (%) or median [IQR].

4.1.2. Laboratory findings

There was no noticeable difference between the study groups based on the findings of the complete blood count that was performed. The levels of hemoglobin, white blood cell count, and platelet count all diverged from one another in the same proportion across the two study groups. Direct stenting group had a higher TC level than the balloon pre-dilatation followed by stenting group, this difference was significant enough to reach the level of statistical significance (5.06 mmol/L *vs.* 4.43 mmol/L; $p = 0.035$). In a similar vein, the level of low-density lipoprotein showed a tendency to be higher in

the group that received direct stenting; however, this tendency achieved statistical significance (3.51 mmol/L *vs.* 3.17 mmol/L; $p = 0.047$). Creatinine clearance did not show a significant difference between the two study groups (40.45 mL/min *vs.* 38.2 mL/min; $p = 0.121$). Neither group showed significant differences in troponin levels between samples taken upon admission and after 24 hours. In addition, the values of platelet aggregation with adenosine diphosphate, which reflect the effect of platelet aggregation inhibitors, did not differ significantly between the two study groups (26.5 *vs.* 28.5; $p = 0.341$) (Table 4.1.2.1).

4.1.3. Echocardiographic findings

There was no statistically significant difference between the two groups in terms of LVEF assessed after primary PCI (42.00% *vs.* 40.00%; $p = 0.913$), nonetheless, this was short-lived, as the LVEF in the direct stenting group recovered significantly faster at one year follow-up (48.00% *vs.* 45.00%; $p = 0.003$) (Table 4.1.2.1).

Table 4.1.2.1. *Laboratory and echocardiographic parameters of patients with ST-elevation myocardial infarction, categorized by percutaneous coronary intervention technique*

Parameters	Overall (n = 210)	Direct stenting (n = 98)	Balloon pre-dilatation stenting (n = 112)	*p*-value
Laboratory test				
Hemoglobin (g/L)	136.0 [119.0, 148.0]	137.0 [121.0, 146.8]	135.0 [118.0, 148.3]	0.631
White blood cell count ($\times 10^9$/L)	9.86 [8.22, 12.09]	9.78 [8.09, 12.07]	10.05 [8.38, 12.10]	0.742
Platelets ($\times 10^9$/L)	240.5 [204.0, 273.0]	242.0 [212.5, 273.8]	240.0 [200.0, 271.5]	0.635
Total cholesterol (mmol/L)	4.64 [3.75, 5.79]	5.06 [4.07, 6.01]	4.43 [3.60, 5.57]	***0.035***
Low-density lipoprotein (mmol/L)	3.26 [2.37, 4.31]	3.51 [2.66, 4.46]	3.17 [2.23, 4.08]	***0.047***
High-density lipoprotein (mmol/L)	1.12 [0.92, 1.35]	1.11 [0.94, 1.36]	1.13 [0.91, 1.32]	0.568
Triglycerides (mmol/L)	1.16 [0.82, 1.65]	1.11 [0.82, 1.72]	1.17 [0.85, 1.57]	0.896
Creatinine clearance (mL/min)	39.5 [34.95, 47.5]	40.45 [35.28, 48.68]	38.20 [34.80, 47.10]	0.121
Basal troponin I (μg/L)	2.19 [0.81, 3.71]	2.22 [0.96, 3.89]	2.18 [0.76, 3.29]	0.427
Peak troponin I (μg/L)	45.0 [27.0, 64.0]	42.0 [26.25, 67.75]	46.0 [28.0, 62.0]	0.830
High-sensitivity C-reactive protein (mg/L)	3.80 [1.85, 10.52]	4.22 [1.85, 10.06]	3.66 [1.94, 10.77]	0.872

Table 4.1.2.1. *Laboratory and echocardiographic parameters of patients with ST-elevation myocardial infarction, categorized by percutaneous coronary intervention technique*

Parameters	Overall (n = 210)	Direct stenting (n = 98)	Balloon pre-dilatation stenting (n = 112)	*p*-value
Echocardiographic parameters				
Post-PCI left ventricular ejection fraction (%)	40.0 [36.25, 45.75]	42.0 [38.5, 45.0]	40.0 [35.75, 46.25]	0.913
12-month left ventricular ejection fraction (%)	45.0 [40.0, 50.0]	48.0 [40.0, 55.0]	45.0 [35.0, 50.0]	**0.003**

CMD – Coronary microvascular dysfunction; PCI – percutaneous coronary intervention. Values are n (%) or median [IQR]. In bold and italics significant *p*-values (< 0.05).

4.1.4. Angiographic findings

The overall time it took patients to seek medical attention after the onset of symptoms did not differ significantly between the two groups (348 min *vs.* 278.5 min; $p = 0.166$). Similarly, the time it took medical personnel to diagnose, respond, and revascularize the culprit vessel did not vary significantly between study groups (41.50 min *vs.* 39.00 min; $p = 0.318$). TIMI flow both before and after PCI was nearly evenly distributed across study groups. Despite the fact that the left anterior descending artery was identified as the culprit vessel in the majority of STEMI patients 118 (56.19%), this did not make a significant difference because the distribution was relatively close in both study groups (54.08% *vs.* 58.04%; $p = 0.771$). In the investigation, patients presenting with single vessel disease were systematically excluded, while the cohort predominantly comprised individuals diagnosed with two-vessel disease, accounting for 58.57% of the sample; conversely, the remaining 41.43% manifested three-vessel disease, with no statistically significant disparity observed in the distribution of these pathologies between the between the direct stenting group and the balloon pre-dilatation followed by stenting group ($p = 0.801$) (Table 4.1.4.1).

Table 4.1.4.1. *Coronary angiography and physiology parameters of ST-elevation myocardial infarction patients, categorized by percutaneous coronary intervention technique*

Parameters	Overall (n = 210)	Direct stenting (n = 98)	Balloon pre-dilatation stenting (n = 112)	*p*-value
Angiographic				
Pain-to-door time (minutes)	314 [107.75, 592.25]	348.0 [112.0, 677.75]	278.5 [108.75, 460.25]	0.166
Door-to-balloon (minutes)	40 [29.25, 52.0]	41.5 [31.0, 51.75]	39.0 [29.0, 52.25]	0.318
Pre-PCI TIMI flow				
0	130 (61.90%)	55 (56.12%)	75 (66.96%)	0.305
1	8 (3.81%)	3 (3.06%)	5 (4.46%)	
2	44 (20.95%)	25 (25.51%)	19 (16.96%)	
3	28 (13.33%)	15 (15.31%)	13 (11.61%)	
Post-PCI TIMI flow				
0	2 (0.95%)	1 (1.02%)	1 (0.89%)	0.824
1	1 (0.48%)	0 (0.0%)	1 (0.89%)	
2	22 (10.48%)	10 (10.20%)	12 (10.71%)	
3	185 (88.1%)	87 (88.78%)	98 (87.50%)	
Culprit Vessel				
Left anterior descending artery	118 (56.19%)	53 (54.08%)	65 (58.04%)	0.771
Circumflex artery	49 (23.33%)	25 (25.51%)	24 (21.43%)	
Right coronary artery	43 (20.48%)	20 (20.41%)	23 (20.54%)	
Number of diseased vessels				
2-vessel disease	123 (58.57%)	56 (57.14%)	67 (59.82%)	0.801
3-vessel disease	87 (41.43%)	42 (42.86%)	45 (40.18%)	
Intracoronary interventions				
Intracoronary heparin infusion	104 (49.52%)	56.0 (57.14%)	48.0 (42.86%)	0.054
Intracoronary glycoprotein IIb/IIIa inhibitor	46 (21.9%)	21.0 (21.43%)	25.0 (22.32%)	1
Aspiration thrombectomy	52 (24.76%)	25.0 (25.51%)	27.0 (24.11%)	0.940
Stent diameter (millimeters)	3.0 [3.0, 3.5]	3.0 [3.0, 3.5]	3.0 [3.0, 3.5]	0.699

Table 4.1.4.1. *Continued*

Parameters	Overall (n = 210)	Direct stenting (n = 98)	Balloon pre-dilatation stenting (n = 112)	*p*-value
Stent length (millimeters)	24.0 [19.0, 26.0]	24.0 [19.0, 26.0]	24.0 [19.0, 26.0]	0.293
Maximal stent pressure (atm)	14.0 [14.0, 16.0]	15.0 [14.0, 17.0]	14.0 [13.0, 16.0]	0.160
Contrast dose (milliliters)	100.0 [90.0, 110.0]	100.0 [90.0, 110.0]	100.0 [90.0, 111.25]	0.262
Coronary physiology at 3-month follow-up				
Coronary flow reserve	2.81 [2.54, 2.98]	2.87 [2.65, 3.14]	2.70 [2.16, 2.95]	***0.003***
Fractional flow reserve	0.92 [0.87, 0.97]	0.92 [0.87, 0.97]	0.92 [0.86, 0.97]	0.452
Index of Microcirculatory resistance	20 [15.0, 29.0]	19.5 [14.0, 22.0]	22.0 [15.0, 42.0]	***0.001***
Coronary microvascular dysfunction	57 (27.14%)	12.0 (12.24%)	45.0 (40.18%)	***< 0.001***

PCI – percutaneous coronary intervention; TIMI – Thrombolysis in Myocardial Infarction. Values are n (%) or median [IQR]. In bold and italics significant *p*-values (< 0.05).

4.1.5. Procedural characteristics

The intracoronary administration of heparin was utilized in 104 STEMI patients, which is equivalent to 49.52% of all study participants. These patients were nearly evenly distributed between the groups undergoing direct stenting and balloon pre-dilatation followed by stenting (57.14% *vs.* 42.86%; $p = 0.054$). Despite the fact that only 46 (21.9%) of the patients who participated in the study were given an intracoronary glycoprotein IIb/IIIa inhibitor, the distribution of these patients was comparable between the two study groups 21.43% *vs.* 22.32%; $p = 1$). Aspiration thrombectomy was performed on 52 patients, representing 24.76% of the study population; this technique was used roughly equally in both groups (25.51% *vs.* 24.11%; $p = 0.940$). There were no significant differences in the study groups with regard to contrast dose, stent diameter and length, or maximal inflation pressure (Table 4.1.4.1).

4.1.6. Coronary physiology findings

Insignificantly greater CFR was observed in patients who underwent direct stenting compared to those who were stented after balloon pre-dilatation (2.87 *vs.* 2.70; $p = 0.003$) (Fig. 4.1.6.1, Table 4.1.4.1). The FFR values of patients who had direct stenting were similar to those of patients who underwent balloon pre-dilatation followed by stenting (0.92 *vs.* 0.92; $p = 0.452$). Patients who underwent revascularization with direct stenting rather than balloon pre-dilatation followed by stenting method had an IMR that was significantly lower (19.5 *vs.* 22.0; $p = 0.001$) (Fig. 4.1.6.2, Table 4.1.4.1). After undergoing coronary physiology testing, 57 patients (27.14%) were diagnosed with CMD. However, patients who underwent direct stenting were less likely to suffer from CMD compared to those who were treated using balloon pre-dilatation followed by stenting method (12.24% *vs.* 40.18%; $p < 0.001$) (Fig. 4.1.6.3, Table 4.1.4.1).

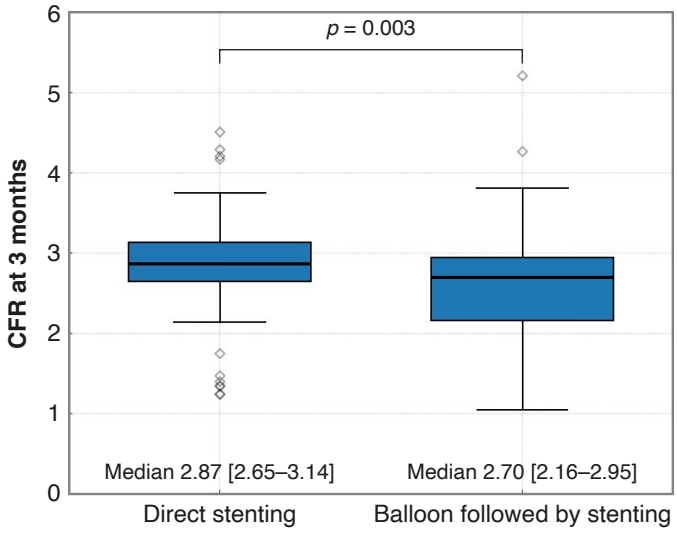

Fig. 4.1.6.1. *Distribution of coronary flow reserve displayed by percutaneous coronary intervention technique*

CFR – coronary flow reserve.

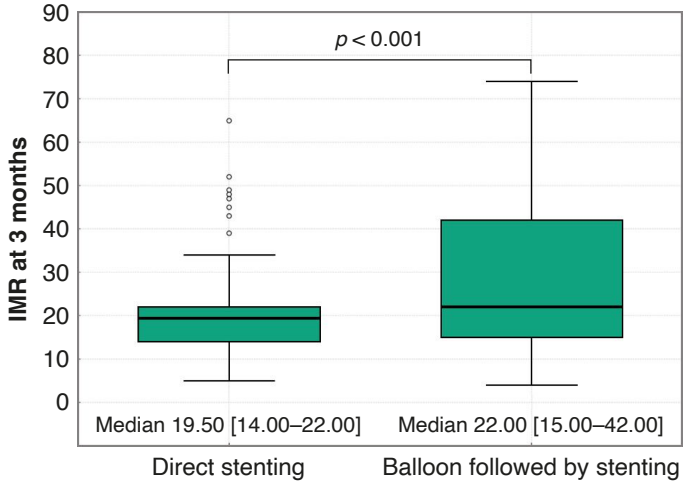

Fig. 4.1.6.2. *Distribution of index of microcirculatory resistance displayed by percutaneous coronary intervention technique*

IMR – index of microcirculatory resistance.

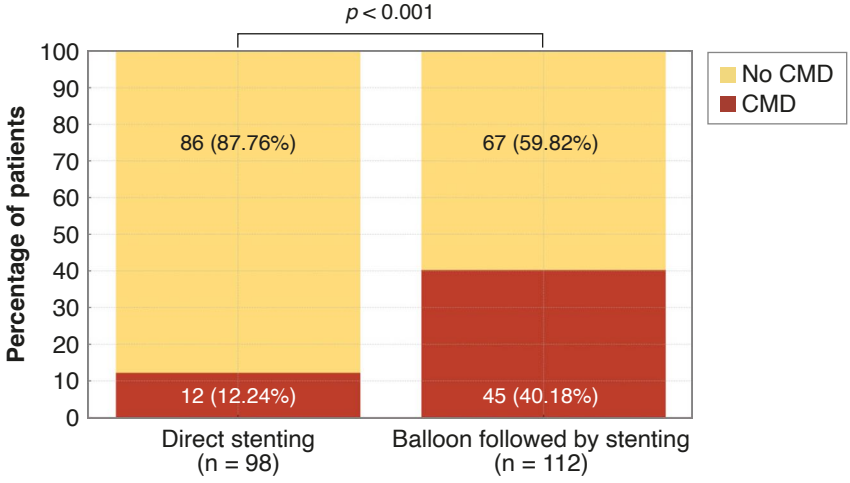

Fig. 4.1.6.3. *Prevalence of coronary microvascular dysfunction displayed by percutaneous coronary intervention technique*

CMD – coronary microvascular dysfunction.

4.1.7. Clinical outcome

The incidence of new onset atrial fibrillation displayed a clear tendency to be higher in the balloon pre-dilatation followed by stenting group (15.18%) compared to the direct stenting group (6.12%), though this difference approached but did not reach statistical significance with a *p*-value of 0.061 (Table 4.1.7.1). All individual components of MACE, such as non-fatal MI, cardiovascular death, and heart failure hospitalization, were numerically more prevalent in the balloon pre-dilatation followed by stenting group compared to the direct stenting group, but these differences did not achieve statistical significance. However, the incidence of stroke was significantly higher in the balloon pre-dilatation followed by stenting group (0 *vs.* 6.25%; $p = 0.033$). While the rate of target vessel revascularization was numerically greater in the direct stenting group, this difference was not statistically significant. During the course of the follow-up, the overall rates of MACE were 20.95%. We found that the rate of MACE in patients treated with balloon pre-dilatation followed by stenting was significantly higher than the rate of MACE in patients treated with direct stenting over a period of 12 months (14.29% *vs.* 26.76%; $p = 0.040$) (Fig. 4.1.7.1).

Table 4.1.7.1. *Twelve-month clinical outcomes of patients presenting with ST-elevation myocardial infarction, categorized by percutaneous coronary intervention technique*

	Overall (n = 210)	**Direct stenting (n = 98)**	**Balloon pre-dilatation stenting (n = 112)**	***p*-value**
New onset atrial fibrillation	23 (10.95%)	6 (6.12%)	17 (15.18%)	0.061
Ischemic stroke	7 (3.33%)	0 (0%)	7 (6.25%)	***0.033***
Nonfatal MI	10 (4.76%)	3 (3.06%)	7 (6.25%)	0.448
Cardiovascular death	6 (2.86%)	1 (1.02%)	5 (4.46%)	0.280
Target vessel revascularization	10 (4.76%)	6 (6.12%)	4 (3.57%)	0.588
Decompensated HF requiring hospitalization	16 (7.62%)	5 (5.10%)	11 (9.82%)	0.305
MACE	44 (20.95%)	14 (14.29%)	30 (26.79%)	***0.040***

MI – myocardial infarction, HF – heart failure, MACE – the composite of stroke, nonfatal myocardial infarction, revascularization, heart failure hospitalization, and cardiovascular death. Values are n (%) or median [IQR]. In bold and italics significant *p*-values (< 0.05).

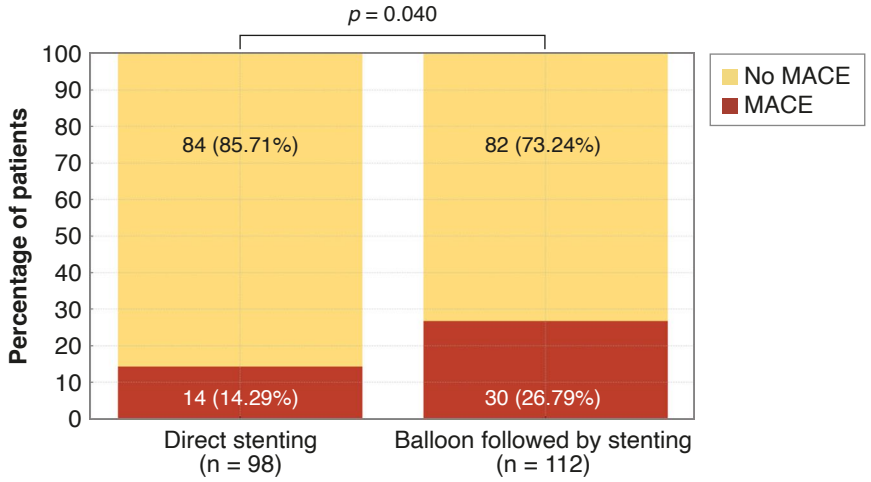

Fig. 4.1.7.1. *Rates of major adverse cardiovascular events displayed by percutaneous coronary intervention technique*

MACE – major adverse cardiovascular events.

The Kaplan-Meier curve revealed an increased incidence of MACE in patients who underwent balloon pre-dilatation stenting (log-rank $p = 0.048$), most noticeably starting at 6 months post-PCI (Fig. 4.1.7.2).

A sensitivity analysis examining the incidence of MACE at 12 months according to IMR category revealed a lower incidence of MACE in patients with an IMR < 25, when compared to those with a $25 \leq IMR \leq 40$ ($p < 0.001$) and those with an IMR > 40 ($p < 0.001$). These was no difference in the incidence of MACE at 12 months in patients with an $25 \leq IMR \leq 40$ and those with an IMR > 40 ($p = 0.352$) (Fig. 4.1.7.3).

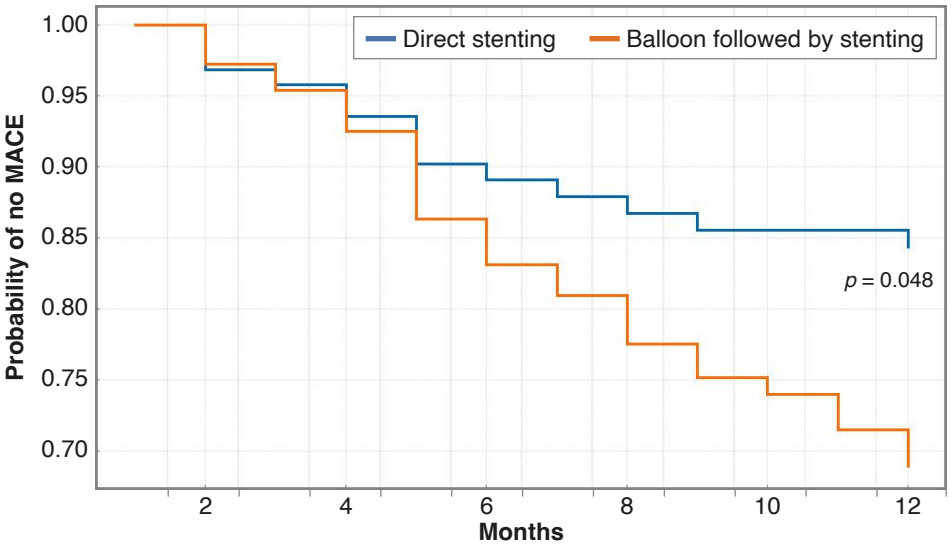

Number at risk (direct stenting)												
98	98	98	98	98	98	91	91	91			91
Number at risk (balloon followed by stenting)												
112	110	110	110	110	108	108	108	108	108	108	108

Fig. 4.1.7.2. *Kaplan-Meier event-free survival curve for occurrence of major adverse cardiovascular events, patients grouped by percutaneous coronary intervention technique*

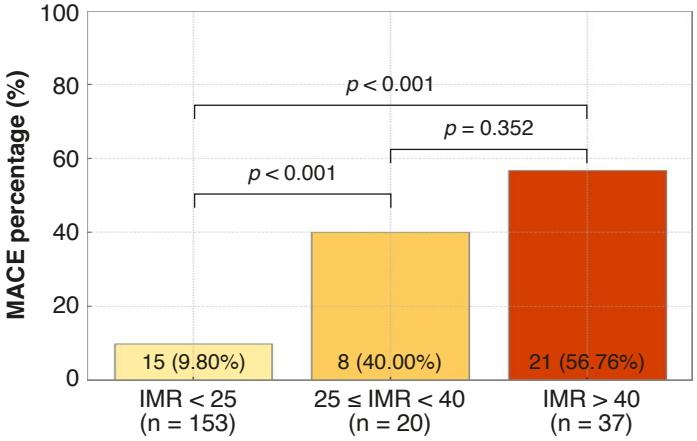

Fig. 4.1.7.3. *Sensitivity analysis examining the incidence of major adverse cardiovascular events at 12 months according to index of microcirculatory resistance category*

MACE – major adverse cardiovascular events; IMR – index of microcirculatory resistance.

4.1.8. Multivariable logistic analysis

The multivariable logistic regression analysis revealed that direct stenting, aspiration thrombectomy, and utilization of glycoprotein IIb/IIIa jointly yielded a ROC AUC of 0.79 (0.71–0.86), indicating a good predictive ability in the binary logistic multivariable analysis (Fig. 4.1.8.1).

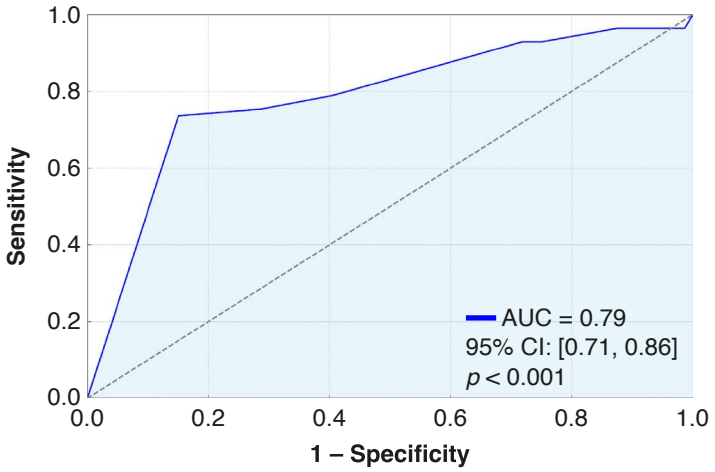

Fig. 4.1.8.1. *Receiver operating characteristic curve for the model of coronary microvascular dysfunction in ST-elevation myocardial infarction patients*

AUC – area under the receiver operating characteristic curve; CI – confidence interval.

In this particular model, we were able to determine that the use of direct stenting as opposed to balloon pre-dilatation before stenting, the utilization of aspiration thrombectomy, and the administration of intracoronary glycoprotein IIb/IIIa were associated with decreased odds of CMD (odds ratio (OR): 0.184, 95% confidence interval (CI): 0.085–0.396, $p < 0.001$), (OR: 0.113, 95% CI: 0.032–0.399, $p = 0.001$), and (OR: 0.175, 95% CI: 0.062–0.495, $p = 0.001$), respectively (Table 4.1.8.1, Fig. 4.1.8.2).

Table 4.1.8.1. *Multivariable binary logistic analysis for prediction of coronary microvascular dysfunction after ST-segment elevation myocardial infarction event*

Effect	Odds ratio	95% confidence limits		*p*-value
Direct stenting *vs.* balloon pre-dilatation stenting	0.184	0.085	0.396	***< 0.001***
Aspiration thrombectomy	0.175	0.062	0.495	***0.001***
Glycoprotein IIb/IIIa	0.113	0.032	0.399	***0.001***

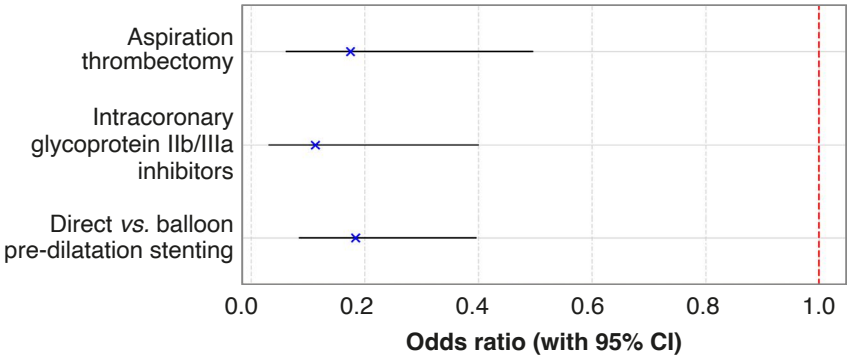

Fig. 4.1.8.2. *Forest plot for the outcome of coronary microvascular dysfunction*

CI – confidence interval.

4.2. Prediction of coronary microvascular dysfunction in ST-elevation myocardial infarction patients via a machine learning approach

4.2.1. Study flow-chart and data set overview

This analysis dataset encompassed data from 200 patients, characterized by a spectrum of 30 variables. This included 12 clinical variables, 17 quantitative biomarkers, and their respective CMD diagnoses (categorized as either No CMD or CMD). Within the timeframe of January 12, 2021, to July 31, 2022, data were collected from 149 patients. Out of this group, 44 individuals (29.5%) were identified with CMD. These 44 cases formed the basis of the training dataset used for developing a CMD risk score through sophisticated machine learning algorithms. Subsequently, an additional cohort of 49 patients was compiled from August 1, 2022, to January 31, 2023. Within this latter group, CMD was diagnosed in 7 patients (13.7%), and this cohort served as the test sample for evaluating the accuracy and generalizability of the Machine Learning-derived CMD risk score, particularly in scenarios where the prevalence of CMD differs from that of the training dataset.

The study's methodology unfolds in a structured manner, beginning with the establishment of the composition and prevalence of the training and test sets. It then moves to the rebalancing method, followed by the identification of specified outcomes and covariates. The process advances with the application of ensemble methods to derive the CMD risk score and ends with the execution of the testing procedure. This sequential approach is visualized in Fig. 4.2.1.1, offering a clear and concise overview of the study's analytical framework.

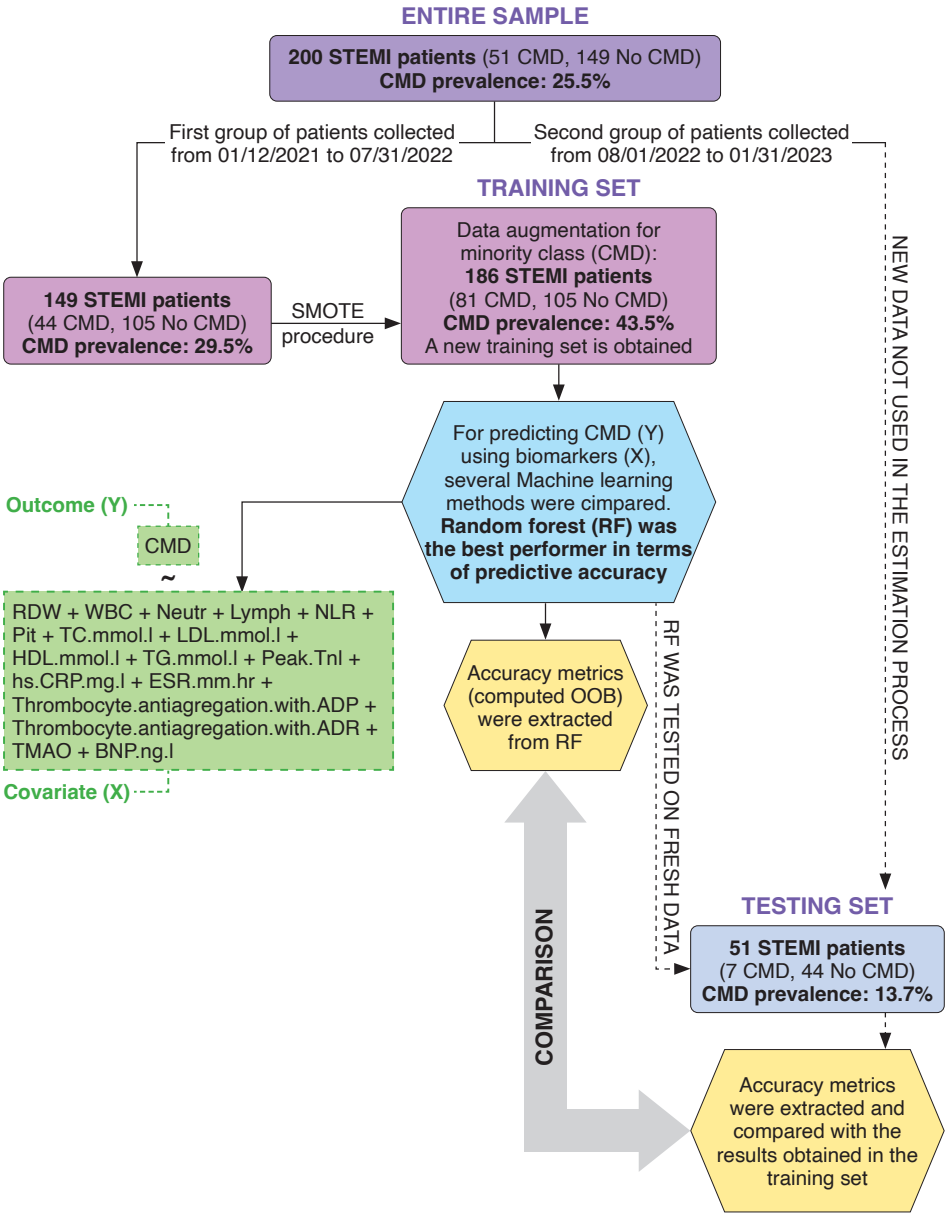

Fig. 4.2.1.1. *Flow-chart of the data and the empirical analyses applied in the study*

STEMI – ST-elevation myocardial infarction; CMD – coronary microvascular dysfunction; SMOTE – synthetic minority over-sampling technique; OOB – out-of-bag; RF – random forest; RDW – red cell distribution width; WBC – white blood cells; Neutr – neutrophil; Lymph – lymphocytes; NLR – neutrophil-to-lymphocyte ratio; PLT – platelets; TC – total cholesterol; LDL – low-density lipoprotein; HDL – high-density lipoprotein; TG – triglycerides; Peak TnI – peak troponin I; hs-CRP – high sensitivity C-reactive protein; ESR – erythrocyte sedimentation rate; ADP – adenosine diphosphate; ADR – epinephrine; BNP – B-type natriuretic peptide; TMAO – trimethylamine N-oxide.

4.2.2. Descriptive analysis of clinical variables in the training and testing sets

Descriptive statistics of the 12 clinical variables within the training set are delineated in Table 4.2.2.1, stratified based on CMD status (No/Yes). Complementarily, Table 4.2.2.2 details the descriptive statistics for the test set. Analysis of Table 4.2.2.1 indicates a significant elevation in the percentage of female patients and those diagnosed with diabetes mellitus among CMD cases, with respective *p*-values of 0.012 and 0.021. Concordant findings are observed in the test sample, as shown in Table 4.2.2.2, where the variables gender and diabetes mellitus exhibit *p*-values less than 0.01, affirming the trends observed in the training set.

Table 4.2.2.1. *Training set characteristics of patients with ST-elevation myocardial infarction stratified by coronary microvascular dysfunction*

Variables	Total (N = 149)	CMD (N = 44)	No CMD (N = 105)	*p*-value
Age (years)				
Mean (SD)	66.70 (11.80)	65.16 (11.25)	67.35 (12.02)	0.302
Median (Q1, Q3)	66.00 (59.00, 76.00)	63.00 (57.75, 73.00)	68.00 (59.00, 76.00)	
Range	41.00–93.00	46.00–91.00	41.00–93.00	
Gender				
Male	85 (57.0%)	18 (40.9%)	67 (63.8%)	***0.012***
Female	64 (43.0%)	26 (59.1%)	38 (36.2%)	
Body mass index (kg/m^2)				
Mean (SD)	28.26 (5.33)	27.57 (5.03)	28.55 (5.45)	0.307
Median (Q1, Q3)	27.78 (24.98, 30.64)	27.26 (24.48, 29.41)	28.26 (25.25, 30.93)	
Range	0.00–43.73	19.15–43.73	0.00–42.87	
History of arterial hypertension				
No	61 (40.9%)	20 (45.5%)	41 (39.0%)	0.472
Yes	88 (59.1%)	24 (54.5%)	64 (61.0%)	
History of coronary artery disease				
No	105 (70.5%)	29 (65.9%)	76 (72.4%)	0.438
Yes	44 (29.5%)	15 (34.1%)	29 (27.6%)	
History of PCI				
No	128 (85.9%)	37 (84.1%)	91 (86.7%)	0.797
Yes	21 (14.1%)	7 (15.9%)	14 (13.3%)	
History of stroke				
No	129 (86.6%)	39 (88.6%)	90 (85.7%)	0.794
Yes	20 (13.4%)	5 (11.4%)	15 (14.3%)	

Table 4.2.2.1. *Continued*

Variables	Total (N = 149)	CMD (N = 44)	No CMD (N = 105)	*p*-value
History of diabetes mellitus				
No	112 (75.2%)	27 (61.4%)	85 (81.0%)	***0.021***
Yes	37 (24.8%)	17 (38.6%)	20 (19.0%)	
History of dyslipidemia				
No	60 (40.3%)	19 (43.2%)	41 (39.0%)	0.715
Yes	89 (59.7%)	25 (56.8%)	64 (61.0%)	
History of alcohol abuse				
No	134 (89.9%)	41 (93.2%)	93 (88.6%)	0.554
Yes	15 (10.1%)	3 (6.8%)	12 (11.4%)	
Smoker				
Never	68 (45.6%)	16 (36.4%)	52 (49.5%)	0.259
Ex-smoker	51 (34.2%)	19 (43.2%)	32 (30.5%)	
Current smoker	30 (20.1%)	9 (20.5%)	21 (20.0%)	
CHA_2DS_2-VASc Score				
1	15 (10.1%)	5 (11.4%)	10 (9.5%)	0.909
2	33 (22.1%)	7 (15.9%)	26 (24.8%)	
3	34 (22.8%)	9 (20.5%)	25 (23.8%)	
4	36 (24.2%)	15 (34.1%)	21 (20.0%)	
5	18 (12.1%)	6 (13.6%)	12 (11.4%)	
6	10 (6.7%)	2 (4.5%)	8 (7.6%)	
7	3 (2.0%)	0 (0.0%)	3 (2.9%)	

PCI – percutaneous coronary intervention; CMD – coronary microvascular dysfunction. In bold and italics significant *p*-values (<0.05).

Table 4.2.2.2. *Test set characteristics of patients with ST-elevation myocardial infarction stratified by coronary microvascular dysfunction*

Variables	Total (N = 51)	CMD (N = 7)	No CMD (N = 44)	*p*-value
Age (years)				
Mean (SD)	65.92 (12.90)	65.29 (16.60)	66.02 (12.44)	0.890
Median (Q1, Q3)	62.00 (56.50, 76.00)	62.00 (52.50, 76.00)	62.50 (56.75, 76.00)	
Range	45.00–94.00	47.00–91.00	45.00–94.00	
Gender				
Male	34 (66.7%)	1 (14.3%)	33 (75.0%)	***0.004***
Female	17 (33.3%)	6 (85.7%)	11 (25.0%)	
Body mass index (kg/m^2)				
Mean (SD)	27.89 (6.30)	24.91 (2.14)	28.37 (6.62)	0.179
Median (Q1, Q3)	26.20 (23.98, 31.23)	24.30 (24.02, 25.96)	26.42 (23.99, 31.63)	
Range	15.96–49.54	21.71–28.38	15.96–49.54	

Table 4.2.2.2. *Continued*

Variables	Total (N = 51)	CMD (N = 7)	No CMD (N = 44)	*p*-value
History of arterial hypertension				
No	21 (41.2%)	2 (28.6%)	19 (43.2%)	0.685
Yes	30 (58.8%)	5 (71.4%)	25 (56.8%)	
History of coronary artery disease				
No	40 (78.4%)	6 (85.7%)	34 (77.3%)	1.000
Yes	11 (21.6%)	1 (14.3%)	10 (22.7%)	
History of PCI				
No	48 (94.1%)	7 (100.0%)	41 (93.2%)	1.000
Yes	3 (5.9%)	0 (0.0%)	3 (6.8%)	
History of stroke				
No	46 (90.2%)	5 (71.4%)	41 (93.2%)	0.133
Yes	5 (9.8%)	2 (28.6%)	3 (6.8%)	
History of diabetes mellitus				
No	39 (76.5%)	2 (28.6%)	37 (84.1%)	***0.005***
Yes	12 (23.5%)	5 (71.4%)	7 (15.9%)	
History of dyslipidemia				
No	26 (51.0%)	3 (42.9%)	23 (52.3%)	0.703
Yes	25 (49.0%)	4 (57.1%)	21 (47.7%)	
History of alcohol abuse				
No	47 (92.2%)	6 (85.7%)	41 (93.2%)	0.457
Yes	4 (7.8%)	1 (14.3%)	3 (6.8%)	
Smoker				
Never	24 (47.1%)	3 (42.9%)	21 (47.7%)	0.291
Ex-smoker	16 (31.4%)	1 (14.3%)	15 (34.1%)	
Current smoker	11 (21.6%)	3 (42.9%)	8 (18.2%)	
CHA_2DS_2-VASc score				
1	8 (15.7%)	0 (0.0%)	8 (18.2%)	0.925
2	7 (13.7%)	0 (0.0%)	7 (15.9%)	
3	18 (35.3%)	1 (14.3%)	17 (38.6%)	
4	9 (17.6%)	2 (28.6%)	7 (15.9%)	
5	5 (9.8%)	2 (28.6%)	3 (6.8%)	
6	4 (7.8%)	2 (28.6%)	2 (4.5%)	
7	0 (0.0%)	0 (0.0%)	0 (0.0%)	

PCI – percutaneous coronary intervention; CMD – coronary microvascular dysfunction. In bold and italics significant *p*-values (<0.05).

4.2.3. Laboratory and biomarkers analysis in the training and testing sets

In the training set, laboratory and biomarker values are categorized according to CMD and presented in Table 4.2.3.1. These quantitative variables do not exhibit a normal distribution, as demonstrated in Fig. 4.2.3.1 (A, B), with all the Shapiro-Wilk test *p*-values being less than 0.001.

Table 4.2.3.1. *Laboratory and biomarker values collected on the training set of patients with ST-elevation myocardial infarction, stratified by coronary microvascular dysfunction*

Variables (unit of measures)	**Total (N = 149)**	**CMD (N = 44)**	**No CMD (N = 105)**	***p*-value**
Red cell distribution width (%)				
Mean (SD)	13.96 (1.53)	14.50 (2.13)	13.73 (1.14)	**0.005**
Median (Q1, Q3)	13.50 (12.90, 14.50)	13.60 (12.97, 16.18)	13.50 (12.90, 14.30)	
Range	11.30–19.00	11.30–19.00	11.63–17.90	
White blood count ($\times 10^9$/L)				
Mean (SD)	9.76 (3.28)	9.91 (2.95)	9.69 (3.42)	0.705
Median (Q1, Q3)	9.48 (7.23, 12.00)	10.15 (7.43, 12.26)	8.60 (7.20, 11.68)	
Range	4.79–22.45	4.79–15.90	4.79–22.45	
Neutrophils ($\times 10^9$/L)				
Mean (SD)	7.59 (5.21)	8.80 (8.43)	7.08 (2.90)	0.066
Median (Q1, Q3)	6.90 (5.28, 8.80)	7.04 (5.68, 9.41)	6.90 (5.12, 8.72)	
Range	2.04–60.60	3.64–60.60	2.04–23.50	
Lymphocytes ($\times 10^9$/L)				
Mean (SD)	2.25 (2.80)	2.80 (4.91)	2.01 (0.98)	0.114
Median (Q1, Q3)	1.75 (1.30, 2.55)	1.75 (1.31, 2.57)	1.75 (1.30, 2.55)	
Range	0.20–33.80	0.67–33.80	0.20–5.44	
Neutrophil-to-Lymphocyte ratio				
Mean (SD)	4.63 (4.29)	4.49 (2.82)	4.68 (4.78)	0.806
Median (Q1, Q3)	3.80 (2.39, 5.77)	3.76 (2.33, 5.88)	3.80 (2.39, 5.35)	
Range	0.65–45.00	1.22–14.65	0.65–45.00	
Platelet count ($\times 10^9$/L)				
Mean (SD)	214.57 (68.60)	210.55 (68.58)	216.26 (68.86)	0.644
Median (Q1, Q3)	210.00 (168.00, 254.00)	206.50 (159.00, 252.50)	211.00 (169.00, 254.00)	
Range	70.00–404.00	80.00–368.00	70.00–404.00	
Total cholesterol (mmol/L)				
Mean (SD)	3.51 (1.15)	4.02 (1.60)	3.29 (0.82)	***< 0.001***
Median (Q1, Q3)	3.21 (2.86, 4.12)	3.77 (2.96, 4.58)	3.14 (2.76, 3.82)	
Range	1.78–8.89	1.91–8.89	1.78–5.34	

Table 4.2.3.1. *Continued*

Variables (unit of measures)	Total (N = 149)	CMD (N = 44)	No CMD (N = 105)	*p*-value
Low-density lipoprotein (mmol/L)				
Mean (SD)	2.18 (0.89)	2.53 (1.26)	2.04 (0.64)	**0.002**
Median (Q1, Q3)	2.11 (1.51, 2.58)	2.06 (1.72, 3.12)	2.12 (1.47, 2.41)	
Range	0.91–6.10	0.91–6.10	1.02–3.75	
High-density lipoprotein (mmol/L)				
Mean (SD)	1.30 (0.29)	1.32 (0.27)	1.29 (0.30)	0.622
Median (Q1, Q3)	1.25 (1.12, 1.48)	1.32 (1.14, 1.51)	1.23 (1.12, 1.48)	
Range	0.71–2.15	0.77–1.97	0.71–2.15	
Triglycerides (mmol/L)				
Mean (SD)	1.24 (0.73)	1.11 (0.48)	1.29 (0.81)	0.188
Median (Q1, Q3)	1.10 (0.75, 1.47)	1.06 (0.80, 1.30)	1.11 (0.74, 1.49)	
Range	0.31–4.21	0.31–2.25	0.32–4.21	
Peak Troponin I (μg/L)				
Mean (SD)	53.34 (32.52)	58.89 (30.22)	51.02 (33.30)	0.179
Median (Q1, Q3)	49.00 (30.00, 69.00)	52.50 (34.50, 81.25)	47.00 (28.00, 67.00)	
Range	4.50–250.00	15.00–136.00	4.50–250.00	
Hs-CRP (mg/L)				
Mean (SD)	4.37 (2.35)	4.55 (2.37)	4.30 (2.35)	0.550
Median (Q1, Q3)	4.17 (2.44, 6.27)	4.26 (2.48, 6.33)	4.06 (2.27, 6.14)	
Range	0.19–11.50	0.37–11.50	0.19–10.20	
ESR (mm/hr)				
Mean (SD)	13.69 (6.01)	16.23 (6.91)	12.63 (5.28)	***< 0.001***
Median (Q1, Q3)	13.00 (10.00, 17.00)	16.00 (12.00, 21.00)	12.00 (9.00, 16.00)	
Range	1.00–29.00	2.00–29.00	1.00–25.00	
Platelet aggregation with ADP (%)				
Mean (SD)	34.36 (18.85)	34.59 (18.21)	34.26 (19.20)	0.922
Median (Q1, Q3)	32.00 (21.00, 42.00)	31.50 (20.75, 42.50)	32.00 (21.00, 41.00)	
Range	3.00–97.00	7.00–83.00	3.00–97.00	
Platelet aggregation with ADR (%)				
Mean (SD)	32.51 (14.92)	37.50 (15.48)	30.42 (14.23)	***0.008***
Median (Q1, Q3)	32.00 (22.00, 40.00)	40.00 (25.00, 49.25)	31.00 (21.00, 37.00)	
Range	2.00–98.00	2.00–62.00	3.00–98.00	
Trimethylamine N-Oxide (μM)				
Mean (SD)	3.56 (2.59)	5.15 (2.44)	2.90 (2.36)	***< 0.001***
Median (Q1, Q3)	2.97 (1.66, 4.28)	5.07 (3.72, 7.19)	2.39 (1.25, 3.45)	
Range	0.42–14.10	0.42–10.24	0.57–14.10	

Table 4.2.3.1. *Continued*

Variables (unit of measures)	Total (N = 149)	CMD (N = 44)	No CMD (N = 105)	*p*-value
B-type natriuretic peptide (ng/L)				
Mean (SD)	60.55 (64.85)	87.11 (93.33)	49.42 (44.26)	***0.001***
Median (Q1, Q3)	40.00 (28.00, 69.00)	69.50 (28.75, 88.00)	37.00 (27.00, 57.00)	
Range	9.00–412.00	9.00–412.00	10.00–304.00	

Hs-CRP – high-sensitivity C-reactive protein; ESR – erythrocyte sedimentation rate; ADP – adenosine diphosphate; ADR – epinephrine in bold and italics significant *p*-values (< 0.05).

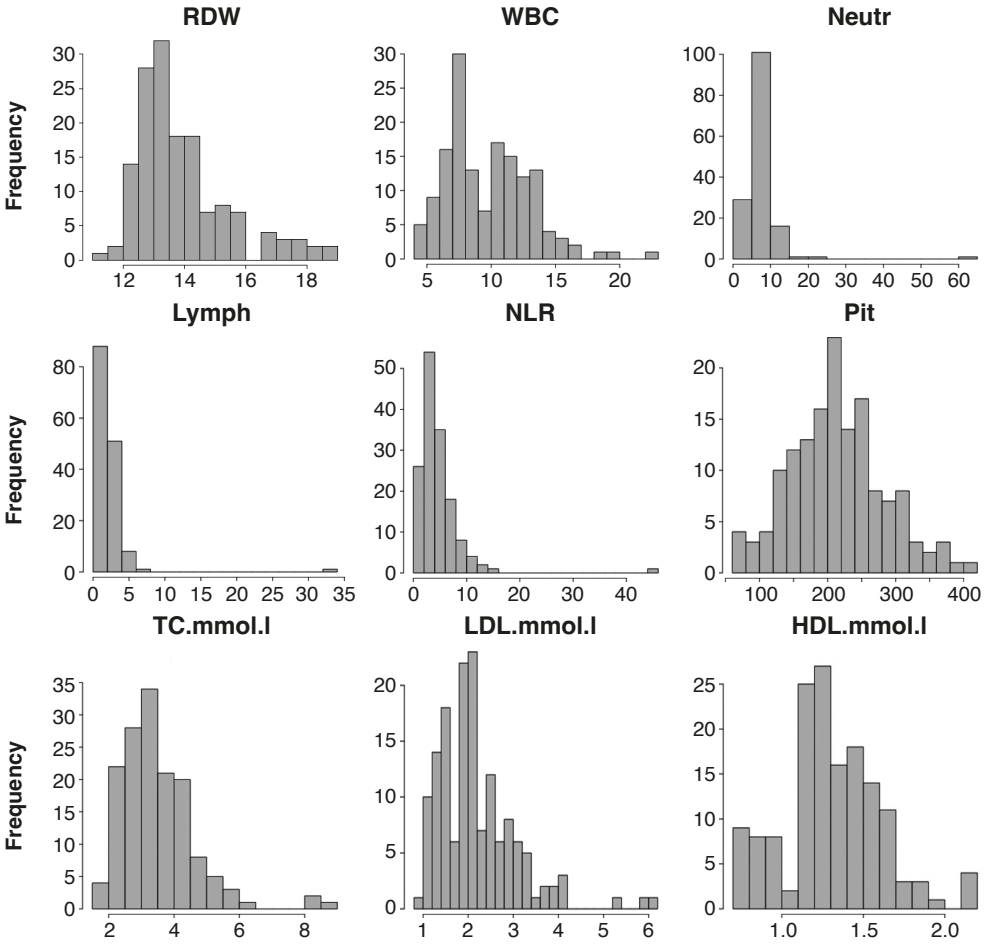

Fig. 4.2.3.1 (A). *Histograms of the 17 biomarkers and body mass index used in the model which evaluating the risk of coronary microvascular dysfunction at baseline*

Biomarkers and body mass index are not normally distributed highlighting distributions with strong positive or negative asymmetries and presence of outliers.

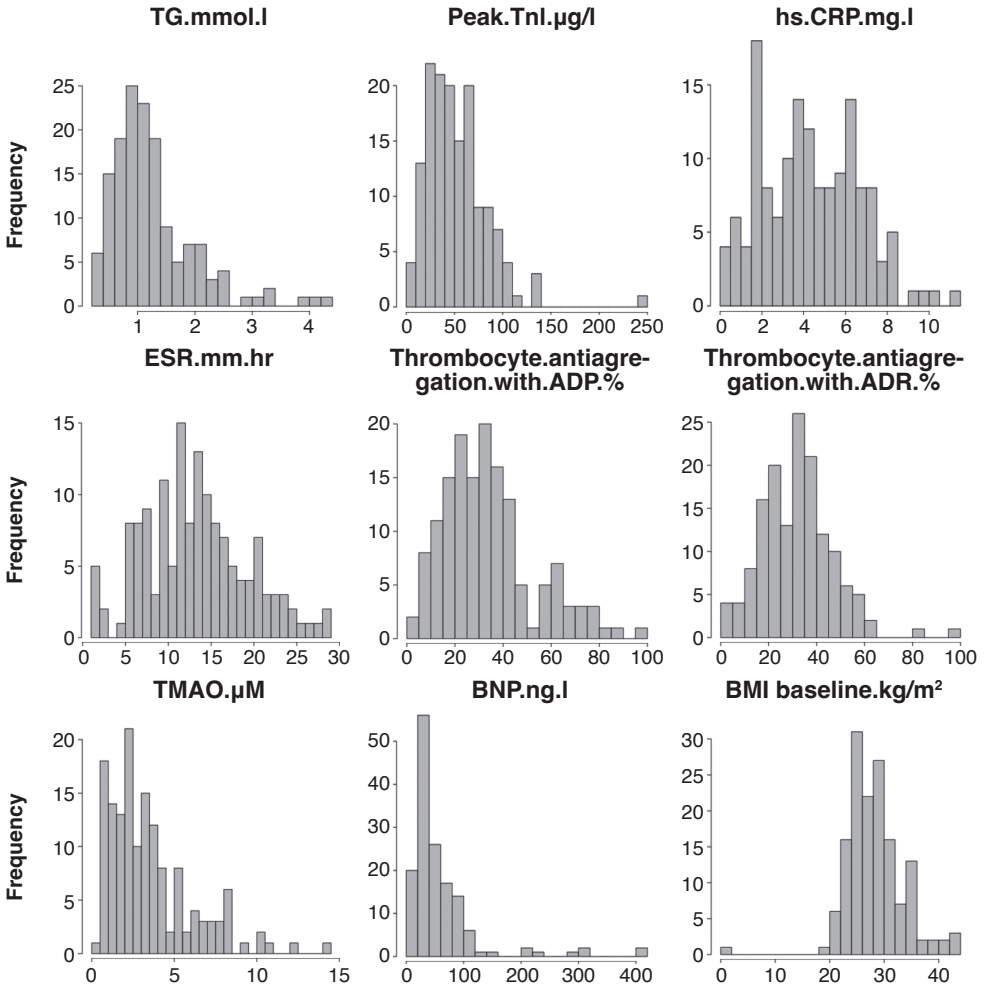

Fig. 4.2.3.1 (B). *Histograms of the 17 biomarkers and body mass index used in the model which evaluating the risk of coronary microvascular dysfunction at baseline*

Biomarkers and body mass index are not normally distributed highlighting distributions with strong positive or negative asymmetries and presence of outliers.

Among the 17 biomarkers, six of them demonstrate noticeably elevated median values in patients with CMD. As demonstrated in Table 4.2.3.1**,** the RDW was 13.50% in CMD patients compared to 13.60%, with a *p*-value of 0.005. The TC level was 3.14 mmol/L compared to 3.77 mmol/L, with a *p*-value of less than 0.001. The ESR was 12.00 mm/hr compared to 16.00 mm/hr, with a *p*-value of less than 0.001. Platelet aggregation with ADR was 31.00% compared to 40.00%, with a *p*-value of 0.008. The TMAO level was 2.39 µM compared to 5.07 µM, with a *p*-value of less than 0.001. The BNP level was

37.00 ng/L compared to 69.00 ng/L, with a *p*-value of 0.001. In contrast, patients with CMD exhibit a noticeably lower median value of LDL (2.06 mmol/L *vs.* 2.12 mmol/L; *p*-value = 0.002).

The test set underwent a parallel analytical process, as detailed in Table 4.2.3.2. Among the six biomarkers identified as correlates of CMD, five exhibited trends consistent with those observed in the training set, affirming that CMD patients typically present with significantly elevated median biomarker values in comparison to their non-CMD counterparts. Specific observations include TC levels of 3.33 mmol/L *vs.* 5.12 mmol/L ($p < 0.001$), ESR values of 12.00 mm/hr versus 22.00 mm/hr ($p < 0.001$), platelet aggregation in response to ADR at 30.00% compared to 47.00% ($p < 0.001$), TMAO concentrations of 2.53 μM versus 5.12 μM ($p = 0.04$), and BNP levels at 34.00 ng/L against 88.00 ng/L ($p < 0.001$). Contrariwise, LDL-C levels presented a divergent pattern from the training dataset, with a notable increase in CMD patients (2.14 mmol/L *vs.* 3.71 mmol/L; $p < 0.001$). Interestingly, RDW demonstrated no significant difference between the two subgroups in the test set ($p = 0.131$). Moreover, Hs-CRP, was observed to significantly increase in CMD patients (3.93 mg/L *vs.* 10.80 mg/L; $p < 0.001$). These findings, highlighting the differences between the training and testing sets, underscore the challenging nature of the testing set for the CMD machine learning algorithm we aim to develop. The robustness and accuracy of this model, when applied to such a diverse set, would be indicative of its generalizability.

Table 4.2.3.2. *Laboratory and biomarker values collected on the test set of patients with ST-elevation myocardial infarction, stratified by coronary microvascular dysfunction*

Variables (unit of measures)	**Total (N = 51)**	**Yes CMD (N = 7)**	**No CMD (N = 44)**	***p*-value**
Red cell distribution width (%)				
Mean (SD)	13.90 (1.50)	14.70 (2.03)	13.78 (1.38)	0.131
Median (Q1, Q3)	13.50 (12.85, 14.50)	14.50 (12.85, 16.30)	13.50 (12.88, 14.25)	
Range	11.63–18.40	12.60–17.50	11.63–18.40	
White blood count ($\times 10^9$/L)				
Mean (SD)	9.91 (3.12)	9.19 (2.08)	10.03 (3.26)	0.517
Median (Q1, Q3)	9.12 (7.67, 11.74)	9.08 (7.96, 10.99)	9.27 (7.68, 12.04)	
Range	4.14–18.52	5.96–11.43	4.14–18.52	
Neutrophils ($\times 10^9$/L)				
Mean (SD)	7.48 (2.29)	7.62 (2.35)	7.46 (2.30)	0.869
Median (Q1, Q3)	7.47 (5.93, 9.03)	7.05 (6.23, 9.05)	7.51 (5.85, 9.02)	
Range	3.38–14.04	4.50–11.19	3.38–14.04	

Table 4.2.3.2. *Continued*

Variables (unit of measures)	Total (N = 51)	Yes CMD (N = 7)	No CMD (N = 44)	*p*-value
Lymphocytes ($\times 10^9$/L)				
Mean (SD)	2.12 (1.01)	2.34 (1.23)	2.09 (0.99)	0.541
Median (Q1, Q3)	1.85 (1.34, 2.64)	2.44 (1.48, 2.60)	1.85 (1.39, 2.69)	
Range	0.67–4.74	1.06–4.74	0.67–4.25	
Neutrophil-to-Lymphocyte ratio				
Mean (SD)	4.51 (2.92)	3.67 (1.10)	4.64 (3.11)	0.419
Median (Q1, Q3)	3.90 (2.44, 5.61)	3.90 (3.27, 4.42)	3.92 (2.36, 6.29)	
Range	0.97–16.27	1.69–4.72	0.97–16.27	
Platelet count ($\times 10^9$/L)				
Mean (SD)	204.49 (53.81)	208.57 (70.47)	203.84 (51.68)	0.831
Median (Q1, Q3)	207.00 (166.00, 241.00)	224.00 (145.50, 259.50)	206.50 (174.00, 241.00)	
Range	70.00–312.00	127.00–299.00	70.00–312.00	
Total cholesterol (mmol/L)				
Mean (SD)	3.66 (1.03)	5.10 (1.07)	3.43 (0.82)	***< 0.001***
Median (Q1, Q3)	3.51 (3.12, 4.18)	5.12 (4.91, 5.56)	3.33 (2.94, 4.03)	
Range	2.01–6.51	3.12–6.51	2.01–6.24	
Low-density lipoprotein (mmol/L)				
Mean (SD)	2.28 (0.83)	3.55 (0.82)	2.08 (0.63)	***< 0.001***
Median (Q1, Q3)	2.14 (1.73, 2.69)	3.71 (3.26, 4.12)	2.14 (1.50, 2.44)	
Range	1.01 –4.41	2.01–4.41	1.01–3.91	
High-density lipoprotein (mmol/L)				
Mean (SD)	1.32 (0.39)	1.17 (0.16)	1.35 (0.41)	0.272
Median (Q1, Q3)	1.29 (1.06, 1.48)	1.23 (1.04, 1.30)	1.33 (1.09, 1.55)	
Range	0.71–3.12	0.95–1.32	0.71–3.12	
Triglycerides (mmol/L)				
Mean (SD)	1.20 (0.68)	1.23 (0.71)	1.19 (0.68)	0.898
Median (Q1, Q3)	1.11 (0.72, 1.41)	1.12 (0.66, 1.52)	1.11 (0.79, 1.41)	
Range	0.41–4.51	0.61–2.51	0.41–4.51	
Peak Troponin I (μg/L)				
Mean (SD)	35.56 (21.36)	28.50 (20.88)	36.68 (21.46)	0.352
Median (Q1, Q3)	30.00 (17.00, 53.00)	22.00 (17.50, 37.00)	32.00 (17.00, 54.25)	
Range	4.50–81.00	4.50–64.00	5.12–81.00	
Hs-CRP (mg/L)				
Mean (SD)	4.79 (3.26)	10.49 (3.06)	3.88 (2.21)	***< 0.001***
Median (Q1, Q3)	4.55 (2.08, 6.27)	10.80 (8.86, 12.05)	3.93 (1.92, 5.67)	
Range	0.57–15.10	5.74–15.10	0.57–8.45	

Table 4.2.3.2. *Continued*

Variables (unit of measures)	Total (N = 51)	Yes CMD (N = 7)	No CMD (N = 44)	*p*-value
ESR (mm/hr)				
Mean (SD)	13.35 (7.05)	19.86 (11.63)	12.32 (5.57)	***0.007***
Median (Q1, Q3)	12.00 (8.50, 16.50)	22.00 (9.50, 29.00)	12.00 (8.00, 15.25)	
Range	2.00–34.00	6.00–34.00	2.00–25.00	
Platelet aggregation with ADP (%)				
Mean (SD)	38.59 (20.81)	49.29 (19.99)	36.89 (20.64)	0.145
Median (Q1, Q3)	35.00 (23.00, 58.00)	49.00 (45.00, 63.50)	31.50 (22.75, 47.00)	
Range	3.00–80.00	10.00–69.00	3.00–80.00	
Platelet aggregation with ADR (%)				
Mean (SD)	32.73 (12.50)	48.57 (9.88)	30.20 (10.99)	***< 0.001***
Median (Q1, Q3)	32.00 (23.50, 38.00)	47.00 (45.50, 55.50)	30.00 (22.00, 36.00)	
Range	3.00–63.00	31.00–60.00	3.00–63.00	
Trimethylamine N-Oxide (μM)				
Mean (SD)	3.67 (2.78)	6.38 (3.84)	3.24 (2.35)	***0.004***
Median (Q1, Q3)	2.75 (1.90, 4.67)	5.12 (4.17, 7.23)	2.53 (1.77, 3.89)	
Range	0.57–14.10	2.64–14.10	0.57–10.74	
B-type natriuretic peptide (ng/L)				
Mean (SD)	45.08 (37.66)	89.14 (65.91)	38.07 (26.01)	***< 0.001***
Median (Q1, Q3)	34.00 (26.50, 48.00)	88.00 (34.00, 119.50)	34.00 (24.25, 44.00)	
Range	6.00–205.00	24.00–205.00	6.00–154.00	

Hs-CRP – high-sensitivity C-reactive protein; ESR – erythrocyte sedimentation rate; ADP – adenosine diphosphate; ADR – epinephrine. In bold and italics significant *p*-values (< 0.05).

4.2.4. Comparative analysis of the training and test sets

When examining the training and test sets, it is evident that the median value of the Peak Troponin is lower in the test set (49.00 μg/L *vs.* 30.00 μg/L; *p*-value < 0.001). Additionally, the prevalence is significantly lower in the test set (29.5% *vs.* 13.7%; *p*-value = 0.026). This evidence is presented in Table 4.2.3.3, which provides a comprehensive comparison of the 30 variables that were involved in the analyses. The notable variance in troponin levels and the lower prevalence of CMD in the test set present additional complexities for our CMD-focused machine learning algorithm. These factors, coupled with the distinct differences observed between the two sets, amplify the challenge faced by the algorithm. If the future model succeeds in successfully navigating these complexities, it would be a strong testament to its accuracy and generalizability.

Table 4.2.3.3. *Characteristics, Laboratory and Biomarker values of patients with ST-elevation myocardial infarction stratified respect training and test set used for the analyses*

Variables (unit of measures)	**Total (N = 200)**	**Test set (N = 51)**	**Training set (N = 149)**	***p*-value**
Age (years)				
Mean (SD)	66.50 (12.06)	65.92 (12.90)	66.70 (11.80)	0.690
Median (Q1, Q3)	65.50 (58.00, 76.00)	62.00 (56.50, 76.00)	66.00 (59.00, 76.00)	
Range	41.00–94.00	45.00–94.00	41.00–93.00	
Gender				
Male	119 (59.5%)	34 (66.7%)	85 (57.0%)	0.251
Female	81 (40.5%)	17 (33.3%)	64 (43.0%)	
Body mass index (kg/m^2)				
Mean (SD)	28.17 (5.58)	27.89 (6.30)	28.26 (5.33)	0.684
Median (Q1, Q3)	27.53 (24.54, 30.74)	26.20 (23.98, 31.23)	27.78 (24.98, 30.64)	
Range	0.00–49.54	15.96–49.54	0.00–43.73	
History of Arterial Hypertension				
No	82 (41.0%)	21 (41.2%)	61 (40.9%)	1.000
Yes	118 (59.0%)	30 (58.8%)	88 (59.1%)	
History of coronary artery disease				
No	145 (72.5%)	40 (78.4%)	105 (70.5%)	0.364
Yes	55 (27.5%)	11 (21.6%)	44 (29.5%)	
History of PCI				
No	176 (88.0%)	48 (94.1%)	128 (85.9%)	0.140
Yes	24 (12.0%)	3 (5.9%)	21 (14.1%)	
History of Stroke				
No	175 (87.5%)	46 (90.2%)	129 (86.6%)	0.627
Yes	25 (12.5%)	5 (9.8%)	20 (13.4%)	
History of diabetes mellitus				
No	151 (75.5%)	39 (76.5%)	112 (75.2%)	1.000
Yes	49 (24.5%)	12 (23.5%)	37 (24.8%)	
History of dyslipidemia				
No	86 (43.0%)	26 (51.0%)	60 (40.3%)	0.194
Yes	114 (57.0%)	25 (49.0%)	89 (59.7%)	
History of alcohol abuse				
No	181 (90.5%)	47 (92.2%)	134 (89.9%)	0.786
Yes	19 (9.5%)	4 (7.8%)	15 (10.1%)	
Smoker				
Never	92 (46.0%)	24 (47.1%)	68 (45.6%)	0.933
Ex-smoker	67 (33.5%)	16 (31.4%)	51 (34.2%)	
Current smoker	41 (20.5%)	11 (21.6%)	30 (20.1%)	

Table 4.2.3.3. *Continued*

Variables (unit of measures)	Total (N = 200)	Test set (N = 51)	Training set (N = 149)	*p*-value
CHA_2DS_2-VASc score				
1	23 (11.5%)	8 (15.7%)	15 (10.1%)	0.434
2	40 (20.0%)	7 (13.7%)	33 (22.1%)	
3	52 (26.0%)	18 (35.3%)	34 (22.8%)	
4	45 (22.5%)	9 (17.6%)	36 (24.2%)	
5	23 (11.5%)	5 (9.8%)	18 (12.1%)	
6	14 (7.0%)	4 (7.8%)	10 (6.7%)	
7	3 (1.5%)	0 (0.0%)	3 (2.0%)	
Red cell distribution width (%)				
Mean (SD)	13.94 (1.52)	13.90 (1.50)	13.96 (1.53)	0.825
Median (Q1, Q3)	13.50 (12.90, 14.50)	13.50 (12.85, 14.50)	13.50 (12.90, 14.50)	
Range	11.30–19.00	11.63–18.40	11.30–19.00	
White blood count ($\times 10^9$/L)				
Mean (SD)	9.80 (3.23)	9.91 (3.12)	9.76 (3.28)	0.765
Median (Q1, Q3)	9.30 (7.40, 11.96)	9.12 (7.67, 11.74)	9.48 (7.23, 12.00)	
Range	4.14–22.45	4.14–18.52	4.79–22.45	
Neutrophils ($\times 10^9$/L)				
Mean (SD)	7.56 (4.64)	7.48 (2.29)	7.59 (5.21)	0.888
Median (Q1, Q3)	7.05 (5.47, 8.88)	7.47 (5.93, 9.03)	6.90 (5.28, 8.80)	
Range	2.04–60.60	3.38–14.04	2.04–60.60	
Lymphocytes ($\times 10^9$/L)				
Mean (SD)	2.21 (2.46)	2.12 (1.01)	2.25 (2.80)	0.759
Median (Q1, Q3)	1.79 (1.29, 2.59)	1.85 (1.34, 2.64)	1.75 (1.30, 2.55)	
Range	0.20–33.80	0.67–4.74	0.20–33.80	
Neutrophil-to-Lymphocyte ratio				
Mean (SD)	4.60 (3.98)	4.51 (2.92)	4.63 (4.29)	0.853
Median (Q1, Q3)	3.81 (2.38, 5.68)	3.90 (2.44, 5.61)	3.80 (2.39, 5.77)	
Range	0.65–45.00	0.97–16.27	0.65–45.00	
Platelet count ($\times 10^9$/L)				
Mean (SD)	212.00 (65.16)	204.49 (53.81)	214.57 (68.60)	0.342
Median (Q1, Q3)	209.00 (167.50, 249.00)	207.00 (166.00, 241.00)	210.00 (168.00, 254.00)	
Range	70.00–404.00	70.00–312.00	70.00–404.00	
Total cholesterol (mmol/L)				
Mean (SD)	3.55 (1.12)	3.66 (1.03)	3.51 (1.15)	0.392
Median (Q1, Q3)	3.25 (2.87, 4.14)	3.51 (3.12, 4.18)	3.21 (2.86, 4.12)	
Range	1.78–8.89	2.01–6.51	1.78–8.89	

Table 4.2.3.3. *Continued*

Variables (unit of measures)	**Total (N = 200)**	**Test set (N = 51)**	**Training set (N = 149)**	***p*-value**
Low-density lipoprotein (mmol/L)				
Mean (SD)	2.21 (0.87)	2.28 (0.83)	2.18 (0.89)	0.500
Median (Q1, Q3)	2.12 (1.52, 2.62)	2.14 (1.73, 2.69)	2.11 (1.51, 2.58)	
Range	0.91–6.10	1.01–4.41	0.91–6.10	
High-density lipoprotein (mmol/L)				
Mean (SD)	1.31 (0.32)	1.32 (0.39)	1.30 (0.29)	0.677
Median (Q1, Q3)	1.25 (1.12, 1.48)	1.29 (1.06, 1.48)	1.25 (1.12, 1.48)	
Range	0.71–3.12	0.71–3.12	0.71–2.15	
Triglycerides (mmol/L)				
Mean (SD)	1.23 (0.71)	1.20 (0.68)	1.24 (0.73)	0.746
Median (Q1, Q3)	1.10 (0.74, 1.47)	1.11 (0.72, 1.41)	1.10 (0.75, 1.47)	
Range	0.31–4.51	0.41–4.51	0.31–4.21	
Peak Troponin I (μg/L)				
Mean (SD)	48.81 (31.01)	35.56 (21.36)	53.34 (32.52)	***< 0.001***
Median (Q1, Q3)	45.00 (27.00, 65.00)	30.00 (17.00, 53.00)	49.00 (30.00, 69.00)	
Range	4.50–250.00	4.50–81.00	4.50–250.00	
Hs-CRP (mg/L)				
Mean (SD)	4.48 (2.61)	4.79 (3.26)	4.37 (2.35)	0.332
Median (Q1, Q3)	4.21 (2.31, 6.28)	4.55 (2.08, 6.27)	4.17 (2.44, 6.27)	
Range	0.19–15.10	0.57–15.10	0.19–11.50	
ESR (mm/hr)				
Mean (SD)	13.61 (6.28)	13.35 (7.05)	13.69 (6.01)	0.741
Median (Q1, Q3)	13.00 (9.00, 17.00)	12.00 (8.50, 16.50)	13.00 (10.00, 17.00)	
Range	1.00–34.00	2.00–34.00	1.00–29.00	
Platelet aggregation with ADP				
Mean (SD)	35.44 (19.40)	38.59 (20.81)	34.36 (18.85)	0.179
Median (Q1, Q3)	32.00 (21.75, 44.25)	35.00 (23.00, 58.00)	32.00 (21.00, 42.00)	
Range	3.00–97.00	3.00–80.00	3.00–97.00	
Platelet aggregation with ADR (%)				
Mean (SD)	32.56 (14.31)	32.73 (12.50)	32.51 (14.92)	0.926
Median (Q1, Q3)	32.00 (22.00, 40.00)	32.00 (23.50, 38.00)	32.00 (22.00, 40.00)	
Range	2.00–98.00	3.00–63.00	2.00–98.00	
Trimethylamine N-oxide (μM)				
Mean (SD)	3.59 (2.63)	3.67 (2.78)	3.56 (2.59)	0.799
Median (Q1, Q3)	2.96 (1.83, 4.37)	2.75 (1.90, 4.67)	2.97 (1.66, 4.28)	
Range	0.42–14.10	0.57–14.10	0.42–14.10	

Table 4.2.3.3. *Continued*

Variables (unit of measures)	Total (N = 200)	Test set (N = 51)	Training set (N = 149)	*p*-value
B-type natriuretic peptide (ng/L)				
Mean (SD)	56.60 (59.41)	45.08 (37.66)	60.55 (64.85)	0.109
Median (Q1, Q3)	37.00 (27.00, 66.25)	34.00 (26.50, 48.00)	40.00 (28.00, 69.00)	
Range	6.00–412.00	6.00–205.00	9.00–412.00	
Microcirculatory disorder				
No	149 (74.5%)	44 (86.3%)	105 (70.5%)	***0.026***
Yes	51 (25.5%)	7 (13.7%)	44 (29.5%)	

PCI – Percutaneous Coronary Intervention; Hs-CRP – High-Sensitivity C-Reactive Protein; ESR – Erythrocyte Sedimentation Rate; ADP – Adenosine diphosphate; ADR – Epinephrine. In bold and italics significant *p*-values (< 0.05).

4.2.5. Variables multicollinearity check

The biomarkers in Tables 4.2.3.1 and 4.2.3.2 have been identified in the literature as critical for the prediction of CMD and used as covariates in a model where the outcome is the diagnosis (No CMD vs CMD). For checking the multicollinearity in the data, two correlation plots (on training and test set) were computed (Fig. 4.2.5.1 A, B). In both graphs, but particularly in the training set, it is evident that some biomarkers are significantly (cells with the pink profile) positively (blue cells) or negatively (red cells) correlated. Additionally, within the study's correlation matrices, a general pattern of weak or random associations between biomarkers suggests the intricate and complex nature of biological interactions. However, several strong expected relationships stand out. A significant correlation is noted between LDL and TC, which aligns with established clinical understanding as LDL cholesterol is factored into the calculation of TC. Similarly, the NLR displays a strong positive correlation with Neutrophil count and a strong negative one with Lymphocyte count, consistent with the definition of NLR as the ratio between these two cell counts. Another anticipated correlation is seen between thrombocyte aggregation with ADP and ADR, reflecting their shared role in platelet aggregation. These particular strong correlations validate known biochemical interactions and therapeutic effects. Conversely, other biomarker correlations within the matrices did not exhibit significant connections, emphasizing the selectivity of substantial correlations within a complex landscape of physiological parameters.

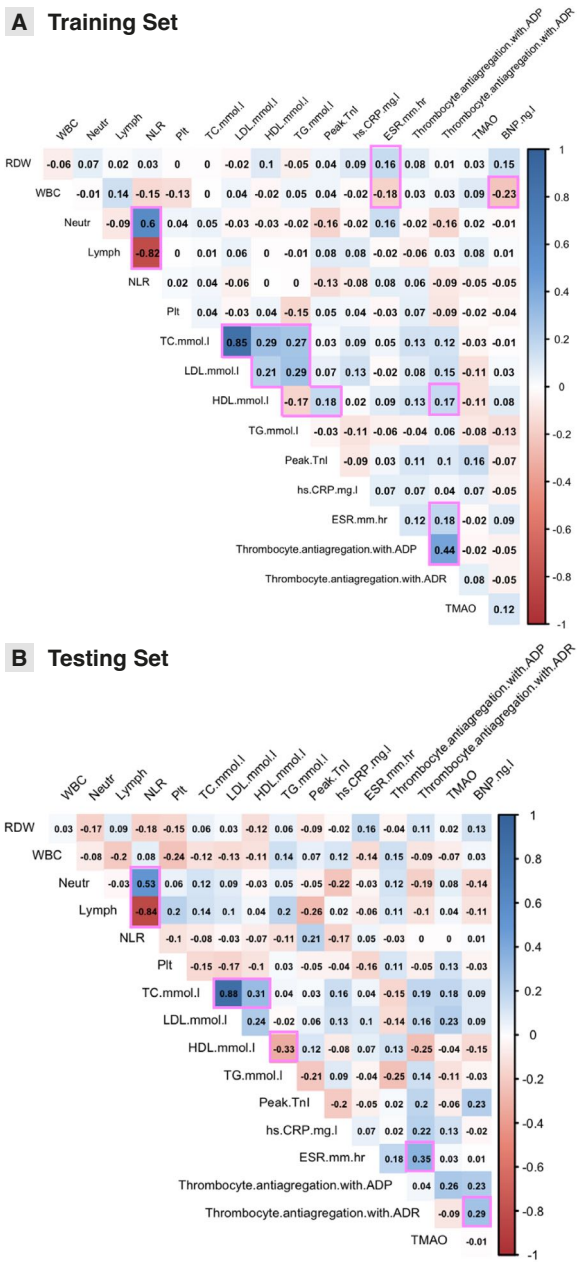

Fig. 4.2.5.1. *Correlation plots on biomarkers used to predict CMD risk*

These upper triangular matrices report in each cell the Spearman correlation (ρ_s) coefficient computed between couples of biomarkers. Figures **A** and **B** evaluate correlations in the training and test set, respectively. The background of the cells is coloured of blue if the relationship is positive ($0 \leq \rho_s \leq 1$); otherwise, the cell is coloured red ($-1 \leq \rho_s \leq 0$). The colors intensity is proportional to the magnitude of ρ_s and the pink profiles identify cells containing significant correlations (correlation test p-value < 0.05).

4.2.6. Employment of machine learning algorithms to address data complexities

To address data complexities including outliers and multicollinearity, a suite of ML algorithms, known for their robustness in handling such challenges, were employed. The training set, characterized by a relatively low CMD prevalence of 29.5%, underwent a SMOTE procedure to achieve balance. This process resulted in a modified cohort of 186 STEMI patients, comprising 81 CMD and 105 non-CMD cases, thereby elevating the prevalence to 43.5%. Leveraging the harmonized training set, an array of sophisticated machine learning algorithms was systematically deployed, each utilizing an identical set of outcomes and covariates to ensure uniformity across experimental conditions. The computational techniques encompassed a diverse suite of models, including RF, GBM, SVM, XGBoost, Super Learner, and Discrete Super Learner. In an endeavor to contextualize the efficacy of these advanced methodologies, a comparative analysis was conducted – predicated on a 10-fold Cross-Validation (CV) risk assessment framework – against the conventional statistical benchmark of logistic Regression. For the purpose of exhaustive analytical rigor, the forest plot pertaining to the logistic regression model was documented in Fig. 4.2.6.1. Furthermore, these varied algorithms were juxtaposed with the meta-analytic learner, SL.mean, utilizing the SuperLearner statistical package implemented within the R programming ecosystem. This multifaceted comparison procedure was crafted to distill insights into the relative predictive veracity and the concomitant risk stratification capabilities intrinsic to each algorithmic model.

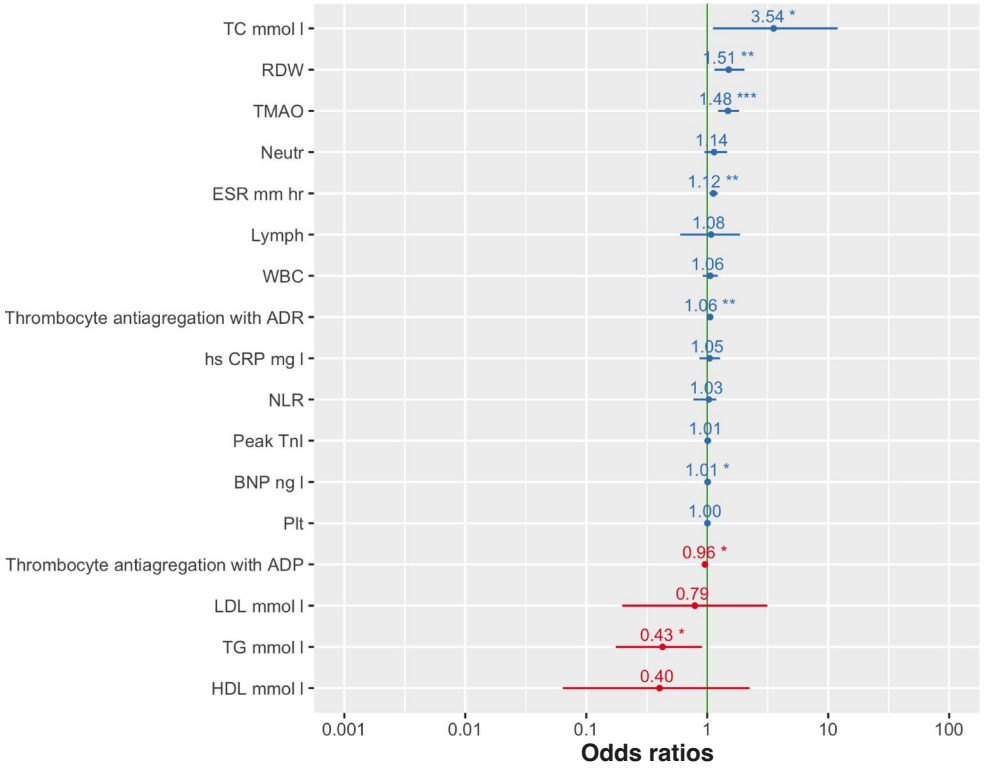

Fig. 4.2.6.1. *Forest plot of the Logistic regression model for the prediction of Coronary Microvascular Dysfunction*

Forest plot of the Logistic regression estimated on rebalanced training set where the outcome is the diagnosis (No CMD/CMD) and the covariates are the 17 biomarkers. The plot visualizes odds ratios (95% CI) computed in correspondence of each biomarker, arranged in descending order based on their values (from the highest at the top of the graph to the lowest at the bottom). Odds ratios ≥ 1 are colored in blue, red otherwise, and when they are significantly different from 1, they are identified by the asterisks.

4.2.7. Performance of machine learning and logistic regression algorithms

While the RF algorithm emerged as the superior model with the lowest 10-fold CV risk (0.120 ± 0.010, as illustrated in Fig. 4.2.7.1), the DeLong test revealed a statistically significant difference between its AUC and those of logistic regression and SL.mean ($p < 0.05$ for both, detailed in Table 4.2.7.1). This finding corroborates the efficacy of ensemble methods in this analytical context, demonstrating comparable predictive accuracy across different approaches.

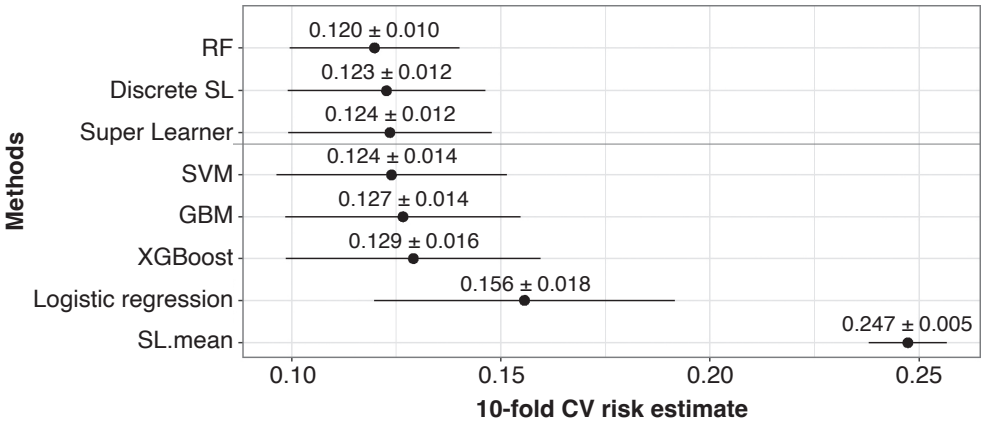

Fig. 4.2.7.1. *Ten-fold cross validation risk in correspondence of each method (± standard error)*

RF – random forest; GBM – gradient boosting machine; SVM – support vector machine; XGBoost – eXtreme gradient boosting; SL – super learner; CV – cross validation.

Table 4.2.7.1. *AUCs (95% confidence interval) of each model compared in the study and p-values of the DeLong test*

Model	AUC (95% CI)	DeLong test *p*-values computed respect the best performer (RF)
RF (best performer)	0.912 (0.89–0.97)	–
Discrete SL	0.911 (0.87–0.96)	0.9305
Super Learner	0.906 (0.86–0.95)	0.5667
SVM	0.900 (0.85–0.95)	0.4797
GBM	0.900 (0.86–0.94)	0.3104
XGBoost	0.894 (0.85–0.94)	0.2567
Logistic regression	0.855 (0.8–0.91)	***0.0138***
SL Mean	0.591 (0.51–0.67)	***< 0.001***

RF – random forest; GBM – gradient boosting machine; SVM – support vector machine; XGBoost – eXtreme gradient boosting; SL – super learner; CV – cross validation; CI – confidence interval. In bold and italics significant *p*-values (< 0.05).

Notwithstanding the similar performance levels, the application of RF is advocated for its provision of two insightful analytical tools: relVIM and 3D-PDP. These tools offer an enhanced understanding of the relationships between the outcome and covariates. Subsequently, the RF model was recalibrated using the random Forest package in R, which facilitates the extraction and utilization of relVIM and 3D-PDP, thereby enriching the interpretability of the model's results.

4.2.8. Relative variable importance measures analysis

In the visual exposition provided by the lollipop graph depicted in Fig. 4.2.8.1, there is a nuanced articulation of the relVIM attributed to the covariates within the RF model. This graphical representation methodically sequences the covariates in a hierarchical schema based on their contributory significance, commencing with the paramount influence of TMAO (relVIM = 100.00%) and descending to the minimal impact exhibited by platelet aggregation with ADP (relVIM = 13.51%). It is of particular interest to note that the graph delineates TMAO, platelet aggregation with epinephrine (relVIM = 50.59%), and BNP (relVIM = 41.15%) as the principal variables exerting considerable sway in the CMD predictive model. Such a stratification intimates that the model's prognostic precision is predominantly contingent upon a cadre of biomarkers. For instance, ESR, with a relVIM of 29.94%, intriguingly falls just shy of the 30% demarcation, suggesting a secondary tier of influence within the model's predictive apparatus.

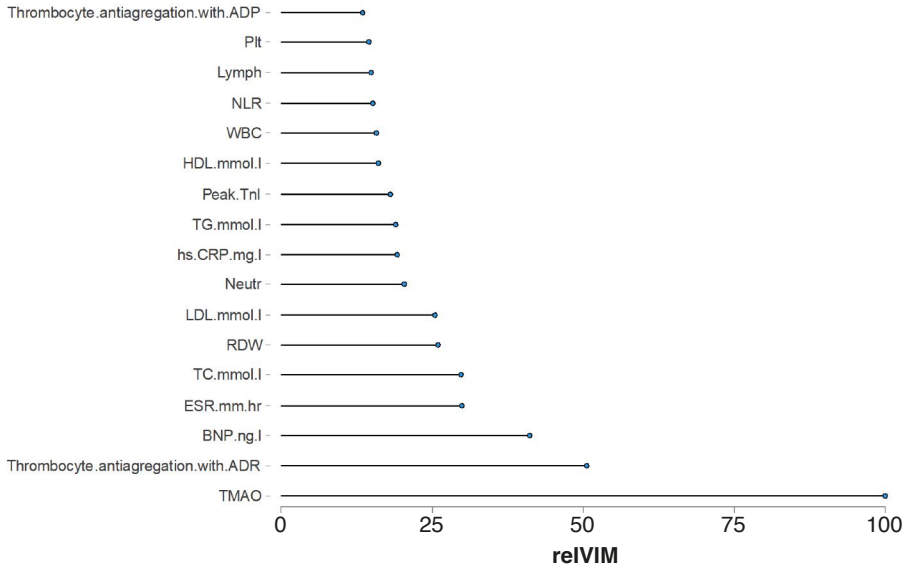

Fig. 4.2.8.1. *Relative variable importance (relVIM) extracted from the random forest*

relVIM identifies which variables had a substantial impact on the diagnosis (No CMD/CMD). It was extracted from the RF estimated on the rebalanced dataset where the diagnosis was the outcome and the 17 biomarkers the covariates. It ranks from the most (TMAO, relVIM = 100.00%) to the least (platelet aggregation with ADP, relVIM = 13.51%) important covariates in the model. RDW – red cell distribution width; WBC – white blood cells count; Neutr – neutrophil count; Lymph – lymphocyte count; NLR – neutrophil-to-lymphocyte ratio; PLT – platelets count; TC – total cholesterol; LDL – low-density lipoprotein; HDL – high-density lipoprotein; TG – triglycerides; Peak TnI – peak troponin I; hs-CRP – high sensitivity C-reactive protein; ESR – erythrocyte sedimentation rate; ADP – adenosine diphosphate; BNP – B-type natriuretic peptide; ADR – epinephrine; TMAO – trimethylamine N-oxide.

Given TMAO's pronounced association with CMD risk, a subsequent RF analysis excluded TMAO to assess the influence of other covariates (Fig. 4.2.8.2). In this adjusted model, platelet aggregation with ADR (relVIM = 100.00%), BNP (relVIM = 92.95%), and TC (relVIM = 60.46%) emerged as the most significant predictors. This alternative analysis underscores that omitting TMAO necessitates monitoring a broader spectrum of biomarkers for maintaining robust predictive capability in the RF model. The analysis identified 12 biomarkers with a relVIM exceeding 30% (including platelet anti-aggregation with epinephrine, BNP, TC, ESR, RDW, LDL, Peak TnI, TG, WBC, hs-CRP, Neutr, and NLR). This not only underscores the complexity and multifactorial essence inherent to CMD prediction but also, in underscoring the potency of TMAO within the predictive framework, it highlights the unique and substantial contribution of this biomarker to the model's overall predictive strength.

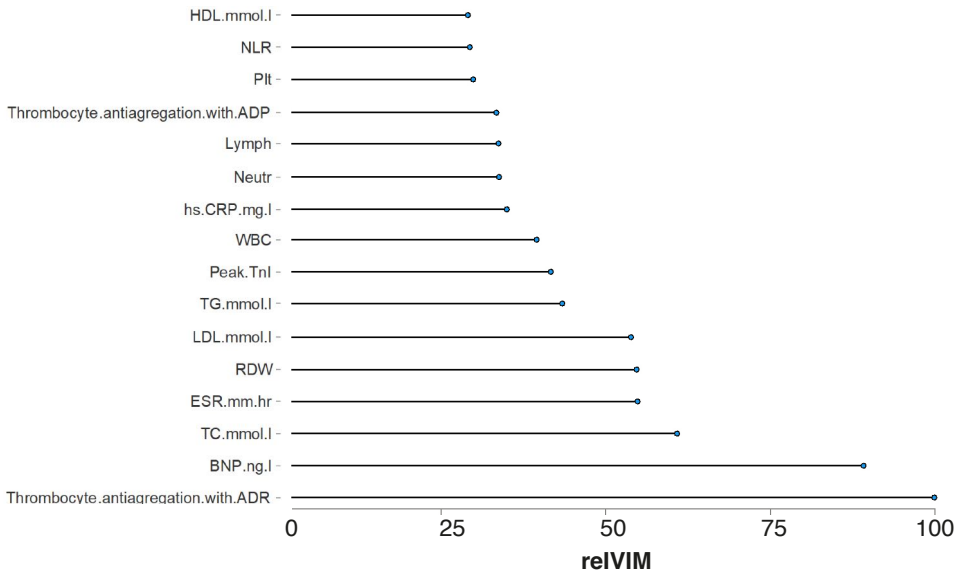

Fig. 4.2.8.2. *Relative variable importance extracted from the random forest, excluding TMAO from the analysis*

relVIM identifies which variables had a substantial impact on the diagnosis (No CMD/CMD). It was extracted from the RF estimated on the rebalanced dataset where the diagnosis was the outcome and the 16 biomarkers the covariates (in this sensitivity analysis TMAO was excluded). It produces a ranking from the most (platelet aggregation with epinephrine (%), relVIM = 100.00%) to the least (HDL(mmol.l), relVIM = 26.07%) significant covariates in predicting the risk of having CMD. RDW – red cell distribution width; WBC – white blood cells; Neutr – neutrophil; Lymph – lymphocytes; NLR – neutrophil-to-lymphocyte ratio; PLT – platelets; TC – total cholesterol; LDL – low-density lipoprotein; HDL – high-density lipoprotein; TG – triglycerides; Peak TnI – peak troponin I; hs-CRP – high sensitivity C-reactive protein; ESR – erythrocyte sedimentation rate; BNP – B-type natriuretic peptide; ADP – adenosine diphosphate; ADR – epinephrine; TMAO – trimethylamine N-oxide.

4.2.9. 3D partial dependence plot analysis

The 3D-PDP elucidates how the probability of CMD diagnosis fluctuates in relation to the levels of key biomarkers identified by the RF algorithm (Fig. 4.2.9.1). This plot is represented in a three-dimensional space, where the colour gradient shifts from blue to yellow, corresponding to an escalating likelihood of being classified as a CMD patient. The directional arrows in the plot, with arrowheads pointing towards higher values, reveal that an increase in all three primary biomarkers is associated with a peak probability of CMD occurrence, reaching approximately 0.7.

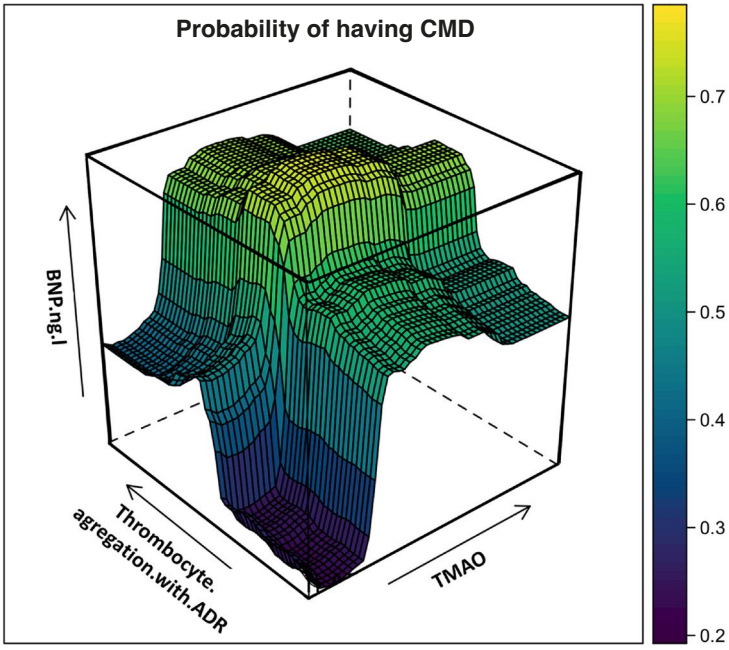

Fig. 4.2.9.1. *3D-PDP extracted from the random forest and based on the three most important variables selected by the relative variable importance measure*

3D-PDP shows how the probability of having CMD changes based on values of the covariates selected by the RF algorithm (TMAO in x-axis, platelet aggregation with epinephrine in y-axis, and BNP.ng.l in z-axis). The colour spectrum shifts from blue to yellow, indicating an increasing probability of being classified as "patient with CMD" (the legend, on the right of the plot, displays the probability magnitude). The arrows on the x, y, and z-axes show the directions in which the values of the three covariates increase. BNP – B-type natriuretic peptide; ADR – epinephrine; TMAO – trimethylamine N-oxide; CMD – coronary microvascular dysfunction.

4.2.10. Random forest model performance and validation

The RF model's performance, as assessed by the OOB error rate on the rebalanced training set, is detailed in Table 4.2.10.1. The model exhibits impressive metrics across various parameters, including accuracy, sensitivity, specificity, Negative Predictive Value (NPV), Positive Predictive Value (PPV), and precision, indicating its strong predictive capabilities.

Table 4.2.10.1. *Performance metrics of the RF on rebalanced training set (OOB) and on the test set*

Metrics	RF on rebalanced training set (OOB)	Test set
Accuracy (95% CI)	0.84 (0.78–0.89)	0.92 (0.81–0.98)
Sensitivity	0.86	0.91
Specificity	0.81	1.00
Positive Predicted Value	0.86	1.00
Negative Predicted Value	0.81	0.64
Precision	0.86	1.00

RF – random forest; CI – confidence interval.

When this model, whose outputs are interpretable as CMD risk scores, is applied to a fresh dataset (comprising 51 patients collected between 08/01/2022 and 01/31/2023), the performance metrics not only remain robust but show improvement in nearly all aspects (except for NPV). This enhancement in model performance on new data, as reported in Table 4.2.10.1, underscores the RF model's generalizability and reliability in predicting CMD, even when confronted with fresh, unobserved data. This result is particularly noteworthy, affirming the model's potential utility in clinical settings for CMD risk assessment.

4.2.11. Efficacy of synthetic minority over-sampling technique rebalancing method

To validate the effectiveness of the SMOTE in rebalancing the dataset for RF modeling, a comparative analysis was conducted between the RF models estimated on the original and the SMOTE-rebalanced datasets. The comparative outcomes are comprehensively presented in Table 4.2.11.1.

Table 4.2.11.1. *Comparison of the performance metrics of the RFs estimated on the rebalanced training set (OOB) vs the original dataset*

Metrics	RF on rebalanced training set	RF on original data
Accuracy (95% CI)	0.84 (0.78–0.89)	0.82 (0.75–0.88)
Sensitivity	0.86	0.94
Specificity	0.81	0.52
Positive predicted value	0.86	0.82
Negative predicted value	0.81	0.79
Precision	0.86	0.82

RF – random forest; CI – confidence interval.

Intriguingly, the analysis revealed that the RF model trained on the original dataset exhibited a decline in several performance metrics compared to the SMOTE-rebalanced data. Specifically, there was a decrease in accuracy by 2.4%, specificity by 35.8%, PPV by 4.7%, NPV by 2.5%, and precision by 4.7%. These findings underscore the impact of dataset imbalance on model performance and highlight the efficacy of SMOTE in enhancing the predictive capabilities of the RF model.

Further, the AUC for the RF model was higher on the rebalanced training set (0.84 with a 95% [CI] of 0.78–0.89) compared to the original dataset (0.73 with a 95% CI of 0.65–0.81). The DeLong test, as reported in Table 4.2.11.2, confirmed a statistically significant difference between these AUCs (p-value = 0.034). This signifies the enhanced discriminatory power of the RF model when applied to the rebalanced data.

Table 4.2.11.2. *Comparison of the area under the curves of random forests estimated on the rebalanced training set (OOB) vs. the original dataset*

RF	AUC	DeLong test p-values
On rebalanced training set	0.84 (0.78–0.89)*	***0.034***
On original data	0.73 (0.65–0.81)	
Comparison of the OOB mean error		
RF	**OOB mean error**	**Wilcoxon rank sum test**
On rebalanced training set	0.16	***<0.001***
On original data	0.19	

In bold and italics significant p-values (< 0.05).
*This AUC (95% CI) was estimated from the random forest (RF) based on rebalanced training set, using the R package random forest (which automatically employs the Out-of-Bag procedure). It differs from the AUC obtained with the package Super Learner (0.912 (0.89–0.97)) since, in that case, the estimates of the different models are based on 10-fold CV which is a procedure less stringent than OOB.

Additionally, the OOB mean error rates for the RF models further corroborated these findings: 0.16 for the rebalanced training set versus 0.19 for the original dataset. The Wilcoxon rank-sum test with continuity correction affirmed the statistical significance of this difference (p-value < 0.01), thereby reinforcing the advantage of utilizing the SMOTE rebalancing method in this context. This comparison not only validates the choice of SMOTE but also emphasizes the necessity of addressing data imbalance for optimizing machine learning model performances in medical research.

4.3. Trimethylamine N-oxide as a predictive biomarker for coronary microvascular dysfunction and prognosis in ST-elevation myocardial infarction patients

4.3.1. Temporal correlations of Trimethylamine N-oxide levels with coronary microvascular function

The temporal associations between TMAO levels and coronary microvascular function were closely examined. No significant association was found between TMAO levels immediately after primary PCI and CFR, with a Pearson correlation coefficient of r = –0.02 (p = 0.828). Similarly, the correlation between TMAO levels and the IMR was negligible, with an r-value of 0.00 (p = 0.965) (Fig. 4.3.1.1 A, B). At the 3-month follow-up, the relationship between TMAO levels and coronary microvascular function became apparent. There was a significant inverse correlation with CFR (r = –0.41, p < 0.001) and a positive correlation with IMR (r = 0.35, p < 0.001), indicating that higher TMAO levels were significantly associated with a lower CFR and higher IMR, reflective of impaired coronary microvascular health (Fig. 4.3.1.1 C, D). These associations were more pronounced at the 12-month follow-up. The negative correlation between CFR and TMAO became stronger (r = –0.54, p < 0.001), and a correspondingly strong positive correlation was observed between IMR and TMAO (r = 0.54, p < 0.001). These findings suggest that higher levels of TMAO over time may predict a decline in microvascular function (Fig. 4.3.1.1 E, F).

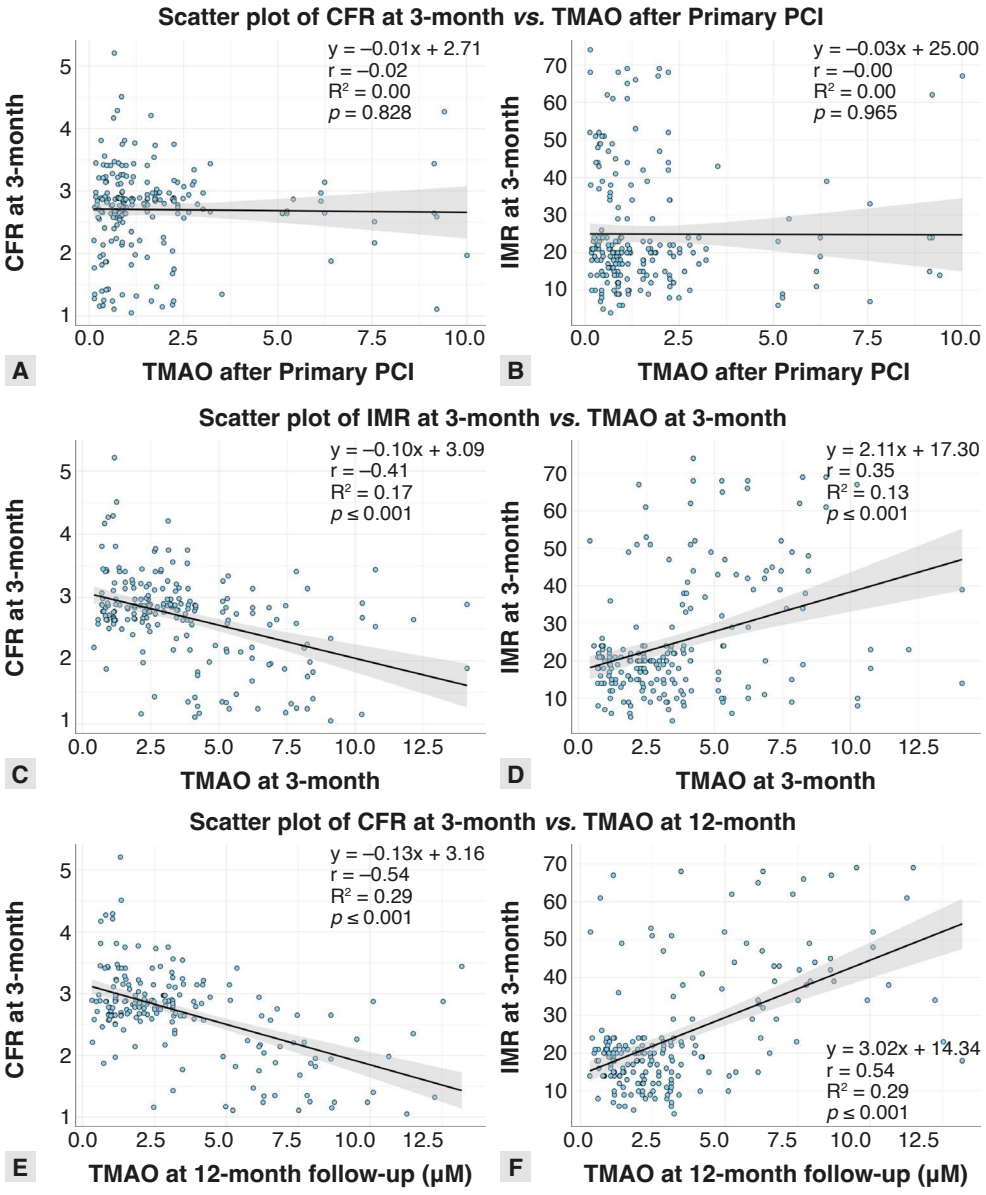

Fig. 4.3.1.1. *Temporal associations between trimethylamine N-oxide levels and microvascular function indicators*

CFR – coronary flow reserve; IMR – index of microcirculatory resistance; TMAO – trimethylamine N-oxide.

4.3.2. Optimal cut-off value determination

In this analysis, the central aim was to establish an optimal cut-off value for TMAO in predicting CMD following primary PCI. The ROC curve

analysis was employed to examine the correlation between TMAO levels post-primary PCI and the presence of CMD at the 3-month follow-up (Fig. 4.3.2.1). The analysis revealed that the area under the ROC curve (AUC) was 0.55 (95% CI: 0.46–0.64), with a *p*-value of 0.426. This result suggested a modest predictive value, establishing an optimal TMAO cut-off value at 0.75 μM. This cut-off correlated with a sensitivity of 0.43 (95% CI: 0.32–0.56) and a specificity of 0.71 (95% CI: 0.63–0.78). In contrast, the ROC analysis for the correlation of TMAO levels at the 3-month follow-up with the presence of CMD demonstrated a more significant predictive value (Fig. 4.3.2.1). The AUC at this stage was 0.80 (95% CI: 0.73–0.87; $p < 0.001$), indicating a robust predictive capability. Accordingly, the optimal cut-off value for TMAO was established at 3.91 μM, yielding a sensitivity of 0.75 (95% CI: 0.63–0.86) and a specificity of 0.82 (95% CI: 0.76–0.88). Given the superior predictive value of the 3-month TMAO levels, the decision was made to dichotomize the patient cohort based on this time point's established cut-off value. This stratification, distinguishing between high and low TMAO groups, is pivotal for subsequent analyses concerning the predictive relevance of TMAO levels in CMD post-PCI.

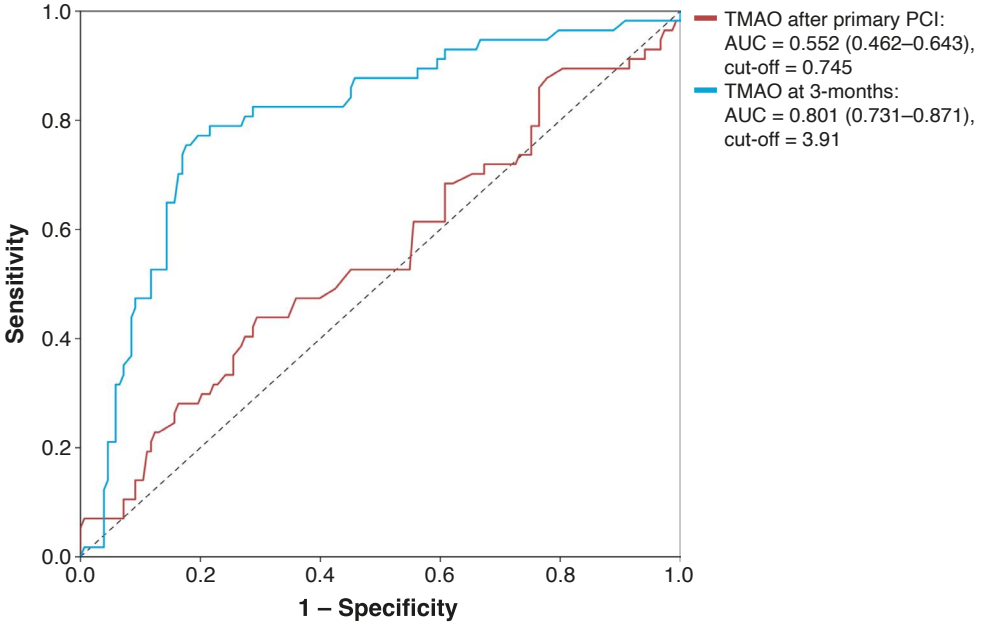

Fig. 4.3.2.1. *Receiver operating characteristic curve analysis of trimethylamine N-oxide for diagnosing coronary microvascular dysfunction*

AUC – area under curve; TMAO – trimethylamine N-oxide.

4.3.3. Baseline characteristics of patients stratified by trimethylamine N-oxide levels

Patients were categorized as presented in Table 4.3.3.1 into two groups based on the determined cut-off value of 3.91 μM. The analysis encompassed a total of 210 patients, with 70 patients (33.33%) presenting with higher TMAO levels (≥ 3.91 μM), while the remaining 140 patients (66.67%) had lower TMAO levels (< 3.91 μM). A notable difference was observed in the gender distribution between the two groups; the higher TMAO group had a significantly larger proportion of female participants (55.71%) compared to the lower TMAO group (32.86%), with a *p*-value of 0.002, indicating statistical significance. The median age of the overall cohort was 65 years, with IQR showing a slightly higher median age in the higher TMAO group (67 years, IQR [59.25, 78.00]) compared to the lower TMAO group (64 years, IQR [56.00, 75.00]); however, this difference was not statistically significant ($p = 0.120$). BMI and BSA were similar across both groups, with median BMIs of 26.75 kg/m² (IQR [24.6, 30.48]) and 27.53 kg/m² (IQR [24.6, 30.75]) and median BSAs of 1.91 m² (IQR [1.81, 2.13]) and 1.94 m² (IQR [1.81, 2.1]) for the higher and lower TMAO groups, respectively.

The primary diagnosis of STEMI was comparable between the groups, with anterior STEMI occurring in 54.29% of the higher TMAO group and 55.71% of the lower TMAO group, and inferior STEMI in 45.71% and 44.29%, respectively. The prevalence of arterial hypertension and a history of CAD showed no significant differences between the two groups. Furthermore, no significant differences were found regarding past PCI, stroke, diabetes mellitus, or dyslipidemia. A history of smoking was slightly more prevalent in the higher TMAO group (54.29% *vs.* 50.71%), but this was not statistically significant.

The distribution of the KILLIP class, which is an indicator of the severity of heart failure, was similar across both groups, with the majority of patients classified in class II. The higher TMAO group had a slightly higher proportion of patients in KILLIP class II (57.14%) compared to the lower TMAO group (50.71%), though this was not statistically significant. Classes III and IV were less common, with no significant differences observed between the two groups.

Table 4.3.3.1. *Baseline demographic and clinical characteristics of patients categorized by trimethylamine N-oxide level thresholds*

Characteristic	Overall (n = 210)	TMAO ≥ 3.91 µM (n = 70)	TMAO < 3.91 µM (n = 140)	*p*-value
Sex (Female)	85 (40.48%)	39 (55.71%)	46 (32.86%)	***0.002***
Age (years)	65.00 [58.00, 76.00]	67.00 [59.25, 78.00]	64.00 [56.00, 75.00]	0.120
Body mass index (kg/m^2)	27.39 [24.56, 30.69]	26.75 [24.6, 30.48]	27.53 [24.6, 30.75]	0.652
Body surface area (m^2)	1.93 [1.81, 2.10]	1.91 [1.81, 2.13]	1.94 [1.81, 2.1]	0.857
Primary diagnosis				
Anterior STEMI	116 (55.24%)	38 (54.29%)	78 (55.71%)	0.961
Inferior STEMI	94 (44.76%)	32 (45.71%)	62 (44.29%)	
Arterial hypertension	123 (58.57%)	42 (60.00%)	81 (57.86%)	0.882
History of coronary artery disease	59 (28.10%)	18 (25.71%)	41 (29.29%)	0.704
History of PCI	26 (12.38%)	8 (11.43%)	18 (12.86%)	0.941
History of stroke	27 (12.86%)	9 (12.86%)	18 (12.86%)	1
History of diabetes mellitus	51 (24.29%)	23 (32.86%)	28 (20.00%)	0.060
History of dyslipidemia	119 (56.67%)	33 (47.14%)	86 (61.43%)	0.069
Smoker (former/current)	109 (51.90%)	38 (54.29%)	71 (50.71%)	0.732
History of alcohol abuse	20 (9.52%)	8 (11.43%)	12 (8.57%)	0.678
KILLIP class				
I	62 (29.52%)	19 (27.14%)	43 (30.71%)	0.698
II	111 (52.86%)	40 (57.14%)	71 (50.71%)	
III	27 (12.86%)	7 (10.00%)	20 (14.29%)	
IV	10 (4.76%)	4 (5.71%)	6 (4.29%)	

STEMI – ST elevation myocardial infarction; PCI – percutaneous coronary intervention. Values are n (%) or median [IQR]. In bold and italics significant *p*-values (< 0.05).

4.3.4. Comparative predictive value of biomarkers for coronary microvascular dysfunction.

Within the scope of evaluating various biomarkers for predicting CMD at a 3-month follow-up. The ROC curve analysis underscores the superior predictive value of TMAO levels at 3 months, which presented an AUC of 0.801 (95% CI: 0.731–0.871) (Fig. 4.3.4.1). This indicator significantly outperformed the other assessed biomarkers, exhibiting a strong statistical significance ($p < 0.05$). CRP, a marker of systemic inflammation, showed a weaker association with CMD at the 3-month mark, with an AUC of 0.619 (95% CI: 0.533–0.706) and a *p*-value of 0.002, indicating a modest but significant predictive capability. BNP, another cardiac biomarker evaluated, had an AUC of 0.672 (95% CI: 0.582–0.762) at 3 months. While this reflects

a moderate predictive value for CMD, it does not reach the predictive strength of TMAO, with the *p*-value suggesting marginal significance ($p = 0.017$). In contrast, LDL cholesterol, often implicated in cardiovascular risk, yielded an AUC of 0.508 (95% CI: 0.415–0.601), which indicates a limited predictive value in this context, as underscored by the statistical analysis ($p < 0.001$). Furthermore, the NLR, considered a marker of systemic inflammation, demonstrated an AUC of 0.512 (95% CI: 0.425–0.598), showing no significant predictive value for CMD at the 3-month follow-up ($p = 0.076$). The comparative analysis, as depicted in Table 4.3.4.1, reveals that among the biomarkers evaluated, TMAO at 3 months shows the most robust association with CMD. This finding highlights the potential of TMAO as a singular biomarker with enhanced predictive capability for CMD, thereby proposing its utility in post-STEMI risk stratification.

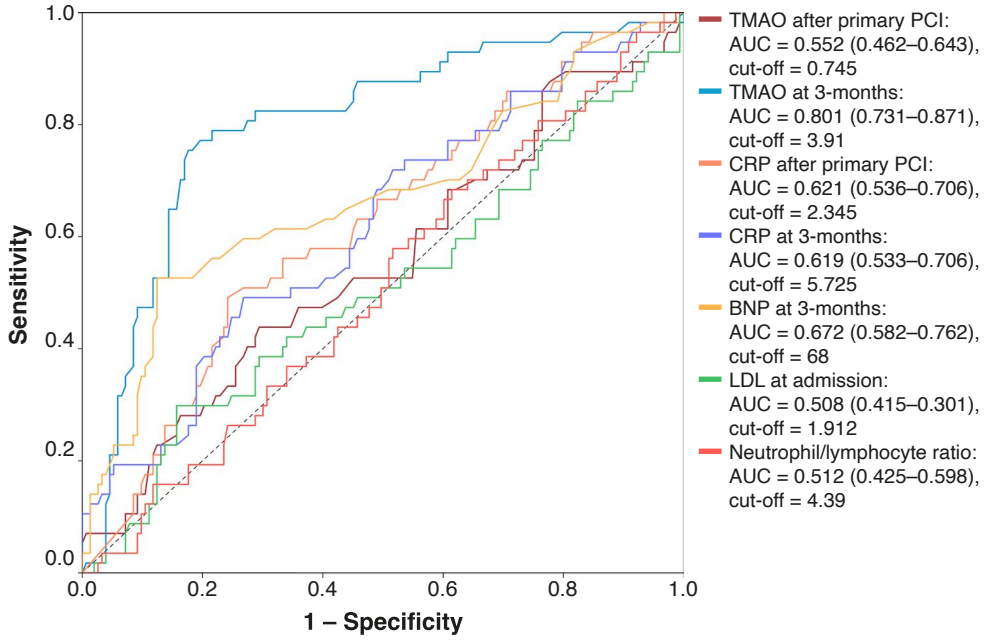

Fig. 4.3.4.1. *Receiver operating characteristic curve analysis of trimethylamine N-oxide and other biomarkers for diagnosing coronary microvascular dysfunction*

AUC – area under curve; LDL – low-density lipoprotein; CRP – C-reactive protein; BNP – B-type natriuretic peptide; TMAO – trimethylamine N-oxide.

Table 4.3.4.1. *Comparison of* receiver operating *characteristic* curves *for diagnosing coronary microvascular dysfunction*

Predictor1	AUC	Predictor2	AUC	*p*-value
TMAO after primary PCI	0.552 (0.462–0.643)	TMAO at 3 months	0.801 (0.731–0.871)	***< 0.001***
TMAO after primary PCI	0.552 (0.462–0.643)	CRP after primary PCI	0.621 (0.536–0.706)	0.284
TMAO after primary PCI	0.552(0.462–0.643)	CRP at 3 months	0.619 (0.533–0.706)	0.357
TMAO after primary PCI	0.552 (0.462–0.643)	BNP at 3 months	0.672 (0.582–0.762)	0.064
TMAO after primary PCI	0.552 (0.462–0.643)	LDL	0.508 (0.415–0.601)	0.491
TMAO after primary PCI	0.552 (0.462–0.643)	Neutrophil/lymphocyte ratio	0.512 (0.425–0.598)	0.559
TMAO at 3 months	0.801 (0.731–0.871)	CRP after primary PCI	0.621 (0.536–0.706)	***0.002***
TMAO at 3 months	0.801 (0.731–0.871)	CRP at 3 months	0.619 (0.533–0.706)	***0.002***
TMAO at 3 months	0.801 (0.731–0.871)	BNP at 3 months	0.672 (0.582–0.762)	***0.017***
TMAO at 3 months	0.801 (0.731–0.871)	LDL	0.508 (0.415–0.601)	***< 0.001***
TMAO at 3 months	0.801 (0.731–0.871)	Neutrophil/lymphocyte ratio	0.512 (0.425–0.598)	***< 0.001***
CRP after primary PCI	0.621 (0.536–0.706)	CRP at 3 months	0.619 (0.533–0.706)	0.981
CRP after primary PCI	0.621 (0.536–0.706)	BNP at 3 months	0.672 (0.582–0.762)	0.474
CRP after primary PCI	0.621 (0.536–0.706)	LDL	0.508 (0.415–0.601)	0.104
CRP after primary PCI	0.621 (0.536–0.706)	Neutrophil/lymphocyte ratio	0.512 (0.425–0.598)	0.061
CRP at 3 months	0.619 (0.533–0.706)	BNP at 3 months	0.672 (0.582–0.762)	0.425
CRP at 3 months	0.619 (0.533–0.706)	LDL	0.508 (0.415–0.601)	0.128
CRP at 3 months	0.619 (0.533–0.706)	Neutrophil/lymphocyte ratio	0.512 (0.425–0.598)	0.076
BNP at 3 months	0.672 (0.582–0.762)	LDL	0.508 (0.415–0.601)	***0.006***
BNP at 3 months	0.672 (0.582–0.762)	Neutrophil/lymphocyte ratio	0.512 (0.425–0.598)	***0.011***
LDL	0.508 (0.415–0.601)	Neutrophil/lymphocyte ratio	0.512 (0.425–0.598)	0.958

AUC – area under curve; LDL – low-density lipoprotein; CRP – C-reactive protein; BNP – B-type natriuretic peptide; TMAO – trimethylamine N-oxide. Values are n (%) or median [IQR].
In bold and italics significant p-values (< 0.05).

4.3.5. Haematological and biochemical markers

The overall median hemoglobin level across the cohort was 136.00 g/L, with no significant difference between the higher and lower TMAO groups ($p = 0.340$) (Table 4.3.5.1). White blood cell count and platelet levels were also consistent across both groups. In lipid profiles, TC levels were significantly lower in the high TMAO group (4.24 mmol/L) compared to the low TMAO group (4.78 mmol/L) with a p-value of 0.008. While LDL and HDL levels exhibited some differences, only HDL showed a significant difference, lower in the high TMAO group ($p = 0.027$). Triglycerides and Creatinine Clearance rates did not differ significantly.

Baseline and Peak Troponin I levels did not demonstrate a significant difference between the groups. However, hs-CRP levels were different at the 3-month mark, with the high TMAO group showing a median of 4.48 mg/L compared to the lower group's 4.14 mg/L, though this was not statistically significant ($p = 0.119$). The 3-month ESR was similar across groups, while BNP levels were significantly higher in the high TMAO group at 3 months ($p = 0.014$).

4.3.6. Echocardiographic parameters

Initial post-PCI LVEF demonstrated a median value of 40.0% [IQR: 36.25, 45.75] across the entire patient population. When categorized by TMAO levels, patients with TMAO ≥ 3.91 μM had a median post-PCI LVEF of 45.0% [IQR: 40.00, 50.00], which was notably higher compared to those with TMAO < 3.91 μM, who had a median LVEF of 40.0% [IQR: 35.00, 45.00]. The difference observed was statistically significant ($p < 0.001$), suggesting that higher TMAO levels may be associated with a more favorable LV function shortly after PCI (Table 4.3.5.1).

Table 4.3.5.1. *Laboratory and echocardiographic parameters of patients with ST-elevation myocardial infarction, categorized by trimethylamine N-oxide level thresholds*

Parameters	Overall (n = 210)	TMAO ≥ 3.91 μM (n = 70)	TMAO < 3.91 μM (n = 140)	*p*-value
Laboratory test				
Hemoglobin (g/l)	136.00 [119.00, 148.00]	139.00 [118.00, 153.00]	135.50 [119.00, 146.00]	0.340
White blood cell count (10^9/L)	9.86 [8.22, 12.09]	10.18 [8.09, 12.06]	9.51 [8.28, 12.10]	0.747
Platelets ($\times 10^9$/L)	240.50 [204.00, 273.00]	239.50 [203.25, 270.25]	244.00 [204.75, 273.25]	0.874
Total cholesterol (mmol/L)	4.64 [3.75, 5.79]	4.24 [3.29, 5.50]	4.78 [3.90, 5.90]	***0.008***
Low-density lipoprotein (mmol/L)	2.93[2.09, 3.93]	2.66 [1.77, 3.86]	3.01 [2.34, 3.96]	0.078
High-density lipoprotein (mmol/L)	1.12 [0.92, 1.35]	1.08 [0.83, 1.27]	1.13 [0.97, 1.36]	***0.027***
Triglycerides (mmol/L)	1.16 [0.82, 1.65]	1.04 [0.85, 1.54]	1.18 [0.82, 1.75]	0.232
Creatinine clearance (ml/min)	39.50 [34.95, 47.50]	39.45 [34.82, 48.18]	39.50 [35.65, 47.35]	0.917
Baseline troponin I (μg/L)	2.19 [0.81, 3.71]	2.20 [0.89, 3.34]	2.16 [0.76, 3.88]	0.671
Peak Troponin I (μg/L)	45.00 [27.00, 64.00]	49.50 [25.00, 64.00]	41.00 [27.00, 64.25]	0.627
High-sensitivity CRP (mg/L)	3.8 [1.85, 10.52]	2.80 [1.39, 8.00]	4.9 [2.36, 11.44]	***0.010***
3-month high-sensitivity CRP (mg/L)	4.28 [2.35, 6.32]	4.48 [2.69, 6.36]	4.14 [2.19, 6.2]	0.119
3-month ESR	13.00 [9.00, 17.00]	13.00 [8.25, 19.75]	13.00 [10.00, 16.00]	0.452
3-month BNP (ng/L)	37.00 [27.00, 66.75]	44 [28, 87.75]	37 [26.75, 57]	***0.014***
Echocardiographic parameters				
Post-PCI LVEF (%)	40.0 [36.25, 45.75]	45.00 [40.00, 50.00]	40.00 [35.00, 45.00]	***< 0.001***
12-month LVEF (%)	45.0 [40.00, 50.00]	40.00 [35.00, 50.00]	48.00 [40.00, 55.00]	***< 0.001***
LVEF change (%)	5.00 [0.00, 10.00]	–5.00 [–10.00, 5.00]	+8.00 [1.50, 10.00]	***< 0.001***
TMAO measurements				
Post-PCI TMAO	0.92 [0.61, 1.93]	1.13 [0.69, 2.23]	0.88 [0.55, 1.74]	0.073
3-month TMAO	2.97 [1.82, 5.06]	6.22 [5.12, 8.06]	2.18 [1.17, 2.97]	***< 0.001***
12-month TMAO	2.44 [1.35, 4.02]	6.18 [4.14, 7.94]	1.83 [1.14, 2.6]	***< 0.001***

CMD – coronary microvascular dysfunction; BNP – brain natriuretic peptide, CRP – C-reactive protein; LVEF – left ventricular ejection fraction; ESR – erythrocyte sedimentation rate; TMAO – trimethylamine N-oxide. Values are n (%) or median [IQR]. In bold and italics significant *p*-values (< 0.05).

At the 12-month follow-up, the trend reversed. The group with higher TMAO levels showed an inferior median LVEF of 40.00% [IQR: 35.00, 50.00], whereas the lower TMAO group showed a superior median of 48.00% [IQR: 40.00, 55.00] (Fig. 4.3.6.1 A). The statistical significance of this difference was maintained ($p < 0.001$), reinforcing the postulate that high TMAO levels may indicate long-term cardiac function deterioration.

The percentage change in LVEF over the 12 months further illuminated these differences. Patients with lower TMAO levels experienced a median increase in LVEF of +8.00% [IQR: 1.50, 10.00], contrasted with a decrease of –5.00% [IQR: –10.00, 5.00] in the higher TMAO group (Fig. 4.3.6.1 B). This stark contrast not only remained statistically significant ($p < 0.001$) but also suggested a potential role of TMAO in cardiac remodelling post-STEMI.

The data elucidates a complex relationship between TMAO levels and LV function recovery in STEMI patients. While initial post-PCI assessments indicated a better LVEF in patients with higher TMAO levels, the 12-month follow-up revealed a reversal in this trend, with these patients exhibiting a decline in LVEF compared to their counterparts with lower TMAO levels (Fig. 4.3.6.1 A). These findings highlight the importance of monitoring TMAO levels not just as a biomarker for immediate post-PCI prognosis but also for understanding long-term cardiac remodelling and recovery trajectories post-STEMI.

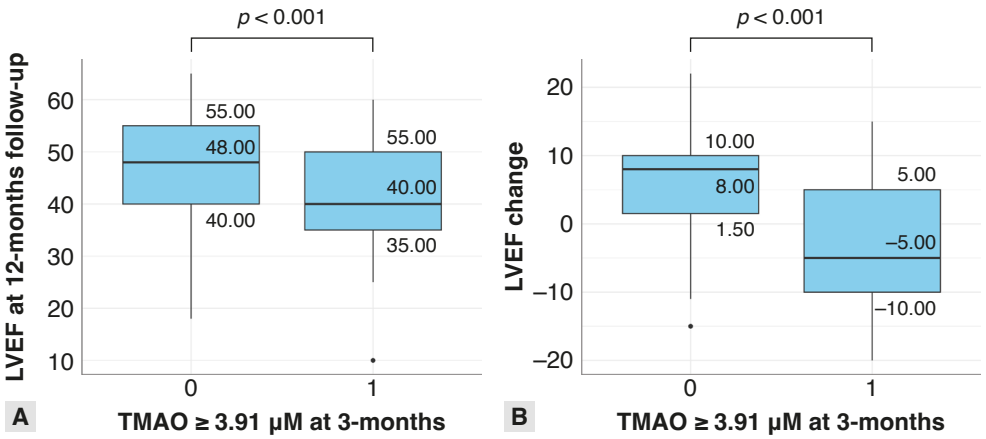

Fig. 4.3.6.1. *12-month left ventricular ejection fraction and change in left ventricular ejection fraction categorized by trimethylamine N-oxide groups*

LVEF – left ventricular ejection fraction; TMAO – trimethylamine N-oxide.

4.3.7. Trajectory of TMAO levels following STEMI

The evolution of TMAO levels following STEMI and primary PCI demonstrates a dynamic profile across the 12-month monitoring period. Initially, after PCI, the median TMAO level was established at 0.92 μM [IQR: 0.61, 1.93], reflecting the baseline state of the patients' metabolic response following acute coronary intervention. A considerable escalation in TMAO levels was observed at the 3-month follow-up, with the median value ascending sharply to 2.97 μM [IQR: 1.82, 5.06]. At the 12-month milestone, the TMAO levels exhibit a slight regression to a median of 2.44 μM [IQR: 1.35, 4.02], indicating a relative stabilization (Table 4.3.5.1). Fig. 4.3.7.1 reflects this trend with many patient lines plateauing or slightly descending, suggesting a chronic phase response where the fluctuations in TMAO levels taper off and reach a new equilibrium.

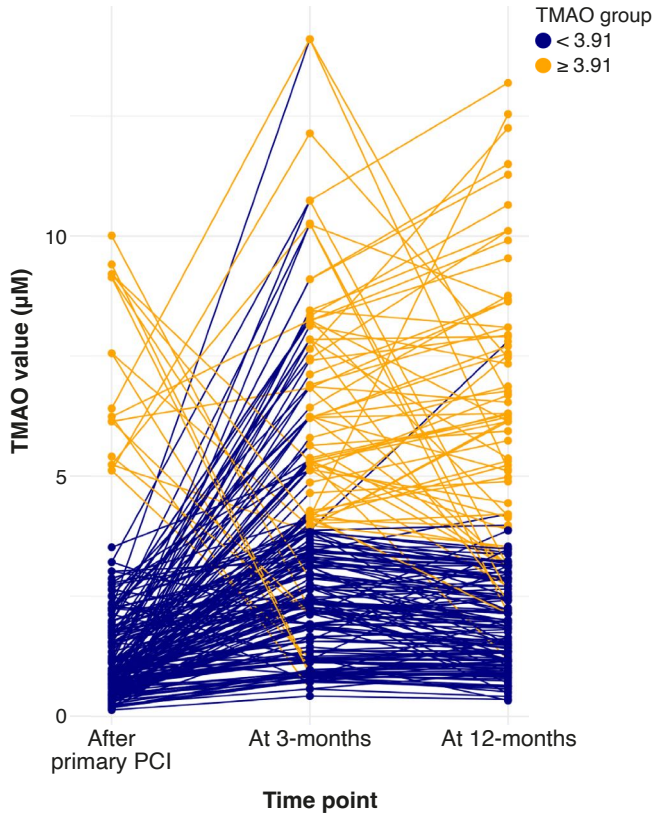

Fig. 4.3.7.1. *Longitudinal changes in trimethylamine N-oxide levels for ST-elevation myocardial infarction patients stratified by trimethylamine N-oxide levels threshold*

PCI – percutaneous coronary intervention; TMAO – trimethylamine N-oxide.

4.3.8. Angiographic parameters

The pain-to-door time, a critical metric in STEMI management, had a median value of 314 minutes [IQR: 107.75, 592.25] across the entire cohort, indicating the time from symptom onset to hospital arrival (Table 4.3.8.1). When comparing between the high TMAO (≥ 3.91 μM) and low TMAO (< 3.91 μM) groups, there was no significant difference, with medians of 352 minutes [IQR: 124.75, 612.00] and 306.50 minutes [IQR: 104.75, 537.25], respectively ($p = 0.246$). The door-to-balloon time, representing the interval from hospital arrival to balloon inflation during PCI, showed a consistent median of 40 minutes [IQR: 29.25, 52.00] overall, which was mirrored in both TMAO stratified groups ($p = 0.649$), reflecting standardized acute care. Pre-PCI TIMI flow grades, which assess coronary artery blood flow, were reported with most patients presenting with grade 0 flow, denoting complete occlusion. The distribution of TIMI flow grades did not show significant variation post-PCI between the two TMAO groups ($p = 0.159$), indicating similar immediate revascularization outcomes. Notably, the post-PCI TIMI flow grade 3, indicative of normal flow, was achieved in 88.1% of the overall patient population. Culprit vessel analysis revealed the left anterior descending artery as the most common site, with no significant difference in distribution across the TMAO groups ($p = 0.135$). Additionally, the number of diseased vessels, reflecting disease severity, was comparable between the two groups.

4.3.9. Physiologic parameters in relation to trimethylamine N-oxide levels

At the 3-month follow-up, there was a notable divergence in coronary physiology parameters based on TMAO levels. The high TMAO group exhibited a lower median CFR of 2.22 [IQR: 1.7, 2.83] compared to the overall median of 2.81 [IQR: 2.54, 2.98], with a significant p-value of < 0.001 (Table 4.3.8.1). This suggests a potential impact of TMAO levels on microvascular function. Conversely, the FFR remained consistent across groups ($p = 0.680$), implying that TMAO levels did not significantly affect epicardial artery stenosis severity.

The IMR, a direct measure of coronary microvascular function, was significantly higher in the high TMAO group, with a median value of 35.5 [IQR: 18.25, 47.75], compared to the overall median of 20.00 [IQR: 15.00, 29.00] ($p < 0.001$).

Table 4.3.8.1. *Coronary angiography and physiology parameters of ST-elevation myocardial infarction patients, categorized by trimethylamine N-oxide levels*

Parameters	Overall (n = 210)	TMAO ≥ 3.91 µM (n = 70)	TMAO < 3.91 µM (n = 140)	*p*-value
Angiographic				
Pain-to-door time (minutes)	314 [107.75, 592.25]	352.00 [124.75, 612.00]	306.50 [104.75, 537.25]	0.246
Door-to-balloon (minutes)	40.00 [29.25, 52.00]	40.00 [31.00, 53.00]	40.00 [29.00, 51.00]	0.649
Pre-PCI TIMI flow				
0	130 (61.90%)	42 (60.00%)	88 (62.86%)	0.109
1	8 (3.81%)	3 (4.29%)	5 (3.57%)	
2	44 (20.95%)	20 (28.57%)	24 (17.14%)	
3	28 (13.33%)	5 (7.14%)	23 (16.43%)	
Post-PCI TIMI flow				0.159
0	2 (0.95%)	1 (1.43%)	1 (0.71%)	
1	1 (0.48%)	1 (1.43%)	0 (0.00%)	
2	22 (10.48%)	10 (14.29%)	12 (8.57%)	
3	185 (88.1%)	58 (82.86%)	127 (90.71%)	
Culprit vessel territory				
Left anterior descending artery	118 (56.19%)	39 (55.71%)	79 (56.43%)	0.135
Circumflex artery	49 (23.33%)	12 (17.14%)	37 (26.43%)	
Right coronary artery	43 (20.48%)	19 (27.14%)	24 (17.14%)	
Number of diseased vessels				
2-vessel disease	123 (58.57%)	43 (61.43%)	80 (57.14%)	0.656
3-vessel disease	87 (41.43%)	27 (38.57%)	60 (42.86%)	
Coronary physiology at 3-month follow-up				
Coronary flow reserve (CFR)	2.81 [2.54, 2.98]	2.22 [1.7, 2.83]	2.87 [2.69, 3.15]	***< 0.001***
Fractional flow reserve (FFR)	0.92 [0.87, 0.97]	0.92 [0.87, 0.97]	0.91 [0.87, 0.97]	0.680
Index of Microcirculatory resistance (IMR)	20.00 [15.00, 29.00]	35.5 [18.25, 47.75]	19 [14, 22]	***< 0.001***

PCI – percutaneous coronary intervention; TIMI – thrombolysis in myocardial infarction; TMAO – trimethylamine N-oxide. Values are n (%) or median [IQR]. In bold and italics significant *p*-values (< 0.05).

4.3.10. Trimethylamine N-oxide and clinical outcomes at 12-month follow-up

In the evaluation of STEMI patients following primary PCI, the 3-month post-procedure phase revealed a pronounced prevalence of CMD in individuals with elevated TMAO levels. Specifically, 61.43% of patients with TMAO levels ≥ 3.91 μM had CMD, contrasting starkly with the 10.00% prevalence in those with lower TMAO levels, indicating a potent correlation between TMAO concentrations and CMD incidence ($p < 0.001$) (Table 4.3.10.1, Fig 4.3.10.1).

Extending the observation period to 12 months post-PCI, the data presented further clinical outcomes stratified by TMAO levels. Notably, the occurrence of nonfatal myocardial infarctions was more frequent in the higher TMAO group, reaching a significant 10.00%, compared to 2.14% in the lower TMAO group ($p = 0.017$). Additionally, mortality rates were higher in the elevated TMAO cohort at 7.14%, against a lower 0.71% in the sub-threshold group ($p = 0.016$). While the need for subsequent revascularization procedures post-PCI did not differ substantially between the groups, a significant disparity emerged in hospitalizations due to heart failure, with 17.14% of patients in the higher TMAO bracket requiring hospital care compared to only 2.86% in the lower bracket ($p < 0.001$).

The study also assessed MACE and POCE. A marked increase in MACE was observed in the higher TMAO group, which reported a 41.43% incidence rate, significantly exceeding the 10.71% rate seen in the lower TMAO group ($p < 0.001$). Similarly, POCE was significantly more common among those with higher TMAO levels, occurring in 27.14% of these patients, compared to 7.86% in those with TMAO levels below the threshold ($p < 0.001$). The Kaplan-Meier curve revealed an increased incidence of MACE in the high TMAO group (log-rank $p < 0.001$), starting from the first-month post-PCI (Fig 4.3.10.2).

These findings collectively underscore the impact of TMAO levels on the prognosis of STEMI patients. Elevated TMAO is evidently associated with an increased risk of CMD in the short term and correlates with a higher incidence of adverse clinical outcomes within a year following the event.

Table 4.3.10.1. *Clinical outcomes of patients presenting with ST-elevation myocardial infarction, categorized by trimethylamine N-oxide levels*

	Overall (n = 210)	**TMAO ≥ 3.91 (n = 70)**	**TMAO < 3.91 (n = 140)**	***p*-value**
3-month physiology diagnosis				
CMD	57 (27.14%)	43 (61.43%)	14 (10.00%)	***< 0.001***
12-month clinical outcome				
Ischemic or hemorrhagic stroke	7 (3.33%)	5 (7.14%)	2 (1.43%)	***0.043***
Nonfatal MI	10 (4.76%)	7 (10.00%)	3 (2.14%)	***0.017***
Death	6 (2.86%)	5 (7.14%)	1 (0.71%)	***0.016***
Revascularization	8 (3.80%)	3 (4.29%)	5 (3.57%)	1
Hospitalization for Heart failure	16 (7.62%)	12 (17.14%)	4 (2.86%)	***< 0.001***
MACE	44 (20.95%)	29 (41.43%)	15 (10.71%)	***< 0.001***
POCE	30 (14.29%)	19 (27.14%)	11 (7.86%)	***< 0.001***

CMD – coronary microvascular dysfunction; POCE – The composite of all-cause mortality, any myocardial infarction, any stroke and any revascularization, MACE – POCE + heart failure hospitalization; TMAO – trimethylamine N-oxide. Values are n (%).
In bold and italics significant p-values (< 0.05).

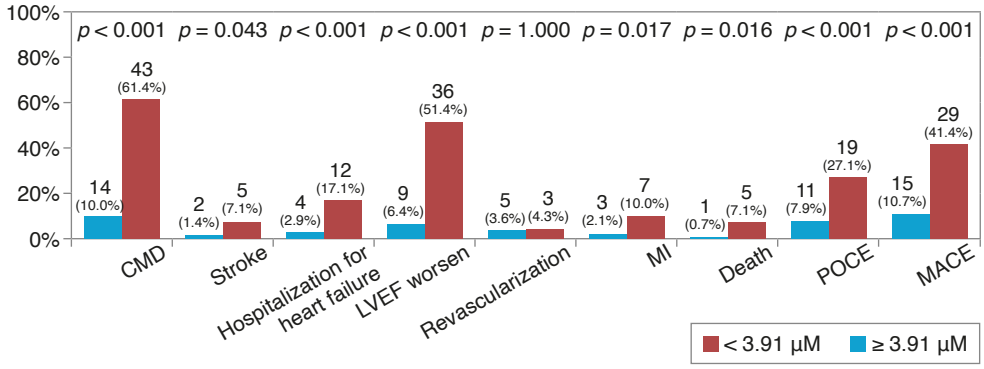

Fig. 4.3.10.1. *Rates of clinical events and major adverse cardiac events displayed by trimethylamine N-oxide levels groups*

CMD – coronary microvascular dysfunction, LVEF – left ventricular ejection fraction, MI – myocardial infarction, POCE – the composite of all-cause mortality, any myocardial infarction, any stroke and any revascularization, MACE = POCE +heart failure hospitalization.

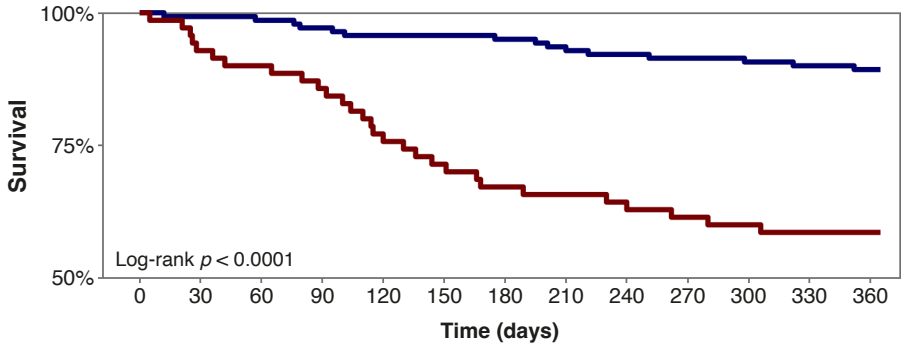

Strata	Number at risk												
TMAO < 3.91	140	139	138	136	134	134	133	131	129	128	127	126	125
TMAO ≥ 3.91	70	65	63	60	54	50	47	46	45	43	42	41	41

Fig 4.3.10.2. *Kaplan-Meier event-free survival curve for occurrence of major adverse cardiac events grouped by trimethylamine N-oxide levels at 3 months*

TMAO – trimethylamine N-oxide.

4.3.11. Relationship between trimethylamine N-oxide levels and odds of coronary microvascular dysfunction

The cubic spline model illustrates the relationship between TMAO concentrations at the 3-month follow-up and the likelihood of developing CMD in post-STEMI patients (Fig. 4.3.11.1). The curve exhibits a distinctive reversed J-shape, indicating a nuanced association between TMAO levels and the odds of CMD.

Initially, at lower concentrations of TMAO, the odds of CMD remain relatively stable with a slight incline. However, as TMAO levels progress beyond the 3.91 μM threshold, there is a discernible sharp escalation in the risk of CMD. This risk intensifies markedly as TMAO levels increase towards the 6 μM mark, suggesting a threshold effect where the odds of CMD rise substantially within this range.

Beyond the 6 μM level, the curve begins to plateau, indicating that while the risk remains elevated, the rate of increase in the odds of CMD does not continue to rise as steeply with higher TMAO levels. This pattern suggests a possible saturation point or a ceiling effect in the relationship between elevated TMAO levels and CMD risk.

This curve not only captures the direct correlation between TMAO levels and the probability of CMD but also highlights a critical concentration window where TMAO levels are most predictive of adverse microvascular outcomes. The delineation of this relationship is crucial for clinicians as it

underscores the potential for TMAO to serve as a biomarker for stratifying patient risk and tailoring post-STEMI management strategies.

The shaded area around the curve represents the CIs, which grow wider at the extremes of TMAO measurements, indicating less certainty in the estimates due to fewer observations at these levels. Nonetheless, within the central, more densely sampled TMAO range, the CIs are narrower, reflecting greater precision in the odds estimation of developing CMD.

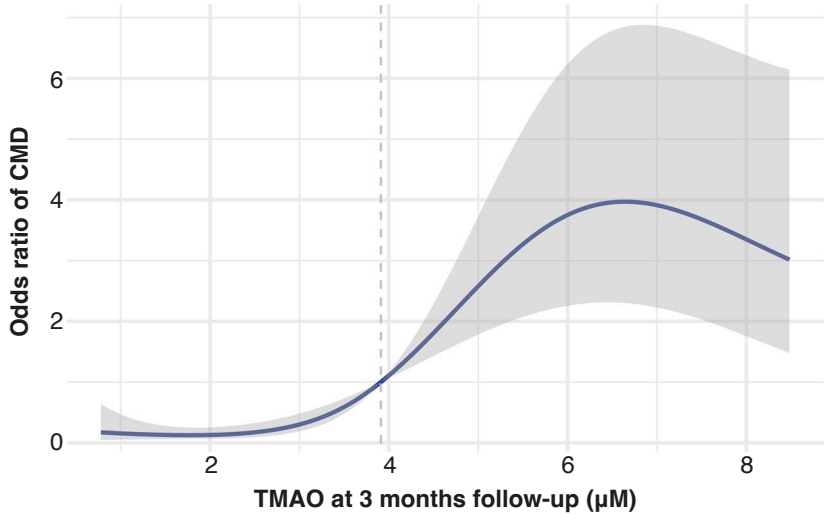

Fig. 4.3.11.1. *Cubic spline analysis of trimethylamine N-oxide levels at 3 months and the associated odds of developing coronary microvascular dysfunction post-ST-elevation myocardial infarction*

CMD – coronary microvascular dysfunction; TMAO – trimethylamine N-oxide.

4.3.12. Multivariable logistic regression analysis

Univariable logistic regression analysis and multivariable analysis with adjustment for variables with $p < 0.05$ in univariable logistic regression were performed to identify the independent risk factors for CMD (Table 4.3.12.1). The model showed that the white blood cell count, creatinine clearance, BNP and CRP at 3-month follow-up, pre-PCI TIMI flow, intracoronary IIb/IIIa inhibitor injection, use of aspiration thrombectomy, and TMAO at 3-month follow-up were the independent predictors for CMD.

Table 4.3.12.1. *Multivariable binary logistic analysis for the prediction of coronary microvascular dysfunction after ST-segment elevation myocardial infarction*

Variable	Univariable		Multivariable	
	Odds ratio	***p*-value**	**Odds ratio**	***p*-value**
Age (years)	0.994 (0.97–1.019)	0.635		
Sex (Female)	3.638 (1.925–6.875)	***< 0.001***	1.064 (0.962–1.178)	0.227
Body mass index (kg/m^2)	0.953 (0.895–1.016)	0.141		
Body surface area (m^2)	0.447 (0.11–1.817)	0.260		
Primary diagnosis	0.951 (0.515–1.755)	0.872		
Arterial hypertension	0.872 (0.472–1.613)	0.663		
History of coronary artery disease	1.412 (0.731–2.728)	0.304		
History of PCI	1.5 (0.627–3.589)	0.362		
History of stroke	1.406 (0.592–3.341)	0.440		
History of diabetes mellitus	3.394 (1.736–6.634)	***< 0.001***	1.118 (0.999–1.251)	0.053
History of dyslipidemia	0.971 (0.526–1.793)	0.925		
Smoker (former/current)	1.393 (0.754–2.574)	0.290		
History of alcohol abuse	0.646 (0.207–2.022)	0.453		
KILLIP class	1.043 (0.708–1.537)	0.831		
Hemoglobin (g/L)	1.01 (0.995–1.026)	0.176		
White blood cell count (×10^9/L)	1.112 (1.003–1.233)	***0.043***	1.026 (1.01–1.043)	***0.002***
Neutrophil lymphocyte ratio	0.972 (0.887–1.065)	0.543		
Platelets (×10^9/L)	1.005 (1–1.009)	0.066		
Total cholesterol (mmol/L)	0.951 (0.774–1.167)	0.630		
Low-density lipoprotein (mmol/ L)	1.025 (0.814–1.29)	0.835		
High-density lipoprotein (mmol/ L)	0.61 (0.237–1.567)	0.304		
Triglycerides (mmol/ L)	0.734 (0.489–1.101)	0.135		
Creatinine clearance (mL/min)	0.951 (0.919–0.985)	***0.005***	0.992 (0.988–0.997)	***0.001***
Baseline troponin I (µg/L)	1.031 (0.978–1.088)	0.255		
Peak troponin I (µg/L)	1.007 (0.997–1.017)	0.170		
Baseline high-sensitivity CRP (mg/L)	0.978 (0.953–1.003)	0.082		
3-month high-sensitivity CRP (mg/L)	1.21 (1.074–1.364)	***0.002***	1.020 (1.001–1.040)	***0.039***
3-month BNP (ng/L)	1.012 (1.006–1.019)	***< 0.001***	1.001(1.000–1.002)	***0.003***
TMAO at primary PCI	0.988 (0.84–1.162)	0.886		
TMAO at 3-month	1.443 (1.262–1.65)	***< 0.001***	1.059 (1.040–1.079)	***<0.001***
Post-PCI LVEF (%)	1.081 (1.028–1.137)	***0.003***	1.007 (1.000–1.014)	***0.043***
Pain-to-door time (minutes)	1.001 (1.000–1.001)	***0.018***	1.000 (1.000–1.000)	0.154
Door-to-balloon (minutes)	1.009 (0.992–1.026)	0.319		

Table 4.3.12.1. *Continued*

Variable	Univariable		Multivariable	
	Odds ratio	*p*-value	Odds ratio	*p*-value
Pre-PCI TIMI flow	0.685 (0.507–0.924)	***0.013***	0.950 (0.912–0.990)	***0.015***
Post-PCI TIMI flow	0.578 (0.302–1.108)	0.099		
Culprit Vessel	1.175 (0.808–1.708)	0.398		
Number of diseased vessels	0.769 (0.411–1.438)	0.411		
Intracoronary glycoprotein IIb/IIIa inhibitor	0.199 (0.068–0.585)	***0.003***	0.827 (0.739–0.926)	***0.001***
Aspiration thrombectomy	0.217 (0.081–0.578)	***0.002***	0.874 (0.782–0.977)	***0.019***
Contrast dose (milliliters)	1.007 (0.987–1.027)	0.519		
Stent diameter (millimeters)	1.037 (0.527–2.04)	0.917		
Stent length (millimeters)	1.046 (0.989–1.106)	0.115		

PCI – percutaneous coronary intervention; CRP – C-reactive protein; BNP – brain natriuretic peptide; LVEF – left ventricular ejection fraction; TMAO – trimethylamine N-oxide. Values are n (%) or median [IQR]. In bold and italics significant *p*-values (< 0.05).

4.4. Validation of the prognostic performance of the novel parameter microvascular resistance reserve in ST-elevation myocardial infarction patients

4.4.1. Study population characteristics

This cohort was stratified based on the presence of CMD, which was defined by a MRR of less than 3 (Table 4.4.1.1). In this analysis, we analyzed all the 210 patients who were presented with STEMI. Patients exhibiting an MRR below this threshold constituted 26.67% of the study population, indicating the presence of CMD. Conversely, patients with an MRR of 3 or above represented the majority, comprising 73.33% of the cohort, indicating the absence of CMD. On the other hand, 57 patients (27.1%) and 33 patients (15.7%) had abnormal IMR (≥ 25) and CFR (< 2.0), respectively. The distribution of patients with abnormal MRR, CFR, and IMR is shown in **fig. 4.4.1.1**. There was a significantly higher female representation in the CMD group compared to the non-CMD group (62.50% *vs.* 32.47%; $p < 0.001$). Although the median age was higher in the CMD group, the difference was not statistically significant when compared to the non-CMD group (67 years *vs.* 63 years; $p = 0.460$). No significant differences were observed in BMI between the CMD and non-CMD groups (26.07 kg/m² *vs.* 27.69 kg/m²; $p = 0.117$). BSA measurements were also similar between the CMD and non-CMD groups (1.89 m² *vs.* 1.94 m²; $p = 0.487$). When looking at the primary diagnosis, the incidence of anterior STEMI was consistent across both groups (55.36% *vs.* 55.19%; $p = 1$), as was the incidence of inferior STEMI (44.64%

vs. 44.81%; $p = 1$). There were no statistically significant differences between groups in terms of arterial hypertension ($p = 0.680$) and history of CAD ($p = 0.337$). Regarding the history of PCI, there were no significant differences between the CMD and non-CMD groups ($p = 0.788$). Stroke history was reported within similar rates between the CMD and non-CMD groups (14.29% *vs.* 12.34%; $p = 0.889$). However, the presence of diabetes mellitus was significantly higher in the CMD group compared to the non-CMD group (39.29% *vs.* 18.83%; $p = 0.004$). Dyslipidemia history was equally distributed between both groups, with no significant difference ($p = 1$). The proportion of smokers was also similar between the CMD and non-CMD groups (53.57% *vs.* 51.30%; $p = 0.892$), as was the history of alcohol abuse (8.93% *vs.* 9.74%; $p = 1$). KILLIP class distribution indicated that most patients fell into class II, but there were no significant differences in KILLIP class distribution between the CMD and non-CMD groups ($p = 0.949$).

Table 4.4.1.1. *Characteristics of ST-elevation myocardial infarction patients classified by coronary microvascular dysfunction according to microvascular resistance reserve*

Characteristic	**Overall (n =210)**	**CMD (MRR < 3.0) (n = 56)**	**No CMD (MRR ≥ 3.0) (n = 154)**	***p*-value**
Sex (Female)	85 (40.48%)	35 (62.50%)	50 (32.47%)	**< 0.001**
Age (years)	65.00 [58.00, 76.00]	67.00 [58.00, 76.00]	63.00 [57.75, 75.25]	0.460
Body mass index (kg/m^2)	27.39 [24.56, 30.69]	26.07 [24.27, 29.41]	27.69 [24.78, 31.04]	0.117
Body surface area (m^2)	1.93 [1.81, 2.10]	1.89 [1.82, 2.10]	1.94 [1.81, 2.11]	0.487
Primary diagnosis				
Anterior STEMI	116 (55.24%)	31 (55.36%)	85 (55.19%)	1
Inferior STEMI	94 (44.76%)	25 (44.64%)	69 (44.81%)	
Arterial hypertension	123 (58.57%)	31 (55.36%)	92 (59.74%)	0.680
History of coronary artery disease	59 (28.10%)	19 (33.93%)	40 (25.97%)	0.337
History of PCI	26 (12.38%)	8 (14.29%)	18 (11.69%)	0.788
History of stroke	27 (12.86%)	8 (14.29%)	19 (12.34%)	0.889
History of diabetes mellitus	51 (24.29%)	22 (39.29%)	29 (18.83%)	**0.004**
History of dyslipidaemia	119 (56.67%)	32 (57.14%)	87 (56.49%)	1
Smoker (former/current)	109 (51.90%)	30 (53.57%)	79 (51.30%)	0.892
History of alcohol abuse	20 (9.52%)	5 (8.93%)	15 (9.74%)	1

Table 4.4.1.1. *Continued*

Characteristic	Overall (n =210)	CMD (MRR < 3.0) (n = 56)	No CMD (MRR ≥ 3.0) (n = 154)	*p*-value
KILLIP class				
I	62 (29.52%)	17 (30.36%)	45 (29.22%)	0.949
II	111 (52.86%)	30 (53.57%)	81 (52.60%)	
III	27 (12.86%)	6 (10.71%)	21 (13.64%)	
IV	10 (4.76%)	3 (5.36%)	7 (4.55%)	

STEMI – ST-elevation myocardial infarction; PCI – percutaneous coronary intervention; MRR – microvascular resistance reserve. Values are n (%) or median [IQR]. In bold and italics significant *p*-values (< 0.05).

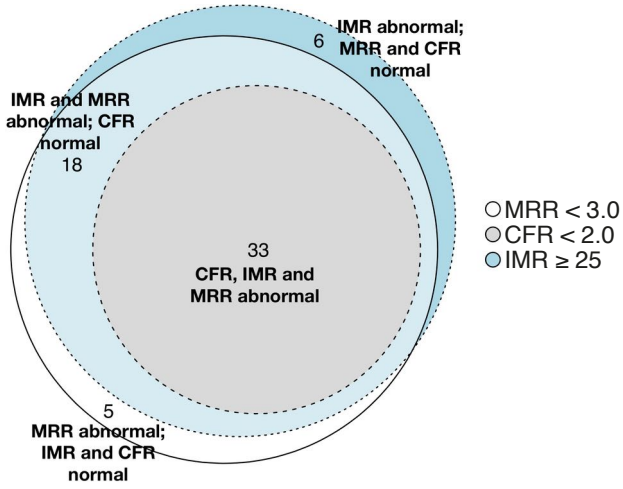

Fig. 4.4.1.1. *Overlap of abnormal coronary flow reserve, index of microcirculatory resistance, and microvascular resistance reserve measurements*

CFR – coronary flow reserve; IMR – index of microcirculatory resistance; MRR – microvascular resistance reserve.

4.4.2. Laboratory findings

Laboratory tests showed that hemoglobin levels, white blood cell count, and platelet count were similar across the overall cohort, with no significant differences between the MRR cut-off groups ($p > 0.05$) (Table 4.4.2.1). The same was true for TC, LDL, HDL, and triglyceride levels, which were comparable between the groups ($p > 0.05$). Creatinine clearance rate was significantly lower in the group with MRR < 3 compared to those with MRR ≥ 3 (37.05 mL/min *vs.* 40.90 mL/min; $p = 0.002$). Troponin levels, both at baseli-

ne and peak, did not differ significantly between the groups ($p > 0.05$). However, 3-month hs-CRP levels were significantly higher in the group with MRR < 3 than in those with MRR ≥ 3 (5.43 mg/L *vs.* 4.02 mg/L; $p = 0.007$). Similarly, BNP levels at 3 months were markedly elevated in those with MRR < 3 (54.00 ng/L *vs.* 37.00 ng/L; $p = 0.005$).

Table 4.4.2.1. *Laboratory and echocardiographic parameters of patients with ST-elevation myocardial infarction, categorized by coronary microvascular dysfunction*

Parameters	**Overall (n = 210)**	**CMD (MRR < 3.0) (n = 56)**	**No CMD (MRR ≥ 3.0) (n = 154)**	***p*-value**
Laboratory test				
Hemoglobin (g/l)	136.00 [119.00, 148.00]	143.50 [118.75, 151.50]	135.00 [119.00, 146.00]	0.163
White blood cell count ($\times 10^9$/L)	9.86 [8.22, 12.09]	10.91 [8.34, 12.52]	9.75 [8.22, 11.96]	0.318
Platelets ($\times 10^9$/L)	240.50 [204.00, 273.00]	242.50 [205.50, 308.25]	238.50 [203.25, 265.00]	0.186
Total cholesterol (mmol/L)	4.64 [3.75, 5.79]	4.55 [3.54, 5.71]	4.65 [3.80, 5.79]	0.755
Low-density lipoprotein (mmol/L)	2.93[2.09, 3.93]	2.92[2.14, 3.91]	3.01[1.88, 4.04]	0.706
High-density lipoprotein (mmol/L)	1.12 [0.92, 1.35]	1.12 [0.88, 1.28]	1.12 [0.95, 1.35]	0.463
Triglycerides (mmol/L)	1.16 [0.82, 1.65]	1.13 [0.84, 1.62]	1.17 [0.82, 1.67]	0.437
Creatinine clearance (mL/min)	39.50 [34.95, 47.50]	37.05 [33.57, 41.97]	40.90 [36.10, 48.60]	***0.002***
Baseline troponin I (μg/L)	2.19 [0.81, 3.71]	2.22 [0.88, 4.12]	2.16 [0.75, 3.56]	0.471
Peak troponin I (μg/l)	45.00 [27.00, 64.00]	50.00 [28.00, 64.00]	41.00 [27.00, 63.50]	0.271
3-month high-sensitivity CRP (mg/L)	3.80 [1.85, 10.52]	5.43 [3.28, 6.77]	4.02 [2.19, 5.88]	***0.007***
3-month BNP (ng/L)	37.00 [27.00, 66.75]	54.00 [28.75, 88.00]	37.00 [27.00, 51.75]	***0.005***
Echocardiographic parameters (post-PCI)				
LVEF (%)	40.0 [36.25, 45.75]	45.00 [40.00, 50.00]	40.00 [35.00, 45.00]	***< 0.001***
Echocardiographic parameters (at follow-up)				
LVEF (%)	45.0 [40.00, 50.00]	40.0 [32.00, 45.00]	50.0 [40.00, 55.00]	***< 0.001***
LVEF change (%)	5.00 [0.00, 10.00]	–10.00 [–12.00, 2.00]	+8.00 [0.00, 10.00]	***< 0.001***

CMD – coronary microvascular dysfunction; BNP – brain natriuretic peptide; CRP – C-reactive protein; LVEF – left ventricular ejection fraction; MRR – microvascular resistance reserve. Values are n (%) or median [IQR]. In bold and italics significant *p*-values (< 0.05).

4.4.3. Echocardiographic findings

Echocardiographically, LVEF just after PCI was higher in patients with MRR < 3 than those with MRR ≥ 3 (45.00% *vs.* 40.00%; $p < 0.001$) (Table 4.4.2.1). Upon follow-up, patients with MRR < 3 exhibited a significantly lower LVEF compared to those with MRR ≥ 3 (40.0% *vs.* 50.0%; $p < 0.001$) (Fig. 4.4.3.1). Additionally, the change in LVEF from post-PCI to 1-year follow-up was significant, with a decrease observed in the MRR < 3 group and an improvement in the MRR ≥ 3 group (–10.00% *vs.* +8.00%; $p < 0.001$) (Fig. 4.4.3.2).

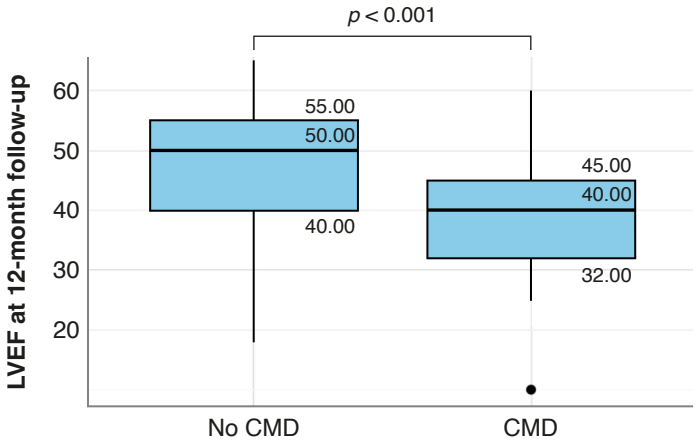

Fig. 4.4.3.1. *Boxplot of left ventricular ejection fraction at 12-month follow-up categorized by coronary microvascular dysfunction according to microvascular resistance reserve*

CMD – coronary microvascular dysfunction; LVEF – left ventricular ejection fraction.

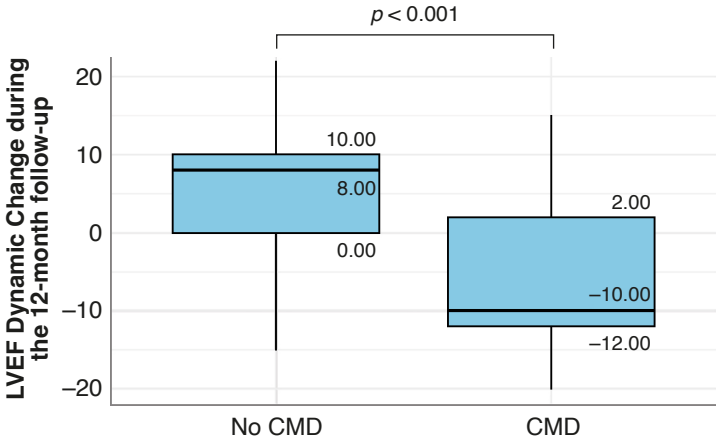

Fig. 4.4.3.2. *12-month change in left ventricular ejection fraction categorized by coronary microvascular dysfunction according to microvascular resistance reserve*

CMD – coronary microvascular dysfunction; LVEF – left ventricular ejection fraction.

4.4.4. Angiographic findings

Patients with an MRR < 3 and those with an MRR ≥ 3 showed no significant difference in pain-to-door time (314.00 minutes for both groups; $p = 0.249$) or door-to-balloon time (40.00 minutes for both groups; $p = 0.420$) (Table 4.4.4.1). TIMI flow grades prior were distributed across the groups without significant disparity. A TIMI flow of 0 was observed in 69.64% of patients with MRR < 3, compared to 59.09% of patients with MRR ≥ 3 ($p = 0.529$). Similarly, the TIMI flow following PCI also did not differ significantly between the groups, with the highest grade (TIMI 3) seen in 82.46% of patients with MRR < 3 and in 90.20% of patients with MRR ≥ 3 ($p = 0.197$). When examining the culprit vessel territory, the left anterior descending artery was the most common in both MRR < 3 and MRR ≥ 3 groups (57.14% *vs.* 55.84%; $p = 0.077$). The number of diseased vessels did not significantly vary between the two groups ($p = 0.392$).

4.4.5. Coronary physiology findings

At the 3-month follow-up, there were significant differences in certain coronary physiological parameters between the groups defined by MRR (Table 4.4.4.1). As expected, a clear difference was observed in CFR values between the groups. Patients with MRR < 3 exhibited a significantly lower CFR compared to those with MRR ≥ 3 counterparts (1.91 *vs.* 2.88; $p = 0.001$). In contrast, FFR values displayed no significant disparity between the two groups (0.92 *vs.* 0.92; $p = 0.593$). Notably, the IMR in patients with MRR < 3

were markedly higher than in those with MRR ≥ 3 (44 *vs.* 18.0; $p < 0.001$). Furthermore, a significant difference in median values was observed when comparing the MRR < 3 group to the MRR ≥ 3 group (2.42 *vs.* 3.66; $p < 0.001$).

Table 4.4.4.1. *Coronary angiography and physiology parameters of ST-elevation myocardial infarction patients, categorized by coronary microvascular dysfunction according to microvascular resistance reserve*

Parameters	**Overall (n = 210)**	**CMD (MRR < 3.0) (n = 56)**	**No CMD (MRR ≥ 3.0) (n = 154)**	***p*-value**
Angiographic				
Pain-to-door time (minutes)	314 [107.75, 592.25]	314.00 [136.75, 648.25]	314.00 [104.00, 524.00]	0.249
Door-to-balloon (minutes)	40.00 [29.25, 52.00]	40.00 [32.75, 53.50]	40.00 [29.00, 51.00]	0.420
Pre-PCI TIMI flow				
0	130 (61.90%)	39 (69.64%)	91 (59.09%)	0.529
1	8 (3.81%)	2 (3.57%)	6 (3.90%)	
2	44 (20.95%)	10 (17.86%)	34 (22.08%)	
3	28 (13.33%)	5 (8.93%)	23 (14.94%)	
Post-PCI TIMI flow				
0	2 (0.95%)	1 (1.79%)	1 (0.65%)	0.197
1	1 (0.48%)	1 (1.79%)	0 (0.00%)	
2	22 (10.48%)	8 (14.29%)	14 (9.09%)	
3	185 (88.1%)	47 (82.46%)	138 (90.20%)	
Culprit Vessel Territory				
Left anterior descending artery	118 (56.19%)	32 (57.14%)	86 (55.84%)	0.077
circumflex artery	49 (23.33%)	8 (14.29%)	41 (26.62%)	
Right coronary artery	43 (20.48%)	16 (28.57%)	27 (17.53%)	
Number of diseased vessels				
2-Vessel Disease	123 (58.57%)	36 (64.29%)	87 (56.49%)	0.392
3-Vessel Disease	87 (41.43%)	20 (35.71%)	67 (43.51%)	

Table 4.4.4.1. *Continued*

Parameters	Overall (n = 210)	CMD (MRR < 3.0) (n = 56)	No CMD (MRR ≥ 3.0) (n = 154)	*p*-value
Coronary physiology at 3-month follow-up				
Coronary flow reserve (CFR)	2.81 [2.54, 2.98]	1.91 [1.35, 2.22]	2.88 [2.77, 3.15]	***< 0.001***
Fractional flow reserve (FFR)	0.92 [0.87, 0.97]	0.92 [0.87, 0.97]	0.92 [0.87, 0.97]	0.593
Index of Microcirculatory resistance (IMR)	20.00 [15.00, 29.00]	44.00 [34.00, 54.25]	18.00 [14.00, 21.00]	***< 0.001***
Microvascular resistance reserve (MRR)	3.46 [2.93, 3.85]	2.42 [1.7, 2.74]	3.66 [3.35, 4.10]	***< 0.001***

PCI – percutaneous coronary intervention; TIMI – thrombolysis in myocardial infarction; MRR – microvascular resistance reserve. Values are n (%) or median [IQR].

In the correlation analysis, MRR showed a slight negative correlation with FFR, which was not statistically significant (r = –0.12; $p = 0.076$; Fig. 4.4.5.1 A). In contrast, a strong positive correlation between MRR and CFR was observed, suggesting a significant relationship (r = 0.93; $p < 0.001$; Fig. 4.4.5.1 B). Additionally, there was a moderate negative correlation between MRR and IMR, which was also statistically significant (r = –0.64; $p < 0.001$; Fig. 4.4.5.1 C).

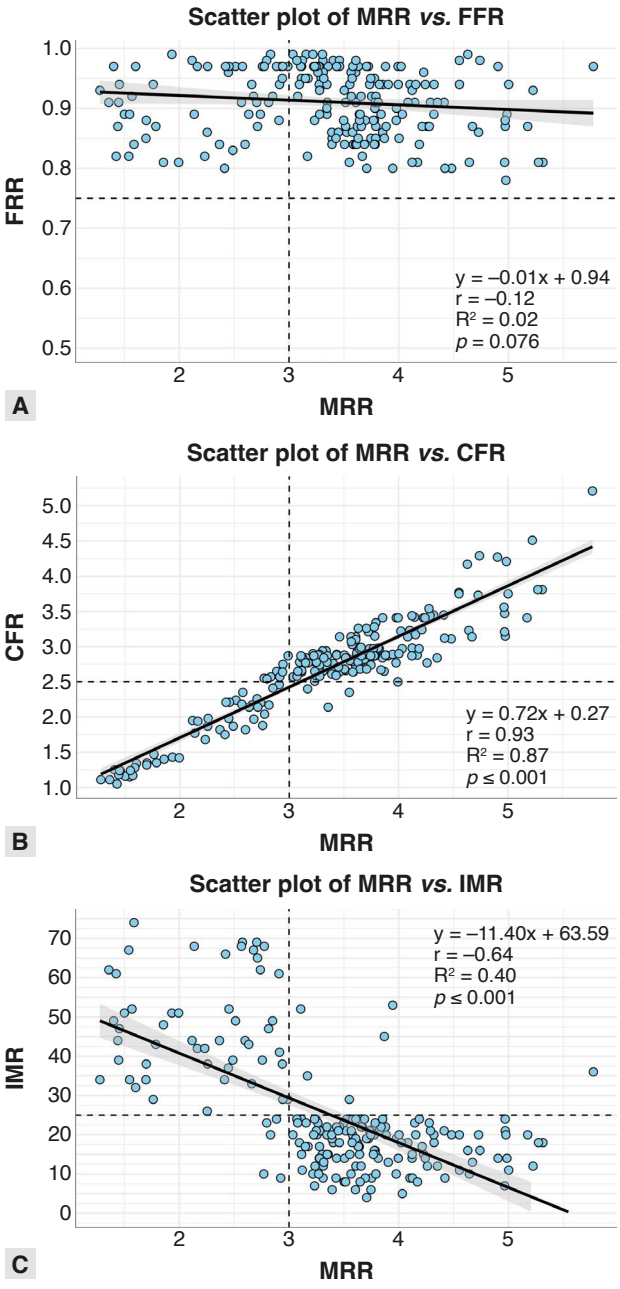

Fig. 4.4.5.1. *Correlation of microvascular resistance reserve with fractional flow reserve, coronary flow reserve, and index of microcirculatory resistance*

FFR – fractional flow reserve, CFR – coronary flow reserve, IMR – index of microcirculatory resistance.

4.4.6. Clinical outcome

A total of 44 patients, or 20.95%, experienced MACE at the 12-month follow-up. When comparing patients with an MRR < 3 to those with an MRR ≥ 3, the incidence of MACE was found to be statistically significant (48.21% *vs.* 11.04%; $p < 0.001$). Event rates of individual components of MACE are reported in Table 4.4.6.1 and illustrated in Fig. 4.4.6.1.

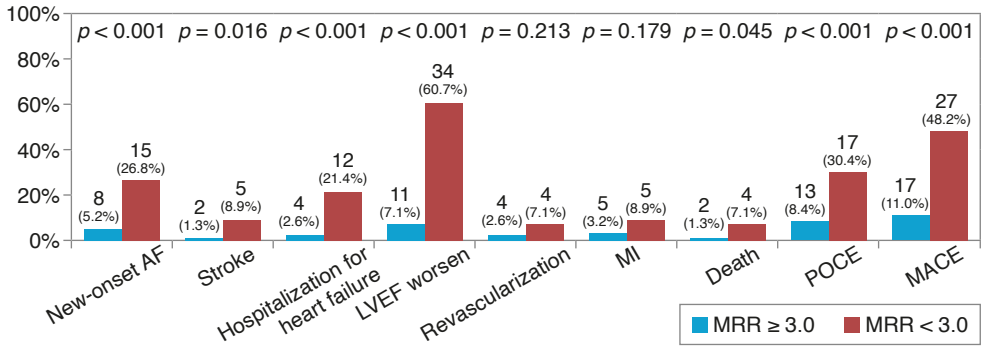

Fig. 4.4.6.1. *Rates of clinical events in high and low microvascular resistance reserve patients*

AF – atrial fibrillation; LVEF – left ventricular ejection fraction, MI – myocardial infarction, POCE – the composite of all-cause mortality, any myocardial infarction, any stroke and any revascularization, MACE – POCE +heart failure hospitalization, MRR – microvascular resistance reserve.

*Table **4.4.6.1.** 12-month clinical outcomes of patients presenting with ST-elevation myocardial infarction, categorized by microvascular dysfunction*

Clinical outcomes	**Overall (n = 210)**	**CMD (MRR < 3.0) (n = 56)**	**No CMD (MRR ≥ 3.0) (n = 154)**	***p*-value**
Ischemic stroke	7 (3.33%)	5 (8.93%)	2 (1.30%)	***0.016***
Nonfatal MI	10 (4.76%)	5 (8.93%)	5 (3.25%)	0.179
Cardiovascular death	6 (2.86%)	4 (7.14%)	2 (1.30%)	0.045
Target vessel revascularization	10 (4.76%)	5 (8.93%)	5 (3.25%)	0.213
Hospitalization for heart failure	16 (7.62%)	12 (21.43%)	4 (2.60%)	***< 0.001***
POCE	30 (14.29%)	17 (30.36%)	13 (8.44%)	***< 0.001***
MACE	44 (20.95%)	27 (48.21%)	17 (11.04%)	***< 0.001***

POCE – the composite of all-cause mortality, any myocardial infarction, any stroke, and any revascularization, MACE – POCE +heart failure hospitalization; MI – myocardial infarction. Values are n (%). In bold and italics significant *p*-values (< 0.05).

During the follow-up period, two cases of stent thrombosis developed; these were classified as MI, and the patients underwent successful revascularization of the culprit coronary artery. Based on the cubic spline curve, it was observed that the probability of MACE increased steeply and significantly when the MRR value was less than three (Fig. 4.4.6.2). Patients with an MRR < 3 also had a higher incidence of ischemic stroke (8.9% *vs.* 1.3%; $p = 0.022$) and heart failure hospitalization (21.4% *vs.* 2.6%; $p < 0.001$). There was no significant difference between the two MRR groups in terms of the occurrence of cardiovascular mortality, non-fatal MI, or target vessel revascularization (Table 4.4.6.1 and Fig. 4.4.6.1). The Kaplan-Meier survival analysis indicated that the incidence of MACE was significantly higher in the group with MRR < 3 compared to the group with MRR ≥ 3 (log-rank $p < 0.001$). Furthermore, there was a discernible divergence in survival curves immediately after one month of discharge (Fig. 4.4.6.3).

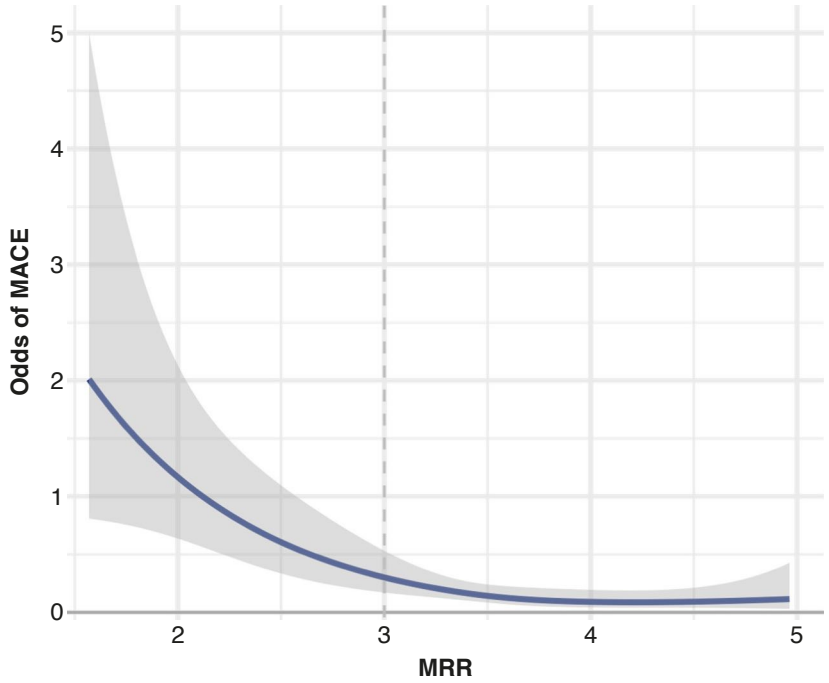

Fig. 4.4.6.2. *Restricted cubic spline curve of microvascular resistance reserve and the odds of major adverse cardiovascular events*

MRR – microvascular resistance reserve; MACE – major adverse cardiovascular events.

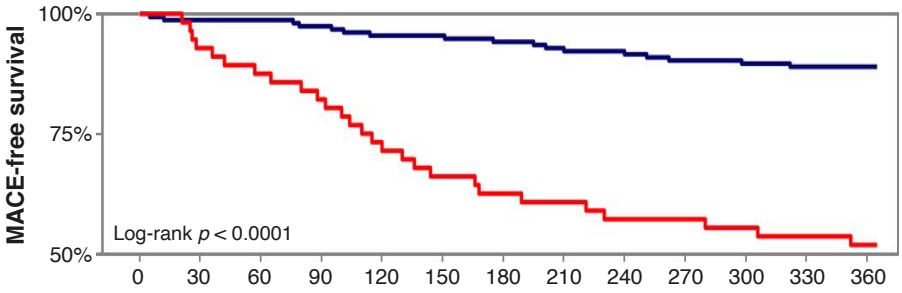

Strata	Number at risk by time												
MRR ≥ 3.0	154	152	152	150	147	147	145	143	142	139	138	137	137
MRR < 3.0	56	52	49	46	41	37	35	34	32	32	31	30	29

Fig. 4.4.6.3. *Kaplan-Meier event-free survival curve for occurrence of major adverse cardiovascular events grouped by coronary microvascular dysfunction according to microvascular resistance reserve*

MRR – microvascular resistance reserve; MACE – major adverse cardiovascular events.

4.4.7. Multivariable Cox analysis

Univariable Cox regression analysis and Multivariable analysis with adjustment for variables with $p < 0.05$ in univariable Cox regression were performed to identify the independent risk factors for MACE (Table 4.4.7.1). The analysis revealed that a lower MRR was a significant predictor of MACE, with the odds decreasing as MRR values were lower (HR 0.45, 95% CI 0.31–0.67; $p < 0.001$). Other variables, such as sex, age, and baseline clinical characteristics, did not show a significant predictive value in the multivariable model. Notably, FFR also emerged as a significant factor, with each unit increase diminishing the likelihood of MACE (HR 0.56, 95% CI: 0.31–0.99; $p = 0.047$).

Table 4.4.7.1. *Multivariable cox regression analysis for the prediction of 12-month major adverse cardiovascular events after ST-elevation myocardial infarction*

Variable	Univariable		Multivariable	
	Hazard Ratio	*p*-value	Hazard Ratio	*p*-value
Sex (Female)	2.38 (1.31–4.34)	***0.005***	1.22 (0.60–2.46)	0.582
Age (years)	1.01 (0.98–1.03)	0.533		
Body mass index (kg/m^2)	1.01 (0.95–1.07)	0.779		
Body surface area (m^2)	1.35 (0.37–4.93)	0.650		
Primary diagnosis	1.02 (0.56–1.85)	0.946		
Arterial hypertension	1.24 (0.67–2.29)	0.492		

Table 4.4.7.1. *Continued*

Variable	Univariable		Multivariable	
	Hazard Ratio	***p*-value**	**Hazard Ratio**	***p*-value**
History of coronary artery disease	0.98 (0.51–1.91)	0.961		
History of PCI	1.14 (0.48–2.69)	0.770		
History of stroke	1.94 (0.93–4.03)	0.077		
History of diabetes mellitus	1.73 (0.93–3.22)	0.085		
History of dyslipidaemia	0.98 (0.54–1.78)	0.954		
Smoker (former/current)	1.28 (0.70–2.32)	0.418		
History of alcohol abuse	0.94 (0.34–2.62)	0.901		
KILLIP class	1.04 (0.72–1.51)	0.823		
Haemoglobin (g/L)	1.00 (0.99–1.02)	0.765		
White Blood Cell Count ($\times 10^9$/L)	1.02 (0.93–1.13)	0.623		
Platelets ($\times 10^9$/L)[$]	1.02 (0.97–1.01)	0.539		
Total cholesterol (mmol/L)	1.08 (0.89–1.31)	0.441		
Low-density lipoprotein (mmol/L)	1.15 (0.92–1.43)	0.212		
High-density lipoprotein (mmol/L)	1.04 (0.78–1.40)	0.777		
Triglycerides (mmol/L)	1.01 (0.96–1.06)	0.786		
Creatinine Clearance (mL/min)	0.98 (0.95–1.01)	0.287		
Baseline Troponin I (µg/L)	1.01 (0.96–1.06)	0.786		
Peak Troponin I (µg/L)[$]	1.04 (0.95–1.13)	0.401		
3-month High-sensitivity CRP (mg/L)	1.12 (1.01–1.25)	***0.039***	0.99 (0.89–1.10)	0.844
3-month BNP (ng/L)	1.01 (1.01–1.01)	***< 0.001***	1.01 (1.00–1.01)	***0.003***
Post-PCI LVEF (%)	1.00 (0.96–1.04)	0.970		
Pain-to-door time (minutes)[$]	1.00 (1.00–1.01)	0.240		
Door-to-balloon (minutes)	1.00(0.98–1.01)	0.737		
Pre-PCI TIMI flow	0.87 (0.66–1.14)	0.310		
Post-PCI TIMI flow	0.72 (0.44–1.20)	0.206		
Culprit vessel	0.99 (0.68–1.43)	0.948		
Number of diseased vessels	0.70 (0.38–1.31)	0.266		
Intracoronary glycoprotein IIb/IIIa inhibitor	0.77 (0.36–1.65)	0.501		
Aspiration thrombectomy	0.45 (0.19–1.05)	0.065		
Stent diameter (millimetres)	1.76 (0.99–3.13)	0.055		
Stent length (millimetres)	1.06 (1.00–1.12)	***0.047***	1.06 (1.00–1.13)	0.062
Maximal stent pressure (atm)	0.93 (0.82–1.05)	0.248		
Contrast dose (millilitres)	0.98 (0.96–1.00)	0.098		
Fractional flow reserve (FFR)*	0.55 (0.33–0.91)	***0.021***	0.56 (0.31–0.99)	***0.047***
Microvascular resistance ratio (MRR)	0.39 (0.28–0.54)	***< 0.001***	0.45 (0.31–0.67)	***< 0.001***

[$] – per 10 unit increment, * – per 0.1 unit increment, all other numerical variables are for 1 unit increment. PCI – percutaneous coronary intervention, CRP – C-reactive protein, BNP – brain natriuretic peptide, LVEF – left ventricular ejection fraction. In bold and italics significant *p*-values (< 0.05).

4.4.8. Prognostic performance of microvascular resistance reserve

The prognostic performance of MRR was investigated using ROC curve analysis, with areas under the ROC curve for predicting POCE at 12 months. The ROC curve analysis highlighted the AUC for MRR at 0.743, CFR at 0.762, and IMR at 0.781, signifying good to strong predictive abilities. The FFR had an AUC of 0.609, reflecting a more modest predictive performance (Fig. 4.4.8.1). Notably, the optimal cut-off values determined for maximizing the prognostic accuracy were 2.75 for MRR, 2.31 for CFR, 33.5 for IMR, and 0.90 for FFR (Fig. 4.4.8.1). When comparing these parameters, the prognostic performance of MRR, CFR, and IMR were statistically superior to that of FFR (Table 4.4.8.1). This suggests that while FFR provides some predictive value, MRR, alongside CFR and IMR, offers stronger and more reliable prognostic information for assessing the risk of POCE. Additionally, a similar prognostic performance was observed among all coronary physiology indices in assessing MACE, as depicted in the accompanying Fig. 4.4.8.2.

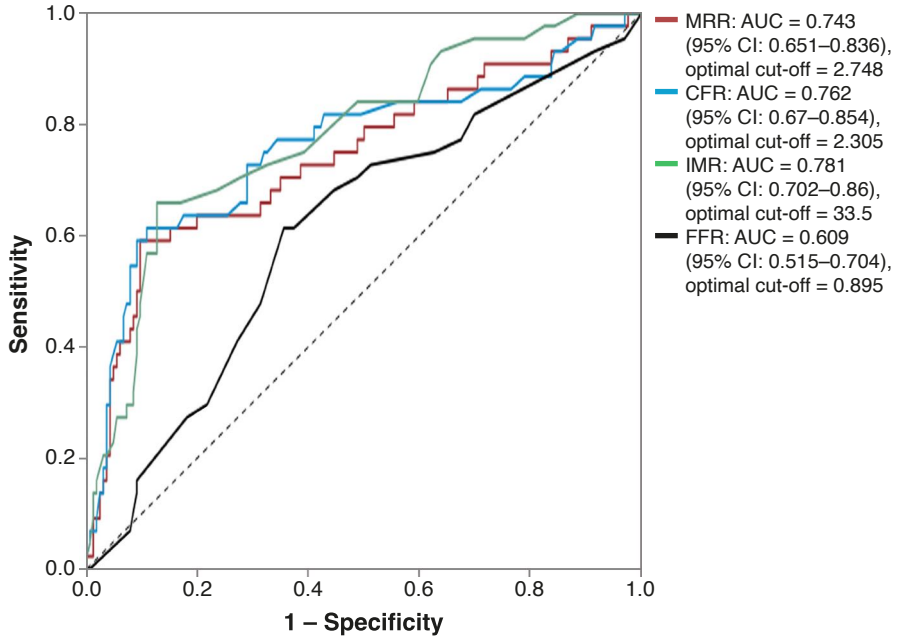

Fig. 4.4.8.1. *Receiver operating characteristic curve for the model of patient-oriented composite endpoint at 12-month follow-up in ST-elevation myocardial infarction patients*

MRR – microvascular resistance reserve; CFR – coronary flow reserve; IMR – index of microcirculatory resistance, FFR – fractional flow reserve. AUC – area under the curve.

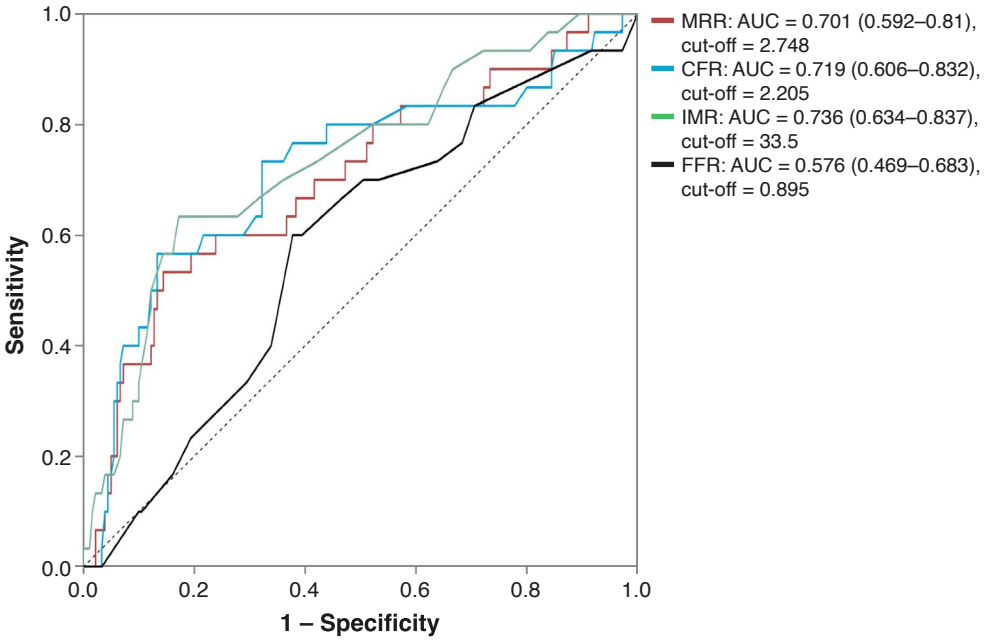

Fig. 4.4.8.2. *Receiver operating characteristic curve for the model of major adverse cardiovascular events at 12-month follow-up in ST-elevation myocardial infarction patients*

MRR – microvascular resistance reserve; CFR – coronary flow reserve; IMR – index of microcirculatory resistance, FFR – fractional flow reserve. AUC – area under the curve.

Table 4.4.8.1. *Comparison of area under the receiver operating characteristic curves for predicting major adverse cardiovascular events*

Predictor1	Predictor2	Delong test *p*-value
MRR	CFR	0.391
MRR	IMR	0.285
CFR	IMR	0.572
MRR	FFR	**0.039**
CFR	FFR	**0.01**
IMR	FFR	**< 0.001**

MRR – microvascular resistance reserve; CFR – coronary flow reserve; IMR – index of microcirculatory resistance, FFR – fractional flow reserve. In bold and italics significant *p*-values (< 0.05).

4.5. Prevalence and prognostic impact of coronary microvascular dysfunction endotypes on 12-month clinical outcomes in ST-elevation myocardial infarction patients

4.5.1. Prevalence and types of coronary microvascular dysfunction in ST-elevation myocardial infarction patients

Among the cohort of 210 patients with STEMI, CMD was identified in 27% (n = 56) of cases. Sub-classification of CMD revealed two distinct endotypes: structural CMD, present in 24% (n = 51) of patients, and functional CMD, observed in 3% (n = 5) of patients (Fig. 4.5.1.1). This indicates a higher likelihood of structural changes over functional alterations within the coronary microvasculature in the STEMI population, highlighting a potential area of focus for targeted therapeutic interventions.

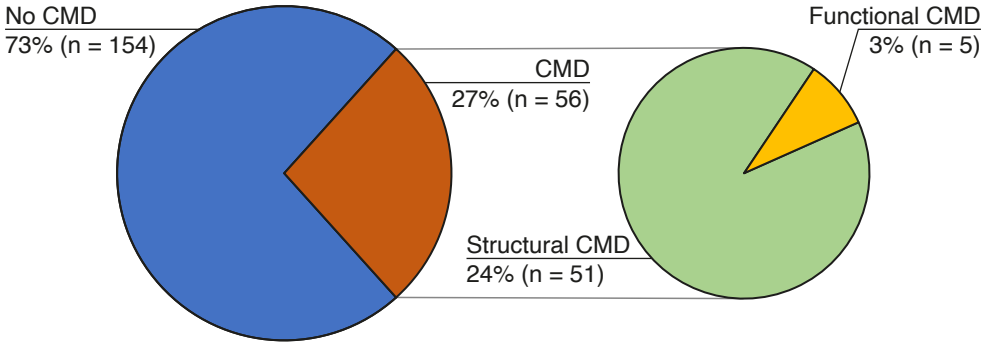

Fig. 4.5.1.1. *Distribution of coronary microvascular dysfunction endotypes in ST-elevation myocardial infarction patients*

CMD – coronary microvascular dysfunction.

4.5.2. Study population characteristics

Analysis of baseline characteristics revealed notable differences in demographic and clinical profiles based on the presence and endotype of CMD (Table 4.5.2.1). In the structural CMD subgroup, a significantly higher proportion of female patients was observed, accounting for 68.63% of this group, a stark contrast to the 32.47% in the no CMD group ($p < 0.001$). Furthermore, Age distribution across the no CMD, functional CMD, and structural CMD groups did not show statistical variance, with median ages closely aligned. This was similarly reflected in the BMI and BSA measurements, where values across the groups did not differ to a significant degree ($p = 0.148$ and $p = 0.650$, respectively), indicating that these factors may not be primary differentiators of CMD presence or type in this clinical context.

A closer look at medical history elements revealed that the incidence of diabetes mellitus was significantly lower in the functional CMD group, with no cases reported, compared to 18.83% in the no CMD group and a considerable 43.14% in the structural CMD group ($p = 0.001$). The absence of diabetes mellitus in the functional CMD subgroup, despite its small size, raises questions about potential differences in pathophysiological mechanisms compared to structural CMD, where diabetes is more prevalent. However, due to the relatively small number of patients with functional CMD, these observations should be interpreted with caution, as they may not be representative of the broader STEMI population. Other clinical parameters, including histories of hypertension, CAD, PCI, stroke, dyslipidemia, and alcohol use, showed no significant differences between the endotypes, as detailed in Table 4.5.2.1. Upon reviewing the data, it appears that smoking is more prevalently associated with the structural CMD endotype rather than the functional CMD endotype. However, the comparable prevalence of smoking between the overall CMD group and the no CMD group suggests that smoking, while potentially contributory, is not the sole determinant in the development of CMD. The lack of a significant difference in smoking prevalence between the CMD and non-CMD groups could indicate that other factors, perhaps in combination with smoking, play a more critical role in the manifestation of CMD endotypes. This observation could point to a multifactorial etiology of CMD, where smoking acts as one of the various elements that may influence the emergence and progression of structural CMD, rather than being a primary causative factor of CMD.

Table 4.5.2.1. *Characteristics of ST-elevation myocardial infarction patients classified by coronary microvascular dysfunction and its endotypes*

Characteristic	Overall (n = 210)	No CMD (n = 154)	Functional CMD (n = 5)	Structural CMD (n = 51)	*p*-value
Sex (Female)	85 (40.48%)	50 (32.47%)	0 (0%)	35 (68.63%)	***< 0.001***
Age (years)	65.00 [58.00, 76.00]	67.00 [58.00, 76.00]	62.00 [61.00, 62.00]	63 [57.5, 75.5]	0.669
Body mass index (kg/m^2)	27.39 [24.56, 30.69]	27.69 [24.78, 31.04]	23.15 [22.04, 24.98]	26.37 [24.47, 29.41]	0.148
Body surface area (m^2)	1.93 [1.81, 2.10]	1.94 [1.81, 2.11]	1.81 [1.75, 1.94]	1.90 [1.83, 2.1]	0.650
Primary diagnosis					
Anterior STEMI	116 (55.24%)	85 (55.19%)	4 (80%)	27 (52.94%)	0.509
Inferior STEMI	94 (44.76%)	69 (44.81%)	1 (20%)	24 (47.06%)	
Arterial hypertension	123 (58.57%)	92 (59.74%)	3 (60%)	28 (54.9%)	0.829
History of coronary artery disease	59 (28.10%)	40 (25.97%)	1 (20%)	18 (35.29%)	0.404
History of PCI	26 (12.38%)	18 (11.69%)	0 (0%)	8 (15.69%)	0.525
History of stroke	27 (12.86%)	19 (12.34%)	0 (0%)	8 (15.69%)	0.566
History of diabetes mellitus	51 (24.29%)	29 (18.83%)	0 (0%)	22 (43.14%)	***0.001***
History of dyslipidemia	119 (56.67%)	87 (56.49%)	4 (80%)	28 (54.9%)	0.556
Smoker (former/current)	109 (51.90%)	79 (51.3%)	0 (0%)	30 (58.82%)	***0.041***
History of alcohol abuse	20 (9.52%)	15 (9.74%)	1 (20%)	4 (7.84%)	0.666
KILLIP class					
I	62 (29.52%)	45 (29.22%)	3 (60%)	14 (27.45%)	0.809
II	111 (52.86%)	81 (52.6%)	2 (40%)	28 (54.9%)	
III	27 (12.86%)	21 (13.64%)	0 (0%)	6 (11.76%)	
IV	10 (4.76%)	7 (4.55%)	0 (0%)	3 (5.88%)	

STEMI – ST-elevation myocardial infarction; PCI – percutaneous coronary intervention; CMD – coronary microvascular dysfunction. Values are n (%) or median [IQR]. In bold and italics significant *p*-values (< 0.05).

4.5.3. Clinical outcome

Kaplan-Meier MACE-free survival analysis indicated a trend toward lower event-free survival in patients with structural CMD compared to those with functional CMD. While this trend neared statistical significance (log-rank $p = 0.054$, Fig. 4.5.3.1), it did not definitively confirm a difference in long-term outcomes between the two CMD endotypes, most probably due to statistical underpower. It is crucial to note that the limited number of patients within the functional CMD category necessitates a cautious interpretation of these results.

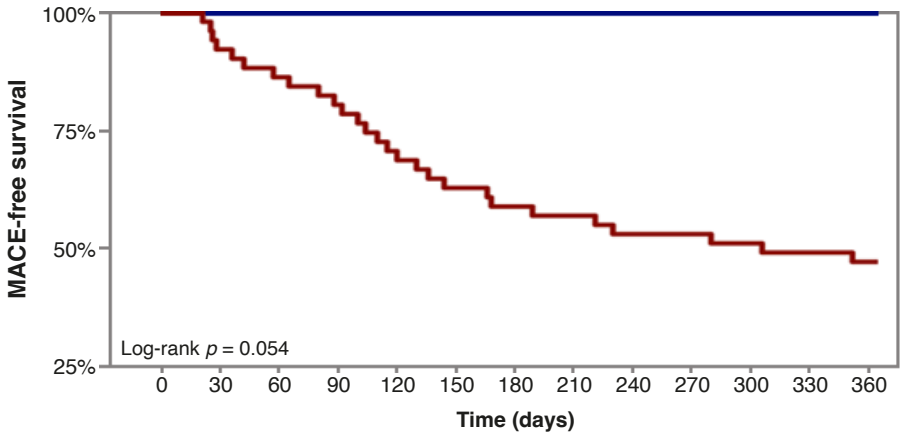

Strata	Number at risk												
Functional CMD	5	5	5	5	5	5	5	5	5	5	5	5	5
Structural CMD	51	47	44	41	36	32	30	29	27	27	26	25	24

Fig. 4.5.3.1. *Kaplan-Meier event-free survival curve for occurrence of major adverse cardiovascular events grouped by coronary microvascular dysfunction endotypes*

CMD – coronary microvascular dysfunction; MACE – major adverse cardiovascular events.

4.6. The impact of coronary microvascular dysfunction on functional left ventricular remodelling, diastolic dysfunction, and clinical outcomes

4.6.1. Study population characteristics

This cohort was stratified based on the presence of CMD, as defined by an IMR value ≥ 25 U or a CFR value of < 2.0 U. A total of 210 individuals were included in the analysis, with 57 patients (27.14%) being diagnosed with CMD and 153 patients (72.86%) not exhibiting CMD (Table 4.6.1.1). Of the total participants, 85 were females, representing 40.48% of the entire study

population. A statistically significant observation was made regarding the prevalence of CMD among female participants; it was notably higher compared to their counterparts who did not exhibit CMD (63.16% *vs.* 32.03%; $p < 0.001$). Patients who exhibited CMD tended to be younger, with a median age of 63 years, the age difference between the two groups of patients participating in the study was never close to being significant. Despite the fact that the study cohort exhibited a tendency towards overweight, as evidenced by a median body mass index of 27.39 kg/m^2, no statistically significant distinction was observed between the two groups. Between the two groups, there was no discernible difference in terms of body surface area, or the location of STEMI events. However, it is noteworthy that individuals with confirmed CMD exhibited a significantly higher prevalence of diabetes compared to those without CMD (24 (42.11%) *vs.* 27 (17.65%); $p < 0.001$). Smokers were almost evenly distributed across study groups. The baseline CHADS2-VASc score was relatively comparable across study groups. The two groups did not differ from one another in any of the risk factors, such as arterial hypertension, hyperlipidemia, Killip classification, or a history of alcohol poisoning, ischemic or hemorrhagic stroke and coronary atherosclerotic disease. To sum up, patients across the study groups were largely similar in terms of general characteristics, with the notable exceptions being a higher prevalence of females and diabetes in the CMD group.

Table 4.6.1.1. *Characteristics of ST-elevation myocardial infarction patients classified by coronary microvascular dysfunction*

Characteristic	Overall (n = 210)	CMD (n = 57)	No CMD (n = 153)	*p*-value
Sex (Female)	85 (40.48%)	36 (63.16%)	49 (32.03%)	***< 0.001***
Age (years)	65.0 [58, 76]	63.00 [57.00, 75.00]	66.00 [58.00, 76.00]	0.572
Body mass index (kg/m^2)	27.39 [24.56, 30.69]	26.37 [24.44, 29.28]	27.58 [24.77, 31.21]	0.146
Body surface area (m^2)	1.93 [1.81, 2.10]	1.90 [1.83, 2.05]	1.95 [1.81, 2.11]	0.292
Primary diagnosis				
Anterior STEMI	116 (55.24%)	32 (56.14%)	84 (57.90%)	0.996
Inferior STEMI	94 (44.76%)	25 (43.86%)	69 (45.10%)	
Arterial hypertension	123 (58.57%)	32 (56.14%)	91 (59.48%)	0.780
History of coronary artery disease	59 (28.10%)	19 (33.33%)	40 (26.14%)	0.391
History of PCI	26 (12.38%)	9 (15.79%)	17 (11.11%)	0.497
History of stroke	27 (12.86%)	9 (15.79%)	18 (11.76%)	0.587
History of diabetes mellitus	51 (24.29%)	24 (42.11%)	27 (17.65%)	***< 0.001***
History of dyslipidemia	119 (56.67%)	32 (56.14%)	87 (56.86%)	1

Table 4.6.1.1. *Continued*

Characteristic	Overall (n = 210)	CMD (n = 57)	No CMD (n = 153)	*p*-value
Smoker (former/current)	109 (51.90%)	33 (57.89%)	76 (49.67%)	0.365
History of alcohol abuse	20 (9.52%)	4 (7.02%)	16 (10.46%)	0.623
KILLIP class				
I	62 (29.52%)	15 (26.32%)	47 (30.72%)	0.796
II	111 (52.86%)	33 (57.89%)	78 (50.98%)	
III	27 (12.86%)	6 (10.53%)	21 (13.73%)	
IV	10 (4.76%)	3 (5.26%)	7 (4.58%)	

CMD – coronary microvascular dysfunction; STEMI – ST-elevation myocardial infarction; PCI – percutaneous coronary intervention. Values are n (%) or median [IQR].
In bold and italics significant *p*-values (< 0.05).

4.6.2. Laboratory findings

There was no noticeable difference between the study groups based on the findings of the complete blood count that was performed (Table 4.6.2.1). The levels of hemoglobin, white blood cell count, and platelet count all diverged from one another in the similar proportion across the two study groups. In the comparison between the CMD and non-CMD groups, differences in the lipid profile, encompassing TC, HDL, LDL, and triglycerides, were found to be statistically insignificant. Creatinine clearance, which is an indicator of kidney function, did show a significant difference between the two study groups (40.70 mL/min *vs.* 37.3 mL/min; $p = 0.003$). Neither group showed statistically significant differences in troponin levels between samples taken upon admission and after 24 hours. However, at 3 months follow-up, the high-sensitivity CRP and the brain natriuretic peptide were significantly higher in patients with CMD (5.21 mg/L *vs.* 3.98 mg/L; $p = 0.008$ and 70.00 ng/L *vs.* 37.00 ng/L; $p < 0.001$, respectively).

Table 4.6.2.1. *Laboratory parameters of patients with ST-elevation myocardial infarction, categorized by coronary microvascular dysfunction*

Parameters	Overall (n = 210)	CMD (n = 57)	No CMD (n = 153)	*p*-value
Laboratory test				
Hemoglobin (g/L)	136.0 [119.0, 148.0]	144.00 [120.00, 153.00]	135.00 [119.00, 146.00]	0.105
White blood cell count ($\times 10^9$/L)	9.86 [8.22, 12.09]	11.32 [8.45, 13.20]	9.66 [8.07, 11.80]	0.062
Platelets ($\times 10^9$/L)	240.5 [204.0, 273.0]	243.00 [206.00, 305.00]	234.00 [203.00, 265.00]	0.148
Total cholesterol (mmol/L)	4.64 [3.75, 5.79]	4.55 [3.54, 5.67]	4.68 [3.84, 5.81]	0.413
Low-density lipoprotein (mmol/L)	2.93 [2.09, 3.93]	2.93 [1.85, 3.94]	2.93 [2.16, 3.92]	0.857
High-density lipoprotein (mmol/L)	1.12 [0.92, 1.35]	1.12 [0.88, 1.31]	1.12 [0.95, 1.35]	0.519
Triglycerides (mmol/L)	1.16 [0.82, 1.65]	1.14 [0.85, 1.54]	1.17 [0.82, 1.68]	0.399
Creatinine clearance (mL/min)	39.5 [34.95, 47.5]	37.30 [32.90, 42.50]	40.70 [36.10, 48.60]	***0.003***
Baseline troponin I (µg/L)	2.19 [0.81, 3.71]	2.22 [0.89, 4.14]	2.17 [0.74, 3.56]	0.373
Peak troponin I (µg/L)	45.0 [27.0, 64.0]	50.00 [30.00, 69.00]	41.00 [26.00, 61.00]	0.145
3-month high-sensitivity CRP (mg/L)	3.80 [1.85, 10.52]	5.21 [3.28, 6.57]	3.98 [1.98, 5.81]	***0.008***
3-month BNP (ng/L)	37.00 [27.00, 66.75]	70.00 [29.00, 88.00]	37.00 [27.00, 51.00]	***< 0.001***

CMD – coronary microvascular dysfunction; BNP – brain natriuretic peptide; CRP – C-reactive protein. Values are n (%) or median [IQR].
In bold and italics significant *p*-values (< 0.05).

4.6.3. Echocardiographic findings

The post-PCI echocardiography showed that the CMD group had significantly higher post-PCI LVEF (42.0% *vs.* 40.0%; $p = 0.005$) and the E/A ratio (1.30 *vs.* 0.80; $p < 0.001$), while the left ventricular end-diastolic volume, left atrial volume index as well as the diastolic function grade were similar between the two groups at post-PCI echocardiography (Table 4.6.3.1). However, at 12-months follow-up, the LVEF became significantly lower in the CMD group (40.00% *vs.* 50.00%; $p < 0.001$) (Fig. 4.6.3.1).

Table 4.6.3.1. *Echocardiographic parameters of patients with ST-elevation myocardial infarction, categorized by coronary microvascular dysfunction*

Parameters	Overall (n = 210)	CMD (n = 57)	No CMD (n = 153)	*p*-value
Echocardiographic parameters (post-PCI)				
LVEF (%)	40.0 [36.25, 45.75]	42.0 [38.5, 45.0]	40.0 [35.75, 46.25]	***0.005***
LVEDV (mL)	85.20 [68.80, 107.10]	86.60 [68.10, 107.10]	85.20 [68.80, 107.10]	0.808
E/A ratio	0.92 [0.70, 1.36]	1.30 [1.12, 1.49]	0.80 [0.66, 1.27]	***< 0.001***
Average e’	8.00 [6.00, 10.00]	8.00 [7.00, 10.00]	8.00 [6.00, 10.00]	0.139
E/e’	8.62 [7.00, 10.67]	8.89 [7.32, 10.18]	8.57 [6.88, 10.71]	0.676
TRpV	2.59 [2.33, 2.80]	2.44 [2.27, 2.70]	2.60 [2.40, 2.81]	0.050
LA volume index	26.19 [22.71, 31.48]	26.41 [23.02, 32.96]	26.08 [22.69, 30.82]	0.290
LV diastolic dysfunction				
Grade 1	196 (93.33%)	56 (98.25%)	140 (91.50%)	0.052
Grade 2	7 (3.33%)	0 (0.00%)	7 (4.58%)	
Grade 3	6 (2.86%)	0 (0.00%)	6 (3.92%)	
NA	1 (0.48%)	1 (1.75%)	0 (0.00%)	
Echocardiographic parameters (at 12-month follow-up)				
LVEF (%)	45.00 [40.00, 50.00]	40.00 [32.00, 42.00]	50.00 [41.50, 55.00]	***< 0.001***
LVEDV (mL)	89.05 [70.88, 107.75]	100.80 [80.40, 124]	85.60 [70.60, 100.2]	***0.005***
E/A ratio	1.23 [0.77, 1.41]	0.72 [0.66, 0.75]	1.32 [1.18, 1.46]	***< 0.001***
Average e’	8.00 [5.00, 10.00]	4.00 [4.00, 5.00]	9.00 [8.00, 10.00]	***< 0.001***
E/e’	9.78 [7.74, 12.65]	15.00 [14.31, 16.00]	8.56 [7.10, 10.57]	***< 0.001***
TRpV	2.60 [2.40, 2.90]	3.10 [2.90, 3.50]	2.40 [2.30, 2.60]	***< 0.001***
LA volume index (mL/m^2)	27.19 [23.02, 35.83]	40.61 [25.75, 45.24]	26.26 [22.73, 31.21]	***< 0.001***
LV diastolic dysfunction				
Grade 1	163 (80.30%)	14 (26.92%)	149 (98.68%)	***<0.001***
Grade 2	40 (19.70%)	38 (73.08%)	2 (1.32%)	
Grade 3	0 (0%)	0 (0%)	0 (0%)	
Echocardiographic remodelling related parameters				
LVEF change (%)	5.00 [10.00, 0.00]	–10.00 [0.00, –12.00]	8.00 [10.00, 1.00]	***< 0.001***
LVEDV change (%)	3.43 [–6.52, 11.26]	9.87 [1.62, 24.08]	–0.56 [–7.03, 7.83]	***< 0.001***
FLVR				
Group 1	148 (72.55%)	15 (28.30%)	133 (88.08%)	***< 0.001***
Group 2	24 (11.76%)	20 (37.74%)	4 (2.65%)	
Group 3	17 (8.33%)	6 (11.32%)	11 (7.28%)	
Group 4	15 (7.35%)	12 (22.64%)	3 (1.99%)	

CMD – coronary microvascular dysfunction; PCI – percutaneous coronary intervention; LVEDV – left ventricular end diastolic volume; LVEF – left ventricular ejection fraction; TRpV – tricuspid regurgitation peak velocity; LA – left atrium; FLVR – functional left ventricular remodelling. Values are n (%) or median [IQR]. In bold and italics significant *p*-values (< 0.05).

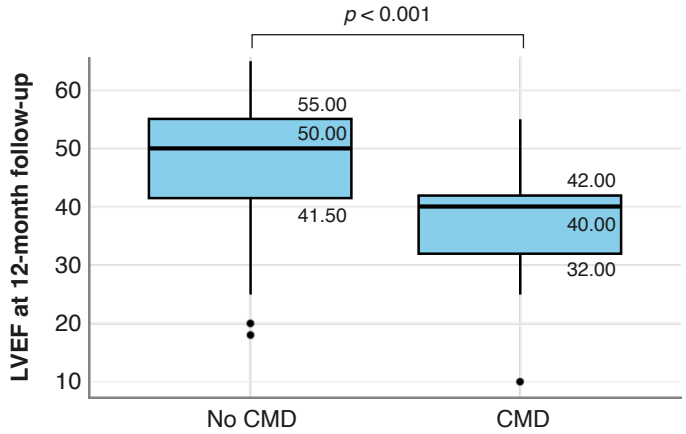

Fig. 4.6.3.1. *Boxplot of left ventricular ejection fraction at 12-month follow-up categorized by coronary microvascular dysfunction*

CMD – coronary microvascular dysfunction; LVEF– left ventricular ejection fraction.

Patients with CMD had significantly worsened LVEF while the patients without CMD had improved LVEF (–10.00% *vs.* 8.00%; $p < 0.001$) (Fig. 4.6.3.2, 4.6.3.3).

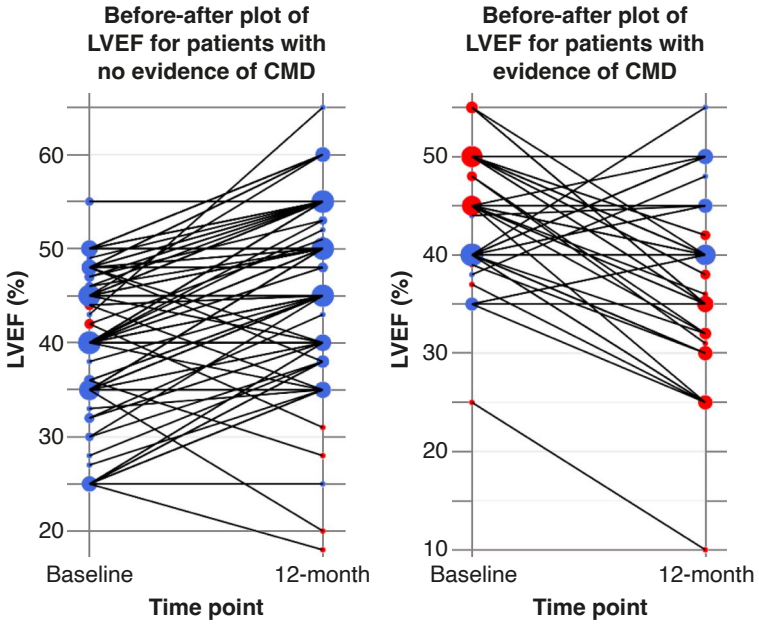

Fig. 4.6.3.2. *Dynamic changes in left ventricular ejection fraction during 12-month follow-up period categorized by coronary microvascular dysfunction*

CMD – coronary microvascular dysfunction; LVEF– left ventricular ejection fraction.

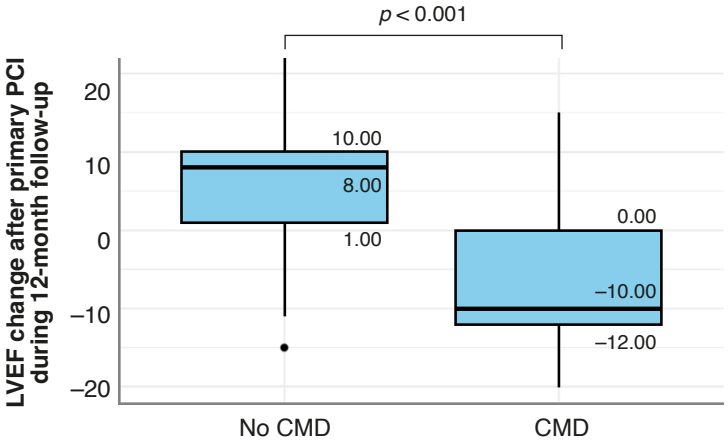

Fig. 4.6.3.3. *12-month change in left ventricular ejection fraction categorized by coronary microvascular dysfunction*

CMD – coronary microvascular dysfunction; LVEF – left ventricular ejection fraction; PCI – percutaneous coronary intervention.

The echocardiographic follow-up showed dynamic changes in diastolic dysfunction grades within the 12-month time frame (Fig. 4.6.3.4).

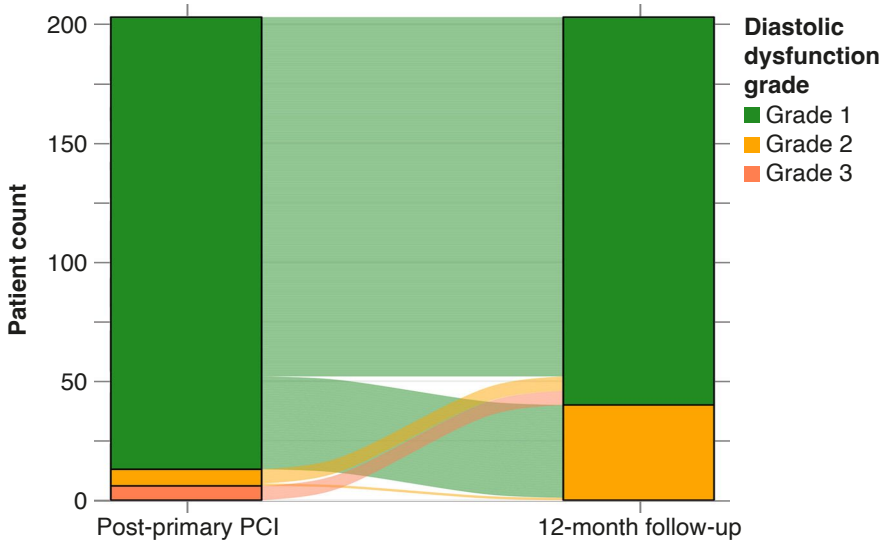

Fig. 4.6.3.4. *Alluvial plot illustrating the dynamic changes in diastolic dysfunction from during 12-month follow-up period*

PCI – percutaneous coronary intervention.

Additionally, the imaging follow-up also revealed that CMD patients had significantly higher LVEDV, LA volume index, E/e', TRpV while the E/A ratio and the average e' were significantly lower. Patients without CMD who had grade 2 and grade 3 diastolic dysfunction at post-PCI, almost all recovered to grade 1 diastolic dysfunction, with few exhibiting grade 2 diastolic dysfunction at 12 months (Fig. 4.6.3.5). Conversely, CMD patients had grade 1 diastolic dysfunction post-PCI, but at 12 months, most of these patients progressed to grade 2 diastolic dysfunction (Fig. 4.6.3.6). The incidence of grade 2 diastolic dysfunction was higher in CMD patients as compared with those without CMD (38 (73.08%) *vs.* 2 (1.32%); $p < 0.001$) (Fig. 4.6.3.7). There were no patients with grade III diastolic dysfunction at 12-month follow-up.

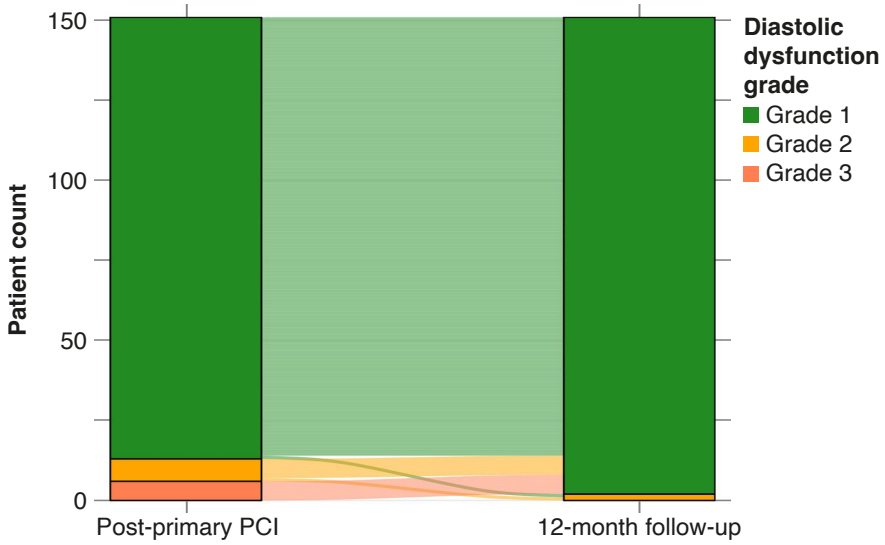

Fig. 4.6.3.5. *Alluvial plot illustrating the dynamic changes in diastolic dysfunction in patients with no coronary microvascular dysfunction during 12-month follow-up period*

PCI – percutaneous coronary intervention.

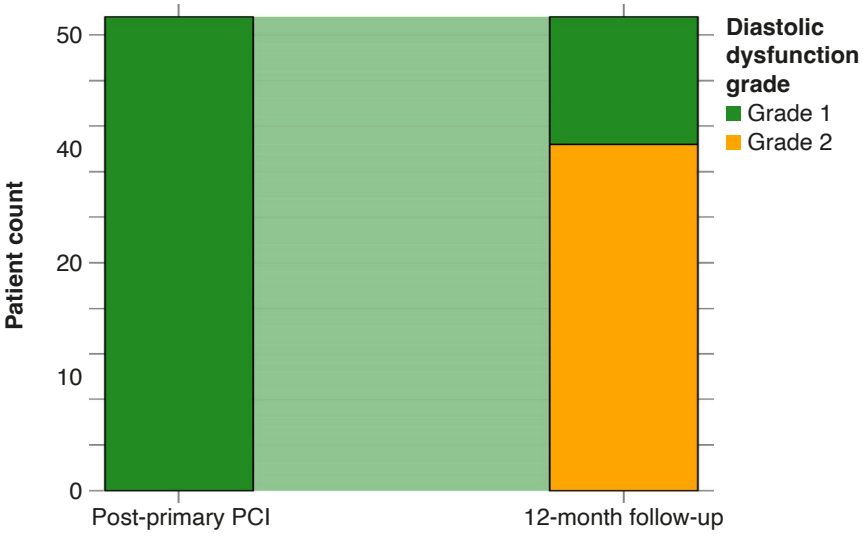

Fig. 4.6.3.6. *Alluvial plot illustrating the dynamic changes in diastolic dysfunction in patients with coronary microvascular dysfunction during 12-month follow-up period*

PCI – percutaneous coronary intervention.

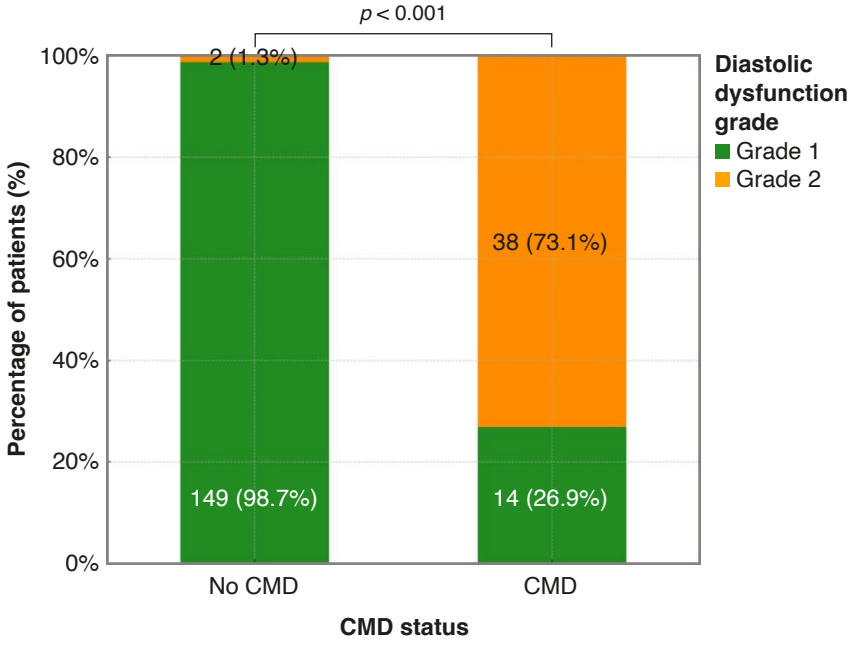

Fig. 4.6.3.7. *Prevalence of diastolic dysfunction displayed by coronary microvascular dysfunction*

CMD – coronary microvascular dysfunction.

Upon further analysis, it was evident that the classification of patients with CMD predominantly aligned with the criteria for Groups 2, 3, and 4 within the FLVR framework. Specifically, for Group 2 there were 20 (37.74%) *vs.* 4 (2.65%), for Group 3 there were 6 (11.32%) *vs.* 11 (7.28%), and for Group 4 there were 12 (22.64%) *vs.* 3 (1.99%); all with $p < 0.001$ (Fig. 4.6.3.8).

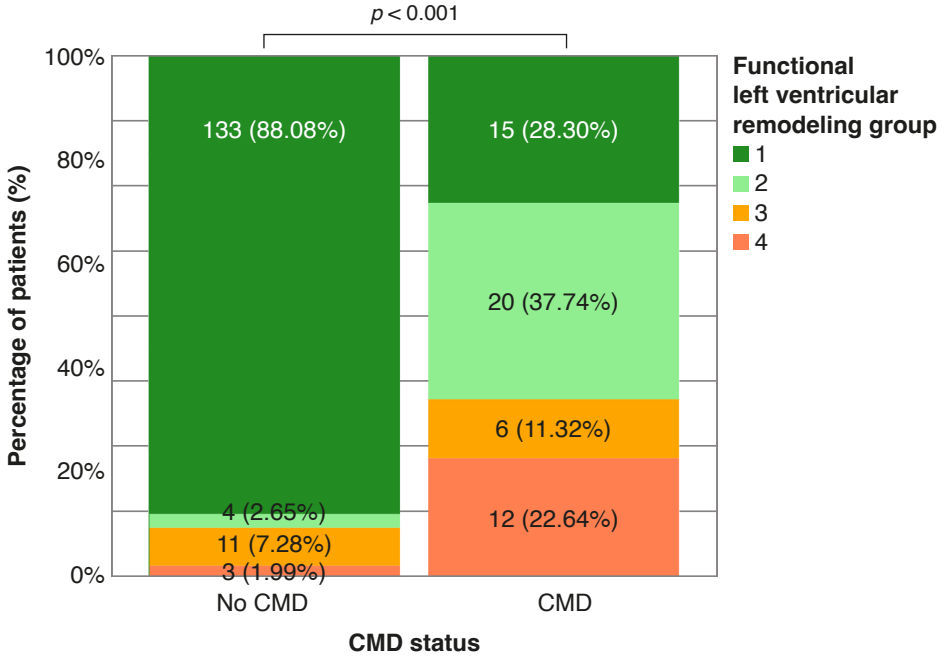

Fig. 4.6.3.8. *Rates of left ventricular remodelling displayed by coronary microvascular dysfunction*

CMD – coronary microvascular dysfunction; LV – left ventricle.

4.6.4. Angiographic findings

The overall time it took patients to seek medical attention after the onset of symptoms did not differ between the two groups (314 min *vs.* 314 min; $p = 0.138$) (Table 4.6.4.1). Similarly, the door-to-balloon time did not vary between study groups (40.0 min *vs.* 40.0 min; $p = 0.128$). TIMI flow both before and after revascularization was nearly evenly distributed across study groups. In our cohort of STEMI patients, the left anterior descending artery was identified as a culprit vessel similarly between both study groups: 33 (57.89%) in the CMD group versus 85 (55.56%) in the non-CMD group. However, some disparities became apparent when examining other arteries. Specifically, the left circumflex artery was more commonly identified as the

culprit in the non-CMD group (7 (12.28%) *vs.* 42 (27.45%)), whereas the right coronary artery was predominant in the CMD group (17 (29.82%) *vs.* 26 (16.99%)). These observed differences achieved statistical significance with a *p*-value of 0.024. In the investigation, the number of diseased vessels was similar between the two groups ($p = 0.505$).

4.6.5. Procedural characteristics

There were no significant differences in the study groups regarding contrast dose (100 ml *vs.* 100 ml; $p = 0.633$), stent diameter (3 mm *vs.* 3 mm; $p = 0.949$) and length (24 mm *vs.* 24 mm; $p = 0.100$), or maximal inflation pressure (15 atm *vs.* 14 atm; $p = 0.797$) (Table 4.6.4.1).

4.6.6. Coronary physiology findings

Distinct differences were observed in CFR values between the groups. Patients diagnosed with CMD exhibited a significantly lower CFR compared to their non-CMD counterparts (1.94 *vs.* 2.88; $p = 0.003$). In contrast, FFR values displayed no significant disparity between the CMD and non-CMD patients (0.91 *vs.* 0.92; $p = 0.452$). Notably, as anticipated, the IMR in CMD patients was markedly higher than in non-CMD patients (44 *vs.* 18.0; $p < 0.001$). Despite the fact that there was no statistically significant difference in hyperemic distal coronary pressure between the two groups (66.42 mmHg *vs.* 66.03 mmHg; $p = 0.003$), the mean transit time was, as anticipated, longer in the CMD group compared to the non-CMD group (0.72 sec *vs.* 0.25 sec; $p < 0.001$) (Table 4.6.4.1).

Table 4.6.4.1. *Coronary angiography and physiology parameters of ST-elevation myocardial infarction patients, categorized by coronary microvascular dysfunction*

Parameters	Overall (n = 210)	CMD (n = 57)	No CMD (n = 153)	*p*-value
Angiographic				
Pain-to-door time (minutes)	314 [107.75, 592.25]	314.00 [141.00, 667.00]	314.00 [104.00, 531.00]	0.138
Door-to-balloon (minutes)	40 [29.25, 52.0]	40.00 [34.00, 55.00]	40.00 [28.00, 51.00]	0.128
Pre-PCI TIMI flow				
0	130 (61.90%)	43 (75.44%)	87 (56.86%)	0.091
1	8 (3.81%)	2 (3.51%)	6 (3.92%)	
2	44 (20.95%)	8 (14.04%)	36 (23.53%)	
3	28 (13.33%)	4 (7.02%)	24 (15.69%)	

Table 4.6.4.1. *Continued*

Parameters	Overall (n = 210)	CMD (n = 57)	No CMD (n = 153)	*p*-value
Post-PCI TIMI flow				
0	2 (0.95%)	1 (1.75%)	1 (0.65%)	0.218
1	1 (0.48%)	1 (1.75%)	0 (0.00%)	
2	22 (10.48%)	8 (14.04%)	14 (9.15%)	
3	185 (88.1%)	47 (82.46%)	138 (90.20%)	
Culprit Vessel				
Left anterior descending artery	118 (56.19%)	33 (57.89%)	85 (55.56%)	***0.024***
Circumflex artery	49 (23.33%)	7 (12.28%)	42 (27.45%)	
Right coronary artery	43 (20.48%)	17 (29.82%)	26 (16.99%)	
Number of diseased vessels				
2-vessel disease	123 (58.57%)	36 (63.16%)	87 (56.86%)	0.505
3-vessel disease	87 (41.43%)	21 (36.84%)	66 (43.14%)	
Intracoronary interventions				
Stent diameter (millimeters)	3.0 [3.0, 3.5]	3.00 [3.00, 3.50]	3.00 [3.00, 3.50]	0.949
Stent length (millimeters)	24.0 [19.0, 26.0]	24.00 [19.00, 26.00]	24.00 [19.00, 26.00]	0.10
Maximal stent pressure (atm)	14.0 [14.0, 16.0]	15.00 [12.00, 17.00]	14.00 [14.00, 16.00]	0.797
Contrast dose (milliliters)	100.0 [90.0, 110.0]	100.00 [90.00, 110.00]	100.00 [90.00, 110.00]	0.633
Coronary physiology at 3-month follow-up				
Coronary flow reserve	2.81 [2.54, 2.98]	1.94 [1.35, 2.24]	2.88 [2.74, 3.15]	***0.003***
Fractional flow reserve	0.92 [0.87, 0.97]	0.91 [0.85, 0.97]	0.92 [0.87, 0.97]	0.452
Index of Microcirculatory resistance	20 [15.0, 29.0]	44.00 [38.00, 53.00]	18.00 [13.00, 21.00]	***0.001***
Hyperemic distal coronary pressure (mmHg)	66.23 [60.04, 76.58]	66.42 [59.64, 78.57]	66.03 [60.14, 75.69]	0.451
Mean transit time (sec)	0.30 [0.20, 0.43]	0.72 [0.51, 0.87]	0.25 [0.18, 0.32]	***<0.001***

PCI – percutaneous coronary intervention; TIMI – thrombolysis in myocardial infarction; CMD – coronary microvascular dysfunction. Values are n (%) or median [IQR]. In bold and italics significant *p*-values (< 0.05).

4.6.7. Clinical outcome

A significant variation in prevalence was observed across almost all individual components of MACE, encompassing ischemic stroke, non-fatal MI, target vessel revascularization, and heart failure hospitalization, when comparing the CMD and non-CMD groups (Table 4.6.7.1). The CMD group demonstrated a notably higher prevalence of ischemic stroke, with 5 (8.77%) instances versus 2 (1.31%) in the non-CMD group ($p = 0.025$). This may, in part, be associated with the higher incidence of atrial fibrillation in this population (28.0% *vs.* 4.5%; $p < 0.001$). Similarly, the prevalence of non-fatal MI was 7 (12.28%) in the CMD group compared to 3 (1.96%) in the non-CMD group ($p = 0.006$). Target vessel revascularization also showed a higher incidence in the CMD group, 6 (10.53%), as opposed to 4 (2.61%) in the non-CMD group ($p = 0.042$). Most pronounced was the disparity in heart failure hospitalization, with the CMD group having 12 (21.05%) cases compared to 4 (2.61%) in the non-CMD group ($p < 0.001$), respectively. While the incidence of cardiovascular mortality in the CMD group was slightly higher, there was no statistically significant difference observed when compared to the non-CMD (4 (7.02%) *vs.* 2 (1.31%); $p = 0.081$). During the course of the follow-up, the overall rates of MACE were 20.95 %. We found that the rate of MACE in CMD patients was significantly higher than the rate of MACE in non-CMD patients over a period of 12 months (25 (50.88%) *vs.* 15 (9.80%); $p < 0.001$) (Fig. 4.6.7.1). The Kaplan-Meier curve revealed an increased incidence of MACE in patients who were diagnosed with CMD (log-rank $p < 0.001$), most noticeably starting at first month post-PCI (Fig. 4.6.7.2).

Table 4.6.7.1. *Twelve-month clinical outcomes of patients presenting with ST-elevation myocardial infarction, categorized by coronary microvascular dysfunction*

	Overall (n = 210)	**CMD (n = 57)**	**No CMD (n = 153)**	***p*-value**
Ischemic stroke	7 (3.33%)	5 (8.77%)	2 (1.31%)	***0.025***
Nonfatal MI	10 (4.76%)	7 (12.28%)	3 (1.96%)	***0.006***
Cardiovascular death	6 (2.86%)	4 (7.02%)	2 (1.31%)	0.081
Target vessel revascularization	10 (4.76%)	6 (10.53%)	4 (2.61%)	***0.042***
HF requiring hospitalization	16 (7.62%)	12 (21.05%)	4 (2.61%)	***< 0.001***
MACE	44 (20.95%)	29 (50.88%)	15 (9.80%)	***< 0.001***

MI – myocardial infarction; HF – heart failure; MACE – the composite of stroke, nonfatal myocardial infarction, revascularization, heart failure hospitalization, and cardiovascular death. Values are n (%). In bold and italics significant *p*-values (< 0.05).

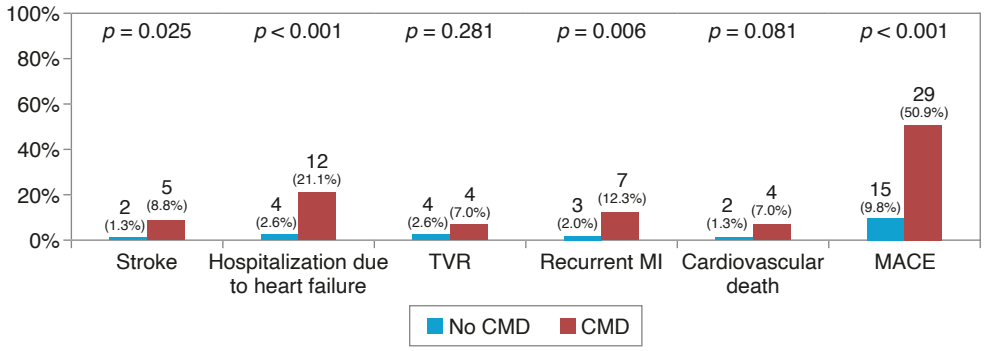

Fig. 4.6.7.1. *Rates of major adverse cardiovascular events and its individual components displayed by coronary microvascular dysfunction*

CMD – coronary microvascular dysfunction; TVR – target vessel revascularization; MI – myocardial infarction; MACE – the composite of stroke, nonfatal myocardial infarction, revascularization, heart failure hospitalization, and cardiovascular death.

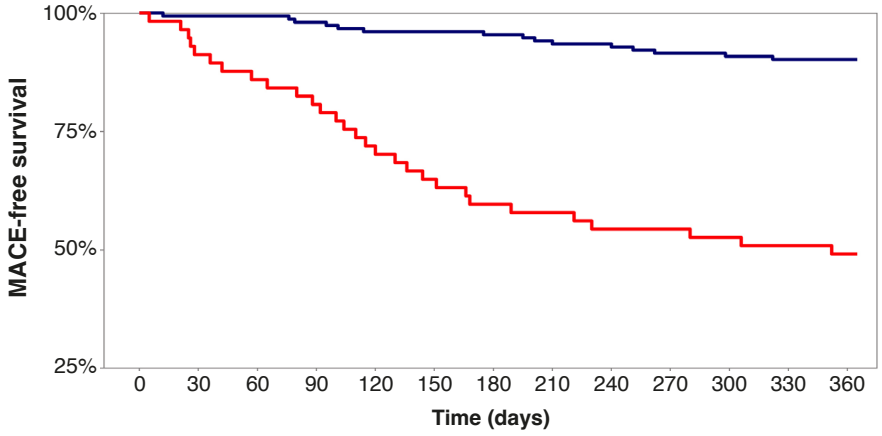

Strata	Number at risk by time												
No CMD	153	152	152	150	147	147	146	144	143	140	139	138	138
CMD	57	52	49	46	41	37	34	33	31	31	30	28	28

Fig. 4.6.7.2. *Kaplan-Meier event-free survival curve for occurrence of major adverse cardiovascular events grouped by coronary microvascular dysfunction*

CMD – coronary microvascular dysfunction; MACE – the composite of stroke, nonfatal myocardial infarction, revascularization, heart failure hospitalization, and cardiovascular death.

4.6.8. Multivariable logistic analysis

Multivariable logistic regression analysis with adjustment for age, gender, BMI, medical history, laboratory data, baseline echocardiography parameters and physiologic analysis was performed to identify the independent risk factors for LV diastolic dysfunction and functional LV remodelling. For LV diastolic dysfunction, the model showed that baseline E/e', and IMR were the independent predictor for LV diastolic dysfunction grade 2 (Table 4.6.8.1). The model with IMR at 3-month follow-up and baseline E/e' yielded a receiver operator characteristic AUC of 0.933 (0.877–0.980; $p < 0.001$), indicating an excellent predictive ability in the binary logistic multivariable analysis (Fig. 4.6.8.1). For the functional LV remodelling, BNP level and IMR at 3 months follow up were independent predictors for group 3 or group 4 remodelling (Table 4.6.8.2). The model with BNP and IMR, yielded a receiver operator characteristic AUC of 0.773 (0.685–0.862; $p < 0.001$), indicating a good predictive ability in the binary logistic multivariable analysis (Fig. 4.6.8.2).

Table 4.6.8.1. *Multivariable binary logistic analysis for prediction of diastolic dysfunction after ST-segment elevation myocardial infarction event*

Variable	Odds ratio	95% confidence limits		*p*-value
Age	0.959	0.906	1.014	0.143
Gender (Female)	1.822	0.408	8.144	0.432
Body mass index (kg/m^2)	0.958	0.823	1.114	0.576
History of arterial hypertension	0.527	0.125	2.231	0.385
History of coronary artery disease	2.422	0.327	17.956	0.387
History of PCI	1.965	0.168	22.966	0.590
History of stroke	1.476	0.224	9.703	0.686
History of diabetes mellitus	0.235	0.045	1.227	0.086
History of dyslipidemia	0.418	0.112	1.565	0.195
Smoking	1.778	0.443	7.132	0.417
History of alcohol abuse	1.510	0.118	19.287	0.751
Hemoglobin (g/dl)	1.027	0.994	1.062	0.110
White blood cell count ($\times 10^9$/L)	1.164	0.933	1.452	0.178
Platelets ($\times 10^9$/L)	1.004	0.993	1.016	0.463
Aspiration thrombectomy	0.301	0.043	2.130	0.229
CRP at 3 months	0.978	0.761	1.258	0.865
BNP at 3 months	0.993	0.982	1.004	0.198
Post PCI LVEF	0.994	0.896	1.103	0.917
Post PCI E/A	0.629	0.110	3.611	0.604
Post PCI E/e*	1.250	1.011	1.545	0.039

Table 4.6.8.1. *Continued*

Variable	Odds ratio	95% confidence limits		*p*-value
Post PCI TRpV (m/s)	4.466	0.484	41.187	0.187
Post PCI LA volume index (mL/m^2)	1.048	0.950	1.155	0.351
Coronary flow reserve at 3 months	0.585	0.217	1.572	0.287
Fractional flow reserve at 3 months (0.1 increment)	1.613	0.508	5.118	0.417
Index of microcirculatory resistance at 3 months	1.173	1.088	1.264	***< 0.001***

PCI – percutaneous coronary intervention, CRP – C-reactive protein, BNP – brain natriuretic peptide, LVEF – left ventricular ejection fraction, TRpV – tricuspid regurgitation peak velocity. In bold and italics significant *p*-values (< 0.05).

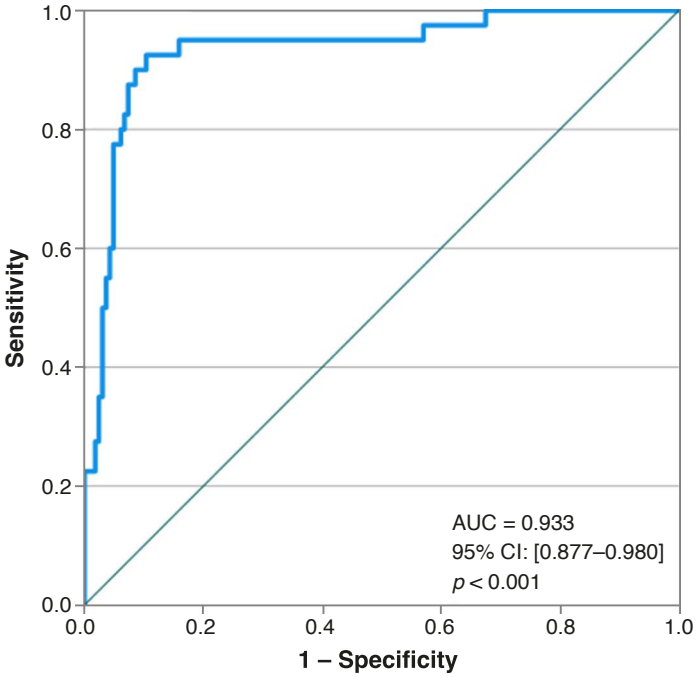

Fig. 4.6.8.1. *Receiver operating characteristic curve for the model of diastolic dysfunction at 12-month follow up in ST-elevation myocardial infarction patients*

AUC – area under the receiver operating characteristic curve; ROC – receiver operating characteristic; CI – confidence interval.

Table 4.6.8.2. *Multivariable binary logistic analysis for functional left ventricular remodelling after ST-segment elevation myocardial infarction event*

Variable	Odds ratio	95% confidence limits		*p*-value
Age	0.966	0.924	1.010	0.124
Gender (Female)	2.760	0.887	8.587	0.080
Body mass index (kg/m^2)	1.041	0.948	1.143	0.400
History of hypertension	0.666	0.238	1.867	0.440
History of coronary artery disease	2.057	0.563	7.513	0.275
History of PCI	0.220	0.027	1.813	0.159
History of stroke	0.950	0.260	3.469	0.938
History of diabetes mellitus	1.871	0.625	5.601	0.263
History of dyslipidemia	0.812	0.289	2.281	0.692
Smoking	1.061	0.360	3.125	0.915
History of alcohol abuse	1.260	0.211	7.521	0.800
Hemoglobin(g/dl)	0.998	0.974	1.022	0.868
White blood cell count ($\times 10^9$/L)	0.967	0.804	1.163	0.725
Platelets ($\times 10^9$/L)	0.997	0.988	1.006	0.489
Aspiration thrombectomy	1.600	0.465	5.506	0.456
High-sensitivity CRP at 3 months	1.033	0.840	1.269	0.761
BNP at 3 months	1.011	1.003	1.019	**0.007**
Post PCI LVEF	0.960	0.892	1.033	0.275
Post PCI E/A	1.357	0.389	4.733	0.632
Post PCI E/e*	1.100	0.923	1.311	0.286
Post PCI TRpV (m/s)	1.097	0.248	4.843	0.903
Post PCI LA volume index (mL/m^2)	1.038	0.961	1.121	0.343
Coronary flow reserve at 3 months	1.638	0.735	3.648	0.228
Fractional flow reserve at 3 months (0.1 increment)	2.590	0.949	7.072	0.063
Index of Microcirculatory resistance at 3 months	1.057	1.015	1.101	**0.007**

PCI – percutaneous coronary intervention, CRP – C-reactive protein, BNP – brain natriuretic peptide, LVEF – left ventricular ejection fraction, TRpV – tricuspid regurgitation peak velocity. In bold and italics significant p-values (< 0.05).

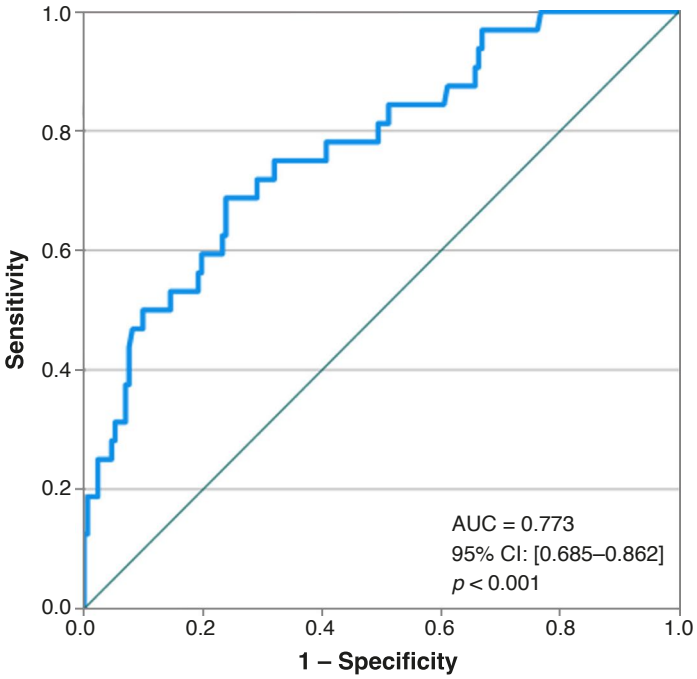

Fig. 4.6.8.2. *Receiver operating characteristic curve for the model of functional left ventricular remodelling at 12-month follow up in ST-elevation myocardial infarction patients*

AUC – area under the receiver operating characteristic curve; ROC – receiver operating characteristic; CI – confidence interval.

5. DISCUSSION

5.1. The impact of percutaneous coronary intervention strategies during ST-elevation myocardial infarction on the prevalence of coronary microvascular dysfunction

5.1.1. Overview of the primary findings

In our prospective, single-blinded cohort study, we observed a significant reduction in CMD and adverse cardiac events through the application of direct stenting, bypassing the pre-dilatation technique, compared to balloon pre-dilatation stenting methods. Additionally, the use of aspiration thrombectomy and glycoprotein IIb/IIIa inhibitors appeared equally effective in reducing CMD risk. With 210 participants, this study is among the largest to explore the effects of varied PCI strategies during STEMI on CMD, using comprehensive coronary invasive physiology assessments.

5.1.2. Timing of coronary physiology assessment post- ST-elevation myocardial infarction

Diverging from previous studies that conducted coronary physiology testing during the acute phase of STEMI, our research opted for a three-month post-STEMI evaluation [349, 350]. This approach aimed to prevent misinterpretation of CMD, which could stem from the altered cardiac physiology during the acute phase of STEMI [351]. Ríos-Navarro et al., in their experimental study, demonstrated a near-complete resolution of CMD 30 days post-reperfusion [352]. This hypothesis found further empirical validation in the research conducted by Demirkiran et al., wherein a marked optimization of CMD indices was observed within the 30-day post-STEMI period. Specifically, data demonstrated a decrement in IMR metrics from a pre-established 38.8 U to a subsequent 25.6 U, concomitant with an augmentation in CFR from an initial measurement of 2.16 U to a later 3.77 U [353]. Our focus was to discern the sustained impact of PCI interventions on CMD.

5.1.3. Revisiting primary percutaneous coronary intervention guidelines in the context of coronary microvascular dysfunction

Current guidelines favor primary PCI as the standard treatment for STEMI patients [4]. Typically, this strategy is effective in restoring blood supply to the myocardium [345]. Yet, it's important to recognize the risk of iatrogenic microvascular obstruction caused by distal embolization of

thrombus or atherosclerotic debris during primary PCI, potentially leading to detrimental clinical outcomes [354].

5.1.4. Direct stenting role in reducing coronary microvascular dysfunction risk

In our comprehensive analysis, the binary logistic multivariable analysis unveiled a significant finding: direct stenting was correlated with a notably lower incidence of CMD, approximately five times less likely, when contrasted with balloon pre-dilatation stenting techniques.

5.1.4.1. Mechanistic insights of direct stenting *vs.* balloon pre-dilatation stenting

The underlying reasons for this disparity are multifaceted. To begin with, balloon manipulations in the target artery during balloon pre-dilatation stenting might inadvertently cause distal thrombus embolization, adversely affecting the microcirculation. Moreover, the process of lesion dilatation can lead to the expulsion of plaque components, known for their potent activation of the coagulation cascade. Furthermore, the pre-dilatation step inherent in balloon pre-dilatation stenting might result in arterial wall endothelial dissection, precipitating rapid thrombus formation. Additionally, there is the concern that pre-dilatation could inflict damage to the endothelial lining of coronary arteries, potentially initiating inflammatory responses. This, in turn, can impede the natural healing process of the endothelium and re-endothelialization around the stented area, subsequently increasing the risk of stent thrombosis and neointimal hyperplasia [355]. Given that patients experiencing STEMI typically present a heightened prevalence of thrombotic material, the adverse effects of these manipulations on the microvascular network might be significantly magnified [356, 357]. Beyond these clinical advantages, direct stenting also presents practical benefits, including potential reductions in radiation exposure, overall healthcare costs, and the procedural duration [358]. Notably, Webb et al. observed that direct stenting in saphenous venous graft lesions resulted in reduced incidents of distal embolization. This was attributed to the entrapment of thrombotic and friable material behind the stent struts [359].

5.1.4.2. Limitations and challenges in direct stenting

Despite its apparent advantages, direct stenting is not devoid of challenges. Critical limitations include the potential underestimation of the actual size of arteries due to the hypo-perfused state of freshly revascularized vessels, which could lead to inadequate stent expansion. Furthermore, the

technique may face difficulties in cases involving tightly constricted coronary lesions, potentially impeding the stent's ability to cross these areas. Additionally, the absence of clearly defined lesion margins can pose challenges in precise stent positioning [360].

5.1.4.3. Clinical outcomes and reperfusion efficacy

Direct stenting is associated with notable improvements in cardiac reperfusion, as evidenced by enhanced ST-segment resolution, a significant decrease in the incidence of no-reflow phenomena, and a reduction in MACE [361–364]. However, these correlations warrant cautious interpretation in light of the study's constraints, which include its primary focus on single-center data, a non-randomized design, and reliance on methodologies not reflective of current clinical practices (e.g., bare metal stent implantation and/or lacking sufficient power to draw a definitive conclusion).

5.1.4.4. Contrasting perspectives in coronary microvascular dysfunction and stenting research

The debate on the differential impacts of stenting techniques on CMD is ongoing. Jie et al.'s investigation into stenting effects on CMD could not conclusively demonstrate the superiority of direct stenting over balloon pre-dilatation stenting methods. The limitations of this study, such as its lack of randomization, relatively small patient cohort (137 participants per arm), and the premature use of CMR imaging for CMD assessment post-STEMI (within one week), raise significant concerns regarding the reliability of its findings [352, 365]. Similarly, Kim et al.'s study, aimed at evaluating the impact of direct stenting on microcirculation, fell short of demonstrating significant results. Criticisms of this study include its small scale (38 patients per group) and the timing of coronary physiology measurements immediately after primary PCI, which risks inaccuracies during the acute phase of STEMI. Furthermore, the study's focus was limited to IMR without considering CFR, a crucial index in CMD diagnosis [349]. Other randomized trials exploring direct stenting and its effect on myocardial perfusion, though methodologically sound, are now considered outdated, having been conducted between the late 1990s and early 2000s. These studies also relied on primitive and less accurate techniques for CMD assessment, such as the TIMI flow count [366–370]. In contrast, a smaller randomized study by Cuisset et al. in Belgium involving stable angina patients presented findings that support a lower incidence of microvascular injury with direct stenting [371].

5.1.5. Aspiration thrombectomy's role in reducing coronary microvascular dysfunction risk

Our current investigation underscores a critical observation: the implementation of aspiration thrombectomy in primary PCI is correlated with a fivefold decrease in the risk of CMD. The efficacy and utility of aspiration thrombectomy during primary PCI are subjects of ongoing debate within the cardiological community, with studies presenting varied outcomes [350, 372–374].

5.1.5.1. Critical analysis of aspiration thrombectomy studies

The Thrombectomy Trialists Collaboration, for instance, reported that combining direct stenting with aspiration thrombectomy did not significantly improve clinical outcomes or myocardial reperfusion metrics [372]. This aligns with current clinical guidelines, which generally discourage the routine application of aspiration thrombectomy [4]. However, a critical point to consider in the Thrombectomy Trialists Collaboration's study is the absence of CMD assessment through invasive thermodilution, CMR, or other precise methodologies. Instead, the study relied on myocardial blush as an indirect marker for CMD, casting doubts on the precision of its CMD evaluation. Hoole et al. embarked on a randomized clinical pilot trial, meticulously conducting IMR measurements at various stages of primary PCI, complemented by CMR analyses at 24-hour and three-month intervals. The trial indicated a trend towards reduced microcirculatory damage in patients who underwent aspiration thrombectomy, although this trend did not achieve statistical significance. Consequently, the study cautiously suggested that aspiration thrombectomy may not be categorically superior to balloon angioplasty in minimizing microcirculatory damage. Notably, the study's interpretive strength is hampered by its limited scale – only 26 patients underwent follow-up CMR analysis, rendering the study statistically underpowered. Moreover, the exclusive reliance on IMR measurements during the acute phase of primary PCI is a notable limitation, given the altered physiological state associated with acute STEMI. The trial also highlighted that smaller-than-recommended balloons were used to minimize the risk of distal embolization, leaving room for speculation that balloon angioplasty with appropriately sized balloons might be less effective compared to aspiration thrombectomy [350].

5.1.5.2. Larger-scale trials and emerging evidence

The MUltidevice Thrombectomy in Acute ST-Segment Elevation Acute Myocardial Infarction (MUSTELA) trial, involving 208 patients with STEMI, represents the largest randomized study to date investigating the impact of aspiration thrombectomy on CMD over a three-month period, utilizing CMR. The findings from this trial were significant, demonstrating a notably lower incidence of CMD in the aspiration thrombectomy group (11.4% *vs.* 26.7%, $p = 0.02$) [375]. Similarly, the Thrombectomy with ExPort catheter in Infarct-Related Artery during primary percutaneous coronary intervention (EXPIRA) trial focused on assessing the influence of aspiration thrombectomy on myocardial blush and ST-elevation resolution during the acute phase of STEMI in a subset of patients. This trial too found a reduced incidence of CMD in the aspiration thrombectomy group compared to the routine PCI group (31.5% *vs.* 72.9%, $p = 0.0005$) [376]. Complementing these findings, a smaller-scale Polish study, though limited by its sample size of 45 patients, revealed a significant reduction in CMD, as assessed by CMR, in patients receiving aspiration thrombectomy compared to those undergoing PCI alone (11.7% *vs.* 22.2%, $p = 0.009$) [374]. While these studies offer promising insights, the relatively small cohort in the Polish study somewhat curtails the generalizability of its findings.

5.1.6. Intracoronary glycoprotein IIb/IIIa inhibitors role in reducing CMD risk

The findings from our study shed light on a pivotal aspect: the administration of intracoronary glycoprotein IIb/IIIa inhibitors, specifically Eptifibatide, during primary PCI is associated with a marked decrease in the risk of CMD, by approximately fivefold. It is widely acknowledged that platelet aggregation plays a critical role in the obstruction of microvasculature [377]. Glycoprotein IIb/IIIa inhibitors function by impeding the final step of the platelet aggregation process, thereby potentially reducing platelet activation and adhesion [377].

5.1.6.1. Mechanistic insights from animal models

In a controlled study using the Sprague-Dawley rat model, the application of a glycoprotein IIb/IIIa inhibitor during a STEMI event was observed to maintain the structural and functional integrity of the microvascular endothelium. This protective mechanism is partly mediated by myocardial endothelial nitric oxide synthesis [378]. Eptifibatide, a glycoprotein IIb/IIIa inhibitor, when administered directly into the coronary circulation during primary PCI, can enhance coronary flow. The rationale behind intracoronary

administration lies in achieving a higher local concentration, leading to augmented binding to platelet and endothelial receptors. This increased efficacy is attributable to the dose-dependency of the inhibitor; higher concentrations more effectively dissolve platelet aggregates [379].

5.1.6.2. Correlation with previous studies and clinical trials

Our results align with previous research demonstrating the efficacy of intracoronary glycoprotein IIb/IIIa inhibitors in reducing CMD [380–382]. In a randomized trial conducted by Akpek et al., patients receiving intracoronary glycoprotein IIb/IIIa inhibitors exhibited improved TIMI flow post-primary PCI compared to a placebo group [382]. Candemir et al. also reported that the administration of this inhibitor significantly reduced infarction size (as indicated by Troponin and CK-MB levels) and CMD (as assessed by TIMI flow count) [381]. However, the methodologies employed in these studies, particularly the use of TIMI flow count to ascertain CMD, have been a subject of contention within the scientific community due to their perceived obsolescence and lack of precision.

5.1.6.3. Comparative efficacy in intracoronary versus intravenous administration

A recent study from China brought a new perspective by comparing CMD prevalence, as determined by CMR, in patients administered intracoronary glycoprotein IIb/IIIa inhibitors versus those receiving it intravenously. This study concluded that intracoronary administration is more effective in reducing CMD [380]. This finding underscores the potential for targeted intracoronary drug delivery in enhancing therapeutic outcomes in the setting of STEMI and CMD.

5.2. Prediction of coronary microvascular dysfunction in ST-elevation myocardial infarction patients via a machine learning approach

5.2.1. Overview of the primary findings

The objective of the present study is to create a predictive model using clinical variables and blood-based biomarkers for CMD, a diagnosis that typically requires advanced imaging techniques or invasive coronary physiology testing. It enrolled 200 patients with STEMI and multivessel CAD. 149 patients were employed in the training set and 51 patients were employed in the validation set. In total, 29 clinical variables were analysed for the outcome of CMD by constructing predictive models for several machine learning techniques. The random forest algorithm yielded the best predictive model,

with a very high sensitivity, specificity, and positive predictive value when tested on the validation set, while logistic regression yielded the least optimal model. The most important variables were TMAO, platelet anti-aggregation with ADR and BNP in the RF model. One of the inherent limitations of machine learning analysis, including the RF technique, is the lack of interpretability compared to logistic regression. The relVIM analysis allows partial insight into the influence of variables on the outcome but does not permit the calculation of metrics like the odds ratio. Further, it is difficult to differentiate causative variables from bystander variables, although delineation is not strictly needed in generating accurate prediction models. Nevertheless, we explore the physiologic relevance of selected variables below.

5.2.2. Trimethylamine N-oxide role in cardiovascular diseases and coronary microvascular dysfunction

The most important variables were TMAO, platelet anti-aggregation with ADR and BNP in the RF model. One of the inherent limitations of machine learning analysis, including the RF technique, is the lack of interpretability compared to logistic regression. The relVIM analysis allows partial insight into the influence of variables on the outcome, but does not permit the calculation of metrics like the odds ratio. Further, it is difficult to differentiate causative variables from bystander variables, although delineation is not strictly needed in generating accurate prediction models. Nevertheless, we explore the physiologic relevance of selected variables below. TMAO is produced via the metabolism of dietary molecules, including L-carnitine and choline, by the intestinal microbiota and liver [383]. It has been implicated in vascular inflammation, foam cell formation, endothelial dysfunction, oxidative stress, and is thought to promote atherosclerosis [275, 384–387]. Despite this, it is unclear whether TMAO plays a causative role in CMD. A study by Jomard et al. found that in obese patients undergoing Roux-en-Y gastric bypass, TMAO increased at 2 years despite sustained weight loss and some improvement in their metabolic profiles [388]. Further, acute TMAO administration to rats did not appear to affect vasodilation, endothelial NO production, thrombus formation or infarct size after transient occlusion of the middle cerebral artery. However, TMAO has been shown to be an independent predictor of clinical events [327, 389]. One study followed 1079 patients with acute myocardial infarction and found that TMAO levels sampled 3–4 days after admission independently correlated with the 2-year risk death or myocardial infarction [327]. Another study found that in 4007 patients who underwent elective coronary angiography and did not have acute

coronary syndrome, TMAO levels independently correlated with the 3-year risk of death, non-fatal myocardial infarction and stroke [389].

5.2.3. Platelet function and coronary microvascular dysfunction

Platelet aggregation by epinephrine was the second most influential variable in the model. Platelet dysfunction is a core mechanism in CMD and is intimately linked to endothelial dysfunction and subsequently alterations in NO, prostaglandin, and cytokine production [390]. Platelet aggregation by adenosine di-phosphate (ADP) was the least influential variable, however this is likely due to the administration of P2Y12 inhibitors to the patients prior to PCI as is the standard of care for STEMI, which prevents the action of ADP on platelets. On the other hand, epinephrine potentiates platelet activation via the α2 receptor and thus better represents the role of platelet dysfunction in the RF model [391].

5.2.4. B-type natriuretic peptide and coronary microvascular dysfunction

The elevated BNP reflects the lower left ventricular ejection fraction in patients with CMD. While the initial left ventricular ejection fraction was similar in patients with and without CMD immediately after PCI [approximately 40%), at 3 months patients with CMD had a lower ejection fraction due chronic ongoing myocardial ischemia. CMD is an established risk factor for heart failure and has been implicated in both heart failure with reduced ejection fraction (HFrEF) and heart failure with preserved ejection fraction (HFpEF) [392, 393]. While CMD appears to be prevalent in both types of heart failure, patients with HFrEF may have a different subtype CMD than patients with HFpEF [394]. Given that BNP levels differ between these two types of heart failure, patients with HFpEF may benefit from a different model for predicting CMD [395].

5.2.5. C-reactive protein and coronary microvascular dysfunction

CRP is a non-specific systemic indicator of inflammation and has been shown to have some predictive value in cardiovascular risk [184, 185]. The Reynolds Risk Score, a scoring system that was derived from the Women's Health Study, incorporates CRP as predictive variable [184]. Prior studies have also shown that patients with CMD typically exhibit elevated levels of CRP than those without CMD [187, 188]. Nevertheless, due to its non-specific nature, high variability on an individual level and propensity to vary throughout the day, CRP is a suboptimal marker for cardiovascular risk in isolation [192].

5.2.6. Immune cells and coronary microvascular dysfunction

Neutrophils are thought to play a pro-inflammatory role through the generation of various inflammatory agents, including myeloperoxidase, oxygen free radicals, and elastase, promoting endothelial dysfunction [206, 207, 210, 211]. In contrast, lymphocytes have been implicated regulating the inflammatory response, with a negative correlation between lymphocyte levels and the inflammatory cytokines associated with endothelial dysfunction [212]. Hence, an elevated NLR is suggestive ongoing of coronary inflammation and endothelial dysfunction. Prior research has demonstrated an independent correlation between an elevated NLR and coronary thrombus in the presence of acute myocardial infarction as well as myocardial perfusion defects in the absence of acute myocardial infarction [209, 217].

5.2.7. Logistic regression versus machine learning

Regression techniques have been traditionally used in biomedical statistics due to their ability to demonstrate relationships between independent variables and outcomes [396]. This is particularly useful when quantifying the contribution of a specific risk factor in the development of disease or the efficacy of a specific intervention in ameliorating it. However, regression techniques are less suited for large datasets, which run the risk of violating the assumptions underlying regression analysis, including the lack of multicollinearity between independent variables, lack of influential outliers and the presence of a linear relationship between continuous independent variables and outcomes of interest. Using regression analysis for large datasets can result in overfitting, reducing the generalizability of the regression model. Further, the large number of variables in larger datasets erodes the interpretability of the regression model, which is a significant advantage of regression. Effective regression analysis requires a careful selection of independent variables to ensure that the analysis adheres to the constraints of regression techniques to produce a stable model. Further

In contrast, machine learning techniques are better suited to analyze large datasets and are becoming increasingly important in biomedical research [397]. Machine learning largely dispenses interpretability in favor of finding patterns in large datasets, particularly those with a larger number of independent variables compared to subjects, without requiring underlying assumptions about the dataset. It excels in generating predictive models and may be particularly useful in modelling complex, non-linear, biological processes, without making assumptions about the relationship between covariates and outcome, but does so at the expense of generating an interpretable model.

Prior studies have exhibited mixed results regarding the predictive ability of machine learning techniques versus logistic regression. For example, a recent analysis utilized 544 hospitalized pediatric patients to predict severe COVID-19 infection [398]. Compared to multivariate logistic regression, the machine learning model was better able to predict whether a patient would develop severe COVID-19 (area under the curve 0.8590 *vs.* 0.7770). However, another study of 4,912 patients who underwent pancreatoduodenectomy did not find that machine learning was superior to logistic regression for predicting post-operative complications [399]. A meta-analysis of 24 studies examined the predictive ability of logistic regression versus machine learning techniques in predicting acute kidney injury [400]. Overall, there was no significant difference in the predictive ability of logistic regression models and the machine learning models. However, GB models were superior to all other machine learning models, except for the RF model, indicating that careful selection of the machine learning techniques is crucial in modelling the biological system.

5.3. Trimethylamine N-oxide as a predictive biomarker for coronary microvascular dysfunction and prognosis in ST-elevation myocardial infarction patients

5.3.1. Overview of the primary findings

In light of the findings from our comprehensive analysis, the role of TMAO in the context of STEMI patients emerges with significant implications. Our study underscores the potential of TMAO not only as a biomarker for detecting CMD but also as a prognostic tool for patient outcomes. The association between elevated TMAO levels and adverse coronary physiology, as well as MACE, highlights a critical avenue for early intervention and tailored patient management. Particularly noteworthy is the marked correlation between TMAO levels at 3-month follow-up and key indicators of coronary microvascular health, such as CFR and IMR, suggesting a time-dependent aspect in TMAO's predictive capacity. This temporal relationship may offer a strategic window for clinicians to identify high-risk patients and potentially modify disease progression. Moreover, the comparison of TMAO with other established biomarkers reveals its superior predictive value, positioning it as a pivotal factor in the landscape of STEMI patient care. As we delve deeper into the discussion, it becomes imperative to contextualize these findings within the broader framework of cardiovascular disease management, exploring the mechanistic pathways of TMAO's influence and its integration into clinical practice.

5.3.2. Trimethylamine N-oxide post-ST-elevation myocardial infarction: from inaccurate to reliable

This comprehensive analysis provides a detailed analysis of the dynamic fluctuations in TMAO levels in patients who have experienced STEMI. Specifically, this study focuses on three critical time points: 24 hours, 3 months, and 12 months following the onset of STEMI. An intriguing aspect of this study is its in-depth investigation into the temporal changes in TMAO levels, thereby offering a novel perspective in the understanding of post-STEMI metabolic alterations.

In the initial phase, within the first 24 hours post-STEMI, a notable decrease in TMAO levels was observed. This finding aligns with those reported in the Dutch study conducted by Almesned et al., which demonstrated a similar decline in TMAO levels immediately following a STEMI, extending up to 24 hours later [401]. Several factors may contribute to this reduction in TMAO levels. These include physiological responses such as decreased appetite and vomiting, as well as adherence to specific dietary protocols typically enforced in a hospital setting during the acute phase of STEMI. Such dietary restrictions often involve fasting, which, as suggested by the findings in Washburn et al.'s pilot study, can significantly impact TMAO levels. This study revealed that a 24-hour period of water-only fasting in healthy individuals precipitated a significant decrease in TMAO levels, which subsequently returned to baseline upon resumption of a regular diet [402]. This suggests that the initial drop in TMAO levels observed in our study could predominantly be a result of reduced oral intake immediately following the STEMI event.

Another intriguing hypothesis emerges from the work of Hazen SL, which identifies the potential role of aspirin in modulating TMAO levels. Zhu's study found that aspirin could significantly lower plasma TMAO levels, particularly in individuals consuming a choline-rich diet [311]. Considering that all patients in our study received a 300 mg loading dose of aspirin post-STEMI, this pharmacological intervention could also be a contributing factor to the lowered TMAO levels observed initially.

At the 3-month follow-up, TMAO levels appeared to stabilize, likely reflecting more accurately the baseline levels. By this time, patients were generally on a lower dose of aspirin (81 mg) and presumably had resumed their typical dietary habits. Thus, the 3-month TMAO levels offer a more representative view of the patients' metabolic state post-STEMI, unaffected by the immediate dietary and pharmacological interventions following the acute event.

This part not only sheds light on the temporal patterns of TMAO levels post-STEMI but also highlights the significant influence of dietary and pharmacological factors on these levels.

5.3.3. Trimethylamine N-oxide and coronary microvascular dysfunction pathogenesis in ST-elevation myocardial infarction

Additionally, this study also offers a comprehensive analysis of TMAO as a biomarker with significant predictive value for CMD in patients who have experienced STEMI. Extensive literature in this field has identified two primary pathophysiological contributors to CMD in the context of STEMI: intraluminal microvascular obstruction and extravascular compression, each with its distinct mechanisms and implications [27].

Focusing on intraluminal microvascular obstruction, key elements include the formation of in situ thrombosis and the presence of endothelial dysfunction. These factors play a pivotal role in the pathogenesis of CMD following STEMI. On the other hand, extravascular compression, primarily attributed to vascular inflammation, is another critical aspect contributing to CMD. The interplay of these two factors creates a complex pathological environment conducive to the development and progression of microvascular obstruction leading to CMD [27].

In relation to TMAO's role, experimental studies have provided compelling evidence of its potential to exacerbate key pathologies associated with CMD, such as thrombosis, endothelial dysfunction, and vascular inflammation [403–405]. Moreover, extensive literature supports the notion that TMAO amplifies platelet responsiveness, thereby heightening the risk of in situ thrombosis. It also plays a significant role in exacerbating vascular inflammation, a crucial factor in the pathogenesis of CMD [310, 405].

Adding to this body of evidence is the experimental study by Brunt et al., which investigates the role of TMAO in contributing to vascular oxidative stress and endothelial dysfunction [406]. These are key elements in the development of CMD, highlighting the multifaceted impact of TMAO in the post-STEMI landscape. Furthermore, a smaller yet insightful pilot study conducted by Kul et al. lends supporting evidence to this theory. This study indicates that elevated levels of TMAO, along with inflammatory biomarkers, are associated with an increased incidence of endothelial dysfunction. They found that higher TMAO levels were inversely correlated with coronary flow reserve, further underscoring the potential role of TMAO in the pathogenesis of CMD [407]. This correlation is particularly significant as it provides a direct link between elevated TMAO levels and impaired vascular function, a cornerstone in the progression of CMD post-STEMI.

In summary, the collected evidence from various studies paints a comprehensive picture of TMAO's role in the development and exacerbation of CMD, particularly in the context of STEMI. By exploring the multifaceted mechanisms through which TMAO influences CMD.

5.3.4. Comparative analysis of Trimethylamine N-oxide levels in diverse geographic cohorts

Furthermore, in this part, we meticulously analyzed the median TMAO levels within our cohort, observing a median value of 2.97 μM. This figure is particularly noteworthy when juxtaposed with data from similar studies conducted in different geographic locations. For instance, when examining cohorts from Switzerland and the Netherlands, the median TMAO levels were recorded at 2.87 μM and 3.1 μM, respectively [401, 408]. These values exhibit a remarkable consistency with our findings, suggesting potential underlying patterns in TMAO levels across European populations.

In stark contrast, however, the Cleveland cohort in the United States reported significantly higher median TMAO levels, registering at 4.28 μM [408]. This discrepancy raises intriguing questions about the factors contributing to such variations in TMAO levels across different populations. One of the primary considerations in this regard is the impact of geographical differences on genetic and dietary factors, which are known to influence TMAO levels [409, 410].

The observation of relatively lower TMAO levels in European cohorts, including our own, may indicate the influence of genetic predispositions that are specific to these populations. Genetic factors can play a significant role in the metabolism of compounds like TMAO, potentially leading to regional variations in baseline TMAO levels [266]. Moreover, dietary habits, which are deeply influenced by cultural and geographical factors, could also contribute to these differences. European diets, for example, might have certain characteristics that result in lower TMAO production compared to diets prevalent in other regions like the United States [411].However, it is crucial to approach these hypotheses with caution. Without comprehensive dietary and genetic data from the various studies, drawing definitive conclusions would be premature. The correlation observed between TMAO levels and geographic location, while suggestive, requires a more in-depth analysis encompassing a broader range of factors, including dietary patterns, lifestyle choices, and genetic backgrounds of the different populations studied.

Additionally, it is important to consider other environmental and socio-economic factors that might influence TMAO levels. These include access to healthcare, levels of urbanization, and even climate, as they can indirectly

impact dietary habits and overall health [412]. It is also possible that differences in study methodologies, such as the timing of sample collection and the methods used for TMAO measurement, could contribute to the observed variations in TMAO levels across different cohorts [413].

In conclusion, the comparison of TMAO levels across different cohorts from Europe and the United States opens a fascinating window into the potential interplay of genetic, dietary, and environmental factors in determining TMAO levels. While our observations hint at geographic influences on TMAO levels, further research incorporating detailed dietary and genetic data is essential to elucidate these complex relationships fully. This line of investigation holds significant promise for understanding the role of TMAO in cardiovascular health and disease, potentially leading to more tailored and effective interventions based on geographic and population-specific factors.

5.3.5. C-reactive protein and B-type natriuretic peptide predictive value for coronary microvascular dysfunction

The exploration of biomarkers for predicting CMD remains a critical area of research, with CRP and BNP being of particular interest. However, the effectiveness of these biomarkers, especially CRP, in reliably predicting CMD is a subject of ongoing debate and investigation.

CRP's role in CMD prediction has been scrutinized in various studies, but its effectiveness remains limited. One notable study by Cosin-Sales et al. explored the relationship between CRP levels and CMD severity. They conducted a detailed analysis involving 137 patients suffering from ischemia with no obstructive coronary arteries (INOCA). This study identified a correlation between higher CRP levels and increased severity of CMD [188]. However, the methodologies employed in this study, such as reliance on patient surveys and the observation of ST-segment changes during 24-hour Holter monitoring, are now considered somewhat outdated. This methodological limitation poses challenges in fully interpreting and generalizing their findings to current clinical practices.

Similarly, the study by Recio-Mayoral et al. took a different approach by utilizing PET to investigate the correlation between hs-CRP levels and CMD. Their findings indicated a positive correlation between hsCRP levels exceeding 3 mg/L and greater impairment in CMD [187]. However, the study's relatively small sample size, consisting of only 21 patients, limits the generalizability of these results.

In our analysis, we observed a moderate predictive ability of CRP for CMD, with an AUC of 0.621, aligning somewhat with the cutoff identified by Recio-Mayoral et al. Despite this, our study, along with the existing

literature, suggests that CRP, by itself, is not robust enough to serve as a standalone biomarker for CMD. This finding is significant as it underscores the need for a more nuanced understanding of biomarkers and their role in CMD prediction.

Shifting focus to BNP, this biomarker has been extensively studied in relation to heart failure and CMD. BNP levels are known to increase in response to elevated left ventricular wall tension, a common feature in heart failure. Additionally, increased arterial stiffness leading to endothelial dysfunction, a key component in CMD pathogenesis, is also associated with elevated BNP levels [243, 414]. Previous research has established a clear link between high BNP levels and microvascular dysfunction. This link was demonstrated through various techniques, including flow-mediated dilation and acetylcholine-induced forearm vasodilation, providing valuable insights into the relationship between BNP and CMD [415–417].

One notable study by Hirakawa et al. employed CMR to analyze a cohort of 55 heart failure patients. They identified a weak to moderate correlation between BNP levels and CMD [418]. However, similar to previous studies, this research was limited by its small sample size, which restricts the breadth of its conclusions.

Furthermore, a study by Prescott et al. employed advanced analytical techniques, such as machine learning and logistic regression, to investigate effective biomarkers for CMD, specifically in females. This study found BNP, among other biomarkers, to be independent predictors of CMD. The AUC values in this study ranged from 0.58 to 0.66, which is in line with the 0.67 value observed in our research [419]. Despite these findings, BNP, much like CRP, is not sufficiently reliable for clinical use as a standalone indicator for CMD.

Both CRP and BNP have emerged as potential biomarkers for CMD. However, their predictive capabilities remain somewhat constrained, primarily due to the limitations inherent in previous studies. These limitations often include small sample sizes and reliance on methodologies that may no longer align with current best practices. Recognizing these challenges, our study aimed to bridge this knowledge gap by employing more contemporary and robust methodologies, coupled with a significantly larger sample size. This approach not only enhances the reliability of our findings but also provides a more accurate assessment of the predictive value of CRP and BNP in the context of CMD.

5.3.6. Trimethylamine N-oxide levels and major adverse cardiovascular events risk

In a pivotal study conducted in 2013, Tang et al. made a groundbreaking discovery, revealing that elevated plasma levels of TMAO are predictive of MACE [324]. This initial observation has since been substantiated by a series of comprehensive meta-analyses, further solidifying the association between high TMAO levels and increased cardiac risk [420–422].

Building upon this foundation, Li et al. conducted an insightful study, which added a new dimension to our understanding of TMAO's role in cardiac health [423]. Their research demonstrated that patients presenting with high plasma TMAO levels upon admission, followed by a decrease in these levels, were at an augmented risk of MACE compared to those with consistently low TMAO levels from the outset. This finding suggests a dynamic relationship between TMAO levels and cardiac risk, where initial high levels, even if reduced, are indicative of increased vulnerability to cardiac events.

Further delving into the metabolic pathways, it was found that dietary components such as choline, carnitine, and butyrobetaine play a significant role in TMAO production. These substances are metabolized by specific gut microbiota, predominantly the Firmicutes and Proteobacteria phyla, into TMA. The TMA is then absorbed into the bloodstream and transformed into TMAO by human flavin-containing monooxygenases, primarily FMO1 and FMO3, located in the liver and kidney respectively [424].

The variance in the composition of gut microbiota, coupled with dietary patterns, particularly those common in Western diets, may partly explain the higher incidence of CVD and MACE observed in certain populations. This is a crucial finding, as it links dietary and microbial factors with cardiac health [425].

Sanhez-Gimenez et al. brought another important aspect into focus: the role of renal function in regulating plasma TMAO concentrations. Their findings highlighted that renal efficiency or dysfunction could significantly influence the levels of TMAO in the bloodstream, thereby impacting the risk of MACE [426].

Intriguingly, recent research has explored the potential of inhibiting the enzymes responsible for TMAO production, particularly human FMO enzymes. FMO1, predominantly expressed in the kidney, and FMO3, more abundant in the liver, are crucial in the metabolic pathway leading to TMAO production. The inhibition of these enzymes, therefore, emerges as a potential therapeutic strategy [427].

In this context, the role of polyphenols, natural enzyme inhibitors, has garnered attention. A notable study investigated the effects of a grape pomace polyphenol nutraceutical. The findings were promising, showing a reduction in plasma TMAO levels and a decrease in biomarkers associated with oxidative stress in human subjects [428]. This suggests that dietary interventions, specifically targeting the TMAO metabolic pathway, could be a viable approach to mitigating the risk of MACE associated with elevated TMAO levels [315, 429].

In summary, the comprehensive analysis of TMAO and its association with MACE has evolved significantly over the years. From the initial discovery of its predictive value to understanding the intricate metabolic pathways and potential intervention strategies, the journey of TMAO research has been both enlightening and transformative. It underscores the complex interplay between diet, microbiota, metabolic processes, and cardiovascular health, and opens avenues for novel therapeutic and dietary strategies to address the MACE issue related to elevated TMAO levels.

5.4. Prognostic performance of microvascular resistance reserve in ST-elevation myocardial infarction patients

5.4.1. Overview of the primary findings

In this comprehensive analysis, we meticulously delineate the prognostic attributes of the MRR, a pioneering and innovative index designed to assess the microvascular vasodilator reserve capacity. Uniquely, MRR operates independently of epicardial CAD, and also accounts for the impact of potent vasodilators on aortic pressure. To our knowledge, this investigation represents the first of its kind to rigorously validate the utility of MRR in the context of STEMI, yielding several key findings:

1. MRR has emerged as a robust and independent predictor for MACE, clinical events, and notably, the recovery trajectory of LV systolic function. This highlights MRR's potential as a valuable tool in assessing patient prognosis post-STEMI.
2. The application of MRR provides a novel avenue for identifying patients with CMD. This is particularly significant as CMD is known to be a harbinger of heightened risk for the progressive deterioration of myocardial function, leading to adverse clinical outcomes. Thus, MRR can play a critical role in early detection and intervention strategies.
3. Our findings also revealed that MRR's prognostic accuracy surpasses that of FFR and is comparable to other established microvascular

indices such as CFR and IMR in predicting clinical outcomes. This comparative superiority and equivalence underline the versatility and efficacy of MRR as a prognostic tool in the realm of cardiac health.

In essence, this study not only establishes MRR as a groundbreaking index in cardiac diagnostics but also paves the way for its potential integration into standard clinical practice, especially for patients undergoing evaluation for STEMI. The insights gained from this research could significantly influence future strategies in the management and treatment of patients with heart conditions, particularly those affected by microvascular complications.

5.4.2. The rationale of microvascular resistance reserve in coronary microvascular dysfunction

The diagnostic process for CMD has historically been shrouded in complexity, with the establishment of consistent diagnostic criteria proving to be a formidable challenge. This complexity is primarily due to the inherent difficulties in visualizing the microcirculation and the varying cut-off values and incidences of CMD reported across different diagnostic techniques [152, 176, 430, 431]. The minuscule and intricate nature of the coronary microcirculation complicates direct observation, and the current CMD assessments, which are predominantly based on distal coronary pressure and/or flow measurements, struggle to accurately and confidently differentiate between the epicardial and microvascular components of the coronary circulation [432].

Moreover, the hemodynamic changes induced by pharmacologically-triggered maximal vasodilatation, a critical step in studying the vasodilatory capacity of the coronary circulation, present another layer of complexity. This process can simultaneously affect other physiological parameters that are essential for the accurate diagnosis of CMD [433]. Consequently, both the CFR and the IMR, though widely used, are encumbered with inherent limitations that challenge their efficacy.

In an effort to surmount these challenges, De Bruyne et al. made a significant advancement by developing a novel metric known as the MRR [175]. This innovative parameter, derived from the precise measurements of absolute coronary blood flow and intracoronary pressures, offers a more nuanced and comprehensive evaluation of the vasodilatory reserve of the coronary microcirculation. Uniquely, MRR can be adapted across various modalities, provided that accurate coronary flow and pressure measurements are available [175, 176]. Its design takes into account the presence of coexisting epicardial CAD and incorporates necessary adjustments. Addi-

tionally, MRR considers the hemodynamic alterations induced by the administration of potent vasodilators on systemic arterial pressures, thereby offering a more holistic assessment.

The prognostic performance of MRR, prior to our study, had been validated in patients with chronic coronary syndromes [434]. However, its application and effectiveness in the context of STEMI patients had not been investigated. Our study fills this significant gap in the research, exploring the utility and implications of MRR in a STEMI patient cohort. This investigation not only contributes to the evolving narrative of CMD diagnosis but also potentially revolutionizes the approach towards understanding and managing microvascular aspects in the context of acute coronary syndromes. By expanding the application of MRR to STEMI patients, our study paves the way for more accurate diagnostics and better-informed therapeutic strategies, ultimately enhancing patient care in this critical area of cardiovascular medicine.

5.4.3. Prognostic characteristics of microvascular resistance reserve

In this analysis, we have successfully illustrated that the MRR, when considered as a continuous variable, exhibits a significant independent association with MACE at a 12-month follow-up. Specifically, we observed a HR of 0.45, with a 95% CI ranging from 0.31 to 0.67, and a highly statistically significant *p*-value of less than 0.001. This association was particularly pronounced in cases of stroke, heart failure, and most notably in the poor recovery of LVEF. Our findings are pivotal as they not only confirm the prognostic relevance of MRR but also substantially widen its application from patients with chronic coronary syndromes to those experiencing ACS.

What sets MRR apart, and is particularly noteworthy, is its independence from the influence of epicardial stenoses and the hemodynamic alterations induced by vasodilator administration. This unique attribute of MRR empowers it to potentially become the primary parameter for assessing microcirculatory dysfunction across a wide range of clinical contexts [435]. The ability to evaluate microcirculatory health without the confounding effects of epicardial artery disease or the systemic impact of pharmacological agents is a significant advancement in cardiovascular diagnostics.

Despite these promising findings, it is important to acknowledge that while traditional indices have effectively established a relationship between microvascular dysfunction and critical clinical outcomes such as residual angina and cognitive dysfunction, these specific outcomes have not yet been evaluated using MRR as a metric [436, 437]. This gap in the research

highlights the need for further studies to assess the utility and effectiveness of MRR in predicting a broader spectrum of clinical outcomes.

Furthermore, the exploration of MRR as a diagnostic tool in the context of microvascular dysfunction opens new avenues for therapeutic interventions and patient management strategies. With its ability to provide a more detailed and nuanced understanding of microcirculatory health, MRR could guide more personalized and targeted treatment plans, particularly in patients with acute coronary syndromes. This could ultimately lead to improved patient outcomes, including enhanced recovery rates, reduced incidence of post-ACS complications, and overall better quality of life for these patients.

This particular analysis represents a significant leap forward in cardiovascular research, particularly in the context of microvascular health assessment. By demonstrating the independent predictive value of MRR for MACE and its potential applicability across various clinical scenarios, we are paving the way for a more comprehensive and accurate approach to diagnosing and managing cardiovascular diseases. However, the full potential of MRR can only be realized through further research and validation studies, particularly in areas that traditional indices have covered, but MRR has not yet been applied. As we continue to explore and understand the capabilities of MRR, it holds great promise in revolutionizing the approach to cardiovascular care, especially in the context of acute coronary syndromes.

5.4.4. Comparison of MRR with other physiology indices

In our study involving a cohort of patients who had undergone complete revascularization, we focused on those with high FFR values. The median FFR in our population was 0.92, with an IQR of 0.87 to 0.97. This high FFR is indicative of optimal epicardial coronary artery patency post-revascularization. Within this context, our research aimed to evaluate the prognostic value of MRR in comparison to other established physiological indices like FFR, IMR, and CFR.

Our findings revealed that MRR holds a prognostic value that not only surpasses that of FFR but also is on par with the predictive capabilities of IMR and CFR. This noteworthy result can be partially attributed to the high correlation observed between CFR and MRR, which was found to be significant ($r = 0.93$, $p < 0.001$). This strong correlation suggests a close relationship between the ability of the coronary microcirculation to dilate in response to stress (as measured by MRR) and the overall flow capacity of the coronary system (as indicated by CFR).

However, it is essential to consider the real-world implications of these findings. In everyday clinical practice, FFR values are often not optimized,

and the presence of epicardial stenoses can significantly influence CFR measurements. In such scenarios, CFR may not accurately reflect microvascular function due to the confounding effect of significant epicardial artery disease. Consequently, an additional adjustment is often required to calculate the correct IMR values, as suggested by previous studies [438, 439]. This adjustment is necessary to ensure that IMR accurately reflects microvascular resistance, independent of any epicardial coronary stenosis.

Given these practical considerations, MRR stands out as a potentially more suitable and practical tool for assessing microvascular function in clinical settings. Its ease of use and straightforward interpretation make it an attractive option for clinicians. The simplicity of obtaining MRR measurements, combined with its strong prognostic value, positions it as a potentially preferable choice in evaluating microcirculatory dysfunction, especially in scenarios where FFR is not optimized or epicardial stenosis affects CFR.

This analysis contributes significantly to the growing body of evidence supporting the use of MRR in clinical practice. By demonstrating its superior prognostic value and ease of use, MRR emerges as a promising tool that could potentially become the test of choice for evaluating coronary microcirculatory dysfunction. This could lead to more accurate diagnostics and better-informed therapeutic strategies, ultimately enhancing patient care and outcomes in the management of CAD.

5.5. Prevalence and prognostic impact of coronary microvascular dysfunction endotypes on 12-month clinical outcomes in ST-elevation myocardial infarction patients

5.5.1. Overview of the primary findings

This groundbreaking study represents the first of its kind to explore the prognostic performance of MRR and various CMD endotypes in patients three months post-revascularization for STEMI. The key findings of our research are both illuminating and significant:

We discovered that CMD was prevalent in more than a quarter of the patients in our study. Notably, the majority of these cases were attributed to the structural CMD endotype. This subgroup of patients demonstrated a discernible trend towards less favorable outcomes when compared to their counterparts with functional CMD. This observation not only provides new insights into the prevalence and implications of different CMD endotypes in post-STEMI patients but also underscores the potential impact of CMD characteristics on patient prognosis and recovery trajectories.

5.5.2. Endotypes of coronary microvascular dysfunction in ST-elevation myocardial infarction patients

In our detailed study, following complete revascularization, a significant subset of our patient cohort, specifically 26.7%, were identified as having CMD, as indicated by a MRR value of less than 3. This assessment was meticulously conducted during the physiological evaluations at the 3-month follow-up mark. Intriguingly, within this subset, a minor fraction (just under one-tenth) exhibited a normal IMR, aligning with what is classified as functional CMD. In stark contrast, a substantial majority, approximately nine-tenths of these patients, presented with an abnormal IMR, indicative of structural CMD.

When juxtaposed with previous studies, the incidence of CMD in our research appears marginally lower. Prior investigations, where coronary physiology was assessed immediately following primary PCI, reported higher prevalence rates [170]. However, it's imperative to consider the dynamic nature of microvascular function. Studies incorporating repeated coronary physiology assessments have consistently demonstrated a tendency for microvascular function to recuperate over time in many patients [353, 440]. Therefore, the timing of our assessments at 3 months post-procedure is a critical factor, suggesting that our findings do not necessarily contradict those of earlier studies but rather offer a different temporal perspective.

The prevalence of CMD endotypes observed in our study presents a striking contrast to findings in patients with non-obstructive CAD. For instance, in the extensive ILAS study focusing on patients with CCS, the ratio of functional to structural CMD was approximately 2:1, a significant deviation from the 1:9 ratio observed in our STEMI cohort [176]. Moreover, while the ILAS study reported similar outcomes for both CMD endotypes, our findings suggest a trend towards fewer clinical events in patients with the functional endotype. This discrepancy could be attributed to the relatively small number of patients in our study presenting with functional CMD.

Further adding to the complexity, if we were to apply the MRR threshold of less than 2.7 – established for the angina with nonobstructive coronary arteries (ANOCA) population – every patient categorized with CMD in our cohort would exhibit an abnormal IMR [441]. This underscores a fundamental difference in the underlying pathophysiology between chronic and acute coronary syndromes, highlighting the distinctive nature of CMD in different cardiac conditions.

Our study, therefore, opens new avenues for understanding the intricate dynamics of CMD post-STEMI. The variations in CMD endotypes, coupled with the temporal aspects of microvascular recovery, emphasize the nuanced

nature of CMD in the context of acute coronary syndromes. To build upon these initial observations and to gain deeper insights into the mechanisms at play, further extensive studies and targeted mechanistic research are crucial. Such investigations would not only enrich our comprehension of CMD in the STEMI population but also potentially guide the development of more effective diagnostic and therapeutic strategies tailored to the unique needs of this patient group.

5.6. Coronary microvascular dysfunction impact on functional left ventricular remodelling, diastolic dysfunction, and clinical outcomes

5.6.1. Overview of the primary findings

This analysis presents several key findings that significantly enhance our understanding of CMD following STEMI. We observed that CMD, as assessed three months post-STEMI, is intricately linked with a spectrum of adverse cardiac outcomes. These include compromised recovery of LV systolic function, the onset of LV diastolic dysfunction, unfavorable LV remodelling, and a heightened incidence of MACE within a 12-month follow-up period.

Further, our data revealed a compelling independent association between the IMR at the 3-month follow-up and more severe forms of LV diastolic dysfunction (specifically grade 2), as well as advanced stages of LV functional remodelling (group 3 and group 4). This relationship underscores the critical role of microvascular integrity in post-STEMI cardiac function and remodelling processes.

To our knowledge, this study constitutes the most extensive cohort to date that investigates the correlation between CMD and the long-term functional status of the LV, both systolic and diastolic. Our findings are significant: they indicate that in about one in four patients, coronary microcirculatory function remains impaired three months following STEMI. This impairment is not an isolated observation but is closely associated with the progressive decline of myocardial function and the emergence of adverse clinical outcomes.

This study, therefore, contributes crucial insights into the post-STEMI trajectory, highlighting the persistent nature of CMD and its substantial impact on cardiac function and patient prognosis. The associations we've identified are pivotal in understanding the comprehensive effects of CMD and underscore the importance of continued monitoring and management of microvascular health in STEMI patients to mitigate long-term cardiac risks.

5.6.2. Coronary microvascular dysfunction and left ventricular systolic function and remodelling

Our analysis has identified a significant association between CMD and suboptimal recovery of LV systolic function, as well as adverse functional LV remodelling. This finding is particularly noteworthy as it adds to a growing body of evidence underscoring the critical role that microvascular integrity plays in the overall health and function of the heart post-STEMI.

Extensive research has previously established that the degree of microvascular dysfunction is a key determinant in the subsequent alterations of left ventricular geometry and function. Patients presenting with impaired microvascular perfusion typically have larger myocardial infarcts, more extensive regions of necrosis, persistent long-term left ventricular wall motion abnormalities, and a noticeable decrease in ejection fraction, which can continue even after successful revascularization of the epicardial vessels [170]. These observations suggest a direct correlation between the health of the microvasculature and the overall functional capacity of the left ventricle.

Kitabata et al. further emphasized this connection through their study, which showed that patients with CMD experienced a marked increase in LV end-diastolic volume over an 8-month period, from 117 ± 21 to 147 ± 21 mL ($p = 0.006$). In contrast, those with normal microvascular function exhibited stable volumes (108 ± 21 mL to 112 ± 30 mL; $p = 0.620$) during the same timeframe [148]. This stark difference underscores the impact of CMD on cardiac remodelling, particularly in the context of left ventricular dilation.

Fearon et al., in their study involving 29 STEMI patients, highlighted that an IMR ≤ 32 post-primary PCI was associated with a significant improvement in left ventricular wall motion score index (from 25.4 ± 6.6 at baseline to 19.5 ± 3.6 at 3-month follow-up; $p = 0.0002$). Conversely, patients with an IMR >32 did not exhibit such improvements in wall motion score index or left ventricular systolic function [165]. This finding not only demonstrates the prognostic value of IMR but also its potential as a predictive marker for cardiac recovery post-STEMI.

Faustino et al. further expanded on these findings in a study of 49 STEMI patients, where CMD was associated with reduced global longitudinal strain and suboptimal recovery in various parameters including LVEF, wall motion score index, and diastolic function, as assessed by the E/e' ratio [442]. This comprehensive analysis provides a multifaceted view of the detrimental effects of CMD on cardiac function.

Moreover, MRI-based studies have validated the independent association of CMD status, as indicated by IMR, with poor myocardial viability and left ventricle functional recovery in AMI patients post-primary

PCI [443]. These imaging-based observations lend further credence to the notion that CMD significantly impairs cardiac recovery following a myocardial infarction.

In a study focused exclusively on post-STEMI patients, Carrick et al. observed that those with CMD had a noticeable increase in LV end-diastolic volume compared to non-CMD patients at a 6-month follow-up (72 *vs.* 60 mL; $p = 0.004$), along with a significant reduction in LVEF (58% *vs.* 64%; $p < 0.001$) [103]. These measurements are crucial as they directly relate to adverse LV remodelling, a condition that can lead to worsening heart failure and other long-term cardiac complications.

The Assessing MICRO-vascular resistances via IMR to predict outcome in STEMI patients with multivessel disease undergoing primary PCI (AMICRO) trial, a recent multicenter prospective study conducted in Italy, provided further insights. In this study, patients with anterior wall STEMI and high IMR exhibited adverse LV remodelling without any improvement in LVEF. However, the study did not report similar outcomes for non-anterior STEMI patients, which could be attributed to an underpowered sample size [444].

These extensive findings collectively highlight the significant role CMD plays in the progression and prognosis of heart diseases post-STEMI. They underscore the necessity for early detection and management of CMD to mitigate its adverse effects on LV function and remodelling, ultimately improving patient outcomes in the long term.

5.6.3. Coronary microvascular dysfunction and left ventricular diastolic function

The relationship between CMD and LV diastolic function has been an area of considerable interest and research. It is well-established that systemic diseases such as hypertension, hyperlipidemia, diabetes, and chronic pulmonary disease contribute to a chronic proinflammatory state, which in turn can induce CMD [445]. The subsequent pathological cascade from CMD leads to uncontrolled cardiomyocyte hypertrophy, cellular stiffening, and fibrosis, ultimately resulting in diastolic dysfunction. This process is especially relevant as these comorbidities are frequently observed in patients who suffer from diastolic dysfunction or heart failure with preserved ejection fraction (HFpEF).

A causal link between CMD and diastolic dysfunction is further supported by various studies. For instance, a study focusing on exercise training in aged rats found that such training could reverse both CMD and diastolic dysfunction, highlighting the potential for interventional strategies to mitigate

these conditions [446]. The Prevalence and Correlates of Coronary Microvascular Dysfunction in Heart Failure with Preserved Ejection Fraction trial (PROMIS-HFpEF) specifically examined patients with diastolic heart failure, excluding those with un-revascularized macrovascular CAD. This study reported a remarkably high prevalence of CMD (defined as a CFR < 2.5) in this patient population at 75% (95% CI: 69–81) [447].

Our current study builds upon these findings, reporting a significant association between CMD post-STEMI and the progression of diastolic dysfunction. We observed that patients with CMD initially presented with grade 1 diastolic dysfunction post- PCI. However, by the 12-month mark, a majority of these patients had progressed to grade 2 diastolic dysfunction. In contrast, almost all patients without CMD recovered to grade 1 diastolic dysfunction within the same timeframe. This association between CMD and the development of diastolic dysfunction is novel and has not been explicitly reported in prior studies.

Previous research, such as that by Faustino et al., has demonstrated the association between post-PCI IMR and the E/e' ratio [442]. Other studies have also noted the relationship between CMD and parameters of LV diastolic function but have not used the ASE guideline grading [335, 448]. Hong et al. reported a correlation between CMD and diastolic dysfunction in a cohort of 330 patients without LV systolic dysfunction (ejection fraction ≥ 50%) and significant epicardial coronary stenosis (fractional flow reserve > 0.80). Their findings also indicated that both cardiac diastolic dysfunction and CMD were associated with a higher risk of cardiovascular death or admission for heart failure [449].

Our study adds to this body of evidence by observing that diastolic dysfunction can develop over a relatively short period, suggesting rapid adverse and beneficial cardiomyocyte remodelling in patients with and without CMD, respectively. Furthermore, our findings show that while patients with CMD had higher rates of diabetes at baseline, the absence of grade 2 and grade 3 diastolic dysfunction post-PCI in these patients implies a predominant role of CMD in the development of diastolic dysfunction. This hypothesis is further substantiated by our multivariable binary logistic analysis (Table 4.6.8.1), which supports the critical role of CMD in the propagation of diastolic dysfunction.

In summary, our study not only reinforces the existing knowledge about the link between CMD and diastolic dysfunction but also provides novel insights into the progression of diastolic dysfunction post-STEMI. This underscores the importance of early detection and management of CMD to prevent or mitigate diastolic dysfunction and its associated complications. It also highlights the potential for targeted therapeutic interventions to address

CMD, thereby improving cardiac function and patient outcomes in the post-STEMI setting.

5.6.4. Association between coronary microvascular dysfunction and adverse left ventricualr systolic and diastolic dysfunction

The association between CMD and adverse LV systolic and diastolic dysfunction is a critical area of investigation in the realm of cardiovascular medicine. A notable limitation in previous studies on this subject has been the timing of microvascular function assessment, typically conducted either immediately post-PCI or before hospital discharge. However, the short-term resolution of CMD is not an uncommon phenomenon in patients who have suffered a STEMI, as evidenced by various MRI studies [450, 451]. This early resolution may mask the longer-term implications of CMD on cardiac function and remodelling.

Our study addresses this gap by evaluating CMD three months post-STEMI, thereby ensuring the exclusion of transient CMD cases from our analysis. This time frame is critical as it provides a more accurate reflection of persistent CMD and its impact on cardiac recovery and remodelling. Our findings indicate that the IMR measured at this later stage maintains a significant association with LV functional recovery, highlighting the enduring presence and pathophysiological impact of CMD in some patients.

Furthermore, our study stands apart from previous research by examining the association between CMD and LV function through the lens of comprehensive classifications of LV diastolic function and functional LV remodelling. We utilized the ASE's latest guidelines for the evaluation of diastolic function and Surenjav Chimed et al.'s classification of LV remodelling, methodologies that had not been employed in prior studies focusing on this topic [335, 347]. This approach allows for a more nuanced understanding of the relationship between CMD and various aspects of LV function and remodelling.

The progression of CMD post-STEMI largely depends on its underlying etiology, such as whether it involves persistent capillary destruction or transient phenomena like microembolization, vessel spasm, or edema [452]. A significant cause of CMD can be attributed to distal embolization of atherosclerotic debris or thrombotic material [453]. While such occurrences may be temporary, resolving quickly to prevent myocardial necrosis and adverse outcomes, they often persist, leading to sustained damage to the microvasculature [454].

These persistent changes, including reperfusion injury, intramyocardial hemorrhage, interstitial and myocardial cell edema or fibrosis, blistering of

the endothelial layer, and blockage of capillaries due to local inflammation, can have profound effects on myocardial health [455]. Animal studies have shown that irreversible injury from these processes can occur within 90 minutes of temporary coronary occlusion [18]. These alterations in the capillary bed lead to malperfusion of myocytes, resulting in cellular death and myocardial remodelling.

Earlier studies observed improvements in microvascular function soon after primary PCI. However, follow-up studies revealed that many patients continued to exhibit CMD, and this persistent CMD was also associated with LVEF recovery [440, 444]. Therefore, our findings suggest that persistent CMD post-STEMI is a likely contributor to myocardial necrosis and adverse LV remodelling.

In summary, our study adds significant depth to the understanding of CMD's role in post-STEMI cardiac health. By analyzing persistent CMD and its association with LV systolic and diastolic dysfunction using advanced classification systems and a more appropriate assessment timeframe, we provide valuable insights into the long-term impacts of CMD. This knowledge is essential for developing targeted interventions to mitigate the adverse effects of CMD on cardiac function and patient outcomes.

5.6.5. Association between coronary microvascular dysfunction and clinical outcomes

The association between CMD and clinical outcomes, particularly MACE, is a critical aspect of our study focusing on patients post- STEMI. In our patient cohort, we observed that CMD, as assessed three months after STEMI, was linked with a higher incidence of MACE. This observation is in line with the findings of Farissi et al., who also identified a correlation between microvascular function post-primary PCI and MACE [456]. However, it's noteworthy that the event rate in our study was markedly higher than that reported by Farissi et al.

One of the key distinctions between our study and that of Farissi et al. lies in the patient demographics. Our study focused on STEMI patients with multi-vessel CAD, a group typically characterized by more comorbidities and a lower LVEF compared to the cohort studied by Farissi et al. This difference in patient characteristics could partly explain the higher MACE rate observed in our study. Indeed, our findings show a 20% MACE rate at one year, a figure that aligns closely with the results of the Complete Revascularization with Multivessel PCI for Myocardial Infarction (COMPLETE) trial [457]. This similarity underscores the consistency of our findings with other major studies in the field.

Another factor potentially contributing to the high event rate and the observed poor LVEF at follow-up could be attributed to the late presentation of our patients. The pain-to-medical contact time in our cohort averaged 314 minutes, a significant delay, despite the commendable door-to-balloon time of 40 minutes [458]. This delay likely resulted in substantial myocardial loss before the patients received treatment, which can have profound implications on the overall recovery and prognosis.

The extended pain-to-medical contact time might be reflective of several factors, including patient awareness, access to medical care, and variations in the presentation of STEMI symptoms. These aspects emphasize the importance of public health initiatives focusing on early recognition and prompt medical attention for STEMI symptoms.

Furthermore, the impact of CMD on clinical outcomes post-STEMI, as highlighted in our study, underscores the necessity of considering microvascular health in the overall management of STEMI patients. The association between CMD and increased MACE rates, coupled with the fact that CMD persists in some patients despite timely revascularization, underscores the need for a more comprehensive approach to STEMI treatment. This approach should not only focus on prompt revascularization but also on the assessment and management of microvascular function.

In conclusion, our study contributes significantly to the understanding of the relationship between CMD and clinical outcomes in STEMI patients, particularly those with multi-vessel CAD. The insights gained from this study underscore the complexity of treating STEMI and the importance of timely intervention, comprehensive patient assessment, and the consideration of microvascular health in the prognosis and long-term management of these patients.

5.7. Strengths and limitations

The limitations of this PhD thesis, spanning across multiple studies on the impact of PCI strategies on CMD during STEMI, the application of machine learning to predict CMD, the exploration of TMAO as a biomarker, the validation of MRR for assessing CMD endotypes, and the investigation into CMD's role in future FLVR and diastolic dysfunction, reveal several common and study-specific challenges that collectively influence the interpretation and generalizability of the findings. These limitations are outlined below to provide context for the thesis's contributions and areas for future research.

1. *Observational nature and study design.* The observational, non-randomized design of the studies, particularly those examining PCI

strategies and TMAO levels, limits the ability to infer causality from the associations observed. Despite the comprehensive data collected, these design choices may introduce biases that could affect the results.

2. *Sample size and single-center settings.* Although some studies within this thesis are among the largest of their kind, particularly in invasive CMD testing in STEMI patients, the relatively small sample sizes and single-center nature of the research limit the generalizability of the findings. This constraint is particularly relevant when considering the diversity of STEMI presentations and treatments across different populations and healthcare settings.
3. *Assessment timing.* The timing of CMD assessment at 3 months post-STEMI, while designed to avoid the acute phase's transient effects, introduces a limitation in understanding the immediate impact of PCI strategies and the evolution of CMD. This choice also precludes a direct assessment of CMD's presence prior to STEMI or its immediate aftermath, potentially overlooking factors influencing CMD's development and persistence.
4. *Generalizability to broader populations.* The inclusion criteria for several studies, particularly those focusing on patients with multi-vessel CAD requiring staged PCI, may not fully represent the wider STEMI patient population. This limitation is important when considering the applicability of findings to patients with single-vessel CAD or those with different clinical profiles.
5. *Methodological considerations.* The methodologies employed, including the use of bolus thermodilution for coronary flow measurements and the administration of intracoronary glycoprotein IIb/IIIa inhibitors, may influence the accuracy of CMD assessment and the interpretation of PCI strategies' effectiveness. Furthermore, the lack of intravascular imaging during primary PCI and reliance on specific flow and resistance measurements could affect the robustness of MRR validation and the identification of CMD endotypes.
6. *Dietary and microbiota factors.* The absence of detailed dietary data and analysis of gut microbiota composition, particularly in the study on TMAO, limits the understanding of these factors' roles in CMD and cardiovascular outcomes post-STEMI. These elements are crucial for interpreting TMAO levels and their impact on CMD pathophysiology and patient outcomes.
7. *Long-term outcomes and emerging biomarkers.* The 12-month follow-up period, while providing valuable insights, may not capture

the full spectrum of CMD's long-term effects on cardiovascular health and outcomes. Additionally, the focus on specific biomarkers, like TMAO, without exploring a broader range of emerging markers, may not fully elucidate CMD's multifaceted nature.

These limitations underscore the need for future research to address the identified gaps, including multi-center studies with larger, more diverse populations, randomized controlled trials to establish causality, longer follow-up periods to assess chronic outcomes, and comprehensive analyses incorporating dietary, microbiota, and a wider array of biomarkers. Such studies will be essential for validating and expanding upon the findings of this PhD thesis, thereby contributing to improved care and outcomes for STEMI patients.

CONCLUSION

In conclusion, this doctoral thesis represents a multifaceted exploration into the realms of CMD and its intricate associations with clinical outcomes in the context of STEMI. Spanning six distinct yet interrelated studies, this body of work provides a comprehensive understanding of CMD, its patho-physiology, prognostic implications, and potential therapeutic interventions.

1. The first segment of the thesis critically examines various interventional strategies in the management of STEMI. It conclusively demonstrates that direct stenting, aspiration thrombectomy, and the intracoronary administration of glycoprotein IIb/IIIa inhibitors each significantly reduce the prevalence of CMD by a factor of five. Furthermore, direct stenting markedly decreases the incidence of MACE at one year compared to traditional balloon pre-dilatation followed by stenting, reducing the incidence of MACE by approximately 50%, from 26.79% to 14.29%. This study provides crucial insights into optimizing interventional strategies to enhance clinical outcomes in STEMI patients.
2. The TAMIR machine algorithm, utilizing a random forest model, demonstrates promising results in predicting CMD. Key biomarkers such as TMAO, thrombocyte aggregation response to epinephrine, and BNP show high relative variable importance (100%, 50.59%, 41.15%). The model achieved an accuracy of 0.92 (0.81–0.98) on the validation set, with a sensitivity of 0.91, specificity of 1.00, and precision of 1.00. These metrics highlight the algorithm's robust performance and potential clinical utility.
3. The third part of this PhD thesis focuses on TMAO, identified through machine learning as the most critical biomarker for diagnosing CMD in STEMI patients. The study establishes a new threshold value of 3.91 μM for TMAO at three months. High TMAO levels significantly predict CMD with an AUC of 0.8 and are associated with a fourfold increase in MACE (41.4% vs. 10.7%). Additionally, patients with TMAO levels ≥3.91 μM at three months show a decline in LVEF that is 1.6 times greater compared to those with lower TMAO levels. This finding underscores TMAO's utility as a powerful single predictor of CMD, LV remodeling and adverse cardiovascular outcomes.

4. The fourth research component presents MRR as a superior prognostic indicator for STEMI patients compared to FFR and comparable to CFR and IMR. Based on the ROC curves, MRR achieved an AUC of 0.701, outperforming FFR, which had an AUC of 0.576. The prognostic performance of MRR is similar to CFR (AUC = 0.719) and IMR (AUC = 0.736), highlighting its reliability in predicting MACE at 12-month follow-up.
5. The fifth study confirms that CMD is present in over a quarter of patients, predominantly exhibiting a structural endotype. This subset of patients tends to experience poorer clinical outcomes than those with functional CMD, underscoring the need for differentiated therapeutic approaches based on CMD endotypes.
6. The final part concludes that the presence of CMD at three months post-STEMI is a significant predictor of adverse outcomes. Diastolic dysfunction was significantly worse in CMD patients, with 73.08% progressing to grade 2 diastolic dysfunction versus only 1.32% in non-CMD patients, reflecting a more than 55-fold increase. CMD was also associated with a substantial increase in adverse LV remodeling, with 37.74% of CMD patients exhibiting severe remodeling compared to 2.65% in non-CMD patients, representing a nearly 14-fold increase. Furthermore, patients with CMD had a significantly higher incidence of MACE at one year, with rates of 50.88% compared to 9.80% in patients without CMD, indicating more than a fivefold increase. This part advocates for further expansive research, suggesting the potential benefits of early CMD identification and intervention to mitigate these adverse outcomes.

Collectively, these studies paint a comprehensive picture of CMD in the context of STEMI, providing novel insights into its diagnosis, prognosis, and potential therapeutic targets. The findings underscore the necessity of continued research in this field, particularly regarding the implementation of these insights into clinical practice to improve patient outcomes in STEMI and beyond.

PRACTICAL RECOMMENDATIONS

This PhD thesis presents comprehensive findings on the impact of PCI strategies on CMD during STEMI, the effectiveness of predictive biomarkers and machine learning for CMD detection, the importance of TMAO as a key biomarker, and the groundbreaking validation and application of MRR in STEMI patients, then utilizing it to identify the predominant CMD endotype. Additionally, it elucidates CMD's role in the progression of FLVR and diastolic dysfunction and the potential of it being a prognosticator for these outcomes. Based on these insights, the following recommendations are designed for cardiologists, interventionalists, and healthcare professionals.

1. Adoption of direct stenting techniques.

Given the evidence supporting the benefits of direct stenting in reducing the incidence of CMD and improving clinical outcomes, it is recommended to prioritize direct stenting over balloon pre-dilatation in STEMI cases whenever clinically feasible. This approach minimizes vascular trauma and distal embolization, thus preserving microvascular integrity.

2. Reassessment of pre-dilatation necessity.

Clinicians should critically reassess the routine application of balloon pre-dilatation in primary PCI procedures. Considering the potential adverse impacts on coronary microvasculature, selective use based on lesion characteristics and patient-specific factors is advisable.

3. Implementation of aspiration thrombectomy.

Aspiration thrombectomy should be considered in STEMI cases with a high thrombus burden, recognizing its potential to reduce CMD risk on the long run. This recommendation is made with an acknowledgment of current guidelines and the necessity for ongoing research to refine patient selection criteria.

4. Use of intracoronary glycoprotein IIb/IIIa inhibitors.

The targeted use of intracoronary glycoprotein IIb/IIIa inhibitors during PCI is recommended to mitigate CMD. This strategy should be tailored based on a thorough evaluation of patient-specific risk profiles and procedural characteristics.

5. **Monitoring and management of TMAO levels.**

It is recommended to monitor TMAO levels at the 3-month follow-up as a predictive biomarker for CMD and adverse outcomes post-STEMI, utilizing the established cutoff value of 3.91 μM. Strategies such as dietary modifications and targeted pharmacological treatments should be considered for managing elevated TMAO levels to improve patient outcomes.

6. **Utilization of machine learning TAMIR prediction model for CMD.**

Incorporating the newly validated TMAIR machine learning prediction model into routine clinical practice is recommended for the early identification of CMD. Leveraging this advanced predictive tool allows for the tailoring of therapeutic strategies to individual patient profiles, thereby optimizing treatment outcomes.

7. **Routine assessment of MRR**

The use of MRR should be routine in clinical assessments post-STEMI for a more accurate prognostic evaluation. This practice can inform therapeutic decisions beyond epicardial coronary interventions, focusing on microvascular health.

8. **Tailoring therapies for structural CMD post-STEMI**

For patients with CMD post-STEMI, it is recommended to address CMD with therapies specifically tailored for the structural endotype. This approach is informed by the study's finding that structural CMD is the predominant endotype in STEMI patients, highlighting the need for targeted treatment strategies to optimize patient care and outcomes.

9. **Early assessment and preventive strategies for heart failure post-STEMI**

Given the PhD thesis findings that CMD can predict future FLVR and diastolic dysfunction, which are common complications after STEMI, it's recommended to perform early CMD assessments. Identifying patients at risk allows for the initiation of preventive therapies for heart failure, potentially mitigating these adverse outcomes.

SANTRAUKA

1. ĮVADAS

Širdies ir kraujagyslių ligos (ŠKL) yra pagrindinė mirštamumo priežastis pasaulyje [1]. Vien 2021 m. nuo širdies ir kraujagyslių sistemos ligų mirė 20,5 mln. žmonių, o tai sudaro maždaug trečdalį visų mirčių pasaulyje. Europos žemyne kas antras žmogus miršta nuo ŠKL [2]. Nors išeminės širdies ligos gydymas pagerėjo, tačiau miokardo infarktas, kai S–T segmentas pakilęs (MIkSTP; angl. *ST-Elevation Myocardial Infarction, santrump. STEMI*), tebėra pagrindinė šių mirčių priežastis [3]. Ankstyvoji reperfuzija, atliekant perodinę transluminalinę vainikinių arterijų angioplastiką (PTVAA; angl. *Percutaneous Coronary Intervention, santrump. PCI*), yra šiuolaikinio MIkSTP gydymo standartas [4]. Nustatytas klinikinis PTVAA veiksmingumas – 95 proc. atkuriamas epikardo kraujagyslių praeinamumas. Tačiau iki 50 proc. pacientų gali nepavykti atkurti vainikinių kraujagyslių mikrocirkuliacijos ir visiškos miokardo perfuzijos [5]. Nepakankama miokardo perfuzija gali sukelti išeminės širdies ligos grandinę: diastolinę disfunkciją, sistolinę disfunkciją ir nepalankią kairiojo skilvelio remodeliaciją nepalankų kairiojo skilvelio remodeliavimąsi. Atlikus detalius tyrimus, paaiškėjo, kad iki 15,5 proc. MIkSTP sergančių pacientų po sėkmingos epikardinių arterijų reperfuzijos ir toliau jaučia angininius simptomus, kurie gali būti susiję su vainikinių mikrokraujagyslių disfunkcija (VMD; angl. *Coronary Microvascular Dysfunction, santrump. CMD*), kuri susijusi su išliekančiais angininiais simptomais, sunkiu kairiojo skilvelio funkcijos atsikūrimu ir nepalankiomis klinikinėmis baigtimis [6].

VMD apima širdies mikrocirkuliacijos anatominių ir funkcinių pakitimų spektrą, dėl kurių sutrinka miokardo aprūpinimas krauju, nulemiantis miokardo išemiją [7]. Pacientams, sergantiems MIkSTP, VMD gali sukelti keletas patofiziologinių mechanizmų, įskaitant mikrovaskulinę okliuziją, intramiokardinį kraujavimą ir uždegimą [8].

Įprastinės angiografijos metu vainikinės mikrokraujagyslės nėra matomos, todėl VMD diagnozuoti reikia invazinių fiziologinių tyrimų arba pažangių vaizdinimo metodų, kurie gali būti brangūs, kelti komplikacijų riziką, o tai nulemia nevisiškai efektyvią diagnostiką [9, 10].

VMD diagnostikai plačiausiai taikomos, geriausiai atkuriamos ir paprasčiausios diagnostikos strategijos yra vainikinių arterijų tėkmės rezervo (angl. *Coronary Flow Reserve*; CFR) ir mikrocirkuliacijos pasipriešinimo indekso (angl. *Index of Microvascular Resistance*; IMR). įvertinimas naudojant slėgio ir temperatūros daviklį [11].

2. DARBO TIKSLAS

Šios daktaro disertacijos tikslas yra ištirti pacientų, kurie sirgo miokardo infarktu, kai S–T segmentas pakilęs, VMD patogenezę, diagnostiką ir klinikines baigtis.

3. DAKTARO DISERTACIJOS UŽDAVINIAI

1. Įvertinti širdies didžiųjų komplikacijų (ŠDK; angl. *Major Adverse Cardiac Events, santrump. MACE*) ir VMD atsiradimo sąsajas su intervencinio gydymo technikomis sergant MIkSTP.
2. Nustatyti biologinius žymenis, prognozuojančius VMD pacientams, sergantiems MIkSTP, naudojant mašininio mokymosi dirbtinio intelekto algoritmą.
3. Ištirti biologinį žymenį, kuris pagal mašininio mokymosi dirbtinio intelekto algoritmą būtų laikomas tinkamiausiu VMD prognozuoti, siekiant nustatyti ribinę jo vertę, palyginti su kitais numanomais biologiniais žymenimis ir išanalizuoti jo ryšį su būklės baigtimis persirgus MIkSTP.
4. Įvertinti ir patvirtinti naujo VA fiziologinio parametro – pacientų mikrocirkuliacijos pasipriešinimo rezervą (MPR, angl. *Microvascular Resistance Reserve, santrump. MRR*) – prognozinę vertę ir atlikti palyginamąją analizę vertinant kitus nustatytus VA fiziologinius parametrus.
5. Ištirti skirtingų VMD endotipų paplitimą ir klinikinę jų reikšmę, siekiant pritaikyti individualizuotojo gydymo metodus MIkSTP sergantiems pacientams.
6. Ištirti ilgalaikį VMD poveikį kairiojo skilvelio funkcijai persirgus MIkSTP, sutelkti dėmesį į funkcinį kairiojo skilvelio remodeliavimąsi (FKSR, angl. *Functional Left Ventricular Remodelling, santrump. FLVR*) ir diastolinės funkcijos sutrikimą.

4. MOKSLINIS DISERTACIJOS NAUJUMAS

Disertaciniame darbe pateikiamas novatoriškas žvilgsnis į esamas paradigmas. Šis biomedicininis tyrimas gerina bendrąsias žinias apie širdies ir kraujagyslių ligas, patobulina VMD diagnostiką. Šie rezultatai galėtų daryti įtaką naujų klinikinių gairių sukūrimui. Vienas iš pagrindinių darbo akcentų yra perodinės transluminalinės vainikinių arterijų angioplastikos (PTVAA; angl. *Percutaneous Coronary Intervention*) technikos, skirtos pacientams, sergantiems MIkSTP, gydyti, detalus įvertinimas. Sistemingai vertindamas efektyviausias PTVAA technikas, šis tyrimas sukuria lyginamųjų intervencinių tyrimų galimybę – tai gali turėti įtakos būsimai efektyvesnei širdies ir kraujagyslių ligų priežiūros praktikai.

Kitas reikšmingas naujumas – dirbtinio intelekto algoritmo integravimas į mašininį mokymąsi diagnozuojant VMD – svarbus širdies ir kraujagyslių ligų diagnostikos žingsnis. Šis proveržis pagrįstas dirbtinio intelekto galia ir pažangia duomenų analize, skirta nuskaityti biologinių žymenų informaciją, naudojamą VMD nustatyti. Metodas yra inovatyvus, sujungiantis mašininį mokymąsi su širdies ir kraujagyslių diagnostikos procesais – iki šiol neištirtu būdu. Disertacija išsiskiria išsamiais biologinių žymenų tyrimais, kurie anksčiau minėtais mašininio mokymosi dirbtinio intelekto algoritmų metodais buvo nustatyti kaip itin svarbūs VMD pasireiškimui. Tiriami su VMD susiję medžiagų apykaitos rodikliai, galintys iš esmės pakeisti supratimą apie VMD mechanizmus bei diagnostikos metodus, reikšmingai prisidedančius prie širdies ir kraujagyslių ligų gydymo.

Šiame tyrime pateikiamas MPR rodiklis, kuris kaip prognozinis žymuo gali būti ypač svarbus pacientams, sergantiems MIkSTP. Šis tyrimas patvirtina MPR naudingumą ne tik lėtinio vainikinių arterijų sindromo (LVAS; angl. *chronic coronary syndrome*) atveju, taip pat jis yra patikimas prognozės rodiklis pacientams, sergantiems MIkSTP. Šie duomenys tik pabrėžia disertacijos vaidmenį plečiant mikrocirkuliacijos tyrimo galimybes bei jos poveikį širdies ir kraujagyslių ligoms.

Taip pat buvo tirti VMD endotipai pacientams, sergantiems MIkSTP. Tai, mano duomenimis, yra vienas pirmųjų kartų, bandant suklasifikuoti ir suprasti VMD pasireiškimo įvairovę šioje pacientų grupėje.

VMD yra svarbus veiksnys, darantis įtaką širdies atsigavimui persirgus MIkSTP, nes žinoma, jog vieniems pacientams KS atsigauna daug ilgiau nei kitiems. Nustatytos VMD sąsajos su FKSR ir diastolinės funkcijos sutrikimu persirgus MIkSTP – reikšmingas indėlis į ateities širdies ir kraujagyslių ligų prognozinius tyrimus.

Būtent dėl šių naujovių, jungiančių inovatyvias metodikas, kritinę analizę bei atradimus, ši disertacija gali pagerinti VMD diagnostiką, gydymą, sumažinti MI komplikacijas bei blogas baigtis.

5. TYRIMO METODIKA

Tai perspektyvusis, stebimasis tyrimas, atliktas Lietuvos sveikatos mokslų universiteto ligoninės Kauno klinikose 2021 m. sausio–2023 m. rugpjūčio mėn.

5.1. Įtraukimo ir neįtraukimo kriterijai

Į tyrimą įtraukti 40 metų ir vyresni suaugusieji, kuriems diagnozuotas MIkSTP. Įtraukimo ir neįtraukimo kriterijai pavaizduoti 1 pav. Į tyrimą buvo įtraukti tik tie tiriamieji, kuriems, praėjus trims mėnesiams nuo pirminės

procedūros, buvo numatyta kitų VA hemodinamiškai reikšmingų susiaurėjimų PTVAA.

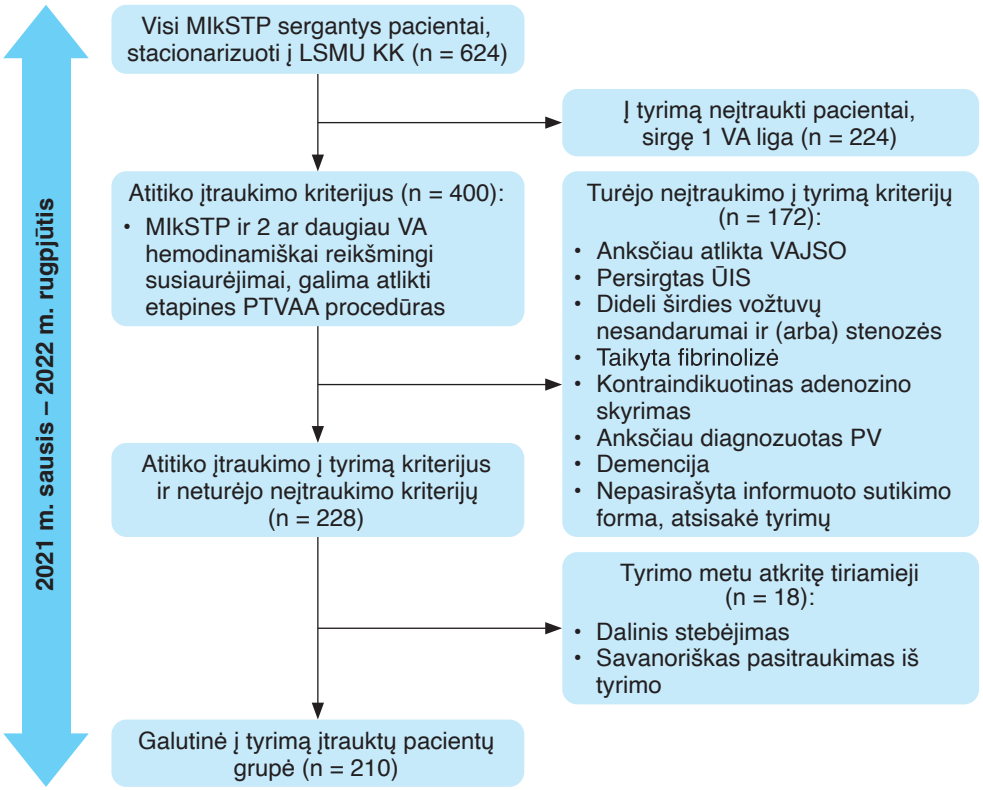

1 pav. *Pacientų priėmimo ir registracijos schema*

LSMU KK – Lietuvos sveikatos mokslų universiteto Kardiologijos klinika, MIkSTP – miokardo infarktas, kai S–T segmentas pakilęs; PTVAA – perodinė transluminalinė vainikinių arterijų angioplastika; PV – prieširdžių virpėjimas; ŪIS – ūminės išemijos sindromas; VA – vainikinė arterija; VAJSO – vainikinių arterijų jungčių suformavimo operacija.

5.2. Pacientų priėmimo ir užregistravimo schema

Į Lietuvos sveikatos mokslų universiteto ligoninę Kauno klinikas (toliau – Kauno klinikos) 2021 m. sausio–2022 m. rugpjūčio mėn. buvo stacionarizuoti 624 pacientai, sirgę MIkSTP, kuriems buvo atlikta pirminė PTVAA. Iš jų 400-ams pacientų buvo nustatyta ne tik priežastinės VA pažeidimas, bet ir kitų 1 ar 2 VA hemodinamiškai reikšmingi susiaurėjimai, kuriems buvo reikalinga pakartotinė PTVAA. Pritaikius neįtraukimo kriterijus, 172 pacientai buvo pašalinti iš tyrimo, todėl pirminės analizės metu liko 228 pacientai. Vėliau dėl įvairių priežasčių iš tyrimo buvo pašalinta dar 18 pacientų. Galiausiai tyrime liko 210 pacientų grupė, kaip ir pavaizduota 1 pav.

5.3. Nuoseklus tiriamųjų stebėjimas

MI metu visiems pacientams buvo atlikta PTVAA – tiesioginis stentavimas arba balioninė dilatacija, po kurios atliktas stentavimas – gydytojai rinkosi atitinkamą metodą atsižvelgdami į individualius klinikinius paciento poreikius. Echokardiografija ir kraujo tyrimai buvo atlikti per pirmąsias 24 valandas po PTVAA. Trijų mėnesių stebėjimo metu buvo atliekami papildomi VMD tyrimai. Tiriamųjų registracija baigta 2022 m. rugpjūčio mėn., bet stebėjimas pratęstas iki 2023 m. rugpjūčio mėn. Po 12 mėnesių kartota echokardiografija, stebėtos didžiosios širdies ir smegenų komplikacijos. Tiriamųjų stebėjimo schema pavaizduota 2 pav.

5.4. Intervencinės procedūros

Intervenciniai kardiologai, remdamiesi klinikiniu vertinimu ir konkretaus atvejo ypatybėmis, galėjo pasirinkti taikyti atitinkamą gydymo metodą: balioninę dilataciją, po kurios atliekamas stentavimas, arba tiesioginį stentavimą, kai stentuojama iš karto, neatliekant plėtimo balionu.

Aspiracinio kateterio naudojimas (Thrombuster II, Kaneka Inc., Osaka, Japonija) ir intrakoronarinis glikoproteino IIb / IIIa inhibitoriaus eptifibatido (*Integrilin, Millennium Pharmaceuticals*) skyrimas buvo parenkamas gydančio gydytojo nuožiūra. Eptifibatidas dažniausiai buvo naudojamas, kai po revaskuliarizacijos nebuvo pasiektas trombolizės, sergant miokardo infarktu (TIMI), srauto balas 3, o jo skyrimas buvo atidžiai apsvarstytas pacientams, turintiems galimų kontraindikacijų.

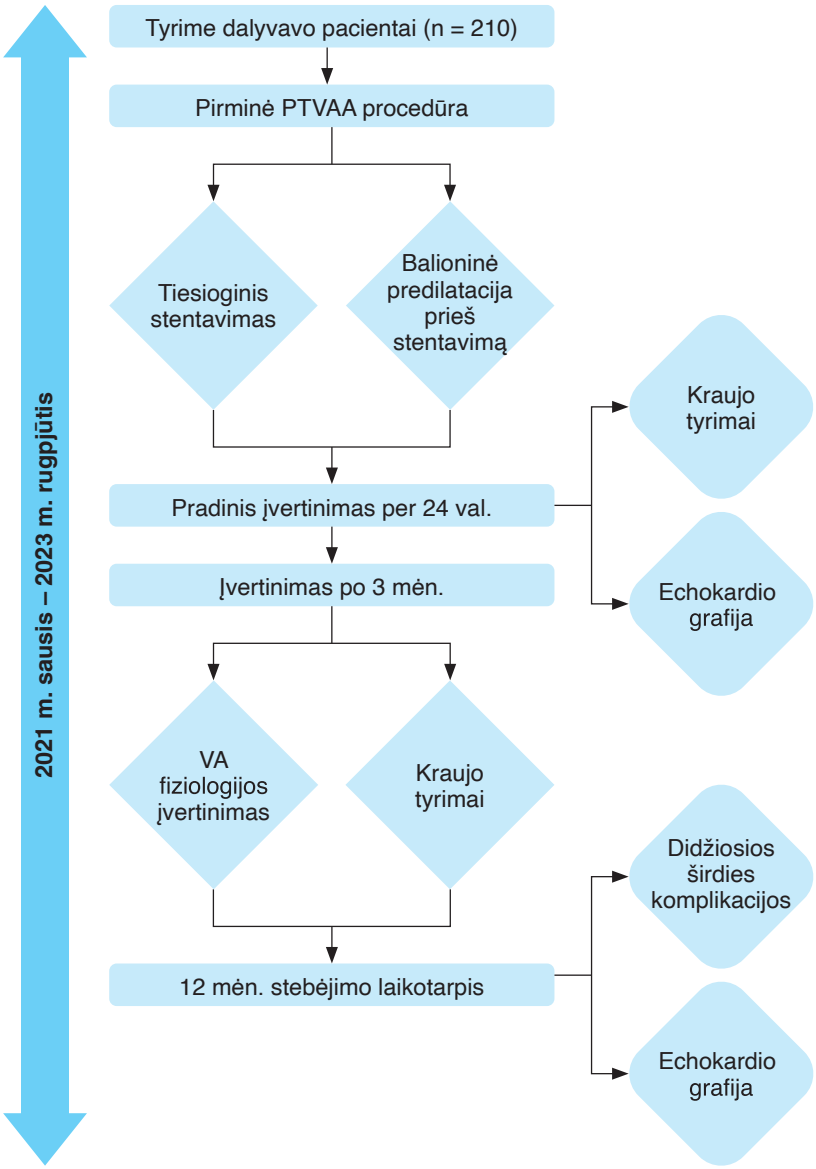

2 pav. *Nuoseklus tyrimo dalyvių stebėsenos protokolas*

PTVAA – perodinė transluminalinė vainikinių arterijų angioplastika; VA – vainikinė arterija.

5.5. Echokardiografijos vertinimo protokolas

Echokardiografiją atliko patyręs kardiologas, kuris neturėjo galimybės pažiūrėti konkrečių tyrimo duomenų – taip užtikrintas nešališkas vertinimas. Pirminė echokardiografija buvo atlikta per pirmąsias ūminio MIkSTP 24 valandas ir po 1 metų.

Echokardiografijos metu buvo vertinami šie rodikliai:

1. Kairiojo skilvelio išstūmio frakcija (KSIF): KSIF buvo tiksliai pamatuota taikant Simpsono diskų sumavimo metodą, laikantis Europos širdies ir kraujagyslių vaizdinių tyrimų asociacijos (angl. *European Association of Cardiovascular Imaging*) ir Amerikos echokardiografijos draugijos (angl. *American Society of Echocardiography*) standartų (3 pav.), naudojant pritaikytą formulę:

$$\text{KS IF} = [(\text{KS GDT} - \text{KS GST})) \,/\, \text{KS GDT}] \times 100 \text{ proc.}$$

KS IF – kairiojo skilvelio išstūmio frakcija; KS GDT – kairiojo skilvelio galinis diastolinis tūris; KS GST – kairiojo skilvelio galinis sistolinis tūris.

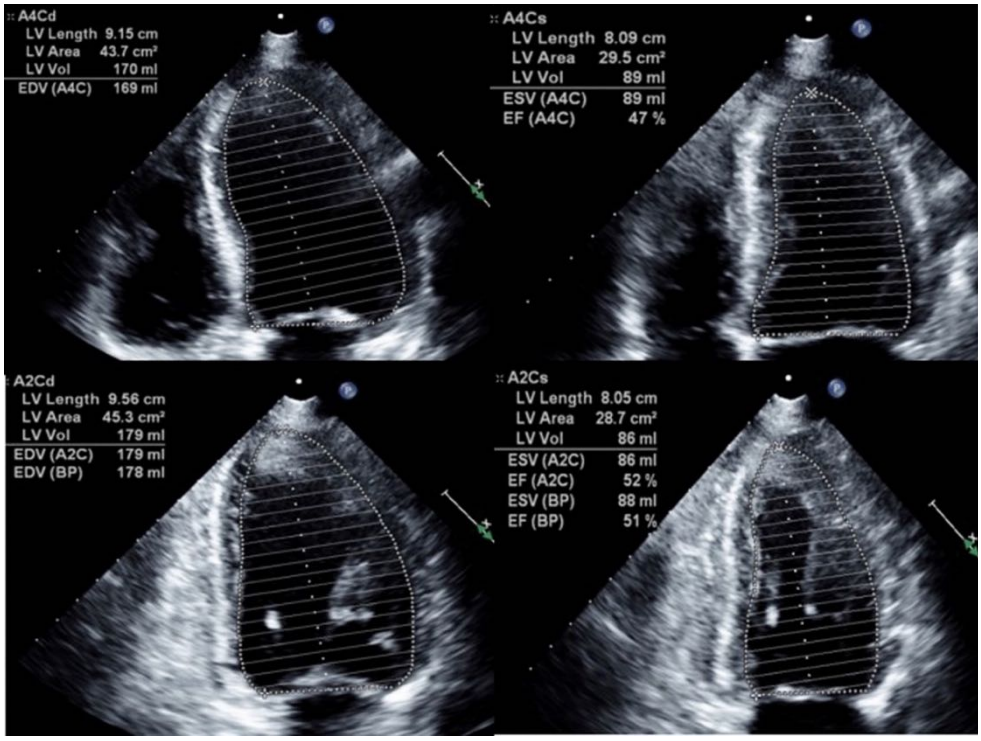

3 pav. *Kairiojo skilvelio išstūmio frakcijos įvertinimo vizualizavimas taikant Simpsono diskų sumavimo metodą*

Kairiojo skilvelio išstūmio frakcijos vertinimas taikant Simpsono diskų sumavimo metodą. Viršutinės nuotraukos rodo 4 kamerų vaizdą, apatinėse – 2 kamerų vaizdas, diastolė rodoma kairėje, o sistolė – dešinėje.

2. Kairiojo prieširdžio (KP) tūrio įvertinimas: kairiojo prieširdžio tūriui įvertinti skilvelio sistolės pabaigoje buvo taikomas modifikuotas Simpsono diskų sumavimo metodas, naudojant viršūninius 4 kamerų ir 2 kamerų vaizdus, siekiant nustatyti maksimalų KP dydį (4 pav.). Apskaičiavimams naudota formulė:

$$\text{Tūris} = 8 \times (\text{Plotis 1} \times \text{Plotis 2})/(3\pi \times \text{Ilgis})$$

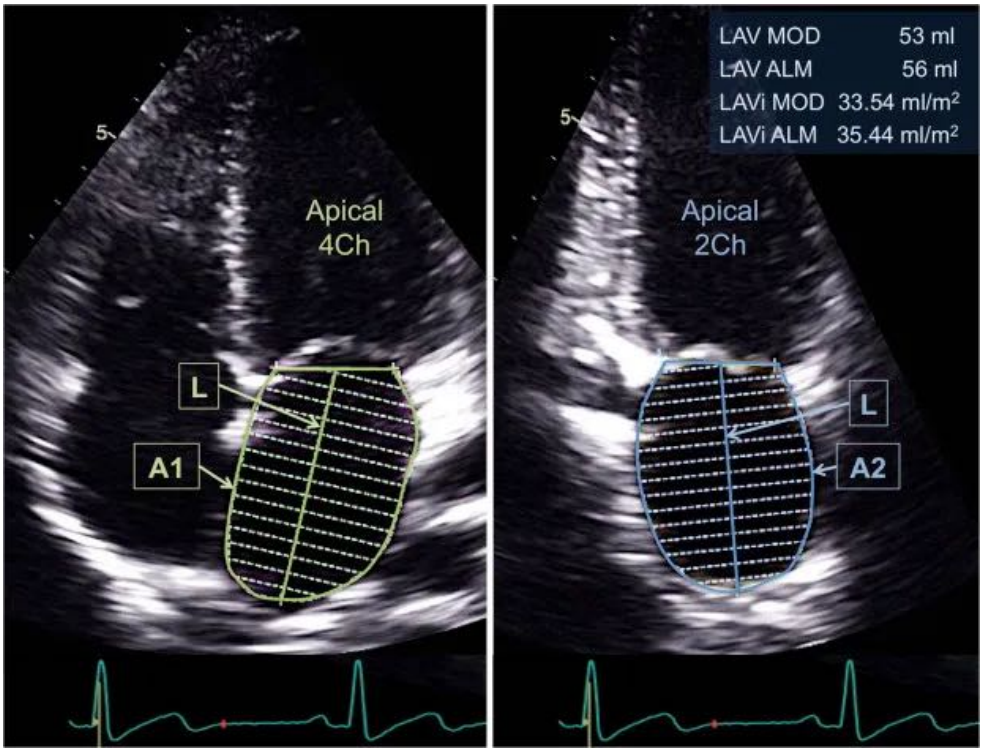

4 pav. *Kairiojo prieširdžio tūrio įvertinimo metodika naudojant modifikuotą Simpsono diskų sumavimo metodą*

Kairiojo prieširdžio tūrio apskaičiavimas taikant modifikuotą Simpsono diskų sumavimo metodą. Kairėje pusėje pavaizduotas 4 kamerų vaizdas, o dešinėje matomas 2 kamerų vaizdas.

3. Diastolinės funkcijos analizė: laikantis 2016 m. Amerikos echokardiografijos draugijos gairių, diastolinė funkcija buvo analizuojama naudojant įvairius parametrus, įskaitant E ir A bangas (5 pav.) ir audinių įvertinimą dopleriu, kuriuo nustatomas žiedo ankstyvasis diastolinis greitis (e') (6 pav.), taip pat pastoviosios bangos doplerio vaizdą, kuriuo nustatomas triburio vožtuvo regurgitacijos maksimalus greitis (TRpV) (7 pav.).

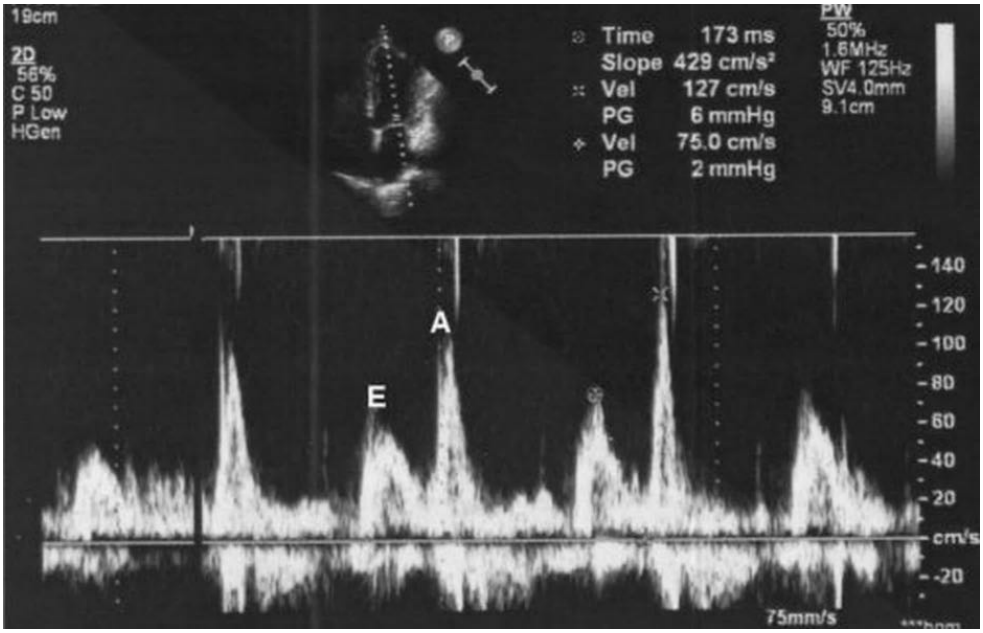

5 pav. *Dviburio vožtuvo žiedo ankstyvojo* ***(E)*** *ir vėlyvojo* ***(A)*** *bangų greičių nustatymo metodikos demonstravimas naudojant impulsinio doplerio metodą*

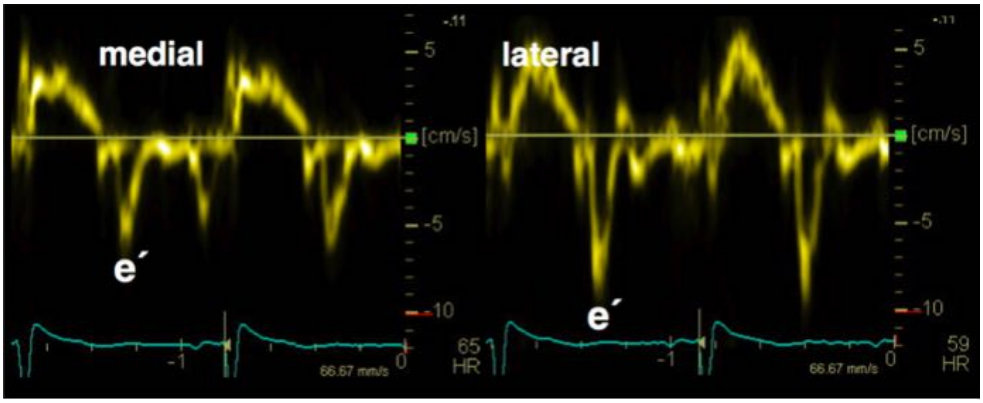

6 pav. *Dviburio žiedo ankstyvojo diastolinio greičio (e') vidurkio nustatymo metodikos demonstravimas naudojant impulsinį audinių doplerio metodą*

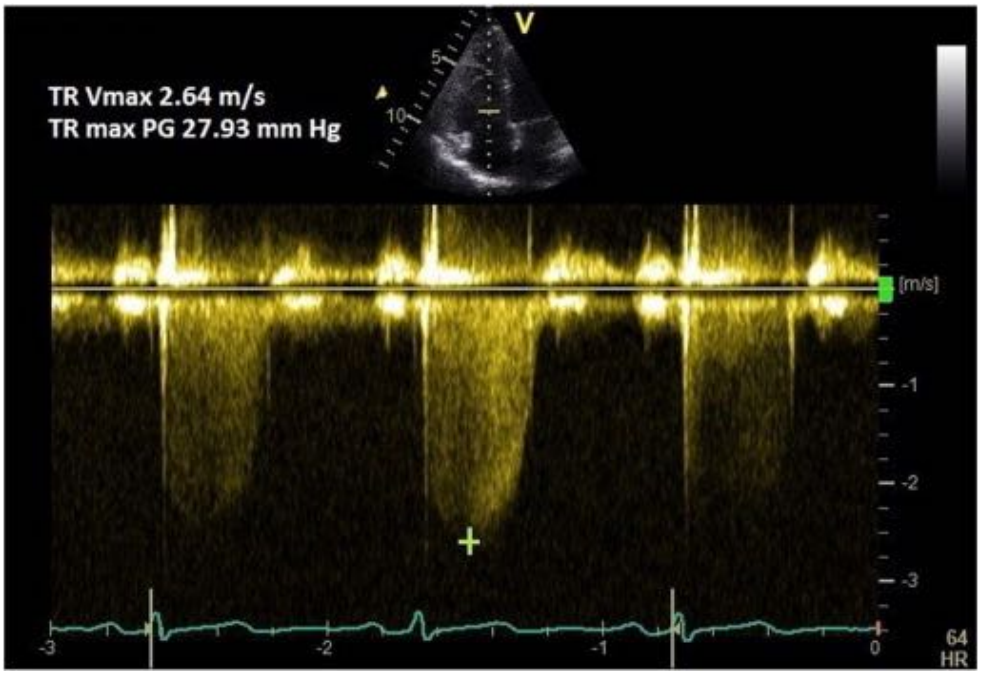

7 pav. *Triburio vožtuvo regurgitacijos maksimalaus greičio nustatymo metodikos demonstravimas naudojant pastoviosios bangos doplerio metodą*

5.6. Vainikinių arterijų fiziologijos vertinimo protokolas

VA fiziologijos vertinimas buvo atliktas po 3 mėnesių persirgus MIkSTP, kad būtų galima nustatyti mikrocirkuliacijos būklę po ūminės obstrukcijos išnykimo. Siekiant išlaikyti tyrimo vientisumą, duomenis surinko patyręs intervencinis kardiologas, kuris neturėjo specifinės informacijos apie pacientus ir jiems pradinio PTVAA metu naudotus revaskuliarizacijos metodus. Šis aklas tyrimas buvo būtinas siekiant užtikrinti fiziologinių vertinimų objektyvumą ir patikimumą. *CoroFlow* sistema iš Coroventis Research AB, Upsala, Švedija, turinti spaudimo daviklį X iš *Abbott Vascular*, Santa Clara, CA, buvo naudojama matuoti vainikinių arterijų tėkmės rezervą (angl. *Coronary Flow Reserve*; CFR), frakcinį tėkmės rezervą (angl. *Fractional Flow Reserve*; FFR) ir mikrocirkuliacijos pasipriešinimo indeksą (angl. *Index of Microvascular Resistance*; IMR). Sistema integruota su spaudimo ir temperatūros jutiklio davikliu leido įvertinti mikrovaskulinę disfunkciją. Vainikinių arterijų fiziologijos matavimas atliktas pagal griežtą protokolą, kuris išsamiai pavaizduotas 8 pav.

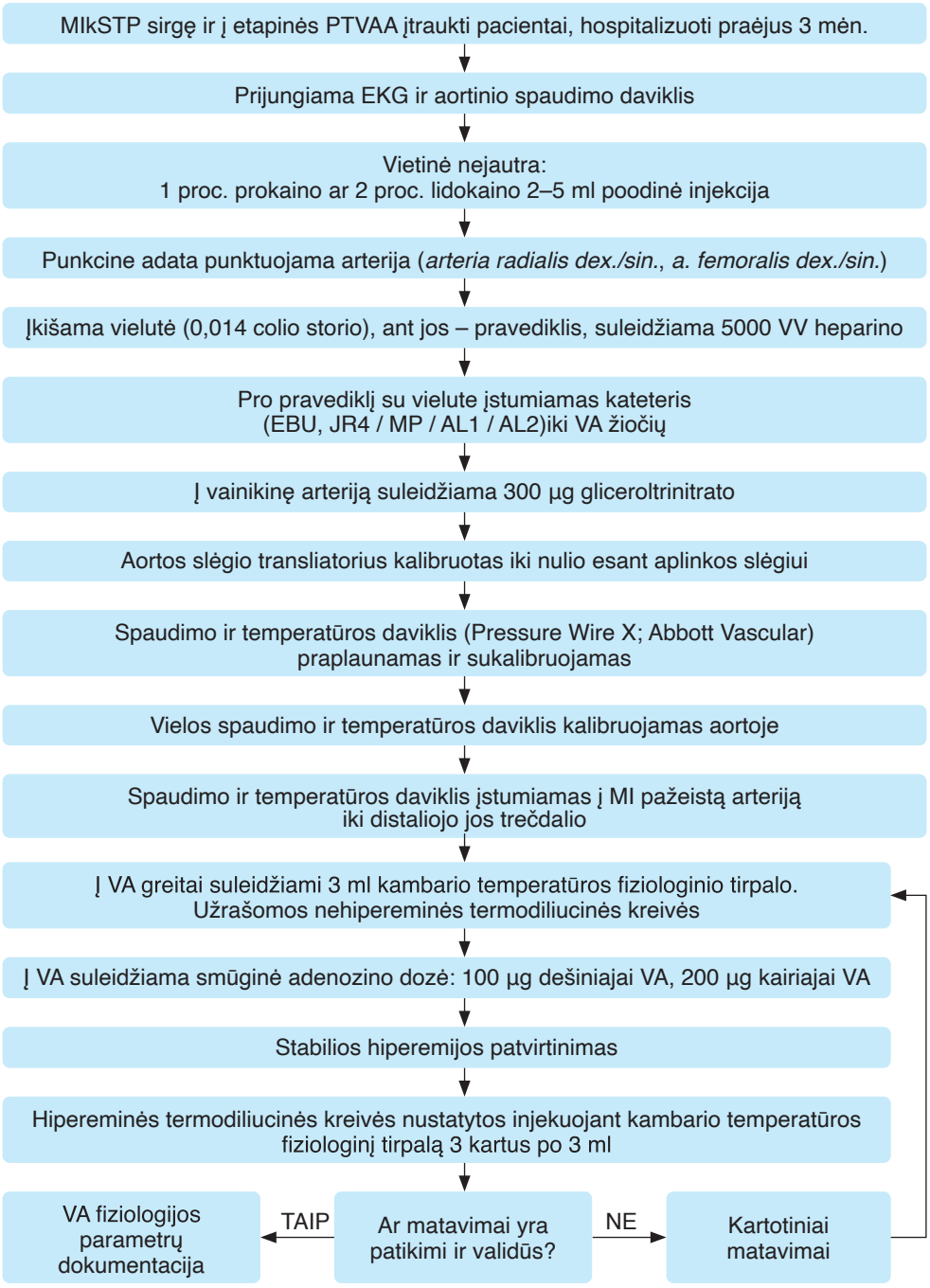

8 pav. *Detalus vainikinių arterijų fiziologijos vertinimo protokolas*

PTVAA – perkutaninė vainikinių arterijų intervencija; MIkSTP– miokardo infarktas, kai S–T segmentas pakilęs; kateteriai EBU, JR, MP, AL.

5.7. Vainikinių arterijų fiziologinių rodiklių apskaičiavimo protokolas

1. CFR – įvertinamas visų VA, įskaitant tiek epikardo kraujagysles, tiek mikrokraujagysles, geba reaguoti į padidėjusį miokardo deguonies poreikį. Jis apskaičiuojamas palyginus vidutinį kraujo tėkmės laiką (T_{mn}) ramybės metu su laiku, reikalingu hiperemijos metu:

$$\mathrm{CFR} = (1/\mathrm{T_{mn\ (hiperemija)}})/(1/\mathrm{T_{mn\ (ramybės\ metu)}}) = \\ = \mathrm{T_{mn\ (ramybės\ metu)}}/\mathrm{T_{mn\ (hiperemija)}}$$

2. IMR – matuoja pasipriešinimą VA mikrocirkuliacijos tinkle, rodantį mikrokraujagyslių gebą palengvinti kraujo pratekėjimą, esant padidėjusiam tėkmės poreikiui. Jis apskaičiuojamas naudojant distalinį VA spaudimą (P_d) ir vidutinį tėkmės laiką (T_{mn}) hiperemijos metu:

$$\mathrm{IMR} = \mathrm{P_d}/(1/\mathrm{T_{vidurkis\ (hiperemija)}}) = \mathrm{P_d} \times \mathrm{T_{vidurkis\ (hiperemija)}}$$

3. FFR – įvertina fiziologinę vainikinių arterijų stenozės reikšmę, palyginus slėgį distaliai nuo stenozės su slėgiu aortoje esant maksimaliai hiperemijai:

$$\mathrm{FFR} = \mathrm{P_d}/\mathrm{P_a}$$

4. MPR – įvertina mikrovaskulinį pasipriešinimą, neatsižvelgiant į epikardo pasipriešinimą, suteikiama papildoma informacija apie mikrovaskulinę funkciją:

$$\mathrm{MPR} = (\mathrm{CFR}/\mathrm{FFR}) \times (\mathrm{P_{a\ (ramybės\ metu)}}/\mathrm{P_{a\ (hiperemija)}})$$

Išskiriant mikrocirkuliacijos pasipriešinimą, MPR suteikia specifinį mikrocirkuliacijos būklės įvertinimą, ypač naudingą tais atvejais, kai epikardo arterijų būklė gali turėti įtakos mikrokraujagyslių funkcijos vertinimui.

5.8. Kraujo mėginių surinkimas ir tyrimai

Veninius kraujo mėginius surinko patyrusi slaugytoja pagal paciento kraujagyslių anatomiją. Po paėmimo mėginiai buvo nedelsiant apdorojami arba laikomi atitinkamomis sąlygomis ir vežami į laboratoriją tyrimui.

Kraujo tyrimus atliko Lietuvos sveikatos mokslų universiteto ligoninės Kauno klinikų ir Lietuvos sveikatos mokslų universiteto Kardiologijos instituto Molekulinės kardiologijos laboratorijos. Atlikti šie tyrimai: bendrasis kraujo tyrimas, trombocitų agregacijos rodikliai, troponino I kiekis, eritrocitų nusėdimo greitis (ENG), kreatinino kiekis, didelio jautrumo C reaktyviojo baltymo (dj-CRB) kiekis, kraujo lipoproteinų koncentracija , B tipo natriure-

zinio peptido (BNP) kiekis, trimetilamino N-oksido (TMAO) koncentracija kraujo plazmoje.

5.9. Vertintos tyrimo baigtys

3 mėn. stebėjimo laikotarpiu buvo vertinta:
1. VMD.
2. VMD endotipai.

12 mėn stebėjimo laikotarpiu buvo vertinta:
1. FKSR.
2. Diastolinės funkcijos sutrikimas.
3. Širdies didžiosios komplikacijos (mirtis, insultas, revaskulizacija, pakartotinis MI, hospitalizacija dėl širdies nepakankamumo).

5.10. Etikos komiteto leidimas

Prieš vykdant tyrimą, gautas (2021 m. sausio mėn.) Kauno regioninio biomedicininių tyrimų etikos komiteto leidimas, kurio numeris BE-2-5. Atliekant tyrimą buvo laikomasi Helsinkio deklaracijos etikos gairių.

5.11. Duomenų analizė: statistiniai metodai ir programinės įrangos naudojimas

Šiame doktorantūros tyrime surinktiems duomenims analizuoti taikyti įvairūs statistiniai metodai, užtikrinantys išvadų patikimumą ir pagrįstumą. Rezultatai buvo pateikti naudojant atitinkamas statistines priemones, o palyginimai tarp grupių atlikti naudojant testus, pritaikytus konkrečiam duomenų tipui ir šių duomenų skirstiniui. Daugiaveiksnės dvinarės logistinės regresijos ir Kokso (angl. *Cox*) regresijos modeliais nustatyti rizikos veiksniai, susiję su VMD, kairiojo skilvelio disfunkcija ir nepageidaujamomis baigtimis, koreguojant atitinkamus rodiklius.

Kaplano ir Mejerio (angl. *Kaplan-Meier*) kreivės analizė leido įvertinti išgyvenamumo rodiklius, o dozės ir atsako ryšys bei tam tikrų biologinių žymenų diagnostinis veiksmingumas buvo tiriami atitinkamai taikant apribotosios kubinės kreivės (angl. *Restricted Cubic Spline*) ir ROC (angl. *Receiver Operating Characteristic*) kreivių analizę, naudojant plotą po šia kreive (angl. *Area under Curve*; AUC). Į tyrimą taip pat buvo įtraukti mašininio dirbtinio intelekto mokymosi algoritmai, skirti numatyti VMD atsiradimą, naudojant suderinamus metodus ir vertinant modelius taikant kryžminį patikrinimą. Taikant *Random Forest* algoritmą, gauti tiksliausi rezultatai. Algoritmo veikimas buvo patvirtintas įtraukiant naują tiriamųjų – patvirtinimo imtį. Statistinė

analizė buvo atlikta naudojant IBM SPSS *Statistics* 27 ir R programinę įrangą. Skirtumai laikyti statistiškai reikšmingais, jei $p < 0,05$.

6. REZULTATAI

6.1. PTVAA strategijų įtaka VMD atsirasti įvykus MIkSTP

6.1.1. Tiriamoji populiacija, laboratoriniai ir echokardiografiniai radiniai

Ištirta 210 pacientų, kuriems MIkSTP metu buvo atlikta PTVAA. Ligoniai suskirstyti pagal stentavimo strategiją: tiesioginis stentavimas taikytas 46,66 proc. ir balioninė dilatacija, po kurios buvo atliekamas stentavimas, – 53,33 proc. Demografinių veiksnių analizė atskleidė tolygų skirstinį tarp abiejų grupių, be reikšmingų skirtumų pagal lytį, amžių, kūno masės indeksą, kūno paviršiaus plotą, MIkSTP įvykių vietas, cukrinio diabeto paplitimą, rūkymą (nerūko; metęs rūkyti; rūko), arba pradinius CHA_2DS_2-VASc balus. Bendrojo kraujo tyrimai nebuvo reikšmingi, vertinant tiesioginio stentavimo ir balioninės dilatacijos po kurios atliekamas stentavimas, grupes. Tiesioginio stentavimo grupėje buvo matomi statistiškai reikšmingai padidėję bendrojo cholesterolio ir MTL kiekiai, palyginti su stentavimu po balioninės dilatacijos (bendrasis cholesterolis: 5,06 mmol/l ir 4,43 mmol/l; p = 0,035; MTL: 3,51 mmol/l ir 3,17 mmol/l, p = 0,047). Kreatinino klirensas ir troponino I kiekis guldymo stacionare metu ir praėjus 24 valandoms, taip pat ir trombocitų agregacijos tyrimo rodikliai paveikus adenozino difosfatu reikšmingo skirtumo tarp grupių neparodė. Echokardiografiniai radiniai tarp grupių nerodė statistiškai reikšmingų KSIF pokyčių po pirminio PTVAA. Tačiau po vienų metų stebėjimo tiesioginio stentavimo grupės tiriamiesiems nustatytas statistiškai reikšmingai greitesnis KSIF pagerėjimas, palyginti su grupe, kurios tiriamiesiems prieš stentavimą atlikta balioninė dilatacija (48,00 proc ir 45,00 proc., p = 0,003). Šie radiniai rodo, kad nors iš karto po PTVAA laboratoriniai ir echokardiografiniai parametrai buvo panašūs abiejose stentavimo grupėse, tačiau KSIF buvo didesnė tiesioginio stentavimo grupėje.

6.1.2. Angiografijos ir angioplastikos metu gauti duomenys

Atlikus procedūrines intervencijas, pvz.: heparino, glikoproteino IIb / IIIa inhibitorių vartojimas ir aspiracinė trombektomija, kartu su stento ypatumais ir kontrasto dozėmis, nenustatyta reikšmingų skirtumų. Vadinasi, PTVAA technikos atliktos taikant vienodus kriterijus. Šis technikų panašumas leidžia tinkamai įvertinti baigtis, susijusias su mikrovaskuline disfunkcija.

6.1.3. Vainikinių arterijų fiziologiniai radiniai

Pacientams, kuriems atliktas tiesioginis stentavimas, buvo pastebėtas statistiškai reikšmingai šiek tiek didesnis CFR, palyginti su tais, kuriems stentai įstatyti atlikus balioninę dilataciją (2,87 ir 2,70; p = 0,003) (9 pav.). Pacientų, kuriems buvo atliktas tiesioginis stentavimas, FFR vertės buvo panašios kaip ir pacientų, kuriems buvo atlikta balioninė dilatacija ir vėliau – stentavimas (0,92, palyginti su 0,92; p = 0,452). Pacientų, kuriems buvo atlikta revaskuliarizacija taikant tiesioginį stentavimą, bet ne balioninę dilataciją, IMR buvo daug mažesnis (19,5 ir 22,0; p = 0,001) (10 pav.). Atlikus vainikinių arterijų fiziologinius tyrimus, 57 pacientams (27,14 proc.) buvo diagnozuota VMD. Tačiau pacientai, kuriems buvo atliktas tiesioginis stentavimas, statistiškai reikšmingai rečiau sirgo VMD, palyginti su tais, kuriems gydymo pradžioje taikyta balioninė dilatacija bei stentavimas (12,24 proc. ir 40,18 proc.; p < 0,001) (11 pav.).

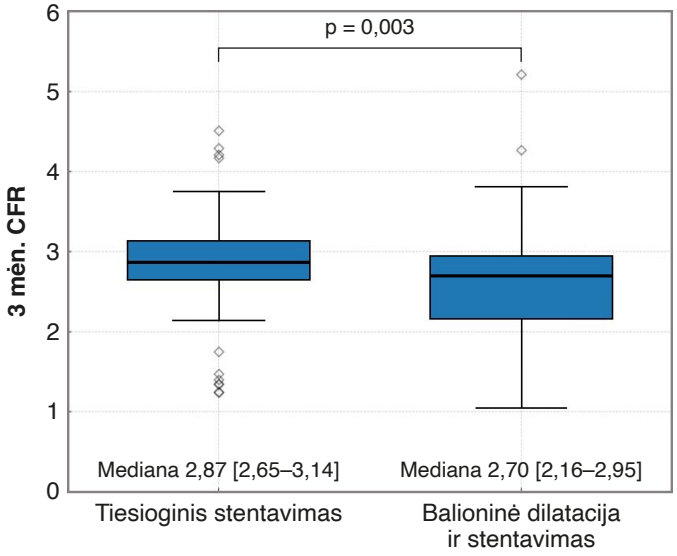

9 pav. *Vainikinių arterijų tėkmės rezervo skirstinys tirtas perkutaninės koronarinės intervencijos metu*

CFR – vainikinių arterijų tėkmės rezervas.

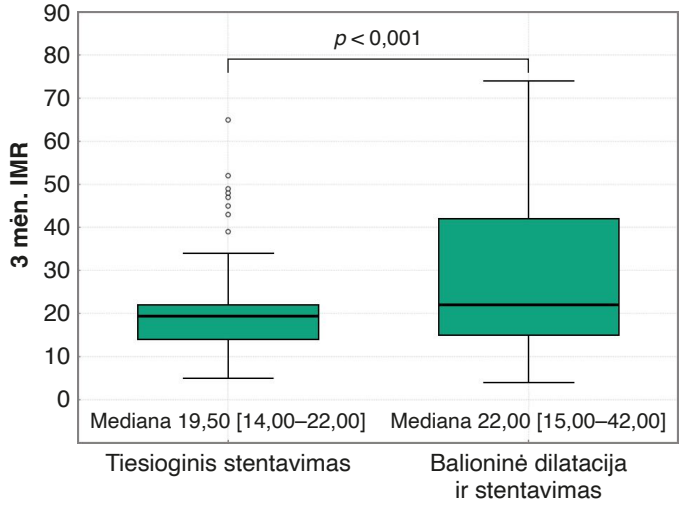

10 pav. *Mikrocirkuliacijos pasipriešinimo indekso skirstinys, tirtas vainikinių arterijų intervencijos metu*

IMR – mikrocirkuliacijos pasipriešinimo indeksas.

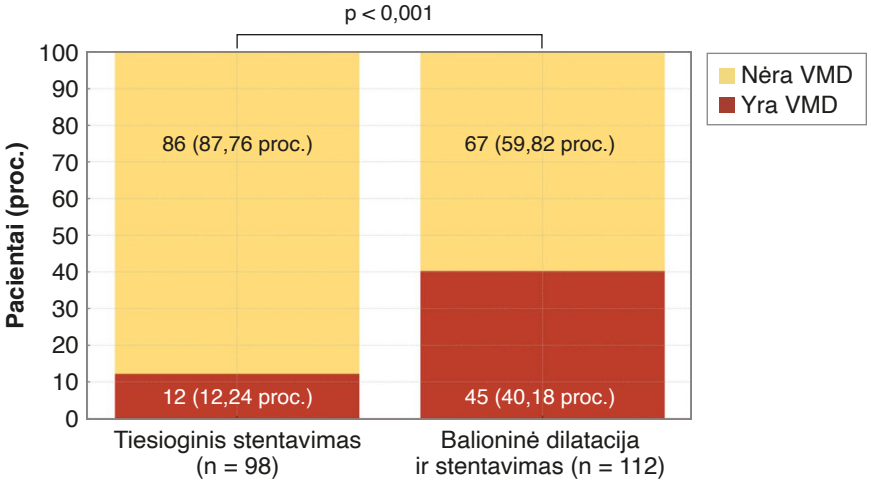

11 pav. *Vainikinių arterijų mikrovaskulinės disfunkcijos tyrimas vainikinių arterijų intervencijos metu*

VMD – vainikinių kraujagyslių mikrocirkuliacijos disfunkcija.

6.1.4. Klinikinės baigtys atsižvelgiant į stentavimo technikas

Grupėje, kurios pacientams buvo atlikta balioninė dilatacija, prieš atliekant stentavimą, dažniau pasireiškė prieširdžių virpėjimas, palyginti su tiesioginio stentavimo grupe (p = 0,061). Be to, pirmojoje grupėje insulto dažnumas buvo daug didesnis, palyginti su tiesioginio stentavimo grupe. Bendrasis

ŠDK dažnumas 12 mėnesių laikotarpiu buvo daug didesnis balioninės dilatacijos ir stentavimo grupėje, palyginti su tiesioginio stentavimo grupe (26,76 proc. *plg.* 14,29 proc.; p = 0,040), vadinasi, stentavimo strategija turėjo įtakos ilgalaikiams rezultatams (12 pav.).

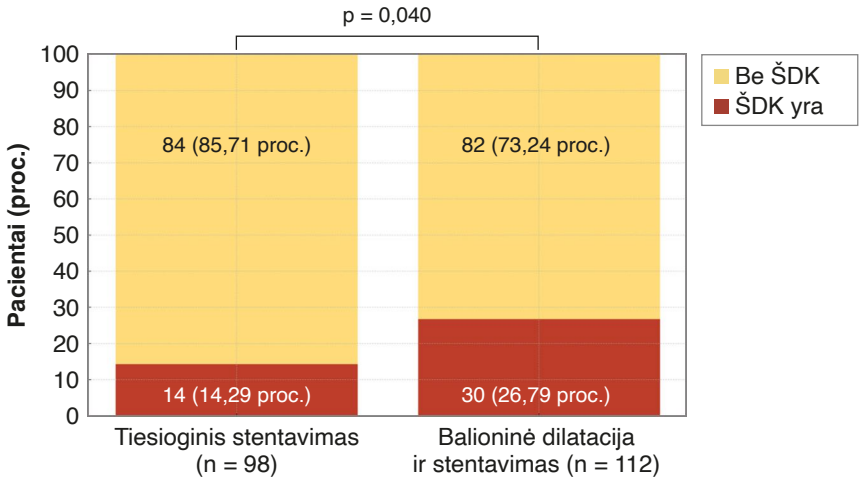

12 pav. *Nepageidaujamų širdies ir kraujagyslių didžiųjų įvykių reiškinių dažnumas vainikinių arterijų intervencijos metu*

ŠDK – širdies didžiosios komplikacijos.

6.1.5. Daugiaveiksnė logistinė regresija

Tiesioginis stentavimas, bet ne balioninė dilatacija ir po jos atliekamas stentavimas, aspiracinė trombektomija ir intrakoronarinio glikoproteino IIb / IIIa skyrimas buvo siejami su reikšmingai sumažėjusia VMD pasireiškimo galimybe (13 pav.).

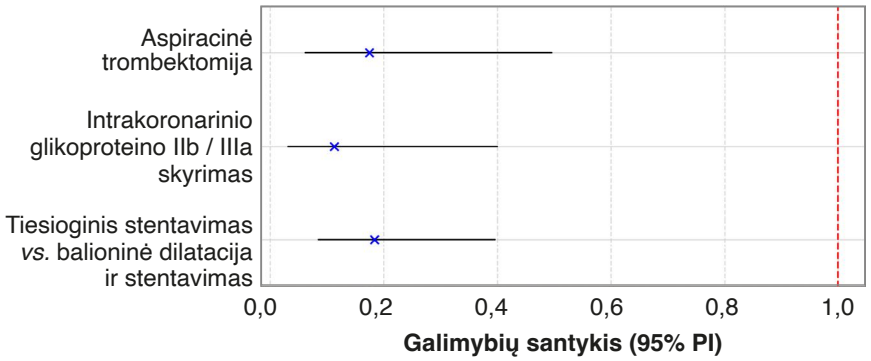

13 pav. *Forest plot vertė, rodanti PTVAA strategijų įtaką vainikinių arterijų mikrovaskulinei disfunkcijai*

PI – pasikliautinasis intervalas.

6.2. VMD prognozavimas pacientams, sergantiems MIkSTP, naudojant mašininio mokymosi dirbtinio intelekto galimybes

Į tyrimą įtraukti 200 pacientų, 30 klinikinių ir biologinių rodiklių. Iš viso – 12 klinikinių kintamųjų, 17 kiekybinių biologinių žymenų ir VMD diagnozės (nesergant VMD ir sergant VMD). Per 2021 m. sausio 12 d.–2022 m. liepos 31 d. laikotarpį duomenys buvo surinkti iš 149 pacientų. Iš šios grupės 44 asmenims (29,5 proc.) buvo nustatyta VMD. Šie 44 atvejai sudarė mokymo duomenų rinkinio, naudojamo kuriant VMD rizikos balą taikant sudėtingus mašininio mokymosi algoritmus, pagrindą. Vėliau 2022 m. rugpjūčio 1 d.–2023 m. sausio 31 d. buvo sudaryta papildoma 49 pacientų kohorta. Pastarojoje grupėje VMD buvo diagnozuota 7 pacientams (13,7 proc.). Ši imtis buvo tiriamoji imtis, kuri leido vertinti mašininio mokymosi būdu gauto VMD rizikos balo tikslumą ir glaustumą. Metodas vizualizuotas 14 pav., kuriame pateikiama aiški ir glausta tyrimo analitinės sistemos apžvalga.

Tyrime taikyti apskaičiavimo metodai, pvz.: *Random Forest (RF), Gradient Boosting Machine (GBM), Support Vector Machine (SVM), eXtreme Gradient Boosting (XGBoost), Super Learner, and Discrete Super Learner.* Siekiant įvertinti šių pažangių metodikų panaudojimą, buvo atlikta palyginamoji analizė, pagrįsta 10-klosčių kryžminio patvirtinimo (CV) rizikos vertinimo sistema. RF algoritmas buvo pranašiausias iš modelių (0,120 ± 0,010, kaip parodyta 15 pav.).

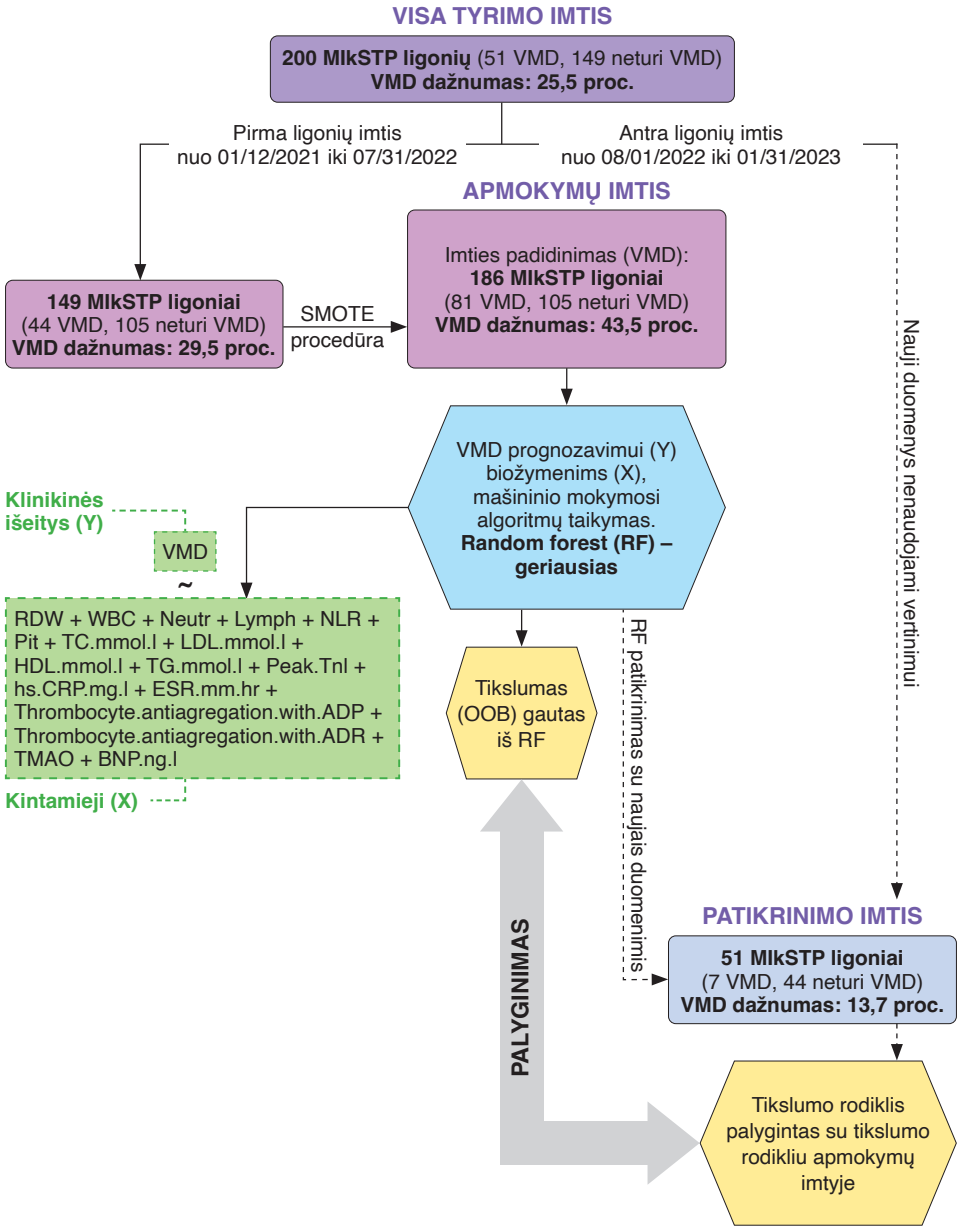

14 pav. *Duomenų schema ir tyrime taikyta empirinė analizė*

MIkSTP – ūminis miokardo infarktas, kai S–T segmentas pakilęs; VMD –vainikinių mikrokraujagyslių disfunkcija; SMOTE – SMOTE technika; OOB – Out-Of-Bag; RF – Random Forest; RDW – eritrocitų pasiskirstymo plotis; WBC – leukocitai; Neutr – neutrofilai; Lymph – limfocitai; NLR – neutrofilų ir limfocitų santykis; PLT – trombocitai; TC – bendrasis cholesterolis; LDL – mažo tankio lipoproteinų cholesterolis; HDL – didelio tankio lipoproteinų cholesterolis; TG – trigliceridų cholesterolis; Peak TnI – didžiausia troponino I koncentracija; hs-CRP – didelio jautrumo C reaktyvusis baltymas; ESR – eritrocitų nusėdimo greitis; ADP – adenozinodifosfatas; ADR – epinefrinas; BNP – B tipo natriurezinis peptidas; TMAO – trimetilamino-N-oksidas.

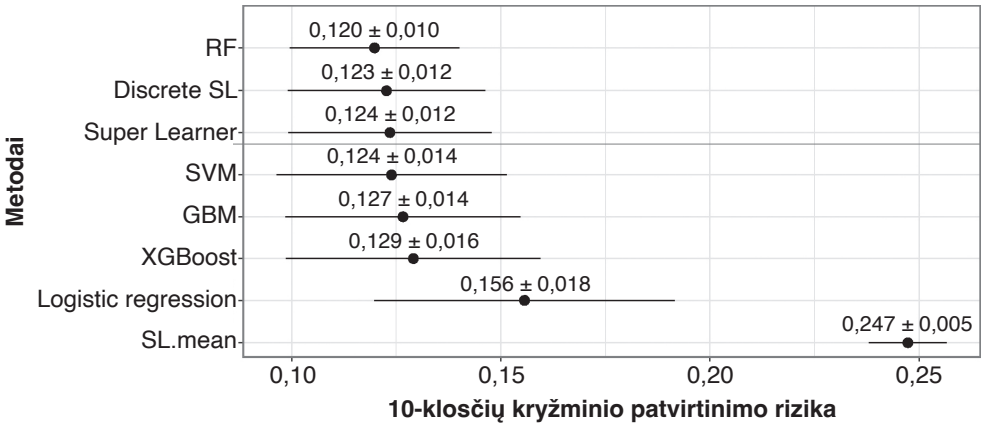

15 pav. *Kryžminio 10-klosčių kryžminio patvirtinimo rizika kiekvienam taikytam metodui (± standartinė paklaida)*

Metodai: RF – Random Forest; GBM – Gradient Boosting Machine; SVM – Support Vector Machine; XGBoost – eXtreme Gradient Boosting; SL – Super Learner; CV – Kryžminis patvirtinimas.

6.2.1. Santykinės kintamųjų svarbos matavimo rodikliai (relVIM) ir trimačiai dalinės priklausomybės brėžiniai (3D-PDP)

relVIM ir 3D-PDP analizė taikyta VMD prognozuoti MIkSTP ligoniams taikant RF.

Kreivė (16 pav.) pabrėžia biologinių žymenų svarbą. TMAO turi didžiausią prognozinę vertę (relVIM = 100 proc.). Mažesnę įtaką turi trombocitų agregacijos rodikliai paveikus epinefrinu bei B tipo natriurezinio peptido (BNP) koncentracija. 3D-PDP analizė (17 pav.) rodo, kad šių pagrindinių biologinių žymenų aktyvumo padidėjimas kraujyje susijęs su didesne VMD tikimybe.

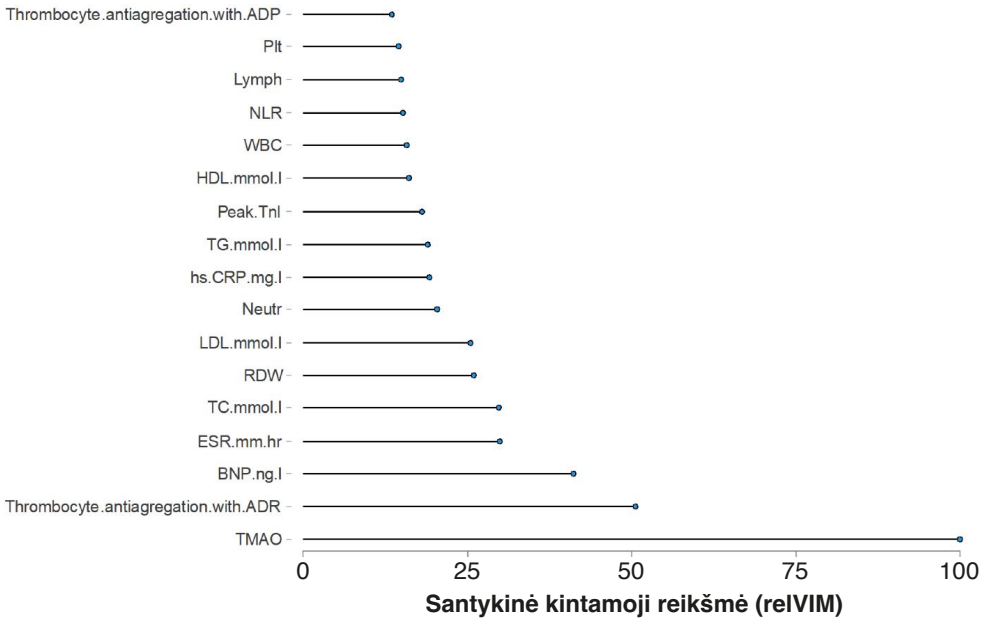

16 pav. *Santykinė kintamoji vertė (relVIM), nustatyta RF metodu*

relVIM nustato, kurie kintamieji turėjo didelę įtaką diagnozei (nėra VMD/yra VMD). RDW – eritrocitų pasiskirstymo plotis; WBC – leukocitai; Neutr – neutrofilai; Lymph – limfocitai; NLR – neutrofilų ir limfocitų santykis; PLT – trombocitai; TC – bendrasis cholesterolis; LDL – mažo tankio lipoproteinų cholesterolis; HDL – didelio tankio lipoproteinų cholesterolis; TG – trigliceridų cholesterolis; Peak TnI – didžiausia troponino I koncentracija; hs-CRP – didelio jautrumo C reaktyvusis baltymas; ESR – eritrocitų nusėdimo greitis; ADP – adenozinodifosfatas; ADR – epinefrinas; BNP – B tipo natriurezinis peptidas; Thrombocyte.antiagregation.with.ADR – trombocitų agregacija paveikus epinefrinu; TMAO – trimetilamino-N-oksidas.

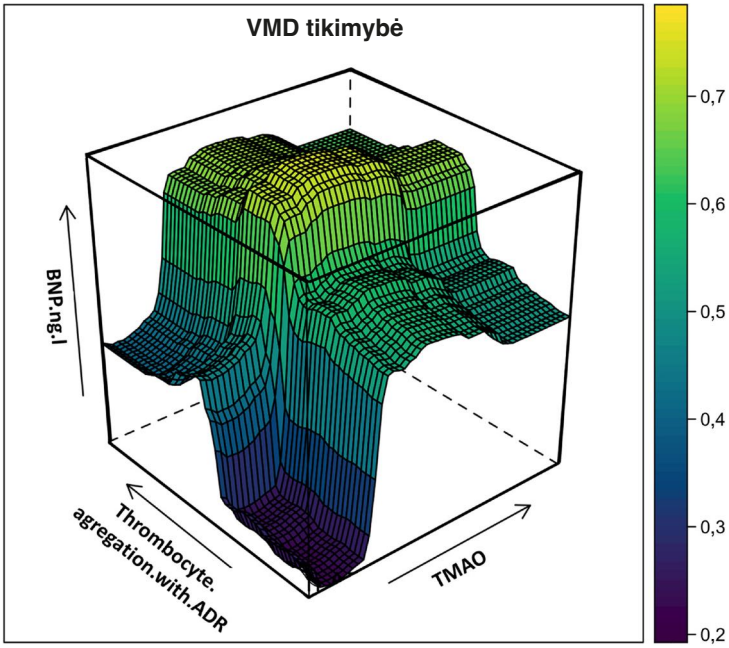

17 pav. *3D-PDP, gaunamas atliekant RF apskaičiavimus ir pagrįstas trimis svarbiausiais kintamaisiais, pasirinktais pagal santykinės kintamosios svarbos matą*

Spalvų spektras kinta nuo mėlynos iki geltonos spalvos, o tai rodo didėjančią tikimybę patekti į grupę „pacientas, turintis VMD“. X, y ir z ašių rodyklės rodo kryptis, kuriomis didėja trijų kintamųjų vertės. BNP – B tipo natriurezinis peptidas; ADR – epinefrinas; TMAO – trimetilamino-N-oksidas; VMD – vainikinių mikrokraujagyslių disfunkcija.

6.2.2. Random Forest (RF) modelio našumas ir patvirtinimas

RF modelio našumas įvertintas pagal *Out-of-Bag* (angl. santrump. OOB) klaidų dažnumą sudarytoje mokymo imtyje (aprašymas 1 lentelėje). Modeliui būdingi puikūs parametrų įverčiai, įskaitant tikslumą, jautrumą, specifiškumą, neigiamą prognozinę vertę (NPV), teigiamą prognozinę vertę (PPV) ir preciziškumą – tai rodo stiprias jo VMD prognozavimo galimybes.

1 lentelė. *RF modelio kokybės kriterijai sudarytoje mokymų imtyje*

Matas	Mokymų imtis	Patikrinimo imtis
Tikslumas (95 proc. PI)	0,84 (0,78–0,89)	0,92 (0,81–0,98)
Jautrumas	0,86	0,91
Specifiškumas	0,81	1,00
Teigiama prognozinė vertė	0,86	1,00
Neigiama prognozinė vertė	0,81	0,64
Preciziškumas	0,86	1,00

RF – Random Forest; PI – pasikliautinasis intervalas.

6.3. TMAO – žymuo, prognozuojantis VMD ligoniams, sergantiems miokardo infarktu, kai S–T segmentas pakilęs

Atsižvelgdami į TMAO svarbą prognozuojant VMD (16 pav.), detaliai ištyrėme ribines jo vertes VMD ir klinikines baigtis gydant ligonius, sergančius MIkSTP.

6.3.1. Optimalios ribinės vertės nustatymas

Pirmieji rezultatai parodė nedidelę TMAO prognozinę vertę iškart po intervencijos. Praėjus 3 mėnesiams po intervencijos, kai optimali TMAO ribinė vertė buvo 3,91 µM, TMAO nustatytas didelis jautrumas ir specifiškumas prognozuojant VMD (18 pav.).

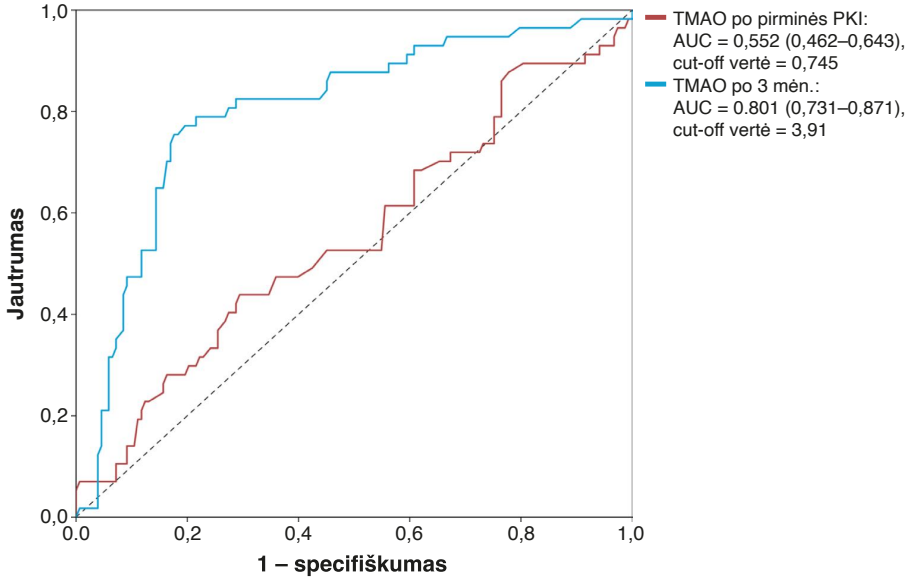

18 pav. *ROC kreivių analizė, rodanti TMAO įtaką diagnozuojant VMD*

TMAO – trimetilamino-N-oksidas; AUC – plotas po kreive.

6.3.2. Prognozinė biologinių žymenų vertė

Vertinant biologinius žymenis, skirtus prognozuoti VMD praėjus 3 mėnesiams po MI, kai S–T segmentas pakilęs, TMAO koncentracijos buvo tiksliausia prognozinė vertė (AUC = 0,801). TMAO rezultatai, palyginti su kitais biologiniais žymenimis, buvo reikšmingai geresni (19 pav.).

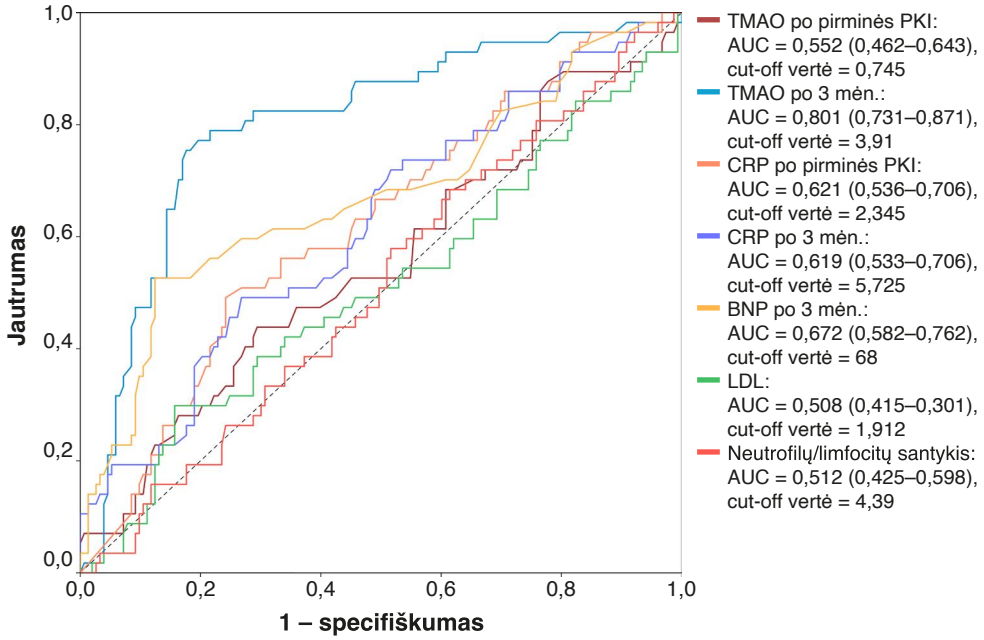

19 pav. *Trimetilamino-N-oksido ir kitų biologinių žymenų ROC kreivės VMD prognozuoti*

TMAO – trimetilamino-N-oksidas; CRP – C reaktyvusis baltymas; BNP – B tipo natriurezinis peptidas; LDL – mažo tankio lipoproteinų cholesterolis; AUC – plotas po kreive.

6.3.3. Echokardiografiniai parametrai

Šis širdies funkcijos ir remodeliavimosi skirtumas, kurį pabrėžė KSIF baigtys vertinant didelio ir mažo TMAO aktyvumo grupes, iliustruojamas 20 pav. (A ir B). Rezultatai patvirtina TMAO įtaką nuspėjant kairiojo skilvelio atsigavimui po MI, kai S–T segmentas pakilęs.

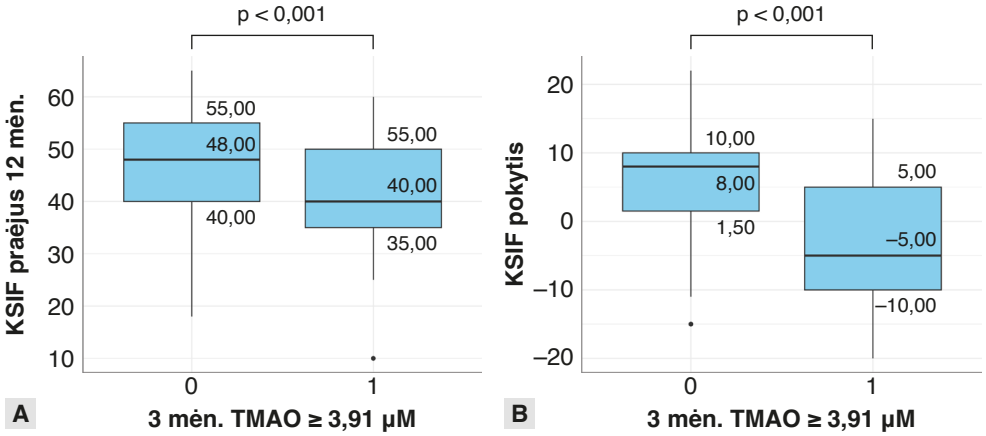

20 pav. *Kairiojo skilvelio išstūmio frakcija ir kairiojo skilvelio išstūmio frakcijos pokytis pagal trimetilamino-N-oksido aktyvumą praėjus 12 mėnesių*

KSIF – kairiojo skilvelio išstumio frakcija; TMAO – trimetilamino-N-oksidas.

6.3.4. Trimetilamino-N-oksido aktyvumas ir klinikinės baigtys 12 mėnesių stebėjimo laikotarpiu

Atlikus pirminę PKI MIkSTP pacientams ir praėjus 3 mėnesiams nuo procedūros atlikimo, nustatytas ryškus ryšys tarp padidėjusio TMAO kiekio (≥ 3,91 µM) ir VMD dažnumo (21 pav.). Ši tendencija stebėta ir praėjus 12 mėnesių laikotarpiui: didesnis TMAO aktyvumas buvo susijęs su padidėjusiu nepageidaujamų klinikinių baigčių dažnumu, įskaitant miokardo infarktus, nesukėlusius mirties, taip pat ir didesniu mirštamumu bei dažnesniu guldymo stacionare dažnumu dėl širdies nepakankamumo. Kaplano ir Meierio kreivė rodo skirtumus tarp ŠDK ir POCE dažnumo tirtų ligonių imtyje (22 pav.).

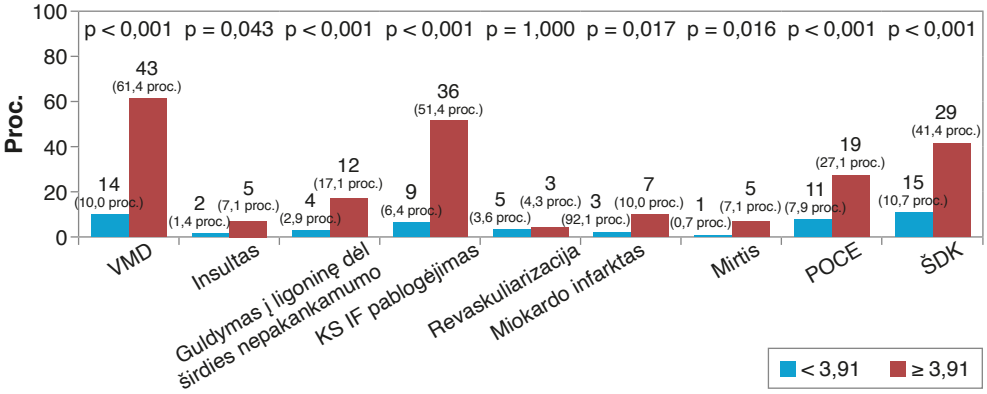

21 pav. *Klinikinių įvykių dažnumas ir nepageidaujamų širdies ir kraujagyslių didžiųjų įvykių rizika, atsižvelgiant į TMAO aktyvumą*

VMD –vainikinių mikrokraujagyslių disfunkcija; LVEF, KSIF – kairiojo skilvelio išstūmio frakcija; POCE – mirštamumas nuo betkokių širdinės kilmės priežasčių; ŠDK – širdies didžiosios komplikacijos; ŠDK = POCE + guldymas stacionare dėl širdies nepakankamumo

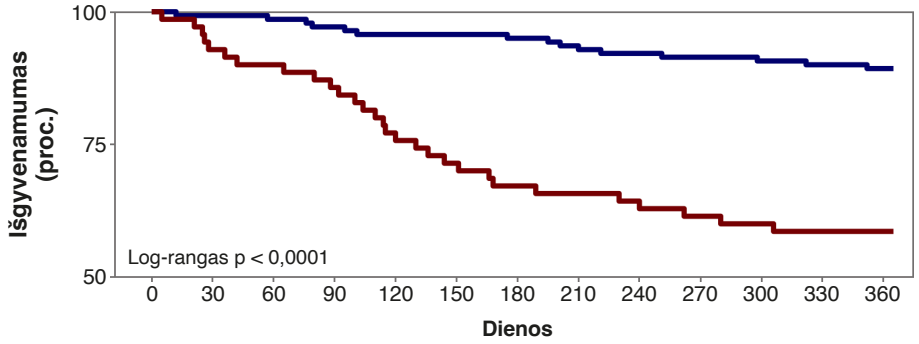

STRATA	Tiriamųjų skaičius rizikos grupėje												
TMAO < 3,91	140	139	138	136	134	134	133	131	129	128	127	126	125
TMAO ≥ 3,91	70	65	63	60	54	50	47	46	45	43	42	41	41

22 pav. *Kaplano ir Mejerio kreivė, kuri rodo ŠDK įvykių dažnumą, priklausomą nuo trimetilamino N-oksido (TMAO), praėjus 3 mėnesiams*

TMAO – trimetilamino N-oksidas, STRATA – tiriama populiacijos dalis.

6.4. MPR patvirtinimas ligoniams, sergantiems miokardo infarktu, kai S–T segmentas pakilęs

6.4.1. Tiriamųjų imtis

Tos pačios kohortos pacientai buvo suskirstyti pagal VMD (buvo arba nebuvo), remiantis MPR ribine verte, kuri lygi 3, ir kitais tyrimais. Iš viso VMD nustatyta 26,67 proc. tiriamųjų (MPR < 3), o 73,33 proc. VMD nenustatyta (MPR ≥ 3). VMD dažniau nustatyta moterims nei vyrams, atitinkamai VMD ir ne VMD grupėse: 62,50 proc. ir 32,47 proc.; p < 0,001). Visų grupių amžiaus mediana buvo panaši. VMD ir ne VMD sergančių pacientų KMI, BSA, MIkSTP vieta, arterinė hipertenzija, vainikinių arterijų ligos anamnezė, ankstesnė PKI, insultas anamnezėje, dislipidemija, rūkymas ar alkoholio vartojimas reikšmingai nesiskyrė tarp grupių. VMD grupės ligoniai dažniau sirgo cukriniu diabetu (39,29 proc. ir 18,83 proc.; p = 0,004).

6.4.2. Echokardiografiniai radiniai

Atlikus PTVAA, pacientų, kurių MPR < 3, KSIF rodikliai buvo geresni nei tų, kurių MPR ≥ 3. Praėjus 1 metams, šie pacientai patyrė reikšmingą KSIF sumažėjimą, palyginti su MPR ≥ 3 grupe. Tai pavaizduota 23 ir 24 pav.

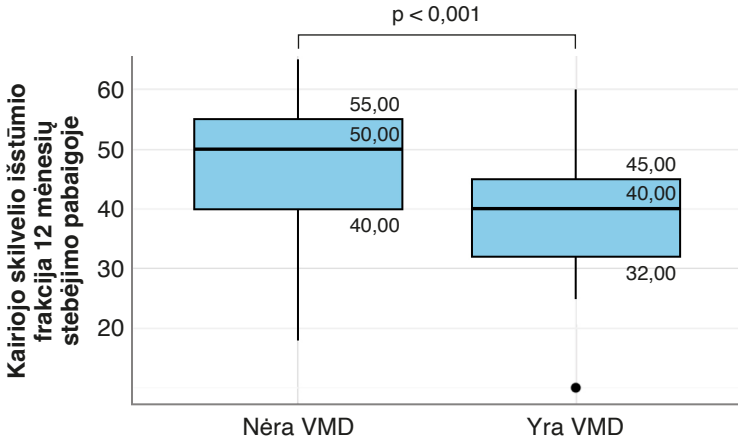

23 pav. *Kairiojo skilvelio išstūmio frakcija praėjus 12 mėnesių nuo PKI, atsižvelgiant į vainikinių arterijų mikrovaskulinę disfunkciją, vertinta remiantis MPR*

VMD – vainikinės mikrocirkuliacijos disfunkcija.

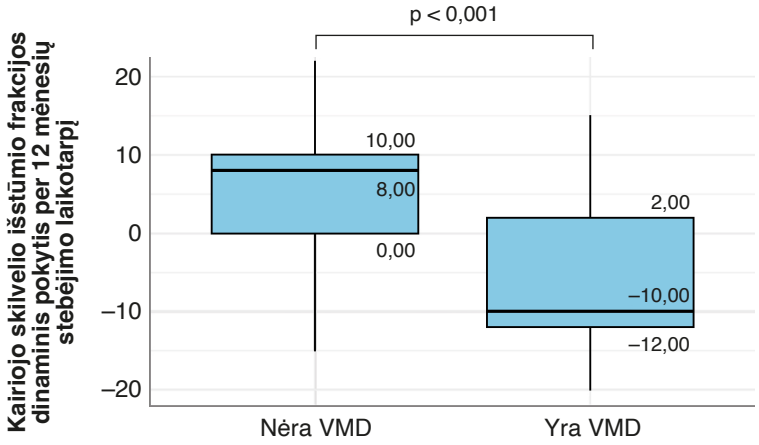

24 pav. *Kairiojo skilvelio išstūmio frakcijos pokyčiai remiantis VMD pagal MPR*

VMD – vainikinės mikrocirkuliacijos disfunkcija.

6.4.3. Klinikinės baigtys remiantis MPR

Šio tyrimo metu 20,95 proc. pacientų, sergančių MIkSTP, patyrė ŠDK 12-kos mėnesių stebėjimo laikotarpiu. Atsižvelgiant į MPR, reikšmingai skyrėsi šių ligonių ŠDK dažnumas: MPR < 3 ir MPR ≥ 3 (48,21 proc. *plg.* 11,04 proc.; p < 0,001), kaip parodyta 25 pav. Pacientai, turintys mažesnius MPR, buvo dažniau hospitalizuojami dėl išeminio insulto ir širdies nepakankamumo.

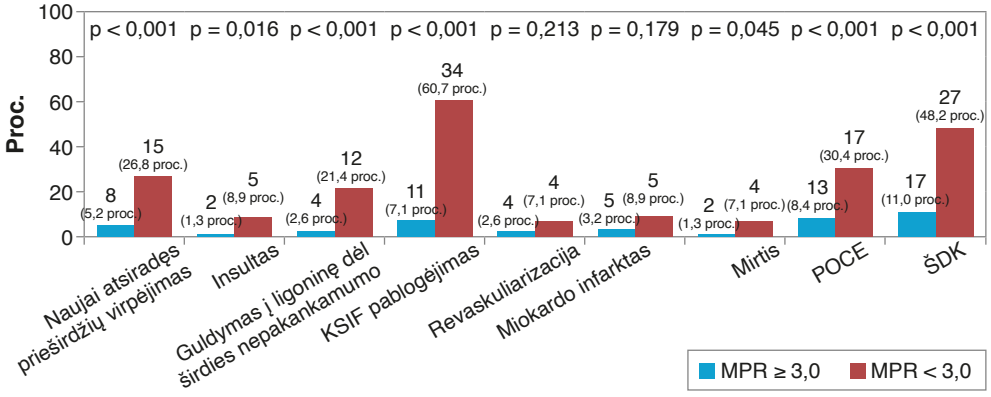

25 pav. *Klinikinių reiškinių dažnumas, atsižvelgiant į MPR*

AF – prieširdžių virpėjimas; LVEF – kairiojo skilvelio išstūmio frakcija; POCE – visų rūšių mirštamumas, sukeltas miokardo infarkto, insulto, revaskuliarizacijos; ŠDK – POCE + stacionarizavimas dėl širdies nepakankamumo; MPR – mikrocirkuliacijos pasipriešinimo rezervo.

Daugiaveiksnė Kokso (angl. *Cox*) analizė parodė, jog mažesnis MPR didina ŠDK įvykių dažnumą – tai pabrėžia riziką, susijusią su mikrokraujagyslių pasipriešinimu. *Cubic spline curve* (26 pav.) ir *Kaplano ir Meierio* išgyvenamumo analizės (27 pav.) rezultatai. *Cubic spline curve* rezultatai pateikti 26 pav., o *Kaplano ir Meierio* išgyvenamumo analizės rezultatai pateikti 27 pav.

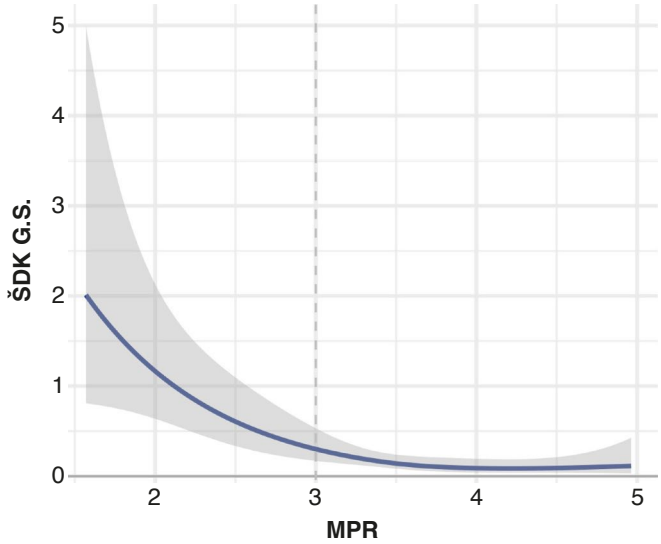

26 pav. *Apribota kubinė kreivė, rodanti MPR ir galimybę įvykti ŠDK*

MPR – mikrocirkuliacijos pasipriešinimo rezervas; ŠDK – širdies didžiosios komplikacijos, G.S. – galimybių santykis.

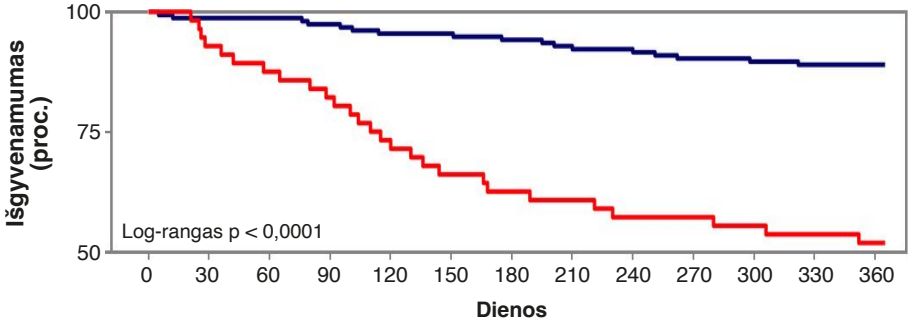

STRATA	Tiriamųjų skaičius rizikos grupėje												
MPR ≥ 3,0	154	152	152	150	147	147	145	143	142	139	138	137	137
MPR < 3,0	56	52	49	46	41	37	35	34	32	32	31	30	29

27 pav. *Kaplano ir Mejerio kreivė, rodanti ŠDK įvykių dažnumą, atsižvelgiant į MPR*

MPR – mikrocirkuliacijos pasipriešinimo rezervas; ŠDK – širdies didžiosios komplikacijos, STRATA – tiriama populiacijos dalis.

6.4.4. Prognozinių rezultatų palyginimas

ROC kreivės analizė parodė, kad MPR, CFR ir IMR turi didelę POCE prognozinę vertę ligoniams 12 mėnesių laikotarpiu. Šių rodiklių AUC, atitinkamai 0,743, 0,762 ir 0,781, buvo geresnis nei FFR AUC, kuris buvo 0,609 (28 pav.). Kiekvienam parametrui buvo nustatytos optimalios ribos, nurodančios jų prognozinį pranašumą prieš FFR numatant POCE. Ši analizė dar kartą patvirtina, kad MPR, CFR ir IMR yra patikimi rodikliai ligoniams po MIkSTP, kaip ir parodyta 28 ir 29 pav.

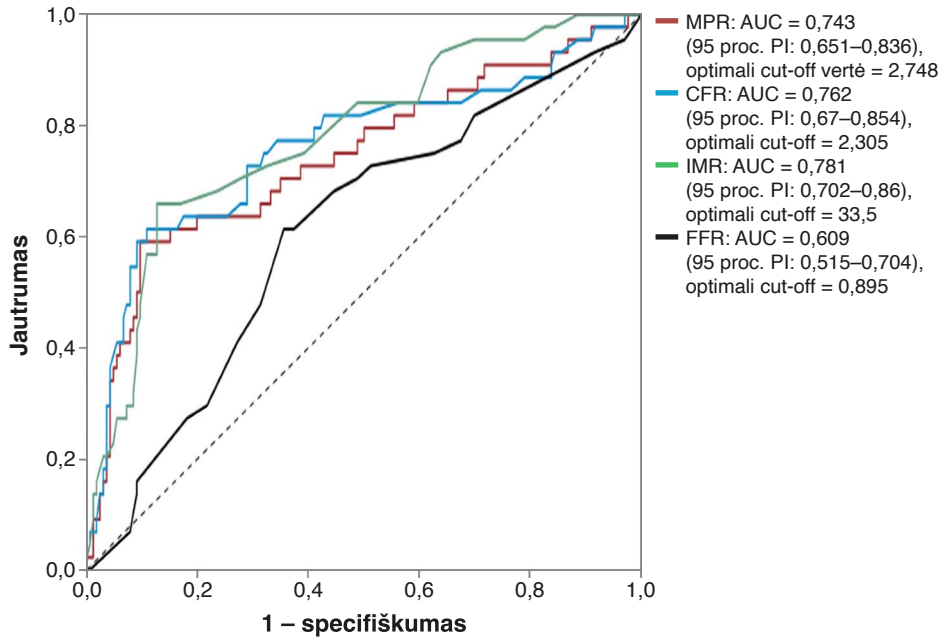

28 pav. *ROC kreivė rodanti, baigtis (POCE) praėjus 12-kai mėnesių MIkSTP ligonių imtyje*

MPR – mikrocirkuliacijos pasipriešinimo rezervas; CFR – vainikinių arterijų tėkmės rezervas; IMR – mikrocirkuliacijos pasipriešinimo indeksas, FFR – frakcinis tėkmės rezervas; AUC – plotas po kreive.

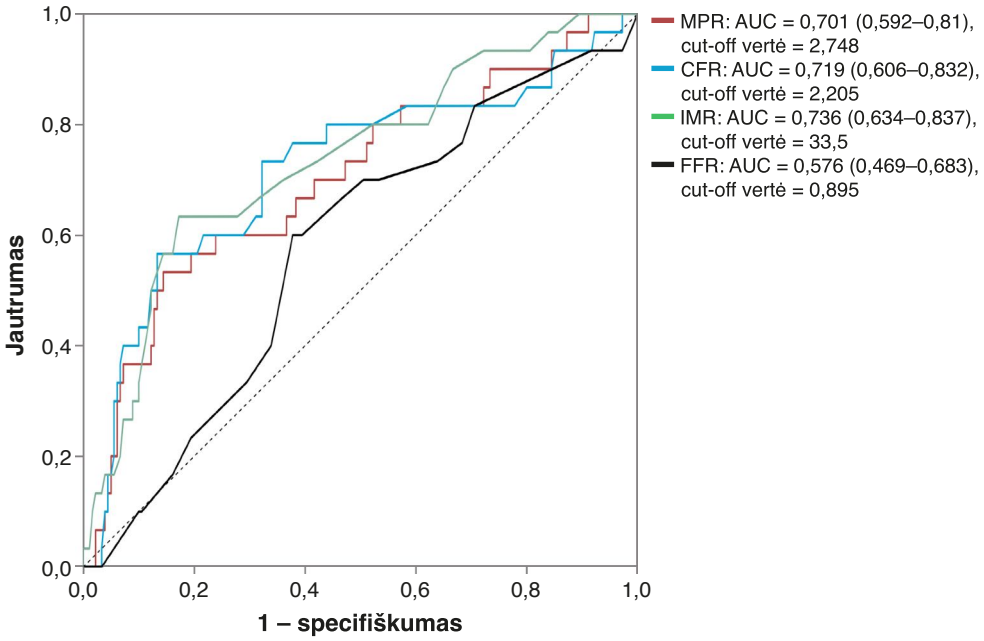

29 pav. *ROC kreivė, rodanti ŠDK praėjus 12-kai mėnesių, ligonių, sergančių MIkSTP imtyje*

MPR – mikrocirkuliacijos pasipriešinimo rezervas; CFR – vainikinių arterijų tėkmės rezervas; IMR – mikrocirkuliacijos pasipriešinimo indeksas, FFR – frakcinis tėkmės rezervas; AUC – plotas po kreive.

6.5. VMD endotipų paplitimas tarp pacientų, sergančių MIkSTP

VMD buvo nustatyta 27 proc. visų pacientų. Daugiausia nustatyta kaip struktūrinė VMD (24 proc.), funkcinė VMD nustatyta 3 proc. pacientų – tai rodo didesnį struktūrinių mikrovaskulinių pokyčių po MIkSTP dažnumą (30 pav.) bei pabrėžia struktūrinio VMD svarbą būsimoms MIkSTP pacientų gydymo strategijoms.

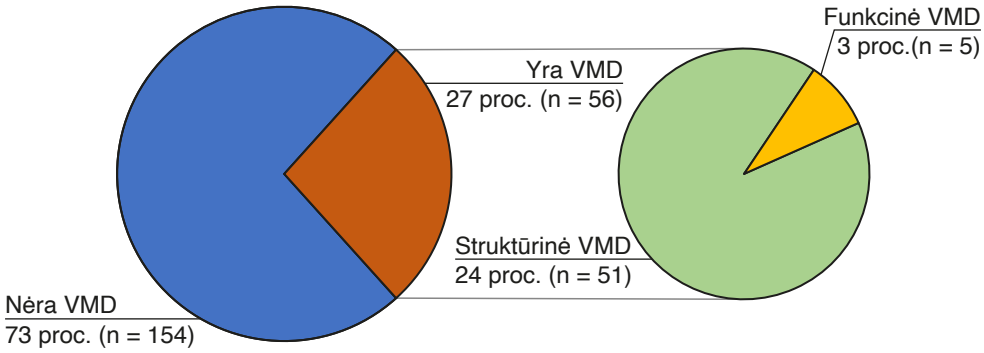

30 pav. *VMD endotipų skirstinys tarp ligonių, sirgusių miokardo infarktu, kai S–T segmentas pakilęs, imtyje*

VMD – vainikinės mikrocirkuliacijos disfunkcija.

6.6. VMD įtaka funkciniam kairiojo skilvelio remodeliavimuisi, diastolinei disfunkcijai ir klinikinėms baigtims

6.6.1. Tyrimų imtis ir laboratoriniai rezultatai stratifikuojant VMD

Pacientai buvo suskirstyti pagal VMD pasireiškimą (IMR ≥ 25 U arba CFR < 2,0 U). Iš viso 27,14 proc. pacientų buvo diagnozuota VMD. VMD dažniau nustatyta moterims, palyginti su vyrais (63,16 proc. *plg.* 32,03 proc.; p < 0,001). Ligoniai, sergantys VMD, dažniau sirgo cukriniu diabetu (42,11 proc. *plg.* 17,65 proc.; p < 0,001). Bendrojo kraujo tyrimo rezultatai tarp skirtingų ligonių grupių reikšmingai nesiskyrė, tačiau kreatinino klirensas skyrėsi reikšmingai (p = 0,003). Tai rodo inkstų funkcijos įtaką VMD atsirasti. Didelio jautrumo CRB ir B tipo natriurezinio peptido lygis praėjus 3 mėnesiams nuo PKI buvo daug didesnis VMD grupės tiriamųjų, o tai rodo ryšį su uždegiminiais procesais.

6.6.2. Echokardiografiniai radiniai

Echokardiografinis tyrimas po PTVAA parodė, kad VMD grupėje tyrimo pradžioje buvo didesnis KSIF ir E/A santykis, palyginti su nesergančiais VMD, o tūriai ir diastolinės funkcijos laipsniai tarp grupių buvo panašūs. Praėjus 12 mėnesių VMD grupėje statistiškai reikšmingai sumažėjo KSIF ir pakito diastolinė funkcija, padidėjo kairiojo skilvelio galutinis diastolinis tūris (KSGT), KP tūrio indeksas ir E/e, kartu sumažėjo E/A santykis ir vidutinis e’. Daugumos pacientų, nesergančių VMD, diastolinė funkcija pagerėjo iki pirmojo laipsnio, o sergančių VMD progresavo iki antrojo laipsnio, tai pabrėžė pablogėjusią VMD sergančių pacientų diastolinę funkciją (31–34 pav.).

Remiantis gautais rezultatais, galima teigti, kad pacientų, sergančių VMD, daugiausiai buvo atitinkančių 2, 3 ir 4 grupių kriterijus pagal funkcinę kairiojo skilvelio remodeliavimosi sistemą (35 pav.).

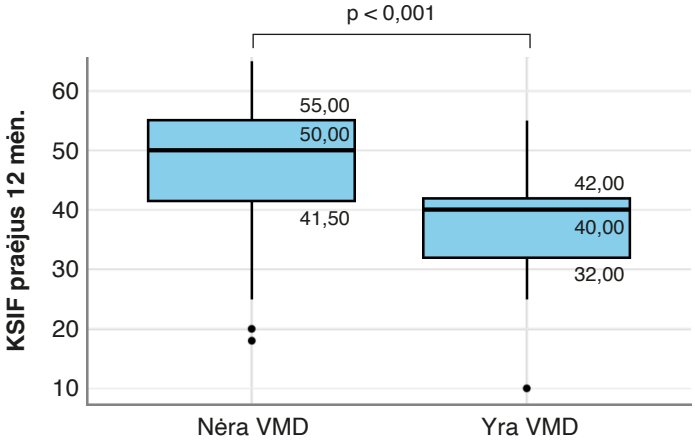

31 pav. *KSIF praėjus 12-kai mėnesių atsižvelgiant į VMD*

VMD – vainikinės mikrocirkuliacijos disfunkcija; KSIF – kairiojo skilvelio išstūmio frakcija.

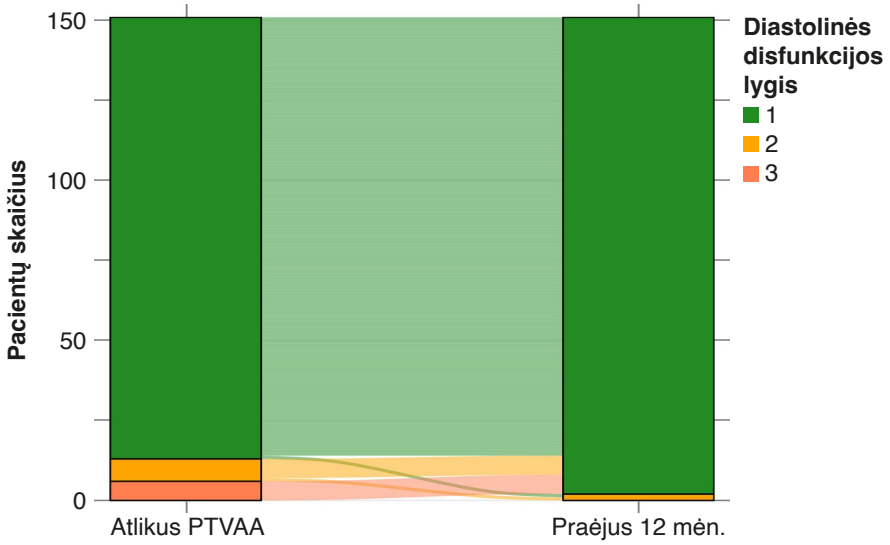

32 pav. *Diagrama vaizduoja dinaminius diastolinės disfunkcijos pokyčius ligoniams, nesirgusiems VMD 12 mėnesių laikotarpiu*

PTVAA – perodinė transluminalinė vainikinių arterijų angioplastika.

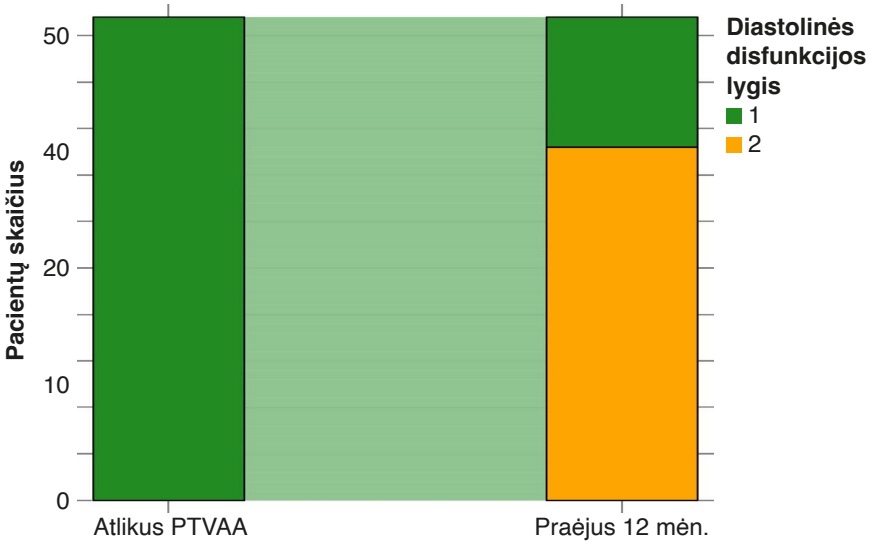

33 pav. *Diagrama vaizduoja dinaminius diastolinės disfunkcijos pokyčius ligoniams, sirgusiems VMD 12 mėnesių laikotarpiu*

PTVAA – perodinė transluminalinė vainikinių arterijų angioplastika.

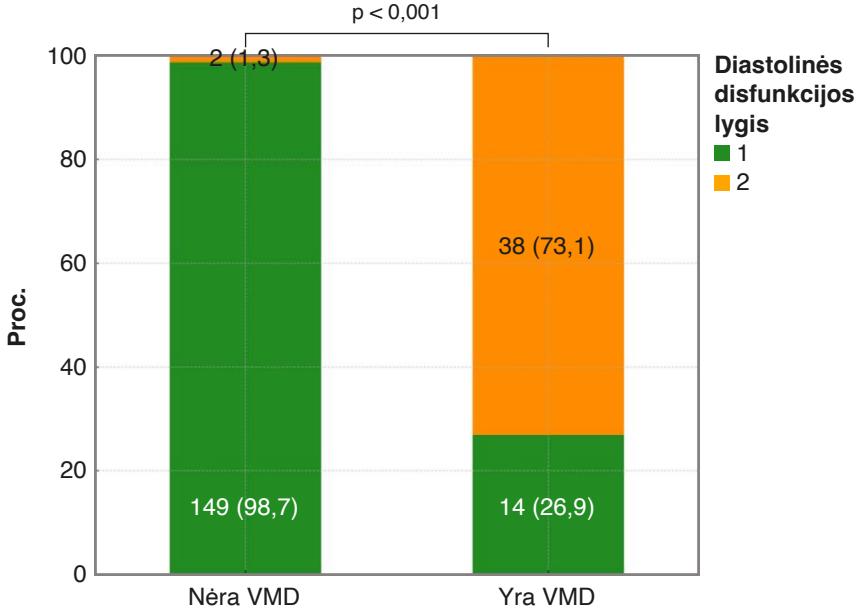

34 pav. *Diastolinės disfunkcijos dažnumas, atsižvelgiant į VMD*

VMD – vainikinės mikrocirkuliacijos disfunkcija.

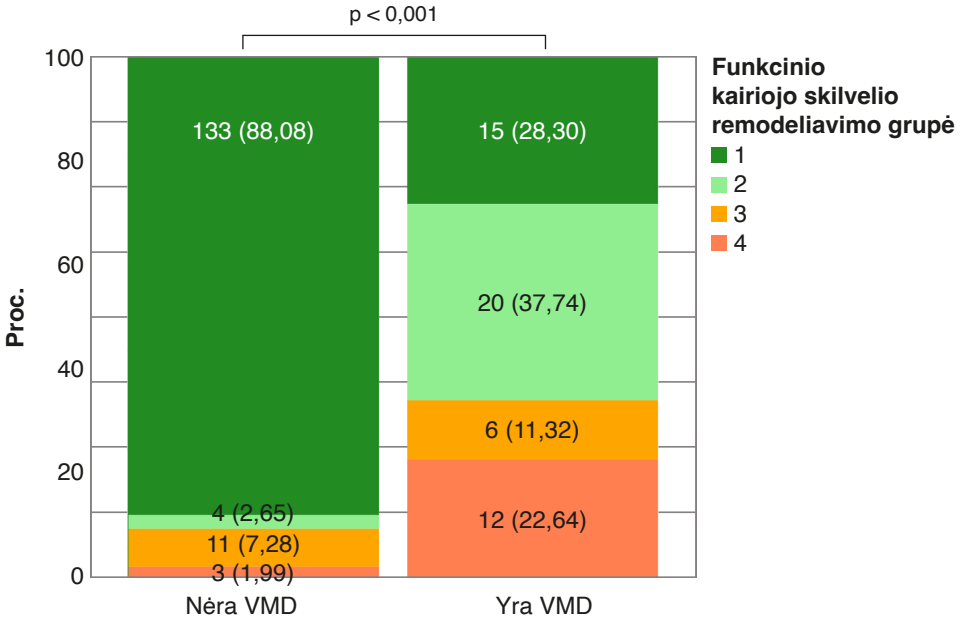

35 pav. *Kairiojo skilvelio remodeliavimasis, atsižvelgiant į VMD*

VMD – vainikinės mikrocirkuliacijos disfunkcija.

6.6.3. Klinikinės baigtys

VMD grupėje dažniau nustatytas išeminis insultas, pasikartojantis miokardo infarktas (MI), kraujagyslių revaskuliarizacija dėl trombozės ir guldymas į ligoninę dėl širdies nepakankamumo, palyginti su VMD nesergančių žmonių grupe. Tai rodo aiškią ir didesnę ŠDK riziką VMD sergantiems pacientams. Mirštamumas nuo širdies ir kraujagyslių ligų VMD grupėje šiek tiek padidėjo, tačiau jis nebuvo statistiškai reikšmingas. Pacientams, sergantiems VMD, 12 mėnesių laikotarpiu po PTVAA reikšmingai dažniau stebėtas ŠDK, palyginti su VMD nesergančiais pacientais (50,88 proc. *plg.* 9,80 proc.; $p < 0,001$), kaip parodyta 36 ir 37 pav. *Kaplano ir Meierio* kreivė parodė, kad ŠDK atvejų VMD grupėje padaugėjo jau pradedant pirmuoju stebėjimo po PTVAA mėnesiu.

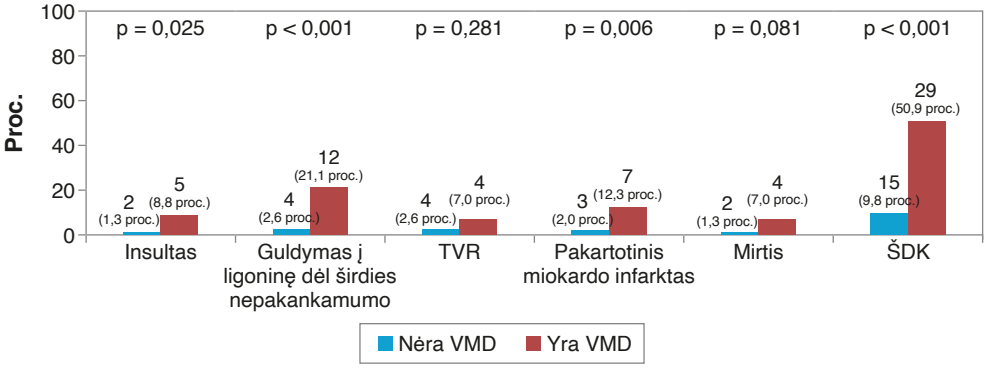

36 pav. *ŠDK sudėtiniai komponentai atsivelgiant į VMD*

VMD – vainikinės mikrocirkuliacijos disfunkcija; TVR – tikslinės kraujagyslės revaskuliarizacija; ŠDK – širdies didžiosios komplikacijos.

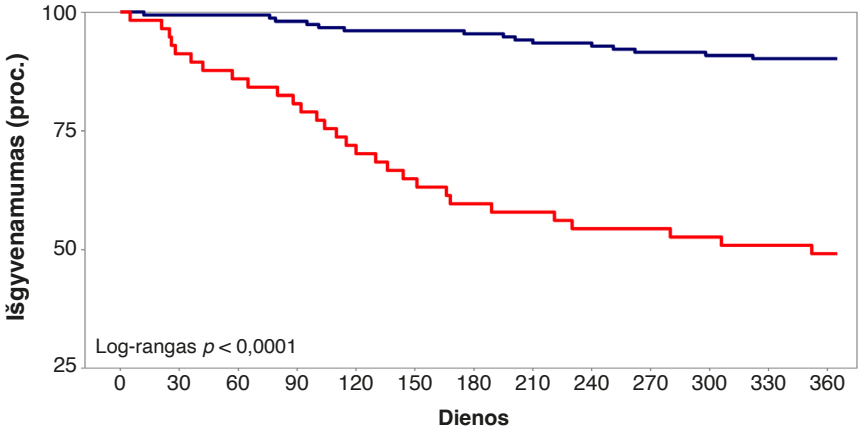

STRATA	Tiriamųjų skaičius rizikos grupėje												
Nėra VMD	153	152	152	150	147	147	146	144	143	140	139	138	138
Yra VMD	57	52	49	46	41	37	34	33	31	31	30	28	28

37 pav. *Kaplano ir Meierio kreivė, rodanti ŠDK įvykius, atsižvelgiant į VMD*

VMD – vainikinės mikrocirkuliacijos disfunkcija, STRATA – tiriama populiacijos dalis.

Daugiaveiksnės logistinės regresijos modelis atskleidė pradinį E/e' ir IMR kaip nepriklausomus antrojo laipsnio KS diastolinės disfunkcijos prognozinius kintamuosius, kurių AUC yra 0,933, o tai galima laikyti geru prognoziniu kintamuoju. FKSRBNP ir 3 mėnesių IMR buvo nustatyti kaip svarbūs prognoziniai sunkesnės remodeliacijos kintamieji (AUC 0,773), tai rodo reikšmingą IMR ir BNP vaidmenį prognozuojant širdies funkcinę būklę po MIkSTP.

7. IŠVADOS

Disertacijoje pateikiama išsami MIkSTP pacientų VMD analizė, atskleidžianti svarbias šešių tarpusavyje susijusių tyrimų įžvalgas.

1. Tiesioginis stentavimas, aspiracinė trombektomija ir individualizuotasis intrakoronarinis gydymas, taikant glikoproteino IIb / IIIa inhibitorius, reikšmingai – 5 kartus – sumažina VMD pasireiškimą, ir perpus – didžiųjų širdies komplikacijų dažnumą vienų metų laikotarpiu, palyginti su balionine dilatacija ir po jos atliekamu stentavimu.
2. Sukūrus ir atlikus pirminį mašininio mokymosi algoritmo patvirtinimą, išryškėjo pagrindinių biologinių žymenų, padedančių prognozuoti VMD, santykinės kintamosios vertės: TMAO, trombocitų atsako paveikus epinefrinu ir BNP (atitinkamai, 100 proc., 50,59 proc., 41,15 proc.). Algoritmui būdingi puikūs parametrų įverčiai, įskaitant tikslumą, jautrumą, specifiškumą (atitinkamai, 1, 0,91, 1).
3. Atlikus tikslinį TMAO tyrimą, nustatyta kritinė šio biologinio žymens koncentracijos vertė – 3,91 μM, kuri pabrėžia prognozinę reikšmę VMD atveju ir jo įtaką klinikiniams rezultatams bei kairiojo skilvelio funkcijos atsigavimui.
4. Mikrocirkuliacijos pasipriešinimo rezervas (MPR) (AUC = 0,701) yra geresnis VMD indikatorius, kuris pagrįstai konkuruoja su tradiciniais indikatoriais, pvz., frakcinės tėkmės rezervu (FFR) (AUC = 0,576).
5. Daugiau nei ketvirtadaliui MIkSTP sergančių pacientų VMD dažniausiai pasireiškia struktūrinio pobūdžio forma, susijusia su blogesne klinikine baigtimi ir individualizuotojo gydymo poreikiu.
6. Praėjus trims mėnesiams po MIkSTP, VMD reikšmingai susijęs su nepalankiu kairiojo skilvelio remodeliavimusi (pasireiškia 14 kartų dažniau), diastoline disfunkcija (pasireiškia 55 kartus dažniau) ir padidėjusiu ŠDK vienų metų laikotarpiu (pasireiškia 5 kartus dažniau).

8. PRAKTINĖS REKOMENDACIJOS

1. Patobulintos PTVAA strategijos ligoniams, sergantiems MIkSTP: pirmenybę teikti tiesioginiam stentavimui, aspiracinei trombektomijai, taikyti intrakoronarinio glikoproteino IIb / IIIa inhibitorius PTVAA metu, norint sumažinti VMD riziką ir pagerinti pacientų gydymo baigtis.
2. Pažangi diagnostika ir individualizuotasis gydymas: stebėti TMAO VMD prognozavimui bei pritaikyti TAMIR mašininio mokymosi modelį tiksliam VMD nustatymui.
3. Standartizuoti MPR tyrimo atlikimą ligoniams, sirgusiems MIkSTP: patikimas VMD diagnostikos įrankis, turintis geresnį prognozinį našumą, palyginti su kitais standartiniais metodais, taikomais klinikinėje praktikoje.
4. Pritaikytas struktūrinio VMD endotipo gydymas: daugiausia STEMI pacientų turi struktūrinės endotipo formos VMD, tai lemia blogesnes klinikines baigtis.
5. Ankstyva intervencija širdies nepakankamumo profilaktikai: atlikti ankstyvą VMD vertinimą, norint įtarti širdies nepakankamumą – ypatingą dėmesį skirti FKSR ir diastolinei disfunkcijai po MIkSTP.

REFERENCES

1. Lindstrom M., DeCleene N., Dorsey H., et al. Global Burden of Cardiovascular Diseases and Risks Collaboration, 1990-2021. J Am Coll Cardiol 2022;80(25):2372–425. Doi: 10.1016/j.jacc.2022.11.001.
2. Townsend N., Wilson L., Bhatnagar P., Wickramasinghe K., Rayner M., Nichols M. Cardiovascular disease in Europe: epidemiological update 2016. Eur Heart J 2016;37(42):3232–45. Doi: 10.1093/eurheartj/ehw334.
3. Pendyal A., Rothenberg C., Scofi JE., et al. National Trends in Emergency Department Care Processes for Acute Myocardial Infarction in the United States, 2005 to 2015. J Am Heart Assoc 2020;9(20). Doi: 10.1161/JAHA.120.017208.
4. Byrne RA., Rossello X., Coughlan JJ., et al. 2023 ESC Guidelines for the management of acute coronary syndromes. Eur Heart J 2023;44(38):3720–826. Doi: 10.1093/eurheartj/ehad191.
5. Bulluck H., Foin N., Tan JW., Low AF., Sezer M., Hausenloy DJ. Invasive Assessment of the Coronary Microcirculation in Reperfused ST-Segment–Elevation Myocardial Infarction Patients. Circ Cardiovasc Interv 2017;10(3). Doi: 10.1161/CIRCINTERVENTIONS.116.004373.
6. Montone RA., Vetrugno V., Santacroce G., et al. Recurrence of angina after ST-segment elevation myocardial infarction: the role of coronary microvascular obstruction. Eur Heart J Acute Cardiovasc Care 2021;10(6):624–32. Doi: 10.1177/2048872619880661.
7. Kaski J-C., Crea F., Gersh BJ., Camici PG. Reappraisal of Ischemic Heart Disease. Circulation 2018;138(14):1463–80. Doi: 10.1161/CIRCULATIONAHA.118.031373.
8. Taqueti VR., Di Carli MF. Coronary Microvascular Disease Pathogenic Mechanisms and Therapeutic Options: JACC State-of-the-Art Review. J Am Coll Cardiol 2018; 72(21):2625–41. Doi: 10.1016/j.jacc.2018.09.042.
9. Rehan R., Yong A., Ng M., Weaver J., Puranik R. Coronary microvascular dysfunction: A review of recent progress and clinical implications. Front Cardiovasc Med 2023;10. Doi: 10.3389/fcvm.2023.1111721.
10. Knuuti J., Bengel F., Bax JJ., et al. Risks and benefits of cardiac imaging: an analysis of risks related to imaging for coronary artery disease. Eur Heart J 2014;35(10):633–8. Doi: 10.1093/eurheartj/eht512.
11. Gallinoro E., Bertolone DT., Fernandez-Peregrina E., et al. Reproducibility of bolus versus continuous thermodilution for assessment of coronary microvascular function in patients with ANOCA. EuroIntervention 2023;19(2):e155–66. Doi: 10.4244/EIJ-D-22-00772.
12. Ford TJ., Stanley B., Sidik N., et al. 1-Year Outcomes of Angina Management Guided by Invasive Coronary Function Testing (CorMicA). JACC Cardiovasc Interv 2020;13(1):33–45. Doi: 10.1016/j.jcin.2019.11.001.
13. Aldujeli A., Haq A., Tsai T-Y., et al. The impact of primary percutaneous coronary intervention strategies during ST-elevation myocardial infarction on the prevalence of coronary microvascular dysfunction. Sci Rep 2023;13(1):20094. Doi: 10.1038/s41598-023-47343-x.
14. Cohen M., Boiangiu C., Abidi M. Therapy for ST-Segment Elevation Myocardial Infarction Patients Who Present Late or Are Ineligible for Reperfusion Therapy. J Am Coll Cardiol 2010;55(18):1895–906. Doi: 10.1016/j.jacc.2009.11.087.

15. van Kranenburg M., Magro M., Thiele H., et al. Prognostic Value of Microvascular Obstruction and Infarct Size, as Measured by CMR in STEMI Patients. JACC Cardiovasc Imaging 2014;7(9):930–9. Doi: 10.1016/j.jcmg.2014.05.010.
16. Reffelmann T., Kloner RA. Microvascular reperfusion injury: rapid expansion of anatomic no reflow during reperfusion in the rabbit. American Journal of Physiology-Heart and Circulatory Physiology 2002;283(3):H1099–107. Doi: 10.1152/ajpheart.00270.2002.
17. Gerber BL., Rochitte CE., Melin JA., et al. Microvascular Obstruction and Left Ventricular Remodeling Early After Acute Myocardial Infarction. Circulation 2000;101(23):2734–41. Doi: 10.1161/01.CIR.101.23.2734.
18. Kloner RA., Ganote CE., Jennings RB. The "No-Reflow" Phenomenon after Temporary Coronary Occlusion in the Dog. Journal of Clinical Investigation 1974; 54(6):1496–508. Doi: 10.1172/JCI107898.
19. Galli M., Niccoli G., De Maria G., et al. Coronary microvascular obstruction and dysfunction in patients with acute myocardial infarction. Nat Rev Cardiol 2023. Doi: 10.1038/s41569-023-00953-4.
20. Krug A., Du Mesnil de Rochemont., Korb G. Blood supply of the myocardium after temporary coronary occlusion. Circ Res 1966;19(1):57–62. Doi: 10.1161/01.res.19.1.57.
21. Ames A., Wright RL., Kowada M., Thurston JM., Majno G. Cerebral ischemia. II. The no-reflow phenomenon. Am J Pathol 1968;52(2):437–53.
22. Kloner RA. No-Reflow Phenomenon: Maintaining Vascular Integrity. J Cardiovasc Pharmacol Ther 2011;16(3–4):244–50. Doi: 10.1177/1074248411405990.
23. Schofer J., Montz R., Mathey DG. Scintigraphic evidence of the "No reflow" phenomenon in human beings after coronary thrombolysis. J Am Coll Cardiol 1985;5(3):593–8. Doi: 10.1016/S0735-1097(85)80381-8.
24. Bates ER., Krell MJ., Dean EN., O'Neill WW., Vogel RA. Demonstration of the "no-reflow" phenomenon by digital coronary arteriography. Am J Cardiol 1986; 57(1):177–8. Doi: 10.1016/0002-9149(86)90976-8.
25. Feld H., Lichstein E., Schachter J., Shani J. Early and late angiographic findings of the "no-reflow" phenomenon following direct angioplasty as primary treatment for acute myocardial infarction. Am Heart J 1992;123(3):782–4. Doi: 10.1016/0002-8703(92)90520-6.
26. Harrison RW., Aggarwal A., Ou F., et al. Incidence and Outcomes of No-Reflow Phenomenon During Percutaneous Coronary Intervention Among Patients With Acute Myocardial Infarction. Am J Cardiol 2013;111(2):178–84. Doi: 10.1016/j.amjcard.2012.09.015.
27. Sezer M., van Royen N., Umman B., et al. Coronary Microvascular Injury in Reperfused Acute Myocardial Infarction: A View From an Integrative Perspective. J Am Heart Assoc 2018;7(21). Doi: 10.1161/JAHA.118.009949.
28. McCartney PJ., Eteiba H., Maznyczka AM., et al. Effect of Low-Dose Intracoronary Alteplase During Primary Percutaneous Coronary Intervention on Microvascular Obstruction in Patients With Acute Myocardial Infarction. JAMA 2019;321(1):56. Doi: 10.1001/jama.2018.19802.
29. Carrick D., Haig C., Ahmed N., et al. Temporal Evolution of Myocardial Hemorrhage and Edema in Patients After Acute ST-Segment Elevation Myocardial Infarction: Pathophysiological Insights and Clinical Implications. J Am Heart Assoc 2016; 5(2). Doi: 10.1161/JAHA.115.002834.

30. van den Bos EJ., Baks T., Moelker AD., et al. Magnetic resonance imaging of haemorrhage within reperfused myocardial infarcts: possible interference with iron oxide-labelled cell tracking? Eur Heart J 2006;27(13):1620–6. Doi: 10.1093/eurheartj/ehl059.
31. Robbers LFHJ., Eerenberg ES., Teunissen PFA., et al. Magnetic resonance imaging-defined areas of microvascular obstruction after acute myocardial infarction represent microvascular destruction and haemorrhage. Eur Heart J 2013;34(30):2346–53. Doi: 10.1093/eurheartj/eht100.
32. Betgem RP., de Waard GA., Nijveldt R., Beek AM., Escaned J., van Royen N. Intramyocardial haemorrhage after acute myocardial infarction. Nat Rev Cardiol 2015;12(3):156–67. Doi: 10.1038/nrcardio.2014.188.
33. Hollander MR., de Waard GA., Konijnenberg LSF., et al. Dissecting the Effects of Ischemia and Reperfusion on the Coronary Microcirculation in a Rat Model of Acute Myocardial Infarction. PLoS One 2016;11(7):e0157233. Doi: 10.1371/journal.pone.0157233.
34. Camici PG., d'Amati G., Rimoldi O. Coronary microvascular dysfunction: mechanisms and functional assessment. Nat Rev Cardiol 2015;12(1):48–62. Doi: 10.1038/nrcardio.2014.160.
35. Pries AR., Reglin B. Coronary microcirculatory pathophysiology: can we afford it to remain a black box? Eur Heart J 2016:ehv760. Doi: 10.1093/eurheartj/ehv760.
36. Cannon RO., Epstein SE. "Microvascular angina" as a cause of chest pain with angiographically normal coronary arteries. Am J Cardiol 1988;61(15):1338–43. Doi: 10.1016/0002-9149(88)91180-0.
37. Lanza GA., Crea F. Primary Coronary Microvascular Dysfunction. Circulation 2010;121(21):2317–25. Doi: 10.1161/CIRCULATIONAHA.109.900191.
38. Niccoli G., Scalone G., Crea F. Acute myocardial infarction with no obstructive coronary atherosclerosis: mechanisms and management. Eur Heart J 2015;36(8):475–81. Doi: 10.1093/eurheartj/ehu469.
39. Tschöpe C., Van Linthout S. New Insights in (Inter)Cellular Mechanisms by Heart Failure with Preserved Ejection Fraction. Curr Heart Fail Rep 2014;11(4):436–44. Doi: 10.1007/s11897-014-0219-3.
40. Herrmann J., Kaski JC., Lerman A. Coronary microvascular dysfunction in the clinical setting: from mystery to reality. Eur Heart J 2012;33(22):2771–83. Doi: 10.1093/eurheartj/ehs246.
41. Yellon DM., Hausenloy DJ. Myocardial Reperfusion Injury. New England Journal of Medicine 2007;357(11):1121–35. Doi: 10.1056/NEJMra071667.
42. Reffelmann T., Hale SL., Li G., Kloner RA. Relationship between no reflow and infarct size as influenced by the duration of ischemia and reperfusion. American Journal of Physiology-Heart and Circulatory Physiology 2002;282(2):H766–72. Doi: 10.1152/ajpheart.00767.2001.
43. Rochitte CE., Lima JAC., Bluemke DA., et al. Magnitude and Time Course of Microvascular Obstruction and Tissue Injury After Acute Myocardial Infarction. Circulation 1998;98(10):1006–14. Doi: 10.1161/01.CIR.98.10.1006.
44. Engler RL., Schmid-Schönbein GW., Pavelec RS. Leukocyte capillary plugging in myocardial ischemia and reperfusion in the dog. Am J Pathol 1983;111(1):98–111.
45. Ambrosio G., Weisman HF., Mannisi JA., Becker LC. Progressive impairment of regional myocardial perfusion after initial restoration of postischemic blood flow. Circulation 1989;80(6):1846–61. Doi: 10.1161/01.CIR.80.6.1846.

46. Orn S., Manhenke C., Greve OJ., et al. Microvascular obstruction is a major determinant of infarct healing and subsequent left ventricular remodelling following primary percutaneous coronary intervention. Eur Heart J 2009;30(16):1978–85. Doi: 10.1093/eurheartj/ehp219.
47. Reffelmann T., Hale SL., Dow JS., Kloner RA. No-Reflow Phenomenon Persists Long-Term After Ischemia/Reperfusion in the Rat and Predicts Infarct Expansion. Circulation 2003;108(23):2911–7. Doi: 10.1161/01.CIR.0000101917.80668.E1.
48. Yunoki K., Naruko T., Inoue T., et al. Relationship of Thrombus Characteristics to the Incidence of Angiographically Visible Distal Embolization in Patients With ST-Segment Elevation Myocardial Infarction Treated With Thrombus Aspiration. JACC Cardiovasc Interv 2013;6(4):377–85. Doi: 10.1016/j.jcin.2012.11.011.
49. Napodano M., Peluso D., Marra MP., et al. Time-Dependent Detrimental Effects of Distal Embolization on Myocardium and Microvasculature During Primary Percutaneous Coronary Intervention. JACC Cardiovasc Interv 2012;5(11):1170–7. Doi: 10.1016/j.jcin.2012.06.022.
50. Okamura A., Ito H., Iwakura K., et al. Clinical Implications of Distal Embolization During Coronary Interventional Procedures in Patients With Acute Myocardial Infarction. JACC Cardiovasc Interv 2008;1(3):268–76. Doi: 10.1016/j.jcin.2008.03.015.
51. Lønborg J., Kelbæk H., Helqvist S., et al. The impact of distal embolization and distal protection on long-term outcome in patients with ST elevation myocardial infarction randomized to primary percutaneous coronary intervention – results from a randomized study. Eur Heart J Acute Cardiovasc Care 2015;4(2):180–8. Doi: 10.1177/2048872614543780.
52. Sharma V., Jolly SS., Hamid T., et al. Myocardial blush and microvascular reperfusion following manual thrombectomy during percutaneous coronary intervention for ST elevation myocardial infarction: insights from the TOTAL trial. Eur Heart J 2016;37(24):1891–8. Doi: 10.1093/eurheartj/ehw157.
53. Kumbhani DJ., Bavry AA., Desai MY., Bangalore S., Bhatt DL. Role of Aspiration and Mechanical Thrombectomy in Patients With Acute Myocardial Infarction Undergoing Primary Angioplasty. J Am Coll Cardiol 2013;62(16):1409–18. Doi: 10.1016/j.jacc.2013.04.025.
54. Lipiecki J., Monzy S., Durel N., et al. Effect of thrombus aspiration on infarct size and left ventricular function in high-risk patients with acute myocardial infarction treated by percutaneous coronary intervention. Results of a prospective controlled pilot study. Am Heart J 2009;157(3):583.e1-583.e7. Doi: 10.1016/j.ahj.2008.11.017.
55. Sirker A., Mamas M., Kwok CS., Kontopantelis E., Ludman P., Hildick-Smith D. Outcomes From Selective Use of Thrombectomy in Patients Undergoing Primary Percutaneous Coronary Intervention for ST-Segment Elevation Myocardial Infarction. JACC Cardiovasc Interv 2016;9(2):126–34. Doi: 10.1016/j.jcin.2015.10.047.
56. Fröbert O., Lagerqvist B., Olivecrona GK., et al. Thrombus Aspiration during ST-Segment Elevation Myocardial Infarction. New England Journal of Medicine 2013;369(17):1587–97. Doi: 10.1056/NEJMoa1308789.
57. Elgendy IY., Huo T., Bhatt DL., Bavry AA. Is Aspiration Thrombectomy Beneficial in Patients Undergoing Primary Percutaneous Coronary Intervention? Circ Cardiovasc Interv 2015;8(7). Doi: 10.1161/CIRCINTERVENTIONS.114.002258.

58. Götz AK., Zahler S., Stumpf P., Welsch U., Becker BF. Intracoronary formation and retention of micro aggregates of leukocytes and platelets contribute to postischemic myocardial dysfunction. Basic Res Cardiol 2005;100(5):413–21. Doi: 10.1007/s00395-005-0540-9.
59. Driesen RB., Zalewski J., Driessche N Vanden., et al. Histological correlate of a cardiac magnetic resonance imaged microvascular obstruction in a porcine model of ischemia–reperfusion. Cardiovascular Pathology 2012;21(3):129–31. Doi: 10.1016/j.carpath.2011.07.008.
60. Sheridan FM., Cole PG., Ramage D. Leukocyte Adhesion to the Coronary Microvasculature During Ischemia and Reperfusion in an In Vivo Canine Model. Circulation 1996;93(10):1784–7. Doi: 10.1161/01.CIR.93.10.1784.
61. Frangogiannis NG., Youker KA., Rossen RD., et al. Cytokines and the Microcirculation in Ischemia and Reperfusion. J Mol Cell Cardiol 1998;30(12):2567–76. Doi: 10.1006/jmcc.1998.0829.
62. Damiano ER. The Effect of the Endothelial-Cell Glycocalyx on the Motion of Red Blood Cells through Capillaries. Microvasc Res 1998;55(1):77–91. Doi: 10.1006/mvre.1997.2052.
63. Faxon DP., Gibbons RJ., Chronos NAF., Gurbel PA., Sheehan F. The effect of blockade of the CD11/CD18 integrin receptor on infarct size in patients with acute myocardial infarction treated with direct angioplasty: the results of the HALT-MI study. J Am Coll Cardiol 2002;40(7):1199–204. Doi: 10.1016/S0735-1097(02)02136-8.
64. Thiele H., Wöhrle J., Hambrecht R., et al. Intracoronary versus intravenous bolus abciximab during primary percutaneous coronary intervention in patients with acute ST-elevation myocardial infarction: a randomised trial. The Lancet 2012;379(9819):923–31. Doi: 10.1016/S0140-6736(11)61872-2.
65. APEX AMI Investigators., Armstrong PW., Granger CB., et al. Pexelizumab for acute ST-elevation myocardial infarction in patients undergoing primary percutaneous coronary intervention: a randomized controlled trial. JAMA 2007;297(1):43–51. Doi: 10.1001/jama.297.1.43.
66. French CJ., Zaman AKMT., Kelm RJ., Spees JL., Sobel BE. Vascular rhexis: loss of integrity of coronary vasculature in mice subjected to myocardial infarction. Exp Biol Med 2010;235(8):966–73. Doi: 10.1258/ebm.2010.010108.
67. Pedersen CM., Barnes G., Schmidt MR., et al. Ischaemia–reperfusion injury impairs tissue plasminogen activator release in man. Eur Heart J 2012;33(15):1920–7. Doi: 10.1093/eurheartj/ehr380.
68. Bach TL., Barsigian C., Yaen CH., Martinez J. Endothelial Cell VE-cadherin Functions as a Receptor for the β15–42 Sequence of Fibrin. Journal of Biological Chemistry 1998;273(46):30719–28. Doi: 10.1074/jbc.273.46.30719.
69. Béguin S., Kumar R., Keularts I., Seligsohn U., Coller BS., Hemker HC. Fibrin-Dependent Platelet Procoagulant Activity Requires GPIb Receptors and von Willebrand Factor. Blood 1999;93(2):564–70. Doi: 10.1182/blood.V93.2.564.
70. Goel MS., Diamond SL. Adhesion of normal erythrocytes at depressed venous shear rates to activated neutrophils, activated platelets, and fibrin polymerized from plasma. Blood 2002;100(10):3797–803. Doi: 10.1182/blood-2002-03-0712.
71. Zhang ZG., Chopp M., Goussev A., et al. Cerebral Microvascular Obstruction by Fibrin is Associated with Upregulation of PAI-1 Acutely after Onset of Focal Embolic Ischemia in Rats. The Journal of Neuroscience 1999;19(24):10898–907. Doi: 10.1523/JNEUROSCI.19-24-10898.1999.

72. Schoots IG., Levi M., Roossink EHP., Bijlsma PB., van Gulik TM. Local intravascular coagulation and fibrin deposition on intestinal ischemia-reperfusion in rats. Surgery 2003;133(4):411–9. Doi: 10.1067/msy.2003.104.
73. Yamada K., Miwa T., Liu J., Nangaku M., Song W-C. Critical Protection from Renal Ischemia Reperfusion Injury by CD55 and CD59. The Journal of Immunology 2004;172(6):3869–75. Doi: 10.4049/jimmunol.172.6.3869.
74. Ami R Ben., Barshtein G., Zeltser D., et al. Parameters of red blood cell aggregation as correlates of the inflammatory state. American Journal of Physiology-Heart and Circulatory Physiology 2001;280(5):H1982–8. Doi: 10.1152/ajpheart.2001.280.5.H1982.
75. Sriramarao P., Languino L., Altieri D. Fibrinogen mediates leukocyte-endothelium bridging in vivo at low shear forces. Blood 1996;88(9):3416–23. Doi: 10.1182/blood.V88.9.3416.bloodjournal8893416.
76. Kupatt C., Habazettl H., Hanusch P., et al. c7E3Fab Reduces Postischemic Leukocyte-Thrombocyte Interaction Mediated by Fibrinogen. Arterioscler Thromb Vasc Biol 2000;20(10):2226–32. Doi: 10.1161/01.ATV.20.10.2226.
77. Sezer M., Oflaz H., Gören T., et al. Intracoronary Streptokinase after Primary Percutaneous Coronary Intervention. New England Journal of Medicine 2007;356(18):1823–34. Doi: 10.1056/NEJMoa054374.
78. Sezer M., Çimen A., Aslanger E., et al. Effect of Intracoronary Streptokinase Administered Immediately After Primary Percutaneous Coronary Intervention on Long-Term Left Ventricular Infarct Size, Volumes, and Function. J Am Coll Cardiol 2009;54(12):1065–71. Doi: 10.1016/j.jacc.2009.04.083.
79. Greco C., Pelliccia F., Tanzilli G., et al. Usefulness of Local Delivery of Thrombolytics Before Thrombectomy in Patients With ST-Segment Elevation Myocardial Infarction Undergoing Primary Percutaneous Coronary Intervention (the Delivery of Thrombolytics Before Thrombectomy in Patients With ST-Segment Elevation Myocardial Infarction Undergoing Primary Percutaneous Coronary Intervention [DISSOLUTION] Randomized Trial). Am J Cardiol 2013;112(5):630–5. Doi: 10.1016/j.amjcard.2013.04.036.
80. Armstrong PW. Intracoronary streptokinase in acute myocardial infarction. Nat Rev Cardiol 2010;7(2):67–9. Doi: 10.1038/nrcardio.2009.230.
81. McCartney PJ., Maznyczka AM., Eteiba H., et al. Low-Dose Alteplase During Primary Percutaneous Coronary Intervention According to Ischemic Time. J Am Coll Cardiol 2020;75(12):1406–21. Doi: 10.1016/j.jacc.2020.01.041.
82. Aversano T., Becker LC. Persistence of coronary vasodilator reserve despite functionally significant flow reduction. American Journal of Physiology-Heart and Circulatory Physiology 1985;248(3):H403–11. Doi: 10.1152/ajpheart.1985.248.3.H403.
83. Heusch G. The Coronary Circulation as a Target of Cardioprotection. Circ Res 2016;118(10):1643–58. Doi: 10.1161/CIRCRESAHA.116.308640.
84. Niccoli G., Rigattieri S., De Vita MR., et al. Open-Label, Randomized, Placebo-Controlled Evaluation of Intracoronary Adenosine or Nitroprusside After Thrombus Aspiration During Primary Percutaneous Coronary Intervention for the Prevention of Microvascular Obstruction in Acute Myocardial Infarction. JACC Cardiovasc Interv 2013;6(6):580–9. Doi: 10.1016/j.jcin.2013.02.009.
85. Nazir SA., McCann GP., Greenwood JP., et al. Strategies to attenuate micro-vascular obstruction during P-PCI: the randomized reperfusion facilitated by local adjunctive therapy in ST-elevation myocardial infarction trial. Eur Heart J 2016;37(24):1910–9. Doi: 10.1093/eurheartj/ehw136.

86. Desai KV., Laine GA., Stewart RH., et al. Mechanics of the left ventricular myocardial interstitium: effects of acute and chronic myocardial edema. American Journal of Physiology-Heart and Circulatory Physiology 2008;294(6):H2428–34. Doi: 10.1152/ajpheart.00860.2007.
87. Schwartz BG., Kloner RA. Coronary no reflow. J Mol Cell Cardiol 2012;52(4):873–82. Doi: 10.1016/j.yjmcc.2011.06.009.
88. Payne AR., Berry C., Kellman P., et al. Bright-Blood T 2 -Weighted MRI Has High Diagnostic Accuracy for Myocardial Hemorrhage in Myocardial Infarction. Circ Cardiovasc Imaging 2011;4(6):738–45. Doi: 10.1161/CIRCIMAGING.111.965095.
89. Gao X-M., Wu Q-Z., Kiriazis H., et al. Microvascular leakage in acute myocardial infarction: characterization by histology, biochemistry, and magnetic resonance imaging. American Journal of Physiology-Heart and Circulatory Physiology 2017;312(5):H1068–75. Doi: 10.1152/ajpheart.00073.2017.
90. Kloner RA., Rude RE., Carlson N., Maroko PR., DeBoer LW., Braunwald E. Ultrastructural evidence of microvascular damage and myocardial cell injury after coronary artery occlusion: which comes first? Circulation 1980;62(5):945–52. Doi: 10.1161/01.CIR.62.5.945.
91. Fernández-Jiménez R., Sánchez-González J., Agüero J., et al. Myocardial Edema After Ischemia/Reperfusion Is Not Stable and Follows a Bimodal Pattern. J Am Coll Cardiol 2015;65(4):315–23. Doi: 10.1016/j.jacc.2014.11.004.
92. Nordlund D., Klug G., Heiberg E., et al. Multi-vendor, multicentre comparison of contrast-enhanced SSFP and T2-STIR CMR for determining myocardium at risk in ST-elevation myocardial infarction. Eur Heart J Cardiovasc Imaging 2016;17(7):744–53. Doi: 10.1093/ehjci/jew027.
93. Fernández-Jiménez R., Barreiro-Pérez M., Martin-García A., et al. Dynamic Edematous Response of the Human Heart to Myocardial Infarction. Circulation 2017;136(14):1288–300. Doi: 10.1161/CIRCULATIONAHA.116.025582.
94. Carrick D., Haig C., Ahmed N., et al. Myocardial Hemorrhage After Acute Reperfused ST-Segment–Elevation Myocardial Infarction. Circ Cardiovasc Imaging 2016;9(1). Doi: 10.1161/CIRCIMAGING.115.004148.
95. Husser O., Monmeneu J V., Sanchis J., et al. Cardiovascular magnetic resonance-derived intramyocardial hemorrhage after STEMI: Influence on long-term prognosis, adverse left ventricular remodeling and relationship with microvascular obstruction. Int J Cardiol 2013;167(5):2047–54. Doi: 10.1016/j.ijcard.2012.05.055.
96. Mather AN., Fairbairn TA., Ball SG., Greenwood JP., Plein S. Reperfusion haemorrhage as determined by cardiovascular MRI is a predictor of adverse left ventricular remodelling and markers of late arrhythmic risk. Heart 2011;97(6):453–9. Doi: 10.1136/hrt.2010.202028.
97. Amier RP., Tijssen RYG., Teunissen PFA., et al. Predictors of Intramyocardial Hemorrhage After Reperfused ST-Segment Elevation Myocardial Infarction. J Am Heart Assoc 2017;6(8). Doi: 10.1161/JAHA.117.005651.
98. Willerson JT., Scales F., Mukherjee A., et al. Abnormal myocardial fluid retention as an early manifestation of ischemic injury. Am J Pathol 1977;87(1):159–88.
99. Mathey DG., Schofer J., Kuck KH., Beil U., Kloppel G. Transmural, haemorrhagic myocardial infarction after intracoronary streptokinase. Clinical, angiographic, and necropsy findings. Heart 1982;48(6):546–51. Doi: 10.1136/hrt.48.6.546.

100. Waller BF., Rothbaum DA., Pinkerton CA., et al. Status of the myocardium and infarct-related coronary artery in 19 necropsy patients with acute recanalization using pharmacologic (streptokinase, r-tissue plasminogen activator), mechanical (percutaneous transluminal coronary angioplasty) or combined types of reperfusion therapy. J Am Coll Cardiol 1987;9(4):785–801. Doi: 10.1016/S0735-1097(87)80234-6.
101. Bulluck H., Rosmini S., Abdel-Gadir A., et al. Residual Myocardial Iron Following Intramyocardial Hemorrhage During the Convalescent Phase of Reperfused ST-Segment–Elevation Myocardial Infarction and Adverse Left Ventricular Remodeling. Circ Cardiovasc Imaging 2016;9(10). Doi: 10.1161/CIRCIMAGING.116.004940.
102. Payne AR., Berry C., Doolin O., et al. Microvascular Resistance Predicts Myocardial Salvage and Infarct Characteristics in ST-Elevation Myocardial Infarction. J Am Heart Assoc 2012;1(4). Doi: 10.1161/JAHA.112.002246.
103. Carrick D., Haig C., Ahmed N., et al. Comparative Prognostic Utility of Indexes of Microvascular Function Alone or in Combination in Patients With an Acute ST-Segment–Elevation Myocardial Infarction. Circulation 2016;134(23):1833–47. Doi: 10.1161/CIRCULATIONAHA.116.022603.
104. Van Herck PL., Carlier SG., Claeys MJ., et al. Coronary microvascular dysfunction after myocardial infarction: increased coronary zero flow pressure both in the infarcted and in the remote myocardium is mainly related to left ventricular filling pressure. Heart 2007;93(10):1231–7. Doi: 10.1136/hrt.2006.100818.
105. Feher A., Sinusas AJ. Quantitative Assessment of Coronary Microvascular Function. Circ Cardiovasc Imaging 2017;10(8). Doi: 10.1161/CIRCIMAGING.117.006427.
106. Murthy VL., Naya M., Taqueti VR., et al. Effects of Sex on Coronary Microvascular Dysfunction and Cardiac Outcomes. Circulation 2014;129(24):2518–27. Doi: 10.1161/CIRCULATIONAHA.113.008507.
107. Taqueti VR., Everett BM., Murthy VL., et al. Interaction of Impaired Coronary Flow Reserve and Cardiomyocyte Injury on Adverse Cardiovascular Outcomes in Patients Without Overt Coronary Artery Disease. Circulation 2015;131(6):528–35. Doi: 10.1161/CIRCULATIONAHA.114.009716.
108. Ziadi MC., deKemp RA., Williams KA., et al. Impaired Myocardial Flow Reserve on Rubidium-82 Positron Emission Tomography Imaging Predicts Adverse Outcomes in Patients Assessed for Myocardial Ischemia. J Am Coll Cardiol 2011;58(7):740–8. Doi: 10.1016/j.jacc.2011.01.065.
109. Herzog BA., Husmann L., Valenta I., et al. Long-Term Prognostic Value of 13N-Ammonia Myocardial Perfusion Positron Emission Tomography. J Am Coll Cardiol 2009;54(2):150–6. Doi: 10.1016/j.jacc.2009.02.069.
110. Gupta A., Taqueti VR., van de Hoef TP., et al. Integrated Noninvasive Physiological Assessment of Coronary Circulatory Function and Impact on Cardiovascular Mortality in Patients With Stable Coronary Artery Disease. Circulation 2017;136(24):2325–36. Doi: 10.1161/CIRCULATIONAHA.117.029992.
111. Kotecha T., Martinez-Naharro A., Boldrini M., et al. Automated Pixel-Wise Quantitative Myocardial Perfusion Mapping by CMR to Detect Obstructive Coronary Artery Disease and Coronary Microvascular Dysfunction. JACC Cardiovasc Imaging 2019;12(10):1958–69. Doi: 10.1016/j.jcmg.2018.12.022.
112. Doyle M., Weinberg N., Pohost GM., et al. Prognostic Value of Global MR Myocardial Perfusion Imaging in Women With Suspected Myocardial Ischemia and No Obstructive Coronary Disease. JACC Cardiovasc Imaging 2010;3(10):1030–6. Doi: 10.1016/j.jcmg.2010.07.008.

113. Rigo F., Sicari R., Gherardi S., Djordjevic-Dikic A., Cortigiani L., Picano E. Prognostic Value of Coronary Flow Reserve in Medically Treated Patients With Left Anterior Descending Coronary Disease With Stenosis 51% to 75% in Diameter. Am J Cardiol 2007;100(10):1527–31. Doi: 10.1016/j.amjcard.2007.06.060.
114. Gan L., Svedlund S., Wittfeldt A., et al. Incremental Value of Transthoracic Doppler Echocardiography-Assessed Coronary Flow Reserve in Patients With Suspected Myocardial Ischemia Undergoing Myocardial Perfusion Scintigraphy. J Am Heart Assoc 2017;6(4). Doi: 10.1161/JAHA.116.004875.
115. Cortigiani L., Rigo F., Gherardi S., et al. Additional Prognostic Value of Coronary Flow Reserve in Diabetic and Nondiabetic Patients With Negative Dipyridamole Stress Echocardiography by Wall Motion Criteria. J Am Coll Cardiol 2007;50(14):1354–61. Doi: 10.1016/j.jacc.2007.06.027.
116. TIMI Study Group. Comparison of invasive and conservative strategies after treatment with intravenous tissue plasminogen activator in acute myocardial infarction. Results of the thrombolysis in myocardial infarction (TIMI) phase II trial. N Engl J Med 1989;320(10):618–27. Doi: 10.1056/NEJM198903093201002.
117. Stone GW., Brodie BR., Griffin JJ., et al. Prospective, Multicenter Study of the Safety and Feasibility of Primary Stenting in Acute Myocardial Infarction: In-Hospital and 30-Day Results of the PAMI Stent Pilot Trial fn1fn1Funding for this study was provided in part by an unrestricted grant from Johnson & Johnson Interventional Systems, Warren, New Jersey. J Am Coll Cardiol 1998;31(1):23–30. Doi: 10.1016/S0735-1097(97)00439-7.
118. Nijveldt R., Beek AM., Hirsch A., et al. 123 Functional recovery after acute myocardial infarction: a comparison between angiography, electrocardiography and cardiovascular magnetic resonance measures of microvascular injury. Journal of Cardiovascular Magnetic Resonance 2008;10(S1):A24. Doi: 10.1186/1532-429X-10-S1-A24.
119. Durante A., Laricchia A., Benedetti G., et al. Identification of High-Risk Patients After ST-Segment–Elevation Myocardial Infarction. Circ Cardiovasc Imaging 2017;10(6). Doi: 10.1161/CIRCIMAGING.116.005841.
120. Caixeta A., Lansky AJ., Mehran R., et al. Predictors of suboptimal TIMI flow after primary angioplasty for acute myocardial infarction: results from the HORIZONS-AMI trial. EuroIntervention 2013;9(2):220–7. Doi: 10.4244/EIJV9I2A37.
121. Gibson CM., Cannon CP., Daley WL., et al. TIMI Frame Count. Circulation 1996;93(5):879–88. Doi: 10.1161/01.CIR.93.5.879.
122. Kunadian V., Harrigan C., Zorkun C., et al. Use of the TIMI frame count in the assessment of coronary artery blood flow and microvascular function over the past 15 years. J Thromb Thrombolysis 2009;27(3):316–28. Doi: 10.1007/s11239-008-0220-3.
123. Manginas A., Gatzov P., Chasikidis C., Voudris V., Pavlides G., Cokkinos D V. Estimation of coronary flow reserve using the Thrombolysis In Myocardial Infarction (TIMI) frame count method. Am J Cardiol 1999;83(11):1562–4. Doi: 10.1016/S0002-9149(99)00149-6.
124. Gibson CM., Murphy SA., Rizzo MJ., et al. Relationship Between TIMI Frame Count and Clinical Outcomes After Thrombolytic Administration. Circulation 1999;99(15):1945–50. Doi: 10.1161/01.CIR.99.15.1945.

125. van ‘t Hof AWJ., Liem A., Suryapranata H., Hoorntje JCA., de Boer M-J., Zijlstra F. Angiographic Assessment of Myocardial Reperfusion in Patients Treated With Primary Angioplasty for Acute Myocardial Infarction. Circulation 1998;97(23): 2302–6. Doi: 10.1161/01.CIR.97.23.2302.
126. Gibson CM., Cannon CP., Murphy SA., et al. Relationship of TIMI Myocardial Perfusion Grade to Mortality After Administration of Thrombolytic Drugs. Circulation 2000;101(2):125–30. Doi: 10.1161/01.CIR.101.2.125.
127. Gibson CM., Schömig A. Coronary and Myocardial Angiography. Circulation 2004;109(25):3096–105. Doi: 10.1161/01.CIR.0000134278.50359.CB.
128. Ungi T., Sasi V., Ungi I., Forster T., Palkó A., Nemes A. Comparison of two visual angiographic perfusion grades in acute myocardial infarction. Ups J Med Sci 2009;114(3):149–53. Doi: 10.1080/03009730902990453.
129. Vicente J., Mewton N., Croisille P., et al. Comparison of the angiographic myocardial blush grade with delayed-enhanced cardiac magnetic resonance for the assessment of microvascular obstruction in acute myocardial infarctions. Catheterization and Cardiovascular Interventions 2009;74(7):1000–7. Doi: 10.1002/ccd.22157.
130. Marra MP., Corbetti F., Cacciavillani L., et al. Relationship between myocardial blush grades, staining, and severe microvascular damage after primary percutaneous coronary intervention. Am Heart J 2010;159(6):1124–32. Doi: 10.1016/j.ahj.2010.03.007.
131. Appelbaum E., Kirtane AJ., Clark A., et al. Association of TIMI Myocardial Perfusion Grade and ST-segment resolution with cardiovascular magnetic resonance measures of microvascular obstruction and infarct size following ST-segment elevation myocardial infarction. J Thromb Thrombolysis 2009;27(2):123–9. Doi: 10.1007/s11239-008-0197-y.
132. Vogelzang M., Vlaar PJ., Svilaas T., Amo D., Nijsten MWN., Zijlstra F. Computer-assisted myocardial blush quantification after percutaneous coronary angioplasty for acute myocardial infarction: a substudy from the TAPAS trial. Eur Heart J 2009;30(5):594–9. Doi: 10.1093/eurheartj/ehn542.
133. Porto I., Hamilton-Craig C., De Maria GL., et al. Quantitative Blush Evaluator accurately quantifies microvascular dysfunction in patients with ST-elevation myocardial infarction: Comparison with cardiovascular magnetic resonance. Am Heart J 2011;162(2):372-381.e2. Doi: 10.1016/j.ahj.2011.04.014.
134. Cole JS., Hartley CJ. The pulsed Doppler coronary artery catheter preliminary report of a new technique for measuring rapid changes in coronary artery flow velocity in man. Circulation 1977;56(1):18–25. Doi: 10.1161/01.CIR.56.1.18.
135. Kawamoto T., Yoshida K., Akasaka T., et al. Can Coronary Blood Flow Velocity Pattern After Primary Percutaneous Transluminal Coronary Angiography Predict Recovery of Regional Left Ventricular Function in Patients With Acute Myocardial Infarction? Circulation 1999;100(4):339–45. Doi: 10.1161/01.CIR.100.4.339.
136. Hirsch A., Nijveldt R., Haeck JDE., et al. Relation Between the Assessment of Microvascular Injury by Cardiovascular Magnetic Resonance and Coronary Doppler Flow Velocity Measurements in Patients With Acute Anterior Wall Myocardial Infarction. J Am Coll Cardiol 2008;51(23):2230–8. Doi: 10.1016/j.jacc.2008.01.064.
137. Furber AP., Prunier F., Nguyen HCP., Boulet S., Delépine S., Geslin P. Coronary Blood Flow Assessment After Successful Angioplasty for Acute Myocardial Infarction Predicts the Risk of Long-Term Cardiac Events. Circulation 2004;110(23): 3527–33. Doi: 10.1161/01.CIR.0000148686.95696.1E.

138. Gould KL., Lipscomb K., Hamilton GW. Physiologic basis for assessing critical coronary stenosis. Am J Cardiol 1974;33(1):87–94. Doi: 10.1016/0002-9149(74)90743-7.
139. van de Hoef TP., van Lavieren MA., Damman P., et al. Physiological Basis and Long-Term Clinical Outcome of Discordance Between Fractional Flow Reserve and Coronary Flow Velocity Reserve in Coronary Stenoses of Intermediate Severity. Circ Cardiovasc Interv 2014;7(3):301–11. Doi: 10.1161/CIRCINTERVENTIONS.113.001049.
140. Bax M., de Winter RJ., Schotborgh CE., et al. Short- and Long-Term recovery of left ventricular function predicted at the time of primary percutaneous coronary intervention in anterior myocardial infarction. J Am Coll Cardiol 2004;43(4):534–41. Doi: 10.1016/j.jacc.2003.08.055.
141. van de Hoef TP., Bax M., Meuwissen M., et al. Impact of Coronary Microvascular Function on Long-term Cardiac Mortality in Patients With Acute ST-Segment–Elevation Myocardial Infarction. Circ Cardiovasc Interv 2013;6(3):207–15. Doi: 10.1161/CIRCINTERVENTIONS.112.000168.
142. Cuculi F., Dall'Armellina E., Manlhiot C., et al. Early change in invasive measures of microvascular function can predict myocardial recovery following PCI for ST-elevation myocardial infarction. Eur Heart J 2014;35(29):1971–80. Doi: 10.1093/eurheartj/eht434.
143. de Bruyne B., Bartunek J., Sys SU., Pijls NHJ., Heyndrickx GR., Wijns W. Simultaneous Coronary Pressure and Flow Velocity Measurements in Humans. Circulation 1996;94(8):1842–9. Doi: 10.1161/01.CIR.94.8.1842.
144. Takahashi T., Hiasa Y., Ohara Y., et al. Usefulness of Coronary Flow Reserve Immediately After Primary Coronary Angioplasty for Acute Myocardial Infarction in Predicting Long-Term Adverse Cardiac Events. Am J Cardiol 2007;100(5):806–11. Doi: 10.1016/j.amjcard.2007.04.015.
145. Kern MJ. Coronary Physiology Revisited. Circulation 2000;101(11):1344–51. Doi: 10.1161/01.CIR.101.11.1344.
146. Nevo E., Nevo S., Beyar R. The physiologic meaning of relative coronary flow reserve. Am J Cardiol 1995;75(4):285–7. Doi: 10.1016/0002-9149(95)80039-U.
147. Kitabata H., Imanishi T., Kubo T., et al. Coronary Microvascular Resistance Index Immediately After Primary Percutaneous Coronary Intervention as a Predictor of the Transmural Extent of Infarction in Patients With ST-Segment Elevation Anterior Acute Myocardial Infarction. JACC Cardiovasc Imaging 2009;2(3):263–72. Doi: 10.1016/j.jcmg.2008.11.013.
148. Kitabata H., Kubo T., Ishibashi K., et al. Prognostic Value of Microvascular Resistance Index Immediately After Primary Percutaneous Coronary Intervention on Left Ventricular Remodeling in Patients With Reperfused Anterior Acute ST-Segment Elevation Myocardial Infarction. JACC Cardiovasc Interv 2013;6(10):1046–54. Doi: 10.1016/j.jcin.2013.05.014.
149. Teunissen PFA., de Waard GA., Hollander MR., et al. Doppler-Derived Intracoronary Physiology Indices Predict the Occurrence of Microvascular Injury and Microvascular Perfusion Deficits After Angiographically Successful Primary Percutaneous Coronary Intervention. Circ Cardiovasc Interv 2015;8(3). Doi: 10.1161/CIRCINTERVENTIONS.114.001786.
150. Maznyczka AM., McCartney P., Berry C. Reference invasive tests of microvascular injury in myocardial infarction. Heart 2018;104(2):90–2. Doi: 10.1136/heartjnl-2017-311695.

151. Jin X., Yoon M-H., Seo K-W., et al. Usefulness of Hyperemic Microvascular Resistance Index as a Predictor of Clinical Outcomes in Patients with ST-Segment Elevation Myocardial Infarction. Korean Circ J 2015;45(3):194. Doi: 10.4070/kcj.2015.45.3.194.
152. Patel N., Petraco R., Dall'Armellina E., et al. Zero-Flow Pressure Measured Immediately After Primary Percutaneous Coronary Intervention for ST-Segment Elevation Myocardial Infarction Provides the Best Invasive Index for Predicting the Extent of Myocardial Infarction at 6 Months. JACC Cardiovasc Interv 2015;8(11):1410–21. Doi: 10.1016/j.jcin.2015.04.029.
153. Shimada K. Assessment of myocardial viability using coronary zero flow pressure after successful angioplasty in patients with acute anterior myocardial infarction. Heart 2003;89(1):71–6. Doi: 10.1136/heart.89.1.71.
154. Ito H., Terai K., Iwakura K., Kawase I., Fujii K. Hemodynamics of microvascular dysfunction in patients with anterior wall acute myocardial infarction. Am J Cardiol 2004;94(2):209–12. Doi: 10.1016/j.amjcard.2004.03.066.
155. Broyd CJ., Davies JE., Escaned JE., Hughes A., Parker K. Wave intensity analysis and its application to the coronary circulation. Glob Cardiol Sci Pract 2017;2017(1). Doi: 10.21542/gcsp.2017.5.
156. Davies JE., Whinnett ZI., Francis DP., et al. Evidence of a Dominant Backward-Propagating "Suction" Wave Responsible for Diastolic Coronary Filling in Humans, Attenuated in Left Ventricular Hypertrophy. Circulation 2006;113(14):1768–78. Doi: 10.1161/CIRCULATIONAHA.105.603050.
157. De Silva K., Foster P., Guilcher A., et al. Coronary Wave Energy. Circ Cardiovasc Interv 2013;6(2):166–75. Doi: 10.1161/CIRCINTERVENTIONS.112.973081.
158. Kobayashi Y., Fearon WF. Invasive Coronary Microcirculation Assessment. Circulation Journal 2014;78(5):1021–8. Doi: 10.1253/circj.CJ-14-0364.
159. Cuculi F., De Maria GL., Meier P., et al. Impact of Microvascular Obstruction on the Assessment of Coronary Flow Reserve, Index of Microcirculatory Resistance, and Fractional Flow Reserve After ST-Segment Elevation Myocardial Infarction. J Am Coll Cardiol 2014;64(18):1894–904. Doi: 10.1016/j.jacc.2014.07.987.
160. Ford TJ., Stanley B., Good R., et al. Stratified Medical Therapy Using Invasive Coronary Function Testing in Angina. J Am Coll Cardiol 2018;72(23):2841–55. Doi: 10.1016/j.jacc.2018.09.006.
161. Fearon WF., Balsam LB., Farouque HMO., et al. Novel Index for Invasively Assessing the Coronary Microcirculation. Circulation 2003;107(25):3129–32. Doi: 10.1161/01.CIR.0000080700.98607.D1.
162. Yong ASC., Ho M., Shah MG., Ng MKC., Fearon WF. Coronary Microcirculatory Resistance Is Independent of Epicardial Stenosis. Circ Cardiovasc Interv 2012;5(1):103–8. Doi: 10.1161/CIRCINTERVENTIONS.111.966556.
163. Fearon WF., Aarnoudse W., Pijls NHJ., et al. Microvascular Resistance Is Not Influenced by Epicardial Coronary Artery Stenosis Severity. Circulation 2004; 109(19):2269–72. Doi: 10.1161/01.CIR.0000128669.99355.CB.
164. Berry C., Corcoran D., Hennigan B., Watkins S., Layland J., Oldroyd KG. Fractional flow reserve-guided management in stable coronary disease and acute myocardial infarction: recent developments. Eur Heart J 2015;36(45):3155–64. Doi: 10.1093/eurheartj/ehv206.
165. Fearon WF., Shah M., Ng M., et al. Predictive Value of the Index of Microcirculatory Resistance in Patients With ST-Segment Elevation Myocardial Infarction. J Am Coll Cardiol 2008;51(5):560–5. Doi: 10.1016/j.jacc.2007.08.062.

166. Ahn SG., Hung OY., Lee J-W., et al. Combination of the Thermodilution-Derived Index of Microcirculatory Resistance and Coronary Flow Reserve Is Highly Predictive of Microvascular Obstruction on Cardiac Magnetic Resonance Imaging After ST-Segment Elevation Myocardial Infarction. JACC Cardiovasc Interv 2016; 9(8):793–801. Doi: 10.1016/j.jcin.2015.12.025.
167. Fearon WF., Low AF., Yong AS., et al. Prognostic Value of the Index of Microcirculatory Resistance Measured After Primary Percutaneous Coronary Intervention. Circulation 2013;127(24):2436–41. Doi: 10.1161/CIRCULATIONAHA.112.000298.
168. Fahrni G., Wolfrum M., De Maria GL., et al. Index of Microcirculatory Resistance at the Time of Primary Percutaneous Coronary Intervention Predicts Early Cardiac Complications: Insights From the OxAMI (Oxford Study in Acute Myocardial Infarction) Cohort. J Am Heart Assoc 2017;6(11). Doi: 10.1161/JAHA.116.005409.
169. McGeoch R., Watkins S., Berry C., et al. The Index of Microcirculatory Resistance Measured Acutely Predicts the Extent and Severity of Myocardial Infarction in Patients With ST-Segment Elevation Myocardial Infarction. JACC Cardiovasc Interv 2010;3(7):715–22. Doi: 10.1016/j.jcin.2010.04.009.
170. De Maria GL., Alkhalil M., Wolfrum M., et al. Index of Microcirculatory Resistance as a Tool to Characterize Microvascular Obstruction and to Predict Infarct Size Regression in Patients With STEMI Undergoing Primary PCI. JACC Cardiovasc Imaging 2019;12(5):837–48. Doi: 10.1016/j.jcmg.2018.02.018.
171. Carrick D., Haig C., Carberry J., et al. Microvascular resistance of the culprit coronary artery in acute ST-elevation myocardial infarction. JCI Insight 2016; 1(6):e85768. Doi: 10.1172/jci.insight.85768.
172. Aarnoudse W., van't Veer M., Pijls NHJ., et al. Direct Volumetric Blood Flow Measurement in Coronary Arteries by Thermodilution. J Am Coll Cardiol 2007;50(24):2294–304. Doi: 10.1016/j.jacc.2007.08.047.
173. De Bruyne B., Adjedj J., Xaplanteris P., et al. Saline-Induced Coronary Hyperemia. Circ Cardiovasc Interv 2017;10(4). Doi: 10.1161/CIRCINTERVENTIONS.116.004719.
174. Keeble TR., Karamasis G V., Rothman MT., et al. Percutaneous haemodynamic and renal support in patients presenting with decompensated heart failure: A multi-centre efficacy study using the Reitan Catheter Pump (RCP). Int J Cardiol 2019;275:53–8. Doi: 10.1016/j.ijcard.2018.09.085.
175. De Bruyne B., Pijls NHJ., Gallinoro E., et al. Microvascular Resistance Reserve for Assessment of Coronary Microvascular Function. J Am Coll Cardiol 2021;78(15): 1541–9. Doi: 10.1016/j.jacc.2021.08.017.
176. Boerhout CKM., Lee JM., de Waard GA., et al. Microvascular resistance reserve: diagnostic and prognostic performance in the ILIAS registry. Eur Heart J 2023;44(30):2862–9. Doi: 10.1093/eurheartj/ehad378.
177. DE MARIA GL., WOPPERER S., KOTRONIAS R., et al. From anatomy to function and then back to anatomy: invasive assessment of myocardial ischemia in the catheterization laboratory based on anatomy-derived indices of coronary physiology. Minerva Cardiology and Angiology 2021;69(6). Doi: 10.23736/S2724-5683.20. 05486-9.
178. Scarsini R., Shanmuganathan M., Kotronias RA., et al. Angiography-derived index of microcirculatory resistance (IMRangio) as a novel pressure-wire-free tool to assess coronary microvascular dysfunction in acute coronary syndromes and stable coronary artery disease. Int J Cardiovasc Imaging 2021;37(6):1801–13. Doi: 10.1007/s10554-021-02254-8.

179. Kotronias RA., Terentes-Printzios D., Shanmuganathan M., et al. Long-Term Clinical Outcomes in Patients With an Acute ST-Segment-Elevation Myocardial Infarction Stratified by Angiography-Derived Index of Microcirculatory Resistance. Front Cardiovasc Med 2021;8. Doi: 10.3389/fcvm.2021.717114.
180. Moncada S., Higgs A. The L-arginine-nitric oxide pathway. N Engl J Med 1993; 329(27):2002–12. Doi: 10.1056/NEJM199312303292706.
181. Meredith IT., Anderson TJ., Uehata A., Yeung AC., Selwyn AP., Ganz P. Role of endothelium in ischemic coronary syndromes. Am J Cardiol 1993;72(8):C27–32. Doi: 10.1016/0002-9149(93)90252-8.
182. Halcox JPJ., Schenke WH., Zalos G., et al. Prognostic Value of Coronary Vascular Endothelial Dysfunction. Circulation 2002;106(6):653–8. Doi: 10.1161/01.CIR. 0000025404.78001.D8.
183. Ridker PM., Cook N. Clinical Usefulness of Very High and Very Low Levels of C-Reactive Protein Across the Full Range of Framingham Risk Scores. Circulation 2004;109(16):1955–9. Doi: 10.1161/01.CIR.0000125690.80303.A8.
184. Ridker PM., Buring JE., Rifai N., Cook NR. Development and Validation of Improved Algorithms for the Assessment of Global Cardiovascular Risk in Women. JAMA 2007;297(6):611. Doi: 10.1001/jama.297.6.611.
185. Cook NR., Paynter NP., Eaton CB., et al. Comparison of the Framingham and Reynolds Risk Scores for Global Cardiovascular Risk Prediction in the Multiethnic Women's Health Initiative. Circulation 2012;125(14):1748–56. Doi: 10.1161/ CIRCULATIONAHA.111.075929.
186. Vaccarino V., Khan D., Votaw J., et al. Inflammation is Related to Coronary Flow Reserve Detected by Positron Emission Tomography in Asymptomatic Male Twins. J Am Coll Cardiol 2011;57(11):1271–9. Doi: 10.1016/j.jacc.2010.09.074.
187. Recio-Mayoral A., Rimoldi OE., Camici PG., Kaski JC. Inflammation and Microvascular Dysfunction in Cardiac Syndrome X Patients Without Conventional Risk Factors for Coronary Artery Disease. JACC Cardiovasc Imaging 2013;6(6): 660–7. Doi: 10.1016/j.jcmg.2012.12.011.
188. Cosín-Sales J., Pizzi C., Brown S., Kaski JC. C-reactive protein, clinical presentation, and ischemic activity in patients with chest pain and normal coronary angiograms. J Am Coll Cardiol 2003;41(9):1468–74. Doi: 10.1016/S0735-1097(03)00243-2.
189. Arroyo-Espliguero R. Chronic inflammation and increased arterial stiffness in patients with cardiac syndrome X. Eur Heart J 2003;24(22):2006–11. Doi: 10.1016/ j.ehj.2003.09.029.
190. On YK., Park R., Hyon MS., Kim SK., Kwon YJ. Are Low Total Serum Antioxidant Status and Elevated Levels of C-Reactive Protein and Monocyte Chemotactic Protein-1 Associated With Cardiac Syndrome X? Circulation Journal 2005;69(10): 1212–7. Doi: 10.1253/circj.69.1212.
191. Tsimikas S., Willerson JT., Ridker PM. C-Reactive Protein and Other Emerging Blood Biomarkers to Optimize Risk Stratification of Vulnerable Patients. J Am Coll Cardiol 2006;47(8):C19–31. Doi: 10.1016/j.jacc.2005.10.066.
192. Qamirani E., Ren Y., Kuo L., Hein TW. C-Reactive Protein Inhibits Endothelium-Dependent NO-Mediated Dilation in Coronary Arterioles by Activating p38 Kinase and NAD(P)H Oxidase. Arterioscler Thromb Vasc Biol 2005;25(5):995–1001. Doi: 10.1161/01.ATV.0000159890.10526.1e.
193. Saadeh C. The erythrocyte sedimentation rate: old and new clinical applications. South Med J 1998;91(3):220–5.

194. Andresdottir MB. Erythrocyte Sedimentation Rate, an Independent Predictor of Coronary Heart Disease in Men and Women: The Reykjavik Study. Am J Epidemiol 2003;158(9):844–51. Doi: 10.1093/aje/kwg222.
195. Gillum R. Erythrocyte sedimentation rate and coronary heart disease: The NHANES I epidemiologic follow-up study. J Clin Epidemiol 1995;48(3):353–61. Doi: 10.1016/0895-4356(94)00156-K.
196. Natali A. Erythrocyte sedimentation rate, coronary atherosclerosis, and cardiac mortality. Eur Heart J 2003;24(7):639–48. Doi: 10.1016/S0195-668X(02)00741-8.
197. Yayan J. Erythrocyte sedimentation rate as a marker for coronary heart disease. Vasc Health Risk Manag 2012:219. Doi: 10.2147/VHRM.S29284.
198. Smith HW., Marshall CJ. Regulation of cell signalling by uPAR. Nat Rev Mol Cell Biol 2010;11(1):23–36. Doi: 10.1038/nrm2821.
199. Thunø M., Macho B., Eugen-Olsen J. suPAR: The Molecular Crystal Ball. Dis Markers 2009;27:504294. Doi: 10.3233/DMA-2009-0657.
200. Cozen AE., Moriwaki H., Kremen M., et al. Macrophage-Targeted Overexpression of Urokinase Causes Accelerated Atherosclerosis, Coronary Artery Occlusions, and Premature Death. Circulation 2004;109(17):2129–35. Doi: 10.1161/01.CIR.0000127369.24127.03.
201. Persson M., Östling G., Smith G., et al. Soluble Urokinase Plasminogen Activator Receptor. Stroke 2014;45(1):18–23. Doi: 10.1161/STROKEAHA.113.003305.
202. Eapen DJ., Manocha P., Ghasemzadeh N., et al. Soluble Urokinase Plasminogen Activator Receptor Level Is an Independent Predictor of the Presence and Severity of Coronary Artery Disease and of Future Adverse Events. J Am Heart Assoc 2014;3(5). Doi: 10.1161/JAHA.114.001118.
203. Sehestedt T., Lyngbæk S., Eugen-Olsen J., et al. Soluble urokinase plasminogen activator receptor is associated with subclinical organ damage and cardiovascular events. Atherosclerosis 2011;216(1):237–43. Doi: 10.1016/j.atherosclerosis.2011.01.049.
204. Eugen-Olsen J., Andersen O., Linneberg A., et al. Circulating soluble urokinase plasminogen activator receptor predicts cancer, cardiovascular disease, diabetes and mortality in the general population. J Intern Med 2010;268(3):296–308. Doi: 10.1111/j.1365-2796.2010.02252.x.
205. Mekonnen G., Corban MT., Hung OY., et al. Plasma soluble urokinase-type plasminogen activator receptor level is independently associated with coronary microvascular function in patients with non-obstructive coronary artery disease. Atherosclerosis 2015;239(1):55–60. Doi: 10.1016/j.atherosclerosis.2014.12.025.
206. Lee M-J., Park S-D., Kwon SW., et al. Relation Between Neutrophil-to-Lymphocyte Ratio and Index of Microcirculatory Resistance in Patients With ST-Segment Elevation Myocardial Infarction Undergoing Primary Percutaneous Coronary Intervention. Am J Cardiol 2016;118(9):1323–8. Doi: 10.1016/j.amjcard.2016.07.072.
207. Ott I., Neumann F-J., Kenngott S., Gawaz M., Schömig A. Procoagulant inflammatory responses of monocytes after direct balloon angioplasty in acute myocardial infarction. Am J Cardiol 1998;82(8):938–42. Doi: 10.1016/S0002-9149(98)00509-8.
208. Marx N., Neumann F-J., Ott I., et al. Induction of Cytokine Expression in Leukocytes in Acute Myocardial Infarction. J Am Coll Cardiol 1997;30(1):165–70. Doi: 10.1016/S0735-1097(97)00116-2.

209. Yilmaz M., Tenekecioglu E., Arslan B., et al. White Blood Cell Subtypes and Neutrophil–Lymphocyte Ratio in Prediction of Coronary Thrombus Formation in Non-ST-Segment Elevated Acute Coronary Syndrome. Clinical and Applied Thrombosis/Hemostasis 2015;21(5):446–52. Doi: 10.1177/1076029613507337.
210. Baldus S., Heeschen C., Meinertz T., et al. Myeloperoxidase Serum Levels Predict Risk in Patients With Acute Coronary Syndromes. Circulation 2003;108(12):1440–5. Doi: 10.1161/01.CIR.0000090690.67322.51.
211. Hansen PR. Role of Neutrophils in Myocardial Ischemia and Reperfusion. Circulation 1995;91(6):1872–85. Doi: 10.1161/01.CIR.91.6.1872.
212. Chen X., Yuan S., Zhang J. Correlation study between blood cytokines and lymphocytes in early postoperative critical patients with compromised immune function. Medicine 2020;99(42):e22459. Doi: 10.1097/MD.0000000000022459.
213. Aurigemma C., Scalone G., Tomai F., et al. Persistent enhanced platelet activation in patients with acute myocardial infarction and coronary microvascular obstruction: clinical implications. Thromb Haemost 2014;111(01):122–30. Doi: 10.1160/TH13-02-0166.
214. van der Laan AM., Hirsch A., Robbers LFHJ., et al. A proinflammatory monocyte response is associated with myocardial injury and impaired functional outcome in patients with ST-segment elevation myocardial infarction. Am Heart J 2012; 163(1):57-65.e2. Doi: 10.1016/j.ahj.2011.09.002.
215. Sezer M., Okcular I., Goren T., et al. Association of haematological indices with the degree of microvascular injury in patients with acute anterior wall myocardial infarction treated with primary percutaneous coronary intervention. Heart 2007;93(3): 313–8. Doi: 10.1136/hrt.2006.094763.
216. Wu KC., Zerhouni EA., Judd RM., et al. Prognostic Significance of Microvascular Obstruction by Magnetic Resonance Imaging in Patients With Acute Myocardial Infarction. Circulation 1998;97(8):765–72. Doi: 10.1161/01.CIR.97.8.765.
217. Williams BA., Merhige ME. Association between neutrophil–lymphocyte ratio and impaired myocardial perfusion in patients with known or suspected coronary disease. Heart & Lung 2013;42(6):436–41. Doi: 10.1016/j.hrtlng.2013.07.013.
218. Dhawan SS., Eshtehardi P., McDaniel MC., et al. The role of plasma aminothiols in the prediction of coronary microvascular dysfunction and plaque vulnerability. Atherosclerosis 2011;219(1):266–72. Doi: 10.1016/j.atherosclerosis.2011.05.020.
219. Alp NJ., Channon KM. Regulation of Endothelial Nitric Oxide Synthase by Tetrahydrobiopterin in Vascular Disease. Arterioscler Thromb Vasc Biol 2004;24(3): 413–20. Doi: 10.1161/01.ATV.0000110785.96039.f6.
220. Napoli C., de Nigris F., Williams-Ignarro S., Pignalosa O., Sica V., Ignarro LJ. Nitric oxide and atherosclerosis: An update. Nitric Oxide 2006;15(4):265–79. Doi: 10.1016/j.niox.2006.03.011.
221. Zhao Y., Vanhoutte PM., Leung SWS. Vascular nitric oxide: Beyond eNOS. J Pharmacol Sci 2015;129(2):83–94. Doi: 10.1016/j.jphs.2015.09.002.
222. Tousoulis D., Kampoli A-M., Tentolouris Nikolaos Papageorgiou C., Stefanadis C. The Role of Nitric Oxide on Endothelial Function. Curr Vasc Pharmacol 2012;10(1): 4–18. Doi: 10.2174/157016112798829760.
223. Russo G., Leopold JA., Loscalzo J. Vasoactive substances. Vascul Pharmacol 2002; 38(5):259–69. Doi: 10.1016/S1537-1891(02)00250-1.
224. Cai H., Harrison DG. Endothelial Dysfunction in Cardiovascular Diseases: The Role of Oxidant Stress. Circ Res 2000;87(10):840–4. Doi: 10.1161/01.RES.87.10.840.

225. Harrison D., Griendling KK., Landmesser U., Hornig B., Drexler H. Role of oxidative stress in atherosclerosis. Am J Cardiol 2003;91(3):7–11. Doi: 10.1016/S0002-9149(02)03144-2.
226. Mkhwanazi BN., Serumula MR., Myburg RB., Van Heerden FR., Musabayane CT. Antioxidant effects of maslinic acid in livers, hearts and kidneys of streptozotocin-induced diabetic rats: effects on kidney function. Ren Fail 2014;36(3):419–31. Doi: 10.3109/0886022X.2013.867799.
227. Qing P., Luo S-H., Guo Y-L., et al. Evaluation of red blood cell distribution width in patients with cardiac syndrome X. Dis Markers 2013;34(5):333–9. Doi: 10.3233/DMA-130977.
228. Molyneux CA., Glyn MC., Ward BJ. Oxidative Stress and Cardiac Microvascular Structure in Ischemia and Reperfusion: The Protective Effect of Antioxidant Vitamins. Microvasc Res 2002;64(2):265–77. Doi: 10.1006/mvre.2002.2419.
229. Bohlen HG., Zhou X., Unthank JL., Miller SJ., Bills R. Transfer of nitric oxide by blood from upstream to downstream resistance vessels causes microvascular dilation. American Journal of Physiology-Heart and Circulatory Physiology 2009; 297(4):H1337–46. Doi: 10.1152/ajpheart.00171.2009.
230. Mangiacapra F., De Bruyne B., Peace AJ., Melikian N., Wijns W., Barbato E. High cholesterol levels are associated with coronary microvascular dysfunction. Journal of Cardiovascular Medicine 2012;13(7):439–42. Doi: 10.2459/JCM.0b013e328351725a.
231. Sitia S., Tomasoni L., Atzeni F., et al. From endothelial dysfunction to atherosclerosis. Autoimmun Rev 2010;9(12):830–4. Doi: 10.1016/j.autrev.2010.07.016.
232. Chatzizisis YS., Coskun AU., Jonas M., Edelman ER., Feldman CL., Stone PH. Role of Endothelial Shear Stress in the Natural History of Coronary Atherosclerosis and Vascular Remodeling. J Am Coll Cardiol 2007;49(25):2379–93. Doi: 10.1016/j.jacc.2007.02.059.
233. Lekakis J., Abraham P., Balbarini A., et al. Methods for evaluating endothelial function: a position statement from the European Society of Cardiology Working Group on Peripheral Circulation. European Journal of Cardiovascular Prevention & Rehabilitation 2011;18(6):775–89. Doi: 10.1177/1741826711398179.
234. Cheng Y., Austin SC., Rocca B., et al. Role of Prostacyclin in the Cardiovascular Response to Thromboxane A 2. Science (1979) 2002;296(5567):539–41. Doi: 10.1126/science.1068711.
235. Martin A-C., Zlotnik D., Bonete GP., et al. Epinephrine restores platelet functions inhibited by ticagrelor: A mechanistic approach. Eur J Pharmacol 2020;866:172798. Doi: 10.1016/j.ejphar.2019.172798.
236. Jennings LK. Role of Platelets in Atherothrombosis. Am J Cardiol 2009;103(3):4A-10A. Doi: 10.1016/j.amjcard.2008.11.017.
237. Michelson AD. Platelets. Academic Press; 2012.
238. Ting HJ., Murad JP., Espinosa EVP., Khasawneh FT. Thromboxane A 2 Receptor. J Cardiovasc Pharmacol Ther 2012;17(3):248–59. Doi: 10.1177/1074248411424145.
239. Michel F., Silvestre J-S., Waeckel L., et al. Thromboxane A2/Prostaglandin H2 Receptor Activation Mediates Angiotensin II–Induced Postischemic Neovascularization. Arterioscler Thromb Vasc Biol 2006;26(3):488–93. Doi: 10.1161/01.ATV.0000201969.93348.74.
240. Houben A. Microvascular effects of atrial natriuretic peptide (ANP) in man: studies during high and low salt diet. Cardiovasc Res 1998;39(2):442–50. Doi: 10.1016/S0008-6363(98)00072-8.

241. Dudek D., Rzeszutko L., Petkow Dimitrow P., et al. Circulating N-terminal brain natriuretic peptide precursor and endothelin levels in patients with syndrome X and left bundle branch block with preserved systolic function. Int J Cardiol 2001;79(1): 25–30. Doi: 10.1016/S0167-5273(01)00400-4.
242. Knaapen P., Germans T., Camici PG., et al. Determinants of coronary microvascular dysfunction in symptomatic hypertrophic cardiomyopathy. American Journal of Physiology-Heart and Circulatory Physiology 2008;294(2):H986–93. Doi: 10.1152/ajpheart.00233.2007.
243. Mitchell A., Misialek JR., Folsom AR., et al. Usefulness of N-terminal Pro–brain Natriuretic Peptide and Myocardial Perfusion in Asymptomatic Adults (from the Multi-Ethnic Study of Atherosclerosis). Am J Cardiol 2015;115(10):1341–5. Doi: 10.1016/j.amjcard.2015.02.040.
244. Fujii K., Kawasaki D., Oka K., et al. The Impact of Pravastatin Pre-Treatment on Periprocedural Microcirculatory Damage in Patients Undergoing Percutaneous Coronary Intervention. JACC Cardiovasc Interv 2011;4(5):513–20. Doi: 10.1016/j.jcin.2011.02.005.
245. Herrmann J., Haude M., Lerman A., et al. Abnormal Coronary Flow Velocity Reserve After Coronary Intervention Is Associated With Cardiac Marker Elevation. Circulation 2001;103(19):2339–45. Doi: 10.1161/01.CIR.103.19.2339.
246. Takashio S., Yamamuro M., Izumiya Y., et al. Coronary Microvascular Dysfunction and Diastolic Load Correlate With Cardiac Troponin T Release Measured by a Highly Sensitive Assay in Patients With Nonischemic Heart Failure. J Am Coll Cardiol 2013;62(7):632–40. Doi: 10.1016/j.jacc.2013.03.065.
247. Park K., Kim M., Cho Y-R., et al. Association between Cardiac Troponin Level and Coronary Flow Reserve in Patients without Coronary Artery Disease: Insight from a Thermodilution Technique Using an Intracoronary Pressure Wire. Korean Circ J 2014;44(3):141. Doi: 10.4070/kcj.2014.44.3.141.
248. Wang Z., Klipfell E., Bennett BJ., et al. Gut flora metabolism of phosphatidylcholine promotes cardiovascular disease. Nature 2011;472(7341):57–63. Doi: 10.1038/nature09922.
249. Koeth RA., Wang Z., Levison BS., et al. Intestinal microbiota metabolism of l-carnitine, a nutrient in red meat, promotes atherosclerosis. Nat Med 2013;19(5):576–85. Doi: 10.1038/nm.3145.
250. Zhu W., Buffa JA., Wang Z., et al. Flavin monooxygenase 3, the host hepatic enzyme in the metaorganismal trimethylamine N-oxide-generating pathway, modulates platelet responsiveness and thrombosis risk. Journal of Thrombosis and Haemostasis 2018;16(9):1857–72. Doi: 10.1111/jth.14234.
251. Landfald B., Valeur J., Berstad A., Raa J. Microbial trimethylamine- N -oxide as a disease marker: something fishy? Microb Ecol Health Dis 2017;28(1):1327309. Doi: 10.1080/16512235.2017.1327309.
252. Janeiro M., Ramírez M., Milagro F., Martínez J., Solas M. Implication of Trimethylamine N-Oxide (TMAO) in Disease: Potential Biomarker or New Therapeutic Target. Nutrients 2018;10(10):1398. Doi: 10.3390/nu10101398.
253. Ferguson JF. Meat-Loving Microbes. Circ Cardiovasc Genet 2013;6(3):308–9. Doi: 10.1161/CIRCGENETICS.113.000213.
254. Bernstein AM., Sun Q., Hu FB., Stampfer MJ., Manson JE., Willett WC. Major Dietary Protein Sources and Risk of Coronary Heart Disease in Women. Circulation 2010;122(9):876–83. Doi: 10.1161/CIRCULATIONAHA.109.915165.

255. Koeth RA., Levison BS., Culley MK., et al. γ-Butyrobetaine Is a Proatherogenic Intermediate in Gut Microbial Metabolism of L-Carnitine to TMAO. Cell Metab 2014;20(5):799–812. Doi: 10.1016/j.cmet.2014.10.006.
256. Koeth RA., Lam-Galvez BR., Kirsop J., et al. l-Carnitine in omnivorous diets induces an atherogenic gut microbial pathway in humans. Journal of Clinical Investigation 2018;129(1):373–87. Doi: 10.1172/JCI94601.
257. Meyer K., Shea J. Dietary Choline and Betaine and Risk of CVD: A Systematic Review and Meta-Analysis of Prospective Studies. Nutrients 2017;9(7):711. Doi: 10.3390/nu9070711.
258. Pignanelli M., Just C., Bogiatzi C., et al. Mediterranean Diet Score: Associations with Metabolic Products of the Intestinal Microbiome, Carotid Plaque Burden, and Renal Function. Nutrients 2018;10(6):779. Doi: 10.3390/nu10060779.
259. Tang WHW., Hazen SL. The contributory role of gut microbiota in cardiovascular disease. Journal of Clinical Investigation 2014;124(10):4204–11. Doi: 10.1172/JCI72331.
260. Zeisel SH., Warrier M. Trimethylamine N -Oxide, the Microbiome, and Heart and Kidney Disease. Annu Rev Nutr 2017;37(1):157–81. Doi: 10.1146/annurev-nutr-071816-064732.
261. Ma J., Li H. The Role of Gut Microbiota in Atherosclerosis and Hypertension. Front Pharmacol 2018;9. Doi: 10.3389/fphar.2018.01082.
262. Yin J., Liao S., He Y., et al. Dysbiosis of Gut Microbiota With Reduced Trimethylamine-N-Oxide Level in Patients With Large-Artery Atherosclerotic Stroke or Transient Ischemic Attack. J Am Heart Assoc 2015;4(11). Doi: 10.1161/JAHA.115.002699.
263. Wu S., Luo T., Wang S., et al. Chronic exposure to fungicide propamocarb induces bile acid metabolic disorder and increases trimethylamine in C57BL/6J mice. Science of The Total Environment 2018;642:341–8. Doi: 10.1016/j.scitotenv.2018.06.084.
264. Romano KA., Vivas EI., Amador-Noguez D., Rey FE. Intestinal Microbiota Composition Modulates Choline Bioavailability from Diet and Accumulation of the Proatherogenic Metabolite Trimethylamine- N -Oxide. MBio 2015;6(2). Doi: 10.1128/mBio.02481-14.
265. Gregory JC., Buffa JA., Org E., et al. Transmission of Atherosclerosis Susceptibility with Gut Microbial Transplantation. Journal of Biological Chemistry 2015;290(9):5647–60. Doi: 10.1074/jbc.M114.618249.
266. Bennett BJ., Vallim TQ de A., Wang Z., et al. Trimethylamine-N-Oxide, a Metabolite Associated with Atherosclerosis, Exhibits Complex Genetic and Dietary Regulation. Cell Metab 2013;17(1):49–60. Doi: 10.1016/j.cmet.2012.12.011.
267. Wang Z., Roberts AB., Buffa JA., et al. Non-lethal Inhibition of Gut Microbial Trimethylamine Production for the Treatment of Atherosclerosis. Cell 2015;163(7):1585–95. Doi: 10.1016/j.cell.2015.11.055.
268. Li T., Chen Y., Gua C., Li X. Elevated Circulating Trimethylamine N-Oxide Levels Contribute to Endothelial Dysfunction in Aged Rats through Vascular Inflammation and Oxidative Stress. Front Physiol 2017;8. Doi: 10.3389/fphys.2017.00350.
269. Belkaid Y., Hand TW. Role of the Microbiota in Immunity and Inflammation. Cell 2014;157(1):121–41. Doi: 10.1016/j.cell.2014.03.011.
270. Shoenfeld Y., Sherer Y., Harats D. Atherosclerosis as an infectious, inflammatory and autoimmune disease. Trends Immunol 2001;22(6):293–5. Doi: 10.1016/S1471-4906(01)01922-6.

271. Rodríguez-Iturbe B., Johnson R. Heat shock proteins and cardiovascular disease. Physiol Int 2018;105(1):19–37. Doi: 10.1556/2060.105.2018.1.4.
272. Wick G., Knoflach M., Xu Q. Autoimmune and Inflammatory Mechanisms in Atherosclerosis. Annu Rev Immunol 2004;22(1):361–403. Doi: 10.1146/annurev.immunol.22.012703.104644.
273. Wick G., Jakic B., Buszko M., Wick MC., Grundtman C. The role of heat shock proteins in atherosclerosis. Nat Rev Cardiol 2014;11(9):516–29. Doi: 10.1038/nrcardio.2014.91.
274. Khandia R., K. Munjal A., M. N. Iqbal H., Dhama K. Heat Shock Proteins: Therapeutic Perspectives in Inflammatory Disorders. Recent Pat Inflamm Allergy Drug Discov 2017;10(2):94–104. Doi: 10.2174/1872213X10666161213163301.
275. Mohammadi A., Vahabzadeh Z., Jamalzadeh S., Khalili T. Trimethylamine-N-oxide, as a risk factor for atherosclerosis, induces stress in J774A.1 murine macrophages. Adv Med Sci 2018;63(1):57–63. Doi: 10.1016/j.advms.2017.06.006.
276. Mohammadi A., Gholamhoseyniannajar A., Yaghoobi MM., Jahani Y., Vahabzadeh Z. Expression levels of heat shock protein 60 and glucose-regulated protein 78 in response to trimethylamine-N-oxide treatment in murine macrophage J774A.1 cell line. Cell Mol Biol (Noisy-Le-Grand) 2015;61(4):94–100.
277. Schroder K., Tschopp J. The Inflammasomes. Cell 2010;140(6):821–32. Doi: 10.1016/j.cell.2010.01.040.
278. Collotteixeira S., Martin J., McDermottroe C., Poston R., McGregor J. CD36 and macrophages in atherosclerosis. Cardiovasc Res 2007;75(3):468–77. Doi: 10.1016/j.cardiores.2007.03.010.
279. Jin P., Bian Y., Wang K., et al. Homocysteine accelerates atherosclerosis via inhibiting LXRα–mediated ABCA1/ABCG1–dependent cholesterol efflux from macrophages. Life Sci 2018;214:41–50. Doi: 10.1016/j.lfs.2018.10.060.
280. Geng J., Yang C., Wang B., et al. Trimethylamine N-oxide promotes atherosclerosis via CD36-dependent MAPK/JNK pathway. Biomedicine & Pharmacotherapy 2018;97:941–7. Doi: 10.1016/j.biopha.2017.11.016.
281. Febbraio M., Podrez EA., Smith JD., et al. Targeted disruption of the class B scavenger receptor CD36 protects against atherosclerotic lesion development in mice. Journal of Clinical Investigation 2000;105(8):1049–56. Doi: 10.1172/JCI9259.
282. Collins HL., Drazul-Schrader D., Sulpizio AC., et al. L-Carnitine intake and high trimethylamine N-oxide plasma levels correlate with low aortic lesions in ApoE−/− transgenic mice expressing CETP. Atherosclerosis 2016;244:29–37. Doi: 10.1016/j.atherosclerosis.2015.10.108.
283. Hoseini Z., Sepahvand F., Rashidi B., Sahebkar A., Masoudifar A., Mirzaei H. NLRP3 inflammasome: Its regulation and involvement in atherosclerosis. J Cell Physiol 2018;233(3):2116–32. Doi: 10.1002/jcp.25930.
284. Takahashi M. NLRP3 Inflammasome as a Novel Player in Myocardial Infarction. Int Heart J 2014;55(2):101–5. Doi: 10.1536/ihj.13-388.
285. Boini KM., Hussain T., Li P-L., Koka SS. Trimethylamine-N-Oxide Instigates NLRP3 Inflammasome Activation and Endothelial Dysfunction. Cellular Physiology and Biochemistry 2017;44(1):152–62. Doi: 10.1159/000484623.
286. Wang R., Wang Y., Mu N., et al. Activation of NLRP3 inflammasomes contributes to hyperhomocysteinemia-aggravated inflammation and atherosclerosis in apoE-deficient mice. Laboratory Investigation 2017;97(8):922–34. Doi: 10.1038/labinvest.2017.30.

287. Chen M., Zhu X., Ran L., Lang H., Yi L., Mi M. Trimethylamine-N-Oxide Induces Vascular Inflammation by Activating the NLRP3 Inflammasome Through the SIRT3-SOD2-mtROS Signaling Pathway. J Am Heart Assoc 2017;6(9). Doi: 10.1161/JAHA.117.006347.
288. Sho T., Xu J. Role and mechanism of ROS scavengers in alleviating NLRP3-mediated inflammation. Biotechnol Appl Biochem 2019;66(1):4–13. Doi: 10.1002/bab.1700.
289. Sun X., Jiao X., Ma Y., et al. Trimethylamine N-oxide induces inflammation and endothelial dysfunction in human umbilical vein endothelial cells via activating ROS-TXNIP-NLRP3 inflammasome. Biochem Biophys Res Commun 2016;481(1–2):63–70. Doi: 10.1016/j.bbrc.2016.11.017.
290. Yue C., Yang X., Li J., et al. Trimethylamine N-oxide prime NLRP3 inflammasome via inhibiting ATG16L1-induced autophagy in colonic epithelial cells. Biochem Biophys Res Commun 2017;490(2):541–51. Doi: 10.1016/j.bbrc.2017.06.075.
291. Tuttolomondo A., Di Raimondo D., Pecoraro R., Arnao V., Pinto A., Licata G. Atherosclerosis as an Inflammatory Disease. Curr Pharm Des 2012;18(28):4266–88. Doi: 10.2174/138161212802481237.
292. Chen K., Zheng X., Feng M., Li D., Zhang H. Gut Microbiota-Dependent Metabolite Trimethylamine N-Oxide Contributes to Cardiac Dysfunction in Western Diet-Induced Obese Mice. Front Physiol 2017;8. Doi: 10.3389/fphys.2017.00139.
293. Rohrmann S., Linseisen J., Allenspach M., von Eckardstein A., Müller D. Plasma Concentrations of Trimethylamine-N-oxide Are Directly Associated with Dairy Food Consumption and Low-Grade Inflammation in a German Adult Population. J Nutr 2016;146(2):283–9. Doi: 10.3945/jn.115.220103.
294. Chou R-H., Chen C-Y., Chen I-C., et al. Trimethylamine N-Oxide, Circulating Endothelial Progenitor Cells, and Endothelial Function in Patients with Stable Angina. Sci Rep 2019;9(1):4249. Doi: 10.1038/s41598-019-40638-y.
295. Baker RG., Hayden MS., Ghosh S. NF-κB, Inflammation, and Metabolic Disease. Cell Metab 2011;13(1):11–22. Doi: 10.1016/j.cmet.2010.12.008.
296. Seldin MM., Meng Y., Qi H., et al. Trimethylamine N-Oxide Promotes Vascular Inflammation Through Signaling of Mitogen-Activated Protein Kinase and Nuclear Factor-κB. J Am Heart Assoc 2016;5(2). Doi: 10.1161/JAHA.115.002767.
297. Ma G., Pan B., Chen Y., et al. Trimethylamine N-oxide in atherogenesis: impairing endothelial self-repair capacity and enhancing monocyte adhesion. Biosci Rep 2017;37(2). Doi: 10.1042/BSR20160244.
298. Cheng X., Qiu X., Liu Y., Yuan C., Yang X. Trimethylamine N-oxide promotes tissue factor expression and activity in vascular endothelial cells: A new link between trimethylamine N-oxide and atherosclerotic thrombosis. Thromb Res 2019;177:110–6. Doi: 10.1016/j.thromres.2019.02.028.
299. Fatkhullina AR., Peshkova IO., Dzutsev A., et al. An Interleukin-23-Interleukin-22 Axis Regulates Intestinal Microbial Homeostasis to Protect from Diet-Induced Atherosclerosis. Immunity 2018;49(5):943-957.e9. Doi: 10.1016/j.immuni.2018.09.011.
300. Wang X., Ota N., Manzanillo P., et al. Interleukin-22 alleviates metabolic disorders and restores mucosal immunity in diabetes. Nature 2014;514(7521):237–41. Doi: 10.1038/nature13564.
301. Glomset JA. The plasma lecithins:cholesterol acyltransferase reaction. J Lipid Res 1968;9(2):155–67.

302. Zárate A., Manuel-Apolinar L., Basurto L., De la Chesnaye E., Saldívar I. Colesterol y aterosclerosis. Consideraciones históricas y tratamiento. Arch Cardiol Mex 2016;86(2):163–9. Doi: 10.1016/j.acmx.2015.12.002.
303. Ding L., Chang M., Guo Y., et al. Trimethylamine-N-oxide (TMAO)-induced atherosclerosis is associated with bile acid metabolism. Lipids Health Dis 2018;17(1):286. Doi: 10.1186/s12944-018-0939-6.
304. Jia L., Betters JL., Yu L. Niemann-Pick C1-Like 1 (NPC1L1) Protein in Intestinal and Hepatic Cholesterol Transport. Annu Rev Physiol 2011;73(1):239–59. Doi: 10.1146/annurev-physiol-012110-142233.
305. Warrier M., Shih DM., Burrows AC., et al. The TMAO-Generating Enzyme Flavin Monooxygenase 3 Is a Central Regulator of Cholesterol Balance. Cell Rep 2015;10(3):326–38. Doi: 10.1016/j.celrep.2014.12.036.
306. Al-Rubaye H., Perfetti G., Kaski J-C. The Role of Microbiota in Cardiovascular Risk: Focus on Trimethylamine Oxide. Curr Probl Cardiol 2019;44(6):182–96. Doi: 10.1016/j.cpcardiol.2018.06.005.
307. Chiang JYL., Kimmel R., Stroup D. Regulation of cholesterol 7α-hydroxylase gene (CYP7A1) transcription by the liver orphan receptor (LXRα). Gene 2001;262(1–2):257–65. Doi: 10.1016/S0378-1119(00)00518-7.
308. Chen M., Yi L., Zhang Y., et al. Resveratrol Attenuates Trimethylamine- N -Oxide (TMAO)-Induced Atherosclerosis by Regulating TMAO Synthesis and Bile Acid Metabolism via Remodeling of the Gut Microbiota. MBio 2016;7(2). Doi: 10.1128/mBio.02210-15.
309. Chen K., Febbraio M., Li W., Silverstein RL. A Specific CD36-Dependent Signaling Pathway Is Required for Platelet Activation by Oxidized Low-Density Lipoprotein. Circ Res 2008;102(12):1512–9. Doi: 10.1161/CIRCRESAHA.108.172064.
310. Zhu W., Gregory JC., Org E., et al. Gut Microbial Metabolite TMAO Enhances Platelet Hyperreactivity and Thrombosis Risk. Cell 2016;165(1):111–24. Doi: 10.1016/j.cell.2016.02.011.
311. Zhu W., Wang Z., Tang WHW., Hazen SL. Gut Microbe-Generated Trimethylamine N-Oxide From Dietary Choline Is Prothrombotic in Subjects. Circulation 2017;135(17):1671–3. Doi: 10.1161/CIRCULATIONAHA.116.025338.
312. Frossard M., Fuchs I., Leitner JM., et al. Platelet Function Predicts Myocardial Damage in Patients With Acute Myocardial Infarction. Circulation 2004;110(11):1392–7. Doi: 10.1161/01.CIR.0000141575.92958.9C.
313. Yang M., Kholmukhamedov A., Schulte ML., et al. Platelet CD36 signaling through ERK5 promotes caspase-dependent procoagulant activity and fibrin deposition in vivo. Blood Adv 2018;2(21):2848–61. Doi: 10.1182/bloodadvances.2018025411.
314. Skye SM., Zhu W., Romano KA., et al. Microbial Transplantation With Human Gut Commensals Containing CutC Is Sufficient to Transmit Enhanced Platelet Reactivity and Thrombosis Potential. Circ Res 2018;123(10):1164–76. Doi: 10.1161/CIRCRESAHA.118.313142.
315. Roberts AB., Gu X., Buffa JA., et al. Development of a gut microbe–targeted nonlethal therapeutic to inhibit thrombosis potential. Nat Med 2018;24(9):1407–17. Doi: 10.1038/s41591-018-0128-1.
316. Shih DM., Zhu W., Schugar RC., et al. Genetic Deficiency of Flavin-Containing Monooxygenase 3 (Fmo3) Protects Against Thrombosis but Has Only a Minor Effect on Plasma Lipid Levels—Brief Report. Arterioscler Thromb Vasc Biol 2019;39(6):1045–54. Doi: 10.1161/ATVBAHA.119.312592.

317. van Mens TE., Büller HR., Nieuwdorp M. Targeted inhibition of gut microbiota proteins involved in TMAO production to reduce platelet aggregation and arterial thrombosis: a blueprint for drugging the microbiota in the treatment of cardiometabolic disease? Journal of Thrombosis and Haemostasis 2019;17(1):3–5. Doi: 10.1111/jth.14331.
318. Zhong Z., Liu J., Zhang Q., et al. Targeted metabolomic analysis of plasma metabolites in patients with coronary heart disease in southern China. Medicine 2019; 98(7):e14309. Doi: 10.1097/MD.0000000000014309.
319. Dong Z., Liang Z., Guo M., Hu S., Shen Z., Hai X. The Association between Plasma Levels of Trimethylamine N-Oxide and the Risk of Coronary Heart Disease in Chinese Patients with or without Type 2 Diabetes Mellitus. Dis Markers 2018;2018:1–7. Doi: 10.1155/2018/1578320.
320. Yu D., Shu X., Rivera ES., et al. Urinary Levels of Trimethylamine-N-Oxide and Incident Coronary Heart Disease: A Prospective Investigation Among Urban Chinese Adults. J Am Heart Assoc 2019;8(1). Doi: 10.1161/JAHA.118.010606.
321. Sheng Z., Tan Y., Liu C., et al. Relation of Circulating Trimethylamine N-Oxide With Coronary Atherosclerotic Burden in Patients With ST-segment Elevation Myocardial Infarction. Am J Cardiol 2019;123(6):894–8. Doi: 10.1016/j.amjcard.2018.12.018.
322. Randrianarisoa E., Lehn-Stefan A., Wang X., et al. Relationship of Serum Trimethylamine N-Oxide (TMAO) Levels with early Atherosclerosis in Humans. Sci Rep 2016;6(1):26745. Doi: 10.1038/srep26745.
323. Meyer KA., Benton TZ., Bennett BJ., et al. Microbiota-Dependent Metabolite Trimethylamine N-Oxide and Coronary Artery Calcium in the Coronary Artery Risk Development in Young Adults Study (CARDIA). J Am Heart Assoc 2016;5(10). Doi: 10.1161/JAHA.116.003970.
324. Tang WHW., Wang Z., Levison BS., et al. Intestinal Microbial Metabolism of Phosphatidylcholine and Cardiovascular Risk. New England Journal of Medicine 2013;368(17):1575–84. Doi: 10.1056/NEJMoa1109400.
325. Li XS., Obeid S., Wang Z., et al. Trimethyllysine, a trimethylamine N-oxide precursor, provides near- and long-term prognostic value in patients presenting with acute coronary syndromes. Eur Heart J 2019;40(32):2700–9. Doi: 10.1093/eurheartj/ehz259.
326. Senthong V., Wang Z., Fan Y., Wu Y., Hazen SL., Tang WHW. Trimethylamine N -Oxide and Mortality Risk in Patients With Peripheral Artery Disease. J Am Heart Assoc 2016;5(10). Doi: 10.1161/JAHA.116.004237.
327. Suzuki T., Heaney LM., Jones DJL., Ng LL. Trimethylamine N-oxide and Risk Stratification after Acute Myocardial Infarction. Clin Chem 2017;63(1):420–8. Doi: 10.1373/clinchem.2016.264853.
328. Haghikia A., Li XS., Liman TG., et al. Gut Microbiota–Dependent Trimethylamine N -Oxide Predicts Risk of Cardiovascular Events in Patients With Stroke and Is Related to Proinflammatory Monocytes. Arterioscler Thromb Vasc Biol 2018;38(9):2225–35. Doi: 10.1161/ATVBAHA.118.311023.
329. Wang Z., Levison BS., Hazen JE., Donahue L., Li X-M., Hazen SL. Measurement of trimethylamine-N-oxide by stable isotope dilution liquid chromatography tandem mass spectrometry. Anal Biochem 2014;455:35–40. Doi: 10.1016/j.ab.2014.03.016.

330. Skagen K., Trøseid M., Ueland T., et al. The Carnitine-butyrobetaine-trimethylamine-N-oxide pathway and its association with cardiovascular mortality in patients with carotid atherosclerosis. Atherosclerosis 2016;247:64–9. Doi: 10.1016/j.atherosclerosis.2016.01.033.
331. Mueller DM., Allenspach M., Othman A., et al. Plasma levels of trimethylamine-N-oxide are confounded by impaired kidney function and poor metabolic control. Atherosclerosis 2015;243(2):638–44. Doi: 10.1016/j.atherosclerosis.2015.10.091.
332. Kaysen GA., Johansen KL., Chertow GM., et al. Associations of Trimethylamine N-Oxide With Nutritional and Inflammatory Biomarkers and Cardiovascular Outcomes in Patients New to Dialysis. Journal of Renal Nutrition 2015;25(4):351–6. Doi: 10.1053/j.jrn.2015.02.006.
333. Lang RM., Badano LP., Mor-Avi V., et al. Recommendations for Cardiac Chamber Quantification by Echocardiography in Adults: An Update from the American Society of Echocardiography and the European Association of Cardiovascular Imaging. Eur Heart J Cardiovasc Imaging 2015;16(3):233–71. Doi: 10.1093/ehjci/jev014.
334. Jiamsripong P., Honda T., Reuss C., et al. Three methods for evaluation of left atrial volume. European Journal of Echocardiography 2007. Doi: 10.1016/j.euje.2007.05.004.
335. Nagueh SF., Smiseth OA., Appleton CP., et al. Recommendations for the Evaluation of Left Ventricular Diastolic Function by Echocardiography: An Update from the American Society of Echocardiography and the European Association of Cardiovascular Imaging. Journal of the American Society of Echocardiography 2016;29(4):277–314. Doi: 10.1016/j.echo.2016.01.011.
336. Pijls NHJ., De Bruyne B., Smith L., et al. Coronary Thermodilution to Assess Flow Reserve. Circulation 2002;105(21):2482–6. Doi: 10.1161/01.CIR.0000017199.09457.3D.
337. Pijls NHJ., de Bruyne B., Peels K., et al. Measurement of Fractional Flow Reserve to Assess the Functional Severity of Coronary-Artery Stenoses. New England Journal of Medicine 1996;334(26):1703–8. Doi: 10.1056/NEJM199606273342604.
338. Krishnaveni P. Assessing the Validity of Friedewald's Formula and Anandraja's Formula For Serum L DL -Cholesterol Calculation. Journal of Clinical and Diagnostic Research 2015. Doi: 10.7860/JCDR/2015/16850.6870.
339. Patrick ME., Schulenberg JE. Prevalence and predictors of adolescent alcohol use and binge drinking in the United States. Alcohol Res 2013;35(2):193–200.
340. Mach F., Baigent C., Catapano AL., et al. 2019 ESC/EAS Guidelines for the management of dyslipidaemias: lipid modification to reduce cardiovascular risk. Eur Heart J 2020;41(1):111–88. Doi: 10.1093/eurheartj/ehz455.
341. Williams B., Mancia G., Spiering W., et al. 2018 ESC/ESH Guidelines for the management of arterial hypertension. Eur Heart J 2018;39(33):3021–104. Doi: 10.1093/eurheartj/ehy339.
342. American Diabetes Association. Standards of Medical Care in Diabetes-2019 Abridged for Primary Care Providers. Clin Diabetes 2019;37(1):11–34. Doi: 10.2337/cd18-0105.
343. Khot UN., Jia G., Moliterno DJ., et al. Prognostic Importance of Physical Examination for Heart Failure in Non–ST-Elevation Acute Coronary Syndromes. JAMA 2003;290(16):2174. Doi: 10.1001/jama.290.16.2174.

344. Winter MA., Guhr KN., Berg GM. Impact of Various Body Weights and Serum Creatinine Concentrations on the Bias and Accuracy of the Cockcroft-Gault Equation. Pharmacotherapy: The Journal of Human Pharmacology and Drug Therapy 2012;32(7):604–12. Doi: 10.1002/j.1875-9114.2012.01098.x.
345. Chang CC., Kogame N., Onuma Y., et al. Defining device success for percutaneous coronary intervention trials: a position statement from the European Association of Percutaneous Cardiovascular Interventions of the European Society of Cardiology. EuroIntervention 2020;15(13):1190–8. Doi: 10.4244/EIJ-D-19-00552.
346. O'Gara PT., Kushner FG., Ascheim DD., et al. 2013 ACCF/AHA Guideline for the Management of ST-Elevation Myocardial Infarction: Executive Summary. J Am Coll Cardiol 2013;61(4):485–510. Doi: 10.1016/j.jacc.2012.11.018.
347. Chimed S., van der Bijl P., Lustosa R., et al. Functional classification of left ventricular remodelling: prognostic relevance in myocardial infarction. ESC Heart Fail 2022;9(2):912–24. Doi: 10.1002/ehf2.13802.
348. Garcia-Garcia HM., McFadden EP., Farb A., et al. Standardized End Point Definitions for Coronary Intervention Trials: The Academic Research Consortium-2 Consensus Document. Circulation 2018;137(24):2635–50. Doi: 10.1161/CIRCULATIONAHA.117.029289.
349. Kim BG., Cho SW., Seo J., et al. Effect of direct stenting on microvascular dysfunction during percutaneous coronary intervention in acute myocardial infarction: a randomized pilot study. Journal of International Medical Research 2022;50(9):030006052211278. Doi: 10.1177/03000605221127888.
350. Hoole SP., Jaworski C., Brown AJ., et al. Serial assessment of the index of microcirculatory resistance during primary percutaneous coronary intervention comparing manual aspiration catheter thrombectomy with balloon angioplasty (IMPACT study): a randomised controlled pilot study. Open Heart 2015;2(1):e000238. Doi: 10.1136/openhrt-2015-000238.
351. Samady H., Lepper W., Powers ER., et al. Fractional Flow Reserve of Infarct-Related Arteries Identifies Reversible Defects on Noninvasive Myocardial Perfusion Imaging Early After Myocardial Infarction. J Am Coll Cardiol 2006;47(11):2187–93. Doi: 10.1016/j.jacc.2006.01.065.
352. Ríos-Navarro C., Hueso L., Miñana G., et al. Coronary Serum Obtained After Myocardial Infarction Induces Angiogenesis and Microvascular Obstruction Repair. Role of Hypoxia-inducible Factor-1A. Revista Española de Cardiología (English Edition) 2018;71(6):440–9. Doi: 10.1016/j.rec.2017.06.019.
353. Demirkiran A., Robbers LFHJ., van der Hoeven NW., et al. The Dynamic Relationship Between Invasive Microvascular Function and Microvascular Injury Indicators, and Their Association With Left Ventricular Function and Infarct Size at 1-Month After Reperfused ST-Segment-Elevation Myocardial Infarction. Circ Cardiovasc Interv 2022;15(11):892–902. Doi: 10.1161/CIRCINTERVENTIONS.122.012081.
354. Papapostolou S., Andrianopoulos N., Duffy SJ., et al. Long-term clinical outcomes of transient and persistent no-reflow following percutaneous coronary intervention (PCI): a multicentre Australian registry. EuroIntervention 2018;14(2):185–93. Doi: 10.4244/EIJ-D-17-00269.
355. Limbruno U., De Carlo M., Pistolesi S., et al. Distal embolization during primary angioplasty: Histopathologic features and predictability. Am Heart J 2005;150(1):102–8. Doi: 10.1016/j.ahj.2005.01.016.

356. Hamadeh A., Aldujeli A., Briedis K., et al. Characteristics and Outcomes in Patients Presenting With COVID-19 and ST-Segment Elevation Myocardial Infarction. Am J Cardiol 2020;131:1–6. Doi: 10.1016/j.amjcard.2020.06.063.
357. Tousoulis D., Davies G., Stefanadis C., Toutouzas P., Ambrose JA. Inflammatory and thrombotic mechanisms in coronary atherosclerosis. Heart 2003;89(9):993–7. Doi: 10.1136/heart.89.9.993.
358. Cosansu K., Ureyen C., Vatan M., Agac M., Kilic H., Akdemir R. Impact of direct stenting on clinical outcomes for small vessel coronary artery disease in patients undergoing primary percutaneous coronary intervention for ST-elevation myocardial infarction. Advances in Interventional Cardiology 2019;15(4):404–11. Doi: 10.5114/aic.2019.90214.
359. Webb JG., Carere RG., Virmani R., et al. Retrieval and analysis of particulate debris after saphenous vein graft intervention. J Am Coll Cardiol 1999;34(2):468–75. Doi: 10.1016/S0735-1097(99)00196-5.
360. Neumann F-J., Gick M. Direct stenting in ST-elevation myocardials infarction: convenient, but not improving outcomes. Eur Heart J 2018;39(26):2480–3. Doi: 10.1093/eurheartj/ehy353.
361. McCormick LM., Brown AJ., Ring LS., et al. Direct stenting is an independent predictor of improved survival in patients undergoing primary percutaneous coronary intervention for ST elevation myocardial infarction. Eur Heart J Acute Cardiovasc Care 2014;3(4):340–6. Doi: 10.1177/2048872614530864.
362. Azzalini L., Millán X., Ly HQ., L'allier PL., Jolicoeur EM. Direct Stenting Versus Pre-Dilation in ST-Elevation Myocardial Infarction: A Systematic Review and Meta-Analysis. J Interv Cardiol 2015;28(2):119–31. Doi: 10.1111/joic.12190.
363. Kalayci A., Oduncu V., Karabay CY., et al. Outcomes of direct stenting in patients with ST-elevated myocardial infarction. Herz 2018;43(5):447–54. Doi: 10.1007/s00059-017-4581-2.
364. Scarparo P., Improta R., Wilschut J., et al. Very Long-Term Clinical Outcomes After Direct Stenting in Patients Presenting With ST-Segment Elevation Myocardial Infarction. Cardiovascular Revascularization Medicine 2022;41:144–50. Doi: 10.1016/j.carrev.2022.01.014.
365. He J., Kong L-C., Zeng J-T., et al. Comparison of direct stenting with conventional strategy on myocardial impairments in ST-segment elevation myocardial infarction: a cardiac magnetic resonance imaging study. Int J Cardiovasc Imaging 2020;36(6):1167–75. Doi: 10.1007/s10554-020-01812-w.
366. Ozdemir R., Sezgin AT., Barutcu I., Topal E., Gullu H., Acikgoz N. Comparison of Direct Stenting Versus Conventional Stent Implantation on Blood Flow in Patients With ST-Segment Elevation Myocardial Infarction. Angiology 2006;57(4):453–8. Doi: 10.1177/0003319706290620.
367. Gasior M., Gierlotka M., Lekston A., et al. Comparison of Outcomes of Direct Stenting Versus Stenting After Balloon Predilation in Patients With Acute Myocardial Infarction (DIRAMI). Am J Cardiol 2007;100(5):798–805. Doi: 10.1016/j.amjcard.2007.04.026.
368. Ballarino MA., Moreyra E., Damonte A., et al. Multicenter randomized comparison of direct vs. conventional stenting: The DIRECTO trial. Catheterization and Cardiovascular Interventions 2003;58(4):434–40. Doi: 10.1002/ccd.10404.
369. Sabatier R., Hamon M., Zhao QM., et al. Could direct stenting reduce no-reflow in acute coronary syndromes? A randomized pilot study. Am Heart J 2002;143(6):1027–32. Doi: 10.1067/mhj.2002.122509.

370. Loubeyre C., Morice M-C., Lefèvre T., Piéchaud J-F., Louvard Y., Dumas P. A randomized comparison of direct stenting with conventional stent implantation in selected patients with acute myocardial infarction. J Am Coll Cardiol 2002;39(1):15–21. Doi: 10.1016/S0735-1097(01)01701-6.
371. Cuisset T., Hamilos M., Melikian N., et al. Direct Stenting for Stable Angina Pectoris Is Associated With Reduced Periprocedural Microcirculatory Injury Compared With Stenting After Pre-Dilation. J Am Coll Cardiol 2008;51(11):1060–5. Doi: 10.1016/j.jacc.2007.11.059.
372. Mahmoud KD., Jolly SS., James S., et al. Clinical impact of direct stenting and interaction with thrombus aspiration in patients with ST-segment elevation myocardial infarction undergoing percutaneous coronary intervention: Thrombectomy Trialists Collaboration. Eur Heart J 2018;39(26):2472–9. Doi: 10.1093/eurheartj/ehy219.
373. Meier D., Fournier S., Masci PG., et al. Impact of manual thrombectomy on microvascular obstruction in STEMI patients. Catheterization and Cardiovascular Interventions 2021;97(6):1141–8. Doi: 10.1002/ccd.28907.
374. Zajdel W., Miszalski-Jamka T., Zalewski J., Legutko J., Żmudka K., Paszek E. Cardiac Magnetic Resonance Shows Improved Outcomes in Patients with an ST-Segment Elevation Myocardial Infarction and a High Thrombus Burden Treated with Adjuvant Aspiration Thrombectomy. J Clin Med 2022;11(17):5000. Doi: 10.3390/jcm11175000.
375. De Carlo M., Aquaro GD., Palmieri C., et al. A Prospective Randomized Trial of Thrombectomy Versus No Thrombectomy in Patients With ST-Segment Elevation Myocardial Infarction and Thrombus-Rich Lesions. JACC Cardiovasc Interv 2012;5(12):1223–30. Doi: 10.1016/j.jcin.2012.08.013.
376. Sardella G., Mancone M., Bucciarelli-Ducci C., et al. Thrombus Aspiration During Primary Percutaneous Coronary Intervention Improves Myocardial Reperfusion and Reduces Infarct Size. J Am Coll Cardiol 2009;53(4):309–15. Doi: 10.1016/j.jacc.2008.10.017.
377. Rubboli A., Patti G. What is the Role for Glycoprotein IIB/IIIA Inhibitor Use in the Catheterization Laboratory in the Current Era? Curr Vasc Pharmacol 2018;16(5):451–8. Doi: 10.2174/1570161116666180117102422.
378. Liu X., Tao G-Z. Effects of tirofiban on the reperfusion-related no-reflow in rats with acute myocardial infarction. J Geriatr Cardiol 2013;10(1):52–8. Doi: 10.3969/j.issn.1671-5411.2013.01.009.
379. Elbadawi A., Gasioch G., Elgendy IY., et al. Intracoronary Eptifibatide During Primary Percutaneous Coronary Intervention in Early Versus Late Presenters with ST Segment Elevation Myocardial Infarction: A Randomized Trial. Cardiol Ther 2016;5(2):203–13. Doi: 10.1007/s40119-016-0073-3.
380. Ma Q., Ma Y., Wang X., et al. Intracoronary compared with intravenous bolus tirofiban on the microvascular obstruction in patients with STEMI undergoing PCI: a cardiac MR study. Int J Cardiovasc Imaging 2020;36(6):1121–32. Doi: 10.1007/s10554-020-01800-0.
381. Candemir B., Kilickap M., Ozcan OU., et al. Intracoronary versus intravenous high-dose bolus plus maintenance administration of tirofiban in patients undergoing primary percutaneous coronary intervention for acute ST elevation myocardial infarction. J Thromb Thrombolysis 2012;34(1):65–72. Doi: 10.1007/s11239-012-0685-y.

382. Akpek M., Sahin O., Sarli B., et al. Acute Effects of Intracoronary Tirofiban on No-Reflow Phenomena in Patients With ST-Segment Elevated Myocardial Infarction Undergoing Primary Percutaneous Coronary Intervention. Angiology 2015;66(6): 560–7. Doi: 10.1177/0003319714545780.
383. Gatarek P., Kaluzna-Czaplinska J. Trimethylamine N-oxide (TMAO) in human health. EXCLI J 2021;20:301–19. Doi: 10.17179/excli2020-3239.
384. Seldin MM., Meng Y., Qi H., et al. Trimethylamine N-Oxide Promotes Vascular Inflammation Through Signaling of Mitogen-Activated Protein Kinase and Nuclear Factor-κB. J Am Heart Assoc 2016;5(2). Doi: 10.1161/JAHA.115.002767.
385. Koeth RA., Wang Z., Levison BS., et al. Intestinal microbiota metabolism of l-carnitine, a nutrient in red meat, promotes atherosclerosis. Nat Med 2013;19(5):576–85. Doi: 10.1038/nm.3145.
386. Chen M-L., Zhu X-H., Ran L., Lang H-D., Yi L., Mi M-T. Trimethylamine-N-Oxide Induces Vascular Inflammation by Activating the NLRP3 Inflammasome Through the SIRT3-SOD2-mtROS Signaling Pathway. J Am Heart Assoc 2017;6(9). Doi: 10.1161/JAHA.117.006347.
387. Ma G., Pan B., Chen Y., et al. Trimethylamine N-oxide in atherogenesis: impairing endothelial self-repair capacity and enhancing monocyte adhesion. Biosci Rep 2017;37(2). Doi: 10.1042/BSR20160244.
388. Jomard A., Liberale L., Doytcheva P., et al. Effects of acute administration of trimethylamine N-oxide on endothelial function: a translational study. Sci Rep 2022;12(1):8664. Doi: 10.1038/s41598-022-12720-5.
389. Tang WHW., Wang Z., Levison BS., et al. Intestinal Microbial Metabolism of Phosphatidylcholine and Cardiovascular Risk. New England Journal of Medicine 2013;368(17):1575–84. Doi: 10.1056/NEJMoa1109400.
390. Kei CY., Singh K., Dautov RF., Nguyen TH., Chirkov YY., Horowitz JD. Coronary "Microvascular Dysfunction": Evolving Understanding of Pathophysiology, Clinical Implications, and Potential Therapeutics. Int J Mol Sci 2023;24(14):11287. Doi: 10.3390/ijms241411287.
391. Lanza F., Beretz A., Stierlé A., Hanau D., Kubina M., Cazenave JP. Epinephrine potentiates human platelet activation but is not an aggregating agent. Am J Physiol 1988;255(6 Pt 2):H1276-88. Doi: 10.1152/ajpheart.1988.255.6.H1276.
392. Toya T., Nagatomo Y., Ikegami Y., Masaki N., Adachi T. Coronary microvascular dysfunction in heart failure patients. Front Cardiovasc Med 2023;10:1153994. Doi: 10.3389/fcvm.2023.1153994.
393. Shah SJ., Lam CSP., Svedlund S., et al. Prevalence and correlates of coronary microvascular dysfunction in heart failure with preserved ejection fraction: PROMIS-HFpEF. Eur Heart J 2018;39(37):3439–50. Doi: 10.1093/eurheartj/ehy531.
394. Paolisso P., Gallinoro E., Belmonte M., et al. Coronary Microvascular Dysfunction in Patients With Heart Failure: Characterization of Patterns in HFrEF Versus HFpEF. Circ Heart Fail 2024;17(1):e010805. Doi: 10.1161/CIRCHEARTFAILURE.123.010805.
395. Meijers WC., van der Velde AR., de Boer RA. Biomarkers in heart failure with preserved ejection fraction. Neth Heart J 2016;24(4):252–8. Doi: 10.1007/s12471-016-0817-7.
396. Stoltzfus JC. Logistic Regression: A Brief Primer. Academic Emergency Medicine 2011;18(10):1099–104. Doi: 10.1111/j.1553-2712.2011.01185.x.
397. Bzdok D., Krzywinski M., Altman N. Machine learning: a primer. Nat Methods 2017;14(12):1119–20. Doi: 10.1038/nmeth.4526.

398. Liu P., Xing Z., Peng X., et al. Machine learning versus multivariate logistic regression for predicting severe COVID-19 in hospitalized children with Omicron variant infection. J Med Virol 2024;96(2):e29447. Doi: 10.1002/jmv.29447.
399. Ingwersen EW., Stam WT., Meijs BJ V., et al. Machine learning versus logistic regression for the prediction of complications after pancreatoduodenectomy. Surgery 2023;174(3):435–40. Doi: 10.1016/j.surg.2023.03.012.
400. Song X., Liu X., Liu F., Wang C. Comparison of machine learning and logistic regression models in predicting acute kidney injury: A systematic review and meta-analysis. Int J Med Inform 2021;151:104484. Doi: 10.1016/j.ijmedinf.2021.104484.
401. Almesned MA., Prins FM., Lipšic E., et al. Temporal Course of Plasma Trimethylamine N-Oxide (TMAO) Levels in ST-Elevation Myocardial Infarction. J Clin Med 2021;10(23):5677. Doi: 10.3390/jcm10235677.
402. Washburn R., Cox J., Muhlestein J., et al. Pilot Study of Novel Intermittent Fasting Effects on Metabolomic and Trimethylamine N-oxide Changes During 24-hour Water-Only Fasting in the FEELGOOD Trial. Nutrients 2019;11(2):246. Doi: 10.3390/nu11020246.
403. Yang S., Li X., Yang F., et al. Gut Microbiota-Dependent Marker TMAO in Promoting Cardiovascular Disease: Inflammation Mechanism, Clinical Prognostic, and Potential as a Therapeutic Target. Front Pharmacol 2019;10. Doi: 10.3389/fphar.2019.01360.
404. Li DY., Tang WHW. Gut Microbiota and Atherosclerosis. Curr Atheroscler Rep 2017;19(10):39. Doi: 10.1007/s11883-017-0675-9.
405. Tilg H. A Gut Feeling about Thrombosis. New England Journal of Medicine 2016;374(25):2494–6. Doi: 10.1056/NEJMcibr1604458.
406. Brunt VE., Gioscia-Ryan RA., Casso AG., et al. Trimethylamine-N-Oxide Promotes Age-Related Vascular Oxidative Stress and Endothelial Dysfunction in Mice and Healthy Humans. Hypertension 2020;76(1):101–12. Doi: 10.1161/HYPERTENSIONAHA.120.14759.
407. Kul S., Caliskan Z., Guvenc TS., et al. Gut microbiota-derived metabolite trimethylamine N-oxide and biomarkers of inflammation are linked to endothelial and coronary microvascular function in patients with inflammatory bowel disease. Microvasc Res 2023;146:104458. Doi: 10.1016/j.mvr.2022.104458.
408. Li XS., Obeid S., Klingenberg R., et al. Gut microbiota-dependent trimethylamine N-oxide in acute coronary syndromes: a prognostic marker for incident cardiovascular events beyond traditional risk factors. Eur Heart J 2017:ehw582. Doi: 10.1093/eurheartj/ehw582.
409. Mei Z., Chen G-C., Wang Z., et al. Dietary factors, gut microbiota, and serum trimethylamine-N-oxide associated with cardiovascular disease in the Hispanic Community Health Study/Study of Latinos. Am J Clin Nutr 2021;113(6):1503–14. Doi: 10.1093/ajcn/nqab001.
410. Yazaki Y., Salzano A., Nelson CP., et al. Geographical location affects the levels and association of trimethylamine N-oxide with heart failure mortality in BIOSTAT-CHF: a post-hoc analysis. Eur J Heart Fail 2019;21(10):1291–4. Doi: 10.1002/ejhf.1550.
411. Clemente-Suárez VJ., Beltrán-Velasco AI., Redondo-Flórez L., Martín-Rodríguez A., Tornero-Aguilera JF. Global Impacts of Western Diet and Its Effects on Metabolism and Health: A Narrative Review. Nutrients 2023;15(12):2749. Doi: 10.3390/nu15122749.

412. Erickson M., Malin S., Wang Z., Brown J., Hazen S., Kirwan J. Effects of Lifestyle Intervention on Plasma Trimethylamine N-Oxide in Obese Adults. Nutrients 2019;11(1):179. Doi: 10.3390/nu11010179.
413. Kühn T., Rohrmann S., Sookthai D., et al. Intra-individual variation of plasma trimethylamine-N-oxide (TMAO), betaine and choline over 1 year. Clinical Chemistry and Laboratory Medicine (CCLM) 2017;55(2):261–8. Doi: 10.1515/cclm-2016-0374.
414. Wilkinson IB., McEniery CM. Arterial Stiffness, Endothelial Function And Novel Pharmacological Approaches. Clin Exp Pharmacol Physiol 2004;31(11):795–9. Doi: 10.1111/j.1440-1681.2004.04074.x.
415. Pauriah M., Khan F., Lim TK., et al. B-type natriuretic peptide is an independent predictor of endothelial function in man. Clin Sci 2012;123(5):307–12. Doi: 10.1042/CS20110168.
416. Chong AY., Blann AD., Patel J., Freestone B., Hughes E., Lip GYH. Endothelial Dysfunction and Damage in Congestive Heart Failure. Circulation 2004;110(13):1794–8. Doi: 10.1161/01.CIR.0000143073.60937.50.
417. Kathiresan S., Gona P., Larson MG., et al. Cross-Sectional Relations of Multiple Biomarkers From Distinct Biological Pathways to Brachial Artery Endothelial Function. Circulation 2006;113(7):938–45. Doi: 10.1161/CIRCULATIONAHA.105.580233.
418. Hirakawa K., Yamamuro M., Uemura T., et al. Correlation between microvascular dysfunction and B-type natriuretic peptide levels in non-ischemic heart failure patients with cardiac fibrosis. Int J Cardiol 2017;228:881–5. Doi: 10.1016/j.ijcard.2016.11.054.
419. Prescott E., Bove KB., Bechsgaard DF., et al. Biomarkers and Coronary Microvascular Dysfunction in Women With Angina and No Obstructive Coronary Artery Disease. JACC: Advances 2023;2(2):100264. Doi: 10.1016/j.jacadv.2023.100264.
420. Yao M-E., Liao P-D., Zhao X-J., Wang L. Trimethylamine-N-oxide has prognostic value in coronary heart disease: a meta-analysis and dose-response analysis. BMC Cardiovasc Disord 2020;20(1):7. Doi: 10.1186/s12872-019-01310-5.
421. Guasti L., Galliazzo S., Molaro M., et al. TMAO as a biomarker of cardiovascular events: a systematic review and meta-analysis. Intern Emerg Med 2021;16(1):201–7. Doi: 10.1007/s11739-020-02470-5.
422. Croyal M., Saulnier P-J., Aguesse A., et al. Plasma Trimethylamine N-Oxide and Risk of Cardiovascular Events in Patients With Type 2 Diabetes. J Clin Endocrinol Metab 2020;105(7):2371–80. Doi: 10.1210/clinem/dgaa188.
423. Li N., Wang Y., Zhou J., et al. Association between the Changes in Trimethylamine N-Oxide-Related Metabolites and Prognosis of Patients with Acute Myocardial Infarction: A Prospective Study. J Cardiovasc Dev Dis 2022;9(11):380. Doi: 10.3390/jcdd9110380.
424. Coutinho-Wolino KS., de F. Cardozo LFM., de Oliveira Leal V., Mafra D., Stockler-Pinto MB. Can diet modulate trimethylamine N-oxide (TMAO) production? What do we know so far? Eur J Nutr 2021;60(7):3567–84. Doi: 10.1007/s00394-021-02491-6.
425. Zhao Y., Wang Z. Impact of trimethylamine N-oxide (TMAO) metaorganismal pathway on cardiovascular disease. J Lab Precis Med 2020;5:16–16. Doi: 10.21037/jlpm.2020.01.01.

426. Sanchez-Gimenez R., Peiró ÓM., Bonet G., et al. Plasma trimethylamine-N-oxide, its precursors and risk of cardiovascular events in patients with acute coronary syndrome: Mediating effects of renal function. Front Cardiovasc Med 2022;9. Doi: 10.3389/fcvm.2022.1000815.
427. Fukami T., Yokoi T., Nakajima M. Non-P450 Drug-Metabolizing Enzymes: Contribution to Drug Disposition, Toxicity, and Development. Annu Rev Pharmacol Toxicol 2022;62(1):405–25. Doi: 10.1146/annurev-pharmtox-052220-105907.
428. Annunziata G., Ciampaglia R., Maisto M., et al. Taurisolo®, a Grape Pomace Polyphenol Nutraceutical Reducing the Levels of Serum Biomarkers Associated With Atherosclerosis. Front Cardiovasc Med 2021;8. Doi: 10.3389/fcvm.2021. 697272.
429. Zhang Q., Guo X., Xie C., et al. Unraveling the metabolic pathway of choline-TMA-TMAO: Effects of gypenosides and implications for the therapy of TMAO related diseases. Pharmacol Res 2021;173:105884. Doi: 10.1016/j.phrs.2021.105884.
430. Konijnenberg LSF., Damman P., Duncker DJ., et al. Pathophysiology and diagnosis of coronary microvascular dysfunction in ST-elevation myocardial infarction. Cardiovasc Res 2020;116(4):787–805. Doi: 10.1093/cvr/cvz301.
431. Serruys PW., Di Mario C., Meneveau N., et al. Intracoronary pressure and flow velocity with sensor-tip guidewires: A new methodologic approach for assessment of coronary hemodynamics before and after coronary interventions. Am J Cardiol 1993;71(14):D41–53. Doi: 10.1016/0002-9149(93)90133-W.
432. Hoffman JIE. Problems of Coronary Flow Reserve. Ann Biomed Eng 2000; 28(8):884–96. Doi: 10.1114/1.1308503.
433. Kodeboina M., Nagumo S., Munhoz D., et al. Simplified Assessment of the Index of Microvascular Resistance. J Interv Cardiol 2021;2021:1–7. Doi: 10.1155/2021/ 9971874.
434. Rahman H., Demir OM., Khan F., et al. Physiological Stratification of Patients With Angina Due to Coronary Microvascular Dysfunction. J Am Coll Cardiol 2020; 75(20):2538–49. Doi: 10.1016/j.jacc.2020.03.051.
435. Jansen TPJ., Crooijmans C., Damman P. Microvascular resistance reserve, does one size fit all? Eur Heart J 2023. Doi: 10.1093/eurheartj/ehad691.
436. Del Buono MG., Montone RA., Camilli M., et al. Coronary Microvascular Dysfunction Across the Spectrum of Cardiovascular Diseases. J Am Coll Cardiol 2021; 78(13):1352–71. Doi: 10.1016/j.jacc.2021.07.042.
437. Mejia-Renteria H., Travieso A., Matías-Guiu JA., et al. Coronary microvascular dysfunction is associated with impaired cognitive function: the Cerebral-Coronary Connection study (C3 study). Eur Heart J 2023;44(2):113–25. Doi: 10.1093/ eurheartj/ehac521.
438. Yong AS., Layland J., Fearon WF., et al. Calculation of the Index of Microcirculatory Resistance Without Coronary Wedge Pressure Measurement in the Presence of Epicardial Stenosis. JACC Cardiovasc Interv 2013;6(1):53–8. Doi: 10.1016/ j.jcin.2012.08.019.
439. Collison D., Didagelos M., Aetesam-ur-Rahman M., et al. Post-stenting fractional flow reserve vs coronary angiography for optimization of percutaneous coronary intervention (TARGET-FFR). Eur Heart J 2021;42(45):4656–68. Doi: 10.1093/ eurheartj/ehab449.
440. Hassell M., Bax M., van Lavieren M., et al. Microvascular dysfunction following ST-elevation myocardial infarction and its recovery over time. EuroIntervention 2017;13(5):e578–84. Doi: 10.4244/EIJ-D-16-00818.

441. de Vos A., Jansen TPJ., van ’t Veer M., et al. Microvascular Resistance Reserve to Assess Microvascular Dysfunction in ANOCA Patients. JACC Cardiovasc Interv 2023;16(4):470–81. Doi: 10.1016/j.jcin.2022.12.012.
442. Faustino M., Baptista SB., Freitas A., et al. The Index of Microcirculatory Resistance as a Predictor of Echocardiographic Left Ventricular Performance Recovery in Patients With ST-Elevation Acute Myocardial Infarction Undergoing Successful Primary Angioplasty. J Interv Cardiol 2016;29(2):137–45. Doi: 10.1111/joic.12278.
443. Yoo S-H., Yoo T-K., Lim H-S., Kim M-Y., Koh J-H. Index of Microcirculatory Resistance as Predictor for Microvascular Functional Recovery in Patients with Anterior Myocardial Infarction. J Korean Med Sci 2012;27(9):1044. Doi: 10.3346/jkms.2012.27.9.1044.
444. Fineschi M., Verna E., Barioli A., et al. One-year results from the Assessing MICRO-vascular resistances via IMR to predict outcome in ST-elevation myocardial infarction patients with multivessel disease undergoing primary PCI (AMICRO) trial. Front Cardiovasc Med 2022;9. Doi: 10.3389/fcvm.2022.1051174.
445. Paulus WJ., Tschöpe C. A Novel Paradigm for Heart Failure With Preserved Ejection Fraction. J Am Coll Cardiol 2013;62(4):263–71. Doi: 10.1016/j.jacc.2013.02.092.
446. Hotta K., Chen B., Behnke BJ., et al. Exercise training reverses age-induced diastolic dysfunction and restores coronary microvascular function. J Physiol 2017;595(12):3703–19. Doi: 10.1113/JP274172.
447. Shah SJ., Lam CSP., Svedlund S., et al. Prevalence and correlates of coronary microvascular dysfunction in heart failure with preserved ejection fraction: PROMIS-HFpEF. Eur Heart J 2018;39(37):3439–50. Doi: 10.1093/eurheartj/ehy531.
448. Taqueti VR., Solomon SD., Shah AM., et al. Coronary microvascular dysfunction and future risk of heart failure with preserved ejection fraction. Eur Heart J 2018;39(10):840–9. Doi: 10.1093/eurheartj/ehx721.
449. Hong D., Shin D., Lee SH., et al. Prognostic Impact of Coronary Microvascular Dysfunction According to Different Patterns by Invasive Physiologic Indexes in Symptomatic Patients With Intermediate Coronary Stenosis. Circ Cardiovasc Interv 2023. Doi: 10.1161/CIRCINTERVENTIONS.122.012621.
450. Mather AN., Fairbairn TA., Artis NJ., Greenwood JP., Plein S. Timing of Cardio-vascular MR Imaging after Acute Myocardial Infarction: Effect on Estimates of Infarct Characteristics and Prediction of Late Ventricular Remodeling. Radiology 2011;261(1):116–26. Doi: 10.1148/radiol.11110228.
451. Wu KC. CMR of microvascular obstruction and hemorrhage in myocardial infarction. Journal of Cardiovascular Magnetic Resonance 2012;14(1):68. Doi: 10.1186/1532-429X-14-68.
452. Kotani J., Nanto S., Mintz GS., et al. Plaque Gruel of Atheromatous Coronary Lesion May Contribute to the No-Reflow Phenomenon in Patients With Acute Coronary Syndrome. Circulation 2002;106(13):1672–7. Doi: 10.1161/01.CIR.0000030189.27175.4E.
453. Piana RN., Paik GY., Moscucci M., et al. Incidence and treatment of “no-reflow” after percutaneous coronary intervention. Circulation 1994;89(6):2514–8. Doi: 10.1161/01.CIR.89.6.2514.
454. Tanaka A., Kawarabayashi T., Nishibori Y., et al. No-Reflow Phenomenon and Lesion Morphology in Patients With Acute Myocardial Infarction. Circulation 2002;105(18):2148–52. Doi: 10.1161/01.CIR.0000015697.59592.07.
455. Buja LM. Myocardial ischemia and reperfusion injury. Cardiovascular Pathology 2005;14(4):170–5. Doi: 10.1016/j.carpath.2005.03.006.

456. El Farissi M., Zimmermann FM., De Maria GL., et al. The Index of Microcirculatory Resistance After Primary PCI. JACC Cardiovasc Interv 2023;16(19):2383–92. Doi: 10.1016/j.jcin.2023.08.030.
457. Mehta SR., Wood DA., Storey RF., et al. Complete Revascularization with Multivessel PCI for Myocardial Infarction. New England Journal of Medicine 2019;381(15):1411–21. Doi: 10.1056/NEJMoa1907775.
458. Goldberg RJ., Spencer FA., Fox KAA., et al. Prehospital Delay in Patients With Acute Coronary Syndromes (from the Global Registry of Acute Coronary Events [GRACE]). Am J Cardiol 2009;103(5):598–603. Doi: 10.1016/j.amjcard.2008.10.038.

LIST OF PUBLICATIONS

Publications related to the results of dissertation

1. Tsai T-Y, **Aldujeli A**, Haq A, Knokneris A, Briedis K, Hughes D, Unikas R, Renkens M, Revaiah PC, Tobe A, Miyashita K, Sharif F, Garg S, Onuma Y, Serruys PW. The Impact of Microvascular Resistance Reserve on the Outcome of Patients with STEMI. *JACC: Cardiovascular Interventions* 2024. Available at: http://dx.doi.org/10.1016/j.jcin.2024.03.024.
2. Čereškevičius D, Zabiela V, **Aldujeli A**, Lesauskaitė V, Zubielienė K, Raškevičius V, Čiapienė I, Žaliaduonytė D, Giedraitienė A, Žvikas V, Jakštas V, Skipskis V, Dobilienė O, Šakalytė G, Tatarūnas V. Impact of CYP2C19 Gene Variants on Long-Term Treatment with Atorvastatin in Patients with Acute Coronary Syndromes. *International Journal of Molecular Sciences* 2024;25:5385. Available at: http://dx.doi.org/10.3390/ijms25105385.
3. **Aldujeli A,** Tsai T, Haq A, Tatarunas V, Knokneris A, Briedis K, Unikas R, Onuma Y, Brilakis ES, Serruys PW. Impact of Coronary Microvascular Dysfunction on Functional Left Ventricular Remodeling and Diastolic Dysfunction. *Journal of the American Heart Association*, 2024;0(0): e033596. https://doi.org/10.1161/JAHA.123.033596
4. **Aldujeli A**, Haq A, Tsai T-Y, Grabauskyte I, Tatarunas V, Briedis K, Rana S, Unikas R, Hamadeh A, Serruys PW, Brilakis ES. The impact of primary percutaneous coronary intervention strategies during ST-elevation myocardial infarction on the prevalence of coronary microvascular dysfunction. *Scientific Reports* 2023;13. Available at: http://dx.doi.org/10.1038/s41598-023-47343-x.
5. **Aldujeli A**, Patel R, Grabauskyte I, Hamadeh A, Lieponyte A, Tatarunas V, Khalifeh H, Briedis K, Skipskis V, Aldujeili M, Jarasuniene D, Rana S, Unikas R, Haq A. The Impact of Trimethylamine N-Oxide and Coronary Microcirculatory Dysfunction on Outcomes following ST-Elevation Myocardial Infarction. *Journal of Cardiovascular Development and Disease* 2023;10:197. Available at: http://dx.doi.org/10.3390/jcdd10050197.
6. Tatarunas V, **Aldujeli A**, Kurnickaite Z, Maciulevicius L, Burkanas M, Venius J, Ciapiene I, Skipskis V, Norvilaite R, Giedraitiene A, Unikas R, Baksyte G, Gustiene O, Sakalyte G, Lesauskaite V. Blood direct PCR: impact of CYP2C19 and CYP4F2 variants for bleeding prediction in ST-elevation myocardial infarction patients with ticagrelor. *Personalized Medicine* 2022;19:207–217. Available at: http://dx.doi.org/10.2217/pme-2021-0152.

Abstracts related to the results of dissertation

1. Patel RH, **Aldujeli A**, Hamadeh A, Haq A. The impact of coronary microcirculatory dysfunction on left ventricular functional remodelling following ST-elevation myocardial infarction. *Journal of the American College of Cardiology* 2024;83:871. Available at: http://dx.doi.org/10.1016/s0735-1097(24)02861-4.
2. **Aldujeli** A, Azani F, Tsai T-Y, Grabauskyte I, Haq A, Briedis K, Rana S, Unikas R, Serruys PW, Brilakis ES. 400.19 Comparative Impact of Direct Stenting, Aspiration Thrombectomy, and Intracoronary Glycoprotein IIb/IIIa Inhibitors Versus Balloon Predilation on Microvascular Function and Long-Term Outcomes in STEMI Patients. *JACC: Cardiovascular Interventions* 2024;17:S47. Available at: http://dx.doi.org/10.1016/j.jcin.2024.01.186.
3. Knokneris A, **Aldujeli A**, Grabauskyte I, Haq A, Briedis K, Tatarunas V, Unikas R. 500.01 The Impact of Gut Microbiota on Left Ventricular Systolic Function Following ST-elevation Myocardial Infarction. *JACC: Cardiovascular Interventions* 2024;17:S51. Available at: http://dx.doi.org/10.1016/j.jcin.2024.01.194.
4. Kireilis, Benas; Grabauskytė, Ingrida; **Aldujeli, Ali**; Bakšytė, Giedrė; Jaruševičius, Gediminas; Visockas, Lukas; Katutytė, Martyna. The influence of coronary microvascular dysfunction on 12-month cardiovascular events // *International Health Sciences Conference for All (IHSC for All) "Precision Medicine"*: Abstract book 2024 : [March 25–26, 2024, Kaunas] / Edited by Ignas Lapeikis, Livija Petrokaitė, p. 272-273, ISSN 3030-0711.
5. **Aldujeli A**, Patel R, Grabauskyte I, Haq A, Karaliute R, Lickunas K, Unikas R, Khalifeh H, Al Dujeili M, Zaliaduonyte D, Plisiene J, Briedis K, Hamadeh A. The Index of Microcirculatory Resistance Is Associated With New Onset of Atrial Fibrillation Following ST-Elevation Myocardial Infarction. *Cardiovascular Revascularization Medicine* 2023;53:S41–S42. Available at: http://dx.doi.org/10.1016/j.carrev.2023.05.096.
6. **Aldujeli A,** Patel R, Grabauskytė I, Sencelikel T, Khalifeh H, Aldujeili M, Briedis K, Unikas R, Hamadeh A, Haq A. Impact of primary PCI techniques on coronary microcirculation in STEMI patients *// PCR Online : EuroPCR 2023 Abstract Book* : [Paris, France, 16–19 May, 2023], p. 1-1.
7. **Aldujeli A**, Unikas R, Grabauskyte I, Tatarunas V, Jarasuniene D, Pranculis A, Patel R, Khalifeh H, Briedis K, Hamadeh A, Ordiene R, Braukyliene R, Haq A. The impact of primary percutaneous coronary intervention strategies during st-elevation myocardial infarction on the preva-

lence of coronary microvascular dysfunction. *European Heart Journal* 2023;44. Available at: http://dx.doi.org/10.1093/eurheartj/ehad655.2129.

8. **Aldujeli A,** Patel R, Haq A, Grabauskytė I, Tatarūnas V, Plisienė J, Hamadeh A, Khalifeh H, Aldujeili M, Briedis K, Jarašūnienė D, Unikas R. The impact of coronary microcirculatory dysfunction on left ventricular functional remodeling following ST-elevation myocardial infarction // *European Journal of Heart Failure*: Abstracts of the Heart Failure 2023 and the World Congress on Acute Heart Failure : May 20-23, 2023, Prague, Czech Republic / Heart Failure Association (HFA), European Society of Cardiology (ESC), t. 25, nr. S2, p. 342 - 343, ISSN 1388-9842, 1879-0844. doi:10.1002/ejhf.2927.
9. **Aldujeli A,** Riddhi P, Grabauskytė I, Haq A, Karaliūtė R, Tatarūnas V, Khalifeh H, Aldujeili M, Briedis K, Plisienė J, Hamadeh A, Jarašūnienė D, Žaliaduonytė D, Unikas R. Novel predictors of newonset atrial fibrillation following the event of ST-elevation myocardial infarction // *European Journal of Heart Failure*: Abstracts of the Heart Failure 2023 and the World Congress on Acute Heart Failure: May 20-23, 2023, Prague, Czech Republic / Heart Failure Association (HFA), European Society of Cardiology (ESC), t. 25, nr. S2, p. 3 - 3, ISSN 1388-9842, 1879-0844. doi:doi:10.1002/ejhf.2927.
10. Kireilis B, Jaruševičius G, **Aldujeli A,** Grabauskytė I. Decoding the Impact of SIRT1 Gene Variants in Coronary Microvascular Dysfunction following ST-Elevation Myocardial Infarction // Læknablaðið. Fylgirit.: *28 Nordic-Baltic Congress of Cardiology* [(NBCC 2023) The Future of Cardiology]: June [8-10] 2023, Reykjavík / [Icelandic Society of Cardiology]. Kópavogur: Læknafélag Íslands (Icelandic Medical Association), 2023, fylgyrit 117, p. 1-1, ISSN 0254-1394.
11. **Aldujeli A**, Patel R, Grabauskyte I, Haq A, Karaliute R, Lickunas K, Unikas R, Khalifeh H, Al Dujeili M, Zaliaduonyte D, Plisiene J, Briedis K, Hamadeh A. CRT-100.76 The Index of Microcirculatory Resistance Is Associated With New Onset of Atrial Fibrillation Following ST-Elevation Myocardial Infarction. *JACC: Cardiovascular Interventions* 2023;16:S29. Available at: http://dx.doi.org/10.1016/j.jcin.2023.01.109.
12. **Aldujeli A,** Haq A, Kurnickaite Z, Lickunas K, Maciulevicius L, Eitminaviciute I, Hamadeh A, Tatarunas V, Al Dujeili M, Briedis K, Tecson KM, Zaliaduonyte D, Unikas R. Increased Plasma Trimethylamine N-Oxide Is Associated With New Onset of Atrial Fibrillation Post-ST-Elevation Myocardial Infarction. *Cardiovascular Revascularization Medicine* 2022;40:26. Available at: http://dx.doi.org/10.1016/j.carrev.2022.06.051.

13. **Aldujeli A**, Haq A, Kurnickaite Z, Lickunas K, Maciulevicius L, Hamadeh A, Eitminaviciute I, Tatarunas V, Al Dujeili M, Briedis K, Baksyte G, Tecson KM, Zaliaduonyte D, Unikas R. CRT-100.49 Impact of On-Admission Trimethylamine N-Oxide Levels on Coronary Blood Flow and Prognosis of Patients with ST-Elevation Myocardial Infarction Undergoing Primary Percutaneous Coronary Intervention in a Real-World Setting. *JACC: Cardiovascular Interventions* 2022;15:S13. Available at: http://dx.doi.org/10.1016/j.jcin.2022.01.108.
14. **Aldujeli A**, Haq A, Kurnickaite Z, Lickunas K, Maciulevicius L, Eitminaviciute I, Hamadeh A, Tatarunas V, Al Dujeili M, Briedis K, Tecson KM, Zaliaduonyte D, Unikas R. CRT-100.31 Increased Plasma Trimethylamine N-Oxide Is Associated With New Onset of Atrial Fibrillation Post-ST-Elevation Myocardial Infarction. *JACC: Cardiovascular Interventions* 2022;15:S8. Available at: http://dx.doi.org/10.1016/j.jcin.2022.01.094.
15. **Aldujeli A**, Haq A, Kurnickaite Z, Lickunas K, Maciulevicius L, Hamadeh A, Eitminaviciute I, Tatarunas V, Al Dujeili M, Briedis K, Baksyte G, Tecson KM, Zaliaduonyte D, Unikas R. Impact of On-Admission Trimethylamine N-Oxide Levels on Coronary Blood Flow and Prognosis of Patients With ST-Elevation Myocardial Infarction Undergoing Primary Percutaneous Coronary Intervention in a Real-World Setting. *Cardiovascular Revascularization Medicine* 2022;40:34. Available at: http://dx.doi.org/10.1016/j.carrev.2022.06.069.
16. **Aldujeli A**, Haq A, Kurnickaite Z, Maciulevicius L, Lickunas K, Al Dujeili M, Eitminaviciute I, Tatarunas V, Briedis K, Krivickas Z, Tecson KM, Hamadeh A, Baksyte G, Zaliaduonyte D, Unikas R. The Relationship Between Trimethylamine N-Oxide and Coronary Collateral Circulation in Patients With ST-Segment Elevation Myocardial Infarction. *Cardiovascular Revascularization Medicine* 2022;40:26–27. Available at: http://dx.doi.org/10.1016/j.carrev.2022.06.052.
17. **Aldujeli A**, Haq A, Kurnickaite Z, Maciulevicius L, Lickunas K, Al Dujeili M, Eitminaviciute I, Tatarunas V, Briedis K, Krivickas Z, Tecson KM, Hamadeh A, Baksyte G, Zaliaduonyte D, Unikas R. CRT-100.32 The Relationship Between Trimethylamine N-Oxide and Coronary Collateral Circulation in Patients With ST-Segment Elevation Myocardial Infarction. *JACC: Cardiovascular Interventions* 2022;15:S8. Available at: http://dx.doi.org/10.1016/j.jcin.2022.01.095.
18. Briedis K, **Aldujeli A**, Briede K, Vajauskas D, Benetis R, Zaliunas R. CRT-700.08 Safety and Feasibility of Dynamic 6-Minute Adenosine Stress Myocardial Perfusion SPECT Imaging in Patients Diagnosed

With Severe Aortic Valve Stenosis. *JACC: Cardiovascular Interventions* 2022;15:S56. Available at: http://dx.doi.org/10.1016/j.jcin.2022.01.220.
19. Briedis K, **Aldujeli A**, Briede K, Vajauskas D, Benetis R, Zaliunas R. CRT-700.06 Comparison of Clinical Characteristics of Intravenous Infusion Versus Intracoronary Injections of Adenosine for Evaluation of Intermediate Coronary Artery Lesions in Patients Diagnosed With Severe Aortic Stenosis. *JACC: Cardiovascular Interventions* 2022;15: S55–S56. Available at: http://dx.doi.org/10.1016/j.jcin.2022.01.218.
20. Briedis K, **Aldujeli A**, Briede K, Vajauskas D, Benetis R, Zaliunas R. Comparison of Clinical Characteristics of Intravenous Infusion Versus Intracoronary Injections of Adenosine for Evaluation of Intermediate Coronary Artery Lesions in Patients Diagnosed With Severe Aortic Stenosis. *Cardiovascular Revascularization Medicine* 2022;40:89–90. Available at: http://dx.doi.org/10.1016/j.carrev.2022.06.201.
21. Briedis K, **Aldujeli A**, Briede K, Vajauskas D, Benetis R, Zaliunas R. Safety and Feasibility of Dynamic 6-Minute Adenosine Stress Myocardial Perfusion SPECT Imaging in Patients Diagnosed With Severe Aortic Valve Stenosis. *Cardiovascular Revascularization Medicine* 2022;40:90. Available at: http://dx.doi.org/10.1016/j.carrev.2022.06.203.

SUPPLEMENT

KAUNO REGIONINIS BIOMEDICININIŲ TYRIMŲ ETIKOS KOMITETAS
Lietuvos sveikatos mokslų universitetas, A. Mickevičiaus g. 9, LT 44307 Kaunas, tel. (+370) 37 32 68 89;el.paštas: kaunorbtek@lsmuni.lt

LEIDIMAS ATLIKTI BIOMEDICININĮ TYRIMĄ

2021-01-12 Nr. BE-2-5

Biomedicininio tyrimo pavadinimas: „Pacientų, sergančių ūmine ir lėtine išemine širdies liga, aterosklerozinės plokštelės morfologijos sąsajos su mikrobiotos metabolitais ir genų variantais“	
Protokolo Nr.:	**1**
Data:	**2021-01-11**
Versija:	**3**
Asmens informavimo forma	**Versija 2; data 2020-12-14 (pagrindinė forma)** **Versija 1; data 2020-11-10 (genetiniams tyrimams)**
Pagrindinis tyrėjas: Biomedicininio tyrimo vieta: Įstaigos pavadinimas: Adresas:	**prof. dr. Ramūnas Unikas** **Lietuvos sveikatos mokslų universito ligoninė Kauno klinikos, Kardiologijos klinika** Eivenių g. 2 LT-50161, Kaunas

Išvada:
Kauno regioninio biomedicininių tyrimų etikos komiteto posėdžio, įvykusio **2021 m. sausio mėn. 5 d.** (protokolo Nr. BE-10-1) sprendimu pritarta biomedicininio tyrimo vykdymui.

Mokslinio eksperimento vykdytojai įsipareigoja: (1) nedelsiant informuoti Kauno Regioninį biomedicininių Tyrimų Etikos komitetą apie visus nenumatytus atvejus, susijusius su studijos vykdymu, (2) iki sausio 15 dienos – pateikti metinį studijos vykdymo apibendrinimą bei, (3) per mėnesį po studijos užbaigimo, pateikti galutinį pranešimą apie eksperimentą.

Kauno regioninio biomedicininių tyrimų etikos komiteto nariai			
Nr.	Vardas, Pavardė	Veiklos sritis	Dalyvavo posėdyje
1.	Doc. dr. Gintautas Gumbrevičius	Klinikinė farmakologija	Taip
2.	Prof. dr. Kęstutis Petrikonis	Neurologija	Taip
3.	Dr. Saulius Raugelė	Chirurgija	Taip
4.	Dr. Lina Jankauskaitė	Pediatrija	Taip
5.	Prof. dr. Džilda Veličkienė	Endokrinologija	Taip
6.	Doc. dr. Eimantas Peičius	Visuomenės sveikata	Taip
7.	Aušra Degutytė	Visuomenės sveikata	Ne
8.	Dr. Žydrūnė Luneckaitė	Visuomenės sveikata	Taip
9.	Viktorija Bučinskaitė	Teisė	Taip

Kauno regioninis biomedicininių tyrimų etikos komitetas dirba vadovaudamasis etikos principais nustatytais biomedicininių tyrimų Etikos įstatyme, Helsinkio deklaracijoje, vaistų tyrinėjimo Geros klinikinės praktikos taisyklėmis.

Kauno RBTEK pirmininkas Doc. dr. Gintautas Gumbrevičius

LIETUVOS SVEIKATOS MOKSLŲ UNIVERSITETAS * KAUNO REGIONINIS BIOMEDICININIŲ TYRIMŲ ETIKOS KOMITETAS

CURRICULUM VITAE

Name, Surname: **Ali Aldujeli**
Address: Lithuanian University of Health Sciences
A. Mickevičiaus 9, LT-44307 Kaunas, Lithuania
Tel.: +370 648 74874
E-mail: ali.aldujeli.medicine@outlook.com

Education:

2020–2024	Doctor of Philosophy (PhD) in Medicine, M001 *Lithuanian University of Health Sciences,* *Kaunas, Lithuania*
2015–2019	Specialty trainee (residency) in Cardiology *Lithuanian University of Health Sciences,* *Kaunas, Lithuania*
2009–2015	Master of Science in Medicine (MSc) *Lithuanian University of Health Sciences,* *Kaunas, Lithuania*

Professional experience:

2020–2022	Assistant at the Department of Cardiology, Faculty of Medicine *Lithuanian University of Health Sciences,* *Kaunas, Lithuania*
Since 2019	Consultant Interventional Cardiologist / Acute Cardiovascular Care Intensivist *Hospital of Lithuanian University of Health Sciences* *Kauno klinikos, Kaunas, Lithuania*
2018–2019	Fellowship in Coronary Interventions *Hospital of Lithuanian University of Health Sciences* *Kauno klinikos, Kaunas, Lithuania*

ACKNOWLEDGMENTS

Completing this PhD has been a profoundly transformative journey, one that I could not have undertaken without the guidance, support, and inspiration from many incredible individuals and institutions.

First and foremost, I extend my deepest gratitude to my supervisor, Prof. Ramunas Unikas, whose mentorship and rigorous academic guidance have been the cornerstone of my research. His wisdom and support have consistently illuminated my path throughout this journey. Similarly, I owe a debt of gratitude to Associate Prof. Vacis Tatarunas, whose meticulous insights and scholarly expertise significantly shaped my research approach and academic growth.

Special acknowledgment is due to Prof. Gediminas Jarusevicius, Dr. Rima Braukyliene and Dr. Arnoldas Janavicius for their profound influence on my professional life. Prof. Jarusevicius has been pivotal in shaping my aspirations and skills as an interventional cardiologist, while Dr. Janavicius offered steadfast support, guiding me through complex challenges with immense patience and wisdom.

I am immensely grateful to the entire team at the Institute of Cardiology for their active involvement in the laboratory testing and procedures essential to my PhD research. Special thanks to the Laboratory of Molecular Cardiology and its head, Prof. Vaiva Lesauskaite, for their crucial contributions.

I would like to especially thank the Cardiology Intensive Care Unit staff, under the compassionate leadership of Prof. Giedre Baksyte, and the dedicated nurses whose meticulous work was fundamental to our study's success. The Catheterization laboratory staff, from nurses to technicians, also deserve my heartfelt thanks for their enthusiastic participation and support during the lengthy and demanding coronary physiology measurement procedures.

The collaboration with the CORRIB Research Centre for Advanced Imaging and Core Laboratory in Galway, Ireland, under the supervision of Prof. Patrick Serruys and his team, was inestimable. Their expertise and resources greatly enhanced the quality of my research. My sincere appreciation also goes to Assistant Professor Marika Vezzoli from Brescia University, Italy, for her guidance through the field of modern machine learning algorithms and their utilization into the statistics of this PhD thesis.

I am thankful for the expertise of Dr. Emmanouil Brilakis and Dr. Ayman Haq from the Minneapolis Heart Institute, USA, whose critical insights and involvement were essential in shaping and executing the protocol of my study.

Associate Professor Ingrida Grabauskyte from the Lithuanian University of Health Sciences deserves special mention for ensuring the statistical integrity throughout my research. Her oversight contributed significantly to the rigorous analysis of our results.

I am also grateful to all the students who participated in the study – Laurynas Maciulevicius, Zemyna Kurnickaite, Karolis Lickunas, and Austeja Lieponyte – for their diligent work and enthusiasm.

To my broader circle of colleagues, your scholarly insights and constructive critiques have ensured that my dissertation meets the highest standards of academic excellence.

My family and friends have provided a foundation of quiet yet steadfast support that has been my stronghold. Special thanks to Greta, whose belief in me has been unwavering and whose presence was a constant source of comfort and motivation.

Lastly, to my parents, whose emotional and spiritual support underpinned this journey: my father, who, even in his battle with pancreatic cancer, showed immense interest in my progress, and my mother, whose strength and encouragement kept me focused during times of despair. This dissertation honours your sacrifices and love.

This acknowledgment extends beyond mere gratitude; it is a reflection of the profound impact each one of you has had on my personal and academic life.